ROČNÍK/*VOL.* **LXVII**
ROK/*YEAR* **2014**
3

Hutnické listy

METALLURGICAL JOURNAL

ODBORNÝ ČASOPIS PRO METALURGII A MATERIÁLOVÉ INŽENÝRSTVÍ
PROFESSIONAL PERIODICAL FOR METALLURGY AND MATERIAL ENGINEERING

WWW.HUTNICKELISTY.CZ
ISSN 0018-8069

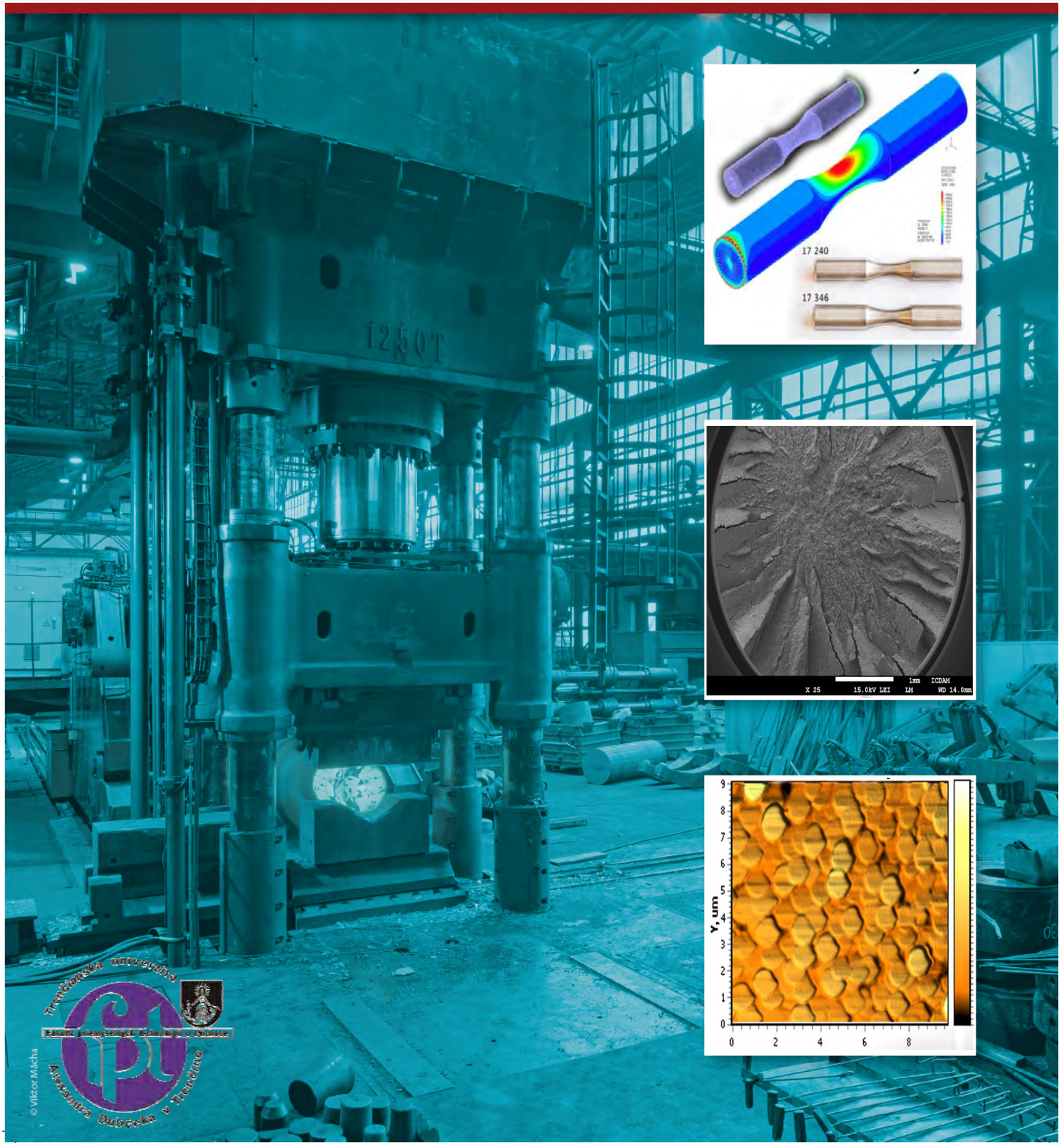

FAKULTA PRIEMYSELNÝCH TECHNOLÓGIÍ V PÚCHOVE

Trenčianska Univerzita Alexandra Dubčeka v Trenčíne

Ivana Krasku 491/30, 020 01 Púchov
tel.:032/7400 814
www.fpt.tnuni.sk

Fakulta priemyselných technológií (FPT) sa každoročne zapája do rôznych mimoškolských aktivít, ktoré umožňujú mladým a poznania chtivým vedátorom spoznávať tajomstvá v oblasti materiálovej vedy a výskumu. V každom akademickom roku otvára FPT svoje brány širokej verejnosti, s možnosťou zoznámenia sa s rôznymi testovacími zariadeniami a prácou materiálových inžinierov.

V dňoch 13. – 15. 11. 2013 počet mladých ľudí, ktorí sa pohybovali v priestoroch FPT v Púchove vzrástol o viac ako 100 %. V rámci celoslovenského Týždňa vedy a techniky fakulta organizovala podujatie „Dni vedy a techniky na FPT v Púchove“, počas ktorého navštívilo fakultu viac ako 500 študentov stredných škôl a žiakov vyššieho stupňa základných škôl púchovského regiónu so svojimi vyučujúcimi. Pracovníci fakulty pre nich pripravili viacero pútavých prednášok spojených s praktickými ukážkami laboratórnych experimentov. Žiaci si v priestoroch laboratórií fakulty vyskúšali prácu so sklom, vlastnoručne si vyrobili kaučukové loptičky, vymodelovali dekoračné predmety z hliny, mali možnosť pomocou experimentov pochopiť, prečo nejesť jablko pred spaním, mohli sledovať mikroštruktúru rôznych materiálov optickým mikroskopom, či vyskúšať si prácu so simulátorom zaťažovania pneumatík. Podujatie bolo zamerané na zvýšenie záujmu mládeže o technický smer štúdia na FPT v Púchove so zameraním na rôzne druhy technických materiálov a celkovo prispelo k popularizácii štúdia technických odborov.






Hutnické listy Metallurgical Journal

Ročník/Volume LXVII
Rok/Year 2014
Číslo/Number 3

květen-červen/May-June
www.hutnickelisty.cz
www.metallurgicaljournal.eu

Registrační číslo/Registration Number
MK ČR E 18087

Mezinárodní standardní číslo
International Standard Serial Number
ISSN 0018-8069

Vydavatel/Publisher
OCELOT s.r.o.
Pohraniční 693/31, 706 02 Ostrava-Vítkovice
IČO 49245848, DIČ CZ 49245848
Registrace v obchodním rejstříku Krajského soudu v Ostravě, oddíl C, vložka 30879

Redakce, kontaktní adresa/ Editorial Office, contact address
OCELOT s.r.o.
Redakce časopisu Hutnické listy
areál VŠB-TU Ostrava, A 534, 17. listopadu 15/2127
708 33 Ostrava - Poruba

Vedoucí redaktor/Chief Editor
Ing. Jan Počta, CSc., tel.: 596995156
e-mail: j.pocta@seznam.cz, redakce@hutnickelisty.cz

Redaktorka/ Editor
Jaroslava Pindorová
e-mail: jaroslava.pindorova@seznam.cz

Grafika titulní strany/Graphic design of the title page
Miroslav Juřica, e-mail: grafik@konstrukce.cz
a red./and Chief Editor

Podkladová fotografie/Underlying photograph
Mgr. Viktor Mácha, viktor.macha@centrum.cz

Tisk/Printing
T-print s.r.o., Průmyslová 1003, 739 65 Třinec

Abstrakty hlavních článků jsou publikovány v české, slovenské a anglické verzi na webových stránkách Hutnických listů.

Časopis vychází 6x ročně. Cena jednotlivého čísla 200 Kč. K ceně se připočítává DPH. Roční předplatné základní 1190 Kč, studentské 20 % sleva proti potvrzení o studiu. K předplatnému se připočítává poštovné vycházející z dodávek každému odběrateli. Po dohodě se zahraničními odběrateli je možno stanovit cenu v Euro (€) jako souhrnnou včetně poštovného. Předplatné se automaticky prodlužuje na další období, pokud je odběratel jeden měsíc před uplynutím abonentního období písemně nezruší prostřednictvím listinné nebo elektronické pošty. Objednávky na předplatné přijímá redakce nebo SEND Předplatné, spol. s r.o., Ve Žlíbku 1800/77, hala A3, 193 00 Praha 9-Horní Počernice (225 985225, send@send.cz). Informace o podmínkách publikace, inzerce a reklamy podává redakce.

Za původnost příspěvků, jejich věcnou a jazykovou správnost odpovídají autoři. Podklady k tisku redakce přijímá v elektronické podobě. Recenzní posudky jsou uloženy v redakci. Žádná část publikovaného čísla nesmí být reprodukována, kopírována nebo elektronicky šířena bez písemného souhlasu vydavatele.

Časopis je zařazen Radou vlády ČR pro výzkum a vývoj do seznamu recenzovaných neimpaktovaných periodik vydávaných v ČR a do mezinárodní databáze CSA Materials Research Database with METADEX, spravované firmou ProQuest, USA.

Abstracts of the main articles are published in Czech, Slovak and English version at the web site of the Metallurgical Journal.

The journal is published 6 times a year. Price of a single issue is CZK 200 without VAT. Net price of basic annual subscription is CZK 1,190, student have 20% discount against the confirmation of study. Forwarding cost (postage) is added to the net price of subscription. Upon agreement with the foreign customers the subscription price, including postage, can be paid in Euro. Subscription is automatically renewed for the next year, unless the customer does not cancel it at the latest one month before the expiry of the subscription period in writing or by electronic mail. Orders are to be sent to the Editorial Office or SEND Předplatné, spol. s r.o., Ve Žlíbku 1800/77, hala A3, 193 00 Praha 9-Horní Počernice (+042 225985225, send@send.cz). Editorial Office provides also information on the conditions of publication of articles and on conditions of advertising.

The authors bear the responsibility for the originality of their articles and for their factual and linguistic accuracy. Editorial Office accepts the articles in electronic form. Peer reviews are archived in the Editorial Office. No part of the published issues may be reproduced or electronically distributed without written permission of the publisher.

The journal was included by the Government Council for Research and Development of the Czech Republic into the list of non-impacted peer-reviewed journals published in the Czech Republic. Abstracts of its articles make part of the international database “CSA Materials Research Database with Metadex”, administered by the database centre ProQuest, USA.

O b s a h/ C o n t e n t

prof. Ing. Ján Vavro, PhD. **4**
Foreword

Recenzované vědecké články/Peer-reviewed scientific papers

prof. Ing. Františka Pešlová, PhD., prof. RNDr. Tatiana Liptáková, PhD., Ing. Michal Bukovina, PhD., Ing. Michaela Ďurovcová, Ing. Pavlína Hájková **5**
Korózne vlastnosti vybraných materiálov pre lopatky vodných turbín
Corrosion Properties of Selected Materials for Blades of Water Turbines
Ing. Zuzana Říhová, Ing. Barbora Roháčová, prof. Ing. Františka Pešlová, PhD. **9**
Hodnocení korozního napadení nelegované oceli průmyslového plynovodu
Evaluation of Unalloyed Steel Corrosion for Industrial Pipeline
Ing. Petra Kováčiková, prof. Ing. Ján Vavro, PhD., Ing. Peter Kopas, PhD., Ing. Marian Handrik, PhD., Ing. Rudolf Valášek, Ing. Ján Vavro, PhD. **13**
Únavová životnosť konštrukčnej ocele pri cyklickom zaťažení
Fatigue Lifetime of the Construction Steel under the Cyclic Loading
Ing. Adriána Pavúčková, Ing. Michaela Ďurovcová, prof. Ing. Františka Pešlová, PhD., Ing. Stanislav Krum **17**
Štruktúrne zmeny vybraných materiálov po teplotných šokoch
Structural Changes of Selected Materials after Thermal Shocks
Ing. Zuzana Harmatová, prof. Ing. Eugen Jóna, DrSc., Ing. Veronika Janíková, Ing. Róbert Janík, PhD., Jozef Miklovič **22**
Štúdium vplyvu rôznych iónov prechodných kovov na termické a spektrálne vlastnosti materiálov s biologicky významnými heterocyklickými zlúčeninami
Study of the Influence of Different Transition Metal Ions on the Thermal and Spectral Properties of Materials with Biologically Important Heterocyclic Compounds
Ing. Ján Vavro, PhD., jr., prof. Ing, Ján Vavro, PhD., Ing. Petra Kováčiková, Ing. Peter Kopas, PhD., Ing. Marián Handrik, PhD., Ing. Radka Bezdedová **25**
Numerická analýza napäťových stavov liatiny s guľôčkovým tvarom grafitu
Numerical Analysis of Stress States for Cast Iron with the Spheroidal Shape of Graphite

Recenzované výzkumné články/Peer-reviewed research papers

Ing. Jan Holec, doc. Ing. Jiří Cejp, CSc., Ing. Stanislav Krum, prof. Ing. Františka Pešlová, PhD. **29**
Abrazivní opotřebení materiálů funkčních součástí vodních turbín
The Abrasive Wear of Materials for Functional Parts of Water Turbines
Ing. Mariana Janeková, Ing. Ľuba Hajduchová, PhD., prof. Ing. Františka Pešlová, PhD. **33**
Porušenie hriadeľa vznikom povrchových vád pri opracovaní
Defect of Shaft Due to Occurrence of Surface Failure during Machining Process
Ing. Daniela Koštialiková, Ing. Ľuba Hajduchová, PhD., prof. Ing. Františka Pešlová, PhD. **37**
Kontiliata guľatina pre výrobu servovalcov z materiálu EN-GJS-700-2
Continuously Cast Round Rod of EN-GJS-700-2 Material for Servo-Cylinder Production
Ing. Natália Luptáková, PhD., prof. Ing. Františka Pešlová, PhD. **42**
Štúdium konečného produktu pri výrobe ZnO
Study of the Final Product in the Production of ZnO
doc. RNDr. Ján Bezecný, CSc., Ing. Andrej Dubec, Ing. Róbert Vavrík **46**
Korózne praskanie demonomerizačnej kolóny
Corrosion Cracking of the Demonomerizing Column
Ing. Jakub Horník, PhD., Ing. Stanislav Krum, Ing. David Tondl, prof. Ing. Františka Pešlová, PhD. **52**
Funkční PVD povlaky pro nástrojové oceli
Functional PVD Coatings for Tool Steels
Ing. Peter Vido, Ing. Jozefína Panáčková, doc. Ing. Jan Krmela, PhD., Ing. Rudolf Valášek **56**
Zhodnotenie interakcie oceľový kord – elastomér v plášti pneumatík
Evaluation of Interaction of Steel Cord – Elastomer in Tire Casing
doc. Ing. Petra Skalková, PhD., Ivan Labaj **60**
Štúdium mechanických vlastností zmesí NR/biopolymér
Study of Mechanical Properties of NR/Biopolymer Blends
Ing. Lenka Špániková, Ing. Michaela Ďurčeková, prof. Ing. Darina Ondrušová, PhD., Ing. Slavomíra Domčeková, Ing. Katarína Holcová **65**
Využitie prírodného a Ca-klinoptilolitu vo funkcii sorbenta zinku z technologickej odpadovej vody- vplyv času a pH
Utilization of Natural and Ca-clinoptilolite in the Function of Sorbent of Zinc from Technological Wastewater-Effect of Time and pH
Ing. Michaela Ďurčeková, Ing. Lenka Špániková, prof. Ing. Darina Ondrušová, PhD. **70**
Odstraňovanie Fe(III) a Pb(II) z vodných roztokov pomocou prírodného a modifikovaného zeolitu
Removal of Fe(III) and Pb(II) from Aqueous Solutions Using Natural and Modified Zeolite
Ing. Dana Bakošová, PhD. **74**
Experimentálne štúdium vplyvu plnív na vybrané mechanické vlastnosti HDPE
Experimental Study of Filler Influence on Mechanical Properties of HDPE
doc. Mgr. Ivan Kopal, PhD. , Ing. Karol Kováč, Ing. Leoš Polka **79**
Analýza teplotnej závislosti termofyzikálnych parametrov tvrdeného polyuretánu
Analysis of the Temperature Dependence of Thermophysical Parameters of Hardened Polyurethane
Ing. Karol Kováč, doc. Mgr. Ivan Kopal, PhD. **83**
Elektrické vlastnosti tvrdeného polyuretánu plneného jednostennými uhlíkovými nanorúrkami s rôznou čistotou
Electrical Properties of Hardened Polyurethane Filled by Single Walled Carbon Nanotubes with Different Purity

Ing. Slavomíra Domčeková, prof. Ing. Darina Ondrušová, PhD., Ing. Lenka Špániková, Ing. Zuzana Jankurová, PhD. **86**
Overenie vplyvu koloidnej siliky v kaučukových zmesiach
Verification of the Colloidal Silica Influence in Rubber Compounds
Ing. Ladislav Janek, PhD., Ing. Vladimíra Krmelová, PhD., doc. Ing. Iva Sroková, PhD., Ing. Jaroslava Janíčková, PhD., RNDr. Vlasta Sasinková **90**
Plnivá na báze organicky modifikovaného MMT a škrobu pre SBR nanokompozity
Fillers for SBR Nanocomposites Based on Organically Modified MMT and Starch
Ing. Michal Pastorek, doc. Ing. Jan Krmela, PhD. **94**
Stanovenie vybraných materiálových charakteristík vybraných častí z rôzne starých plášťov pneumatík
Determination of Selected Material Characteristics for Chosen Parts from Variously Aged Tire Casings
doc. Ing. Petra Skalková, PhD., Ing. Katarína Kostelanská, PhD., Pavol Boško **98**
Vplyv plniva na vulkanizačné charakteristiky zmesí NR/celulóza
Effect of Filler on Curing Characteristics of NR/Cellulose Blends
Ing. Monika Struharňanská, doc. Ing. Jan Krmela, PhD. **102**
Vyhodnocovanie experimentálnych výsledkov vybraných materiálových charakteristík gumárenských zmesí pred a po zostarnutí
Evaluation of Experimental Results for Selected Rubber Compounds before and after Aging Degradation
Ing. Katarína Holcová, prof. RNDr. Mariana Pajtášová, PhD., Ing. Lenka Španiková , Ing. Jana Paliesková, Ing. Zuzana Jankurová PhD., Ing. Marianna Janeková **106**
Štúdium vlastností kaučukových zmesí s obsahom plniva na báze PLA a PP vlákien
Study of the Properties for Rubber Compounds with Fillers Based on PLA and PP Fibers
Ing. Jela Legerská, PhD. **110**
Vplyv väzby na transportné vlastnosti pletenín
Effect of Structure of Knitted Fabric on the Transfer Properties
doc. Ing. Pavol Lizák, PhD., Ing. Anton Schlosser, Ing. Ľubomír Žila **115**
Vplyv koeficientu zaplnenia pleteniny na tepelnú odolnosť a odolnosť proti vodným parám *The Coefficient Influence of Knitted Fabric Packing Density on the Thermal Resistance and Resistance to Water Vapour*
doc. Ing. Pavol Lizák, PhD. **119**
Fyziologická funkcia v odevnom dizajne
Physiological Function in the Clothing Design

Informační články/Informative articles

hutní výroba v ČR a SR/Metallurgical production in Czech Republic and Slovak Republic **122**

ze spolkové činnosti a odborných akcí/Information on associations and professional events **123**

nová literatura/New books **124**

výstavy, veletrhy, konference/Conferences, trade fairs, exhibitions **127**

hutnictví ve světě/Metallurgy in the world **128**

redakční článek **133**

Dodavatelé příspěvků ve všeobecné části:

● Hutnictví železa, a.s. ● pravidelní dopisovatelé ● redakce

Původní autorské texty/Original author´s texts

ISSN 0018-8069

Foreword

Dear readers and all members of academic and scientific community,

I am really pleased that I can write a few words again in relation to the further edition of Metallurgical Journal (2014, Vol. LXVII, No. 3) which comprises the wide range of topics focused on the latest information and outcomes in the field of materials science and engineering. The introduced papers cover a lot of new or additional scientific knowledge related to the most discussed themes in the scientific community with the reference to the current and new scientific approaches and experimental methods of research and development including polymeric materials, metallic materials, inorganic material, textile materials, environmental engineering, physical engineering of materials, numerical analysis, computational modelling and simulations of various processes.

All the papers presented in this edition of the journal are based on the creative and hard work of all scientific and academic staff as well as of doctoral undergraduates at Faculty of Industrial Technologies in Púchov, Alexander Dubček University of Trenčín. The continual investigation by contributors is the reflection of the laborious work leading to the introduced outcomes in this journal and all these outcomes are only the reaction to the most frequently discussed questions and problems which occur on the basis of nowadays needs and wants of the practice.

Presenting their results, all the authors believe that the introduced papers will be the contribution for the improvement of the mutual cooperation between the scientists and engineers and the new gained results will be applied and implemented into the industrial practice. Moreover, this edition with all the investigations can also be the stimulus for the readers in order to cooperate and participate in research with our faculty.

Best regards,

prof. Ing. Ján Vavro, PhD.
Dean of Faculty of Industrial Technologies in Púchov,TnUAD

Recenzované vědecké články

Corrosion Properties of Selected Materials for Blades of Water Turbines

Korózne vlastnosti vybraných materiálov pre lopatky vodných turbín

prof. Ing. Františka Pešlová, PhD.[1], prof. RNDr. Tatiana Liptáková, PhD.[2], Ing. Michal Bukovina, PhD.[2], Ing. Michaela Ďurovcová[3], Ing. Pavlína Hájková[1]

[1]Czech Technical University in Prague, Faculty of Mechanical Engineering, Karlovo nám. 13, 121 32 Prague 2, Czech Republic
[2]University of Žilina in Žilina, Faculty of Mechanical Engineering, Univerzitná 1, 010 26 Žilina, Slovak Republic
[3]Alexander Dubček University of Trenčín, Faculty of Industrial Technologies in Púchov, I. Krasku 491/30, 020 01 Púchov, Slovak Republic

The blades of water turbines are exposed to enormous load from the aspect of dynamic forces, corrosion, erosion and cavitation. According to the mentioned fact, the specialised producer of turbines has to evaluate the material which is used for production of blades and this evaluation is based on the previous knowledge on the degradation process that can be observed in operation and moreover, this evaluation is also based on simulated wear tests. The work deals with the evaluation of two types of materials which can be used for blades of water turbines. There are stainless steel and graphitic cast irons. In the natural water, the cast irons are attacked by the overall non-uniform corrosion. Corrosion grows with the oxygen content under the influence of the water stream, temperature and the presence of free inorganic and organic acids or other aggressive corrosive factors. From an economic and technological point of view, graphitic cast iron is more suitable than steel but it is truth only if the composition and character of the metallic matrix and graphite are in optimum in terms of corrosion.

Keywords: *corrosion resistance, steel, cast iron, blades of water turbines*

Lopatky vodných turbín sú vystavené enormnému zaťaženiu z pohľadu dynamických síl, korózie, erózie a kavitácie. Výrobcovia turbín preto musia návrh materiálu zhodnotiť jednak na základe skúseností z degradácie, ktoré sa vyskytujú v prevádzke a ďalej na základe simulovaných skúšok opotrebenia. Práca sa zaoberá hodnotením dvoch materiálov, ktoré by bolo možné pre lopatky turbín použiť. Jedná sa o nehrdzavejúce ocele a grafitické liatiny. Nehrdzavejúce ocele sú legované ocele s obsahom Cr nad 12 %, čím sa zabezpečí vytvorenie ochrannej oxidickej vrstvy na povrchu kovu. Pre zlepšenie korózných vlastností sa tieto ocele legujú prvkami Ni, Mo, Ti, N, Mn, Cu a pod. podľa požiadaviek na prevádzkové vlastnosti. Pokiaľ sa tieto ocele budú používať v bežnej mineralizovanej vode, tak je známe, že takáto voda nie je pre tieto ocele nebezpečná a ocele sú v nej odolné cca do teploty 60 °C. V bežných riečnych vodách odolávajú korózii i kavitácii pokiaľ nie sú prítomné najmä chloridy. Pre tento typ materiálu sú ďalej nebezpečné štrbiny, baktérie a iné usadeniny na povrchu pretože obmedzujú prístup kyslíka, ktorý zabezpečuje obnovu ochrannej oxidickej vrstvy. Grafitické liatiny sú charakteristické prítomnosťou voľného uhlíka vo forme grafitu. Grafit je korózne odolný materiál ale v spojení s kovovou matricou sa správa ako katóda. V koróznom prostredí sa najskôr rozpúšťa železo a grafitový skelet zostáva. Forma vylúčeného grafitu môže aj celý korózny proces urýchliť (globulárny grafit) alebo spomaliť (lupienkový grafit) pretože na kostre grafitu sa zadržiavajú tuhé korózne produkty. Rýchlosť korózie superponuje charakter kovovej matrice , tvar grafitu, chemické zloženie a štruktúra základného materiálu (perlitický je odolnejší). V prírodných vodách bývajú liatiny napadnuté celkovou nerovnomernou koróziou. V morskej vode s vysokým obsahom chloridov je priemerná hĺbka korózie cca 0,15mm/rok. Korózia rastie s obsahom kyslíka pri prúdení, teplotou a prítomnosťou voľných anorganických a organických kyselín alebo iných agresívnych korózných činiteľov. Z ekonomického aj technologického hľadiska je grafitická liatina výhodnejšia ako oceľ, ale iba za predpokladu, že zloženie a charakter kovovej matrice a grafitu sú optimálne z pohľadu korózie.

Kľúčové slová: *korózna odolnosť, oceľ, liatina, lopatky vodných turbín*

Hutnické listy č. 3/2014, roč. LXVII
ISSN 0018-8069

The subject of the research is connected with the investigation of the material which is commonly used for blades of water turbines and its comparison to the cast iron which has been developed as a new type of material for blades. The chemical composition of evaluated materials is shown in Table 1.

Tab. 1 Chemical composition of the evaluated materials
Tab. 1 Chemické zloženie hodnotených materiálov

Material/ Content in wt.%	Ductile cast iron	Vermicul. cast iron+Al	COR 13-4
C	3.6	3.11	0.05
Si	2.5	2.35	-
Cr	-	-	13.0
Mn	0.1	0.1	-
Mo	-	-	0.5
Al	-	1.9	-
N	-	-	0.5
Cu	0.7	-	-
Ni	1.0	-	4.0
P	0.05	0.05	-
S	0.02	0.02	-

Corrosion tests

The tested materials are commonly subjected to two types of corrosion tests: exposure and electrochemical test. The measurements are performed in mineralised water for drinking and in relation to this water, pH value is determined and it is 5, 6.8 and 8. The addition of HCl leads to the modification of the water with pH = 5 and by this way, there is the increase of the acidity of the solution as well as slight increase of the chloride content (about 0.036 g of Cl to 1liter of water whereas the chloride content in seawater is about 21 g to 1liter of water). In relation to the pH = 8, it is commonly increased by the addition Na_2CO_3 which is the natural part of common water. In this work, attention is paid to selected materials that have been subjected only to the exposure test. Corrosion exposure test was performed by immersing the tested materials to the testing solutions with different pH values. The experimental temperature was 23 ± 2 °C and it corresponded to the ambient temperature. The given samples were immersed for 3 months. The tested samples of materials were cleaned, degreased with diethylether, dried and weighed using analytical balance with an accuracy 10^{-5}. Then the samples were immersed into an aqueous medium of solutions with different pH. After the time of exposure, the samples were cleaned from corrosion products, dried and weighed again using analytical balance. Corrosion rate v_k can be calculated from the weight loss Δm by the formula:

$$v_k = \frac{\Delta m}{S.t}$$

were S – area of the sample (m^2), t – exposure time (year), m – weight (g).

The results of the corrosion tests in water solution with different pH are shown in Table 2. From the experimental results, it is evident that alloyed steel COR 13-4 has a corrosion rate 2.17 $g.m^{-2}.year^{-1}$ at pH = 6.8 and it is negligible corrosion effect. The highest corrosion rate was observed for ductile cast iron ADI. According to the values of corrosion rate, it can be concluded that ductile cast iron MA and vermicular cast iron with aluminium are much more resistant in comparison to cast iron ADI. In the acidic water medium, the corrosion rate is increased for all tested materials and it means that pH represents the increase of the corrosive aggressiveness of water. The most susceptible reaction to the acid environment was observed in the case of the ductile cast iron MA. In relation to the investigation of the alloyed steels, the obtained results are comparable to the results obtained for cast irons because there was also increase in the corrosion rate compared to neutral environment but it can be said that steel COR 13-4 is material with high corrosion resistance. Materials had a different behaviour in alkaline environments. In the case of the alloyed steel COR and ductile cast iron MA, it can be assumed that the chemical composition of the materials and character of the structure is more susceptible to alkaline environment.

Tab. 2 Corrosion rate of the evaluated materials in environments with different pH
Tab. 2 Korózna rýchlosť hodnotených materiálov v prostredí s rôznym pH

Material	COR 13-4	Ductile cast iron ADI	Ductile cast iron MA	Vermicular cast iron+Al
pH 5				
m_1 (g)	17.89567	27.72138	8.70557	27.85175
m_2 (g)	17.89244	27.44088	8.59787	27.65209
S (m^2)	0.001736	0.003263	0.001250	0.002906
Δm (g)	0.00323	0.28050	0.1077	0.19966
v_k ($g.m^{-2}.rok^{-1}$)	7.44	343.86	344.64	274.82
pH 6.8				
m_1 (g)	17.70183	27.70815	8.49514	27.75381
m_2 (g)	17.70089	27.41387	8.41243	27.57727
S (m^2)	0.001736	0.003263	0.001250	0.002906
Δm (g)	0.00094	0.29428	0.08271	0.17654
v_k ($g.m^{-2}.rok^{-1}$)	2.17	360.75	264.67	243.00
pH 8				
m_1 (g)	9.78708	27.49895	8.57391	27.96997
m_2 (g)	9.78569	27.23851	8.46913	27.76226
S (m^2)	0.000965	0.003263	0.001250	0.002906
Δm (g)	0.00139	0.26044	0.10478	0.20771
v_k ($g.m^{-2}.rok^{-1}$)	5.76	319.26	335.30	285.91

After the exposure test, all tested graphite cast irons were covered with black corrosion products while the corrosion was overall as well as non-uniform. The average corrosion rate of cast iron converted to mm/year was in the range from 0.033 to 0.045 mm/year. Areas with missing graphite have local character and depth of the dimples in the structure is markedly different in comparison to the documented microscopic figures. Character of corrosion attack was microscopically evaluated in relation to the all metallographically prepared samples.

Documented microstructure of the materials was investigated for testing solution with pH = 5. Unbroken

surface of sample for alloyed steel COR 13-4 after exposure in water with pH = 5 can be seen in Fig. 1. It is a martensitic structure with a residual austenite among the martensite needles.

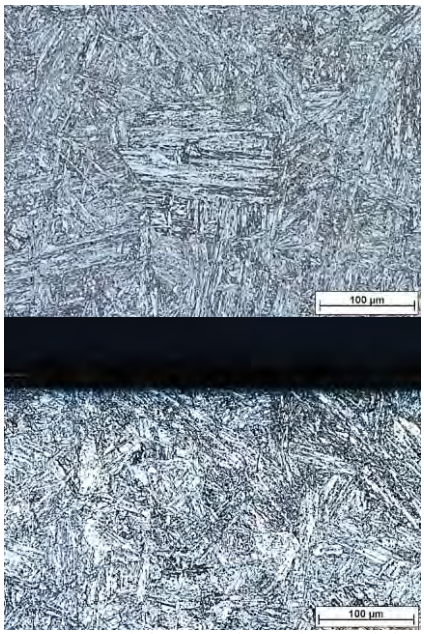

Fig. 1 Microstructure and character of corrosion attack for steeel COR 13-4
Obr. 1 Mikroštruktúra a charakter korózneho napadnutia ocele COR 13-4

Ductile cast iron ADI was exhibited overall as well as no-uniform corrosion attack in relation to its surface (Fig. 2). Missing graphite globules on the surface were the reason for the intensive dissolution of the ferritic matrix around the areas where the graphite globules were fallen out and it led to the influence of the corrosion attack.

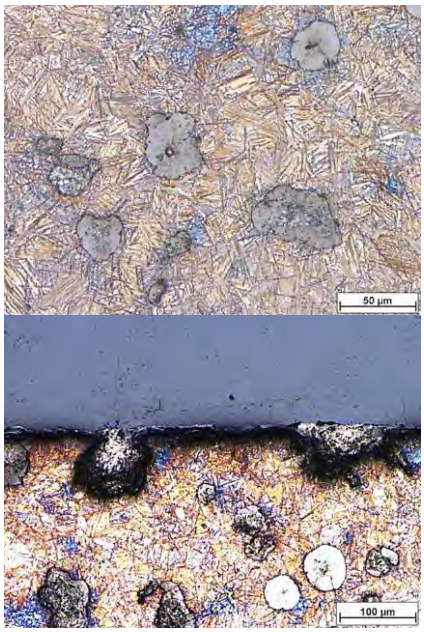

Fig. 2Microstructure and character of corrosion attack for ductile cast iron ADI
Obr. 2 Mikroštruktúra a charakter korózneho napadnutia liatiny ADI

In relation to the corrosive attack, the similar character is observed for of ductile cast iron MA and it is shown in Fig. 3. It can be observed that the size of graphite globules affects the depth of corrosion dimples.

Vermicular cast iron with Al (Fig. 4) exhibits the branching of graphitic particles throughout the whole volume.

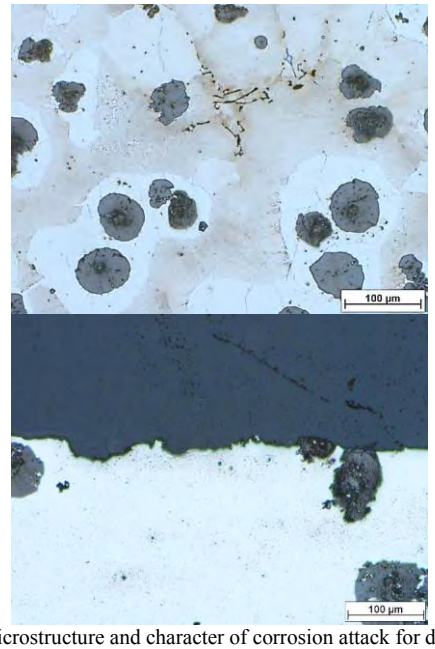

Fig. 3 Microstructure and character of corrosion attack for ductile cast iron MA
Obr. 3 Mikroštruktúra a charakter korózneho napadnutia tvárnej liatiny MA

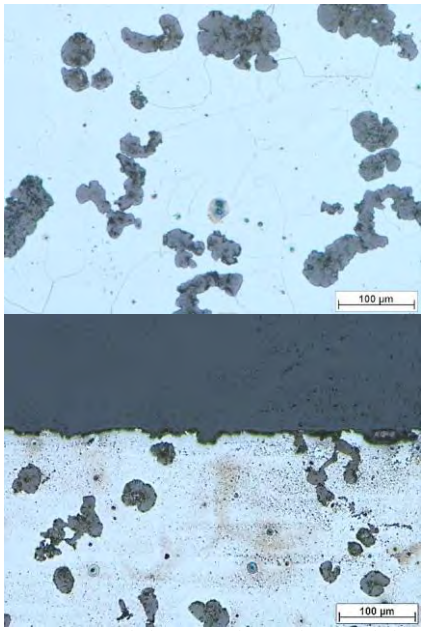

Fig. 4 Microstructure and character of corrosion attack for vermicular cast iron with Al
Obr. 4 Mikroštruktúra a charakter korózneho napadnutia vermikulárnej liatiny s Al

It can be pointed out that if the graphite is fallen out from the surface, the dissolution of ferrite under the effect of cathodic graphite is dominant. Depth of the

Hutnické listy č. 3/2014, roč. LXVII
ISSN 0018-8069

surface attack is related to the morphology of graphite. Corrosion attack is non-uniform in relation to the cast iron surface.

There is not an assumption that the vermicular graphite can fall out in its all volume because parts of the graphitic branches remain locked in metal matrix (in this case, it is ferrite). Comparison of the corrosion rate for graphitic cast irons to corrosion rate for steel COR 13-4 is shown in the Fig. 5.

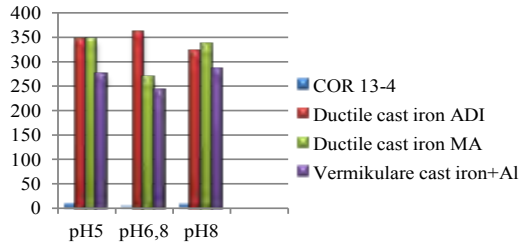

Fig. 5 Comparison of the corrosion rates for the tested materials in dependence on pH
Obr. 5 Porovnanie korózných rýchlostí skúšaných materiálov v závislosti na pH

Conclusions

Alloyed steel COR 13-4, which is commonly used for production of the blades into the water turbine, exhibits high corrosion resistance in waters with lower pH (in our case pH = 5) and in waters with the higher pH (in our case pH = 8), its corrosion attack is negligible.

Cast irons are the materials which are susceptible to acidic as well as basic environment and their susceptibility is influenced be the character of the metal matrix containing graphite. The morphology of the graphite plays important role from the aspect of the immersion and it can be confirmed on the basis of the corrosion tests which showed that vermicular cast iron exhibited the higher corrosion resistance after the immersion to the solutions with different pH in comparison to the globular cast iron.

Average depth of the corrosive attack can be only estimated because the non-uniform corrosion process is influenced by the different size of the graphitic particles which are fallen out.

It is necessary to take into account the synergic effect of the corrosion and cavitation from the aspect of the utilisation of the graphitic cast irons for the hydraulic parts which are commonly loaded by water stream. The overall degradation of the material can be also influenced by character of water pH, angle of water falling and erosive particles because all these phenomena can be commonly seen in the nature.

Literature resources KWOK et al. (2009) confirm that the corrosion process belongs to the processes which cause the overall degradation of the ductile cast iron (1.3 %). The given corrosion process is commonly accompanied by the erosion (73.7 %) and the synergic effect of the corrosion and erosion (25 %).

According to the obtained results and analysis, the vermicular cast iron with Al as alloying element is recommended to be used as the replacement of the alloyed steel. The surface of the given vermicular cast iron can be further treated (coating process) in order to be used under the conditions including the acute angle of water falling.

Acknowledgements
This work has been supported by TAČR No. TA02011121.

Literature

[1] ASM Handbook Properties and Selection. *Nonferrous Alloys and Special-Purpose Material*, 1990, Vol. 2, Priting, USA

[2] KWOK, C.T. WONGA, P.K., MANB, H.C., CHENG, F.T. *Effect of pH on corrosion behavior of CuCrZr in solution without and with NaCl*, 2009, Journal of Nuclear Materials 394, p. 52–62

[3] RANJBAR, K. *Effect off lowinduced corrosion and erosion on failure of a tubular heat exchanger*, January 2010, Materials & Design Volume 31, Issue 1, p. 613–619

[4] LIPTÁKOVÁ, T., FAJNOR, P., DODEK, A. *Evaluation of the flow accelerated corrosion of copper pipe,* 2010, Materials Engineering, Vol. 17, p. 7-13

[5] MALKA, R., SRDJAN, N., GULINO, D. *Erosion–corrosion and synergistic effects in distributed liquid-particle flow*, 2007, Wear 262, p. 791–799

SSI UK má výrobní milník pro oslavu

Steel Guru/Steel Trade Today 22. 3. 2014

Výrobce oceli SSI UK oslavuje další velký milník – přes Teesport vyvezl 5 mil. t ocelových bram. Poslední dodávka bram o celkové hmotnosti byla určena pro SSI v Thajsku. Tento milník přichází téměř dva roky od doby, co se bývalá firma Corus po dvouleté přestávce vrátila k činnosti. Od opětného zapálení vysoké pece téměř před dvěma roky vztahy mezi PD Ports a SSI UK posílily a to umožnilo dosažení takového výrobního milníku, k němuž nyní došlo. Veškerá výroba je vyvážena přes Teesport, v hodnotě okolo 2.7 mld. USD. Tento speciální aspekt činnosti v úzké spolupráci s PD Ports je mimořádně úspěšný.

Evaluation of Unalloyed Steel Corrosion for Industrial Pipeline

Hodnocení korozního napadení nelegované oceli průmyslového plynovodu

Ing. Zuzana Říhová[1], Ing. Barbora Roháčová[2], prof. Ing. Františka Pešlová, PhD.[3]

[1]Czech Technical University in Prague, Faculty of Mechanical Engineering, Department of Materials Engineering, Karlovo náměstí 13, 121 35 Prague 2, Czech Republic
[2]Czech Technical University in Prague, Faculty of Mechanical Engineering, Department of Machining, Process Planning and Metrology, Technická 4, 166 07, Prague 6 Dejvice, Czech Republic
[3]Alexander Dubcek University of Trencin, Faculty of Industrial Technologies in Puchov, Department of Materials Engineering, I. Krasku491/30, 020 01, Puchov, Slovak Republic

The main aim of the presented paper was to analyse the corrosion damage of unalloyed steel pipe. The investigated pipe was the operating part of the pipeline in the heating plant. Corrosion of the inner wall of a natural gas pipeline may occur when the wall is exposed to water and contaminants in the gas, such as O_2, H_2S, CO_2 or chlorides. Corrosion damage of pipe, which was made of steel 12021.1, was subsequently investigated by means of stereo microscopy and optical microscopy. In the experimental part, the pipe was sectioned, grinded, polished and etched. The structure of the pipe is ferrite-pearlite. In relation to the pipe, the occurrence of corrosion which was identified is commonly called as pitting. It is a dangerous kind of corrosion. The corrosion effect involves penetration of the pipe wall and then it is necessary to weld affected pipes. In addition, corrosion was also observed for the outside side of the pipe.

Keywords: *corrosion, pipe, steel, heatexchangers*

V této práci jsme se zabývaly studií korozního napadení oceli 12 021.1 využívané pro trubky průmyslového plynovodu. Jedná se o nelegovanou ocel normalizačně žíhanou s chemickým složením uvedeným níže v tabulce. Tato uhlíková ocel je běžně používána do teplot 300 °C v teplárnách na kotle i potrubí. Při výrobě tepla spalováním zemního plynu dochází nejen k tepelně mechanickému namáhání (creepu) těchto ocelí, ale velkým problémem je I působení koroze.Teplota spalin ve spalovací komoře se pohybuje kolem 800°C a teplota vody uvnitř výparníku je 100 °C/ 16 barů. Z toho důvodu je třeba posuzovat i korozní proces. Práce se zabývá hodnocením degradačního procesu určité části potrubí, u kterého nastal mezní stav opotřebení. Vzhledem k tomu, že se jedná převážně o korozní opotřebení, byla věnovaná pozornost povrchům materiálu. Z napadené části potrubí byly vyřezány vzorky, na kterých semikroskopickyhodnotilastruktura povrchové a podpovrchové části. Prvním krokem bylo zdokumentování vnitřního i vnějšího povrchutrubky na stereomikroskopupomocíněhožbyly detekované nejvíce napadené oblasti.Nežádoucí efekt se ukázal uvnitř membránové stěny, kde došlo ke vzniku úsad a pod nimi narušení mikrostruktury. Korozní porušování odpovídalo důlkové korozi. Důlky se na vnitřní straně vyskytovaly ve značném počtu a různé velikosti.Lze usoudit na nebezpečí působení koroze tak, že může docházet až k lokálnímu proděravění stěny. Vzhledem k tomu, že se jedná o svařitelný materiál opravují se tyto trubky svařováním. Nebezpečí lokální koroze spočívá i v tom, že k perforaci trubek může docházet na předem nepředpokládaných místech membránových stěn, což může způsobit následnou degradaci celého potrubí. Na metalograficky připravených vzorcích v podélném a příčném řezu byla hodnocena mikrostruktura jak z hlediska strukturní charakteristiky, tak z hlediska čistoty materiálu. Na světelném mikroskopu se potvrdila důlkové koroze na vnitřní stěně trubky.Celkové korozní napadení bodovou korozí bylo sledováno i na vnější straně trubky. Mikrostruktura trubek je tvořena feriticko-perlitickou strukturou s výskytem jemných sulfidů na bázi manganu. Na výbrusech je patrné, že se koroze šíří po feritu. Předpokládáme, že úsady jsou na bázi oxidu železa s možnou přítomností chloridů. Chloridy mohou být aktivátorem při spuštění korozních procesů, které se nejvíc projevují za tepla. Doporučujeme provést korozní zkoušky, které by simulovaly i provozní teplotu. Dále je potřebné se zabývat vývojem a možností využití nového čisticího prostředku na čištění vnitřních povrchů trubek. Dnes se v provozu běžně používá čištění pomocí HCl, HF, kyselinou citrónovou, která zanechává stopy na struktuře.

Klíčová slova: *koroze, trubka, ocel, výměníky tepla*

Boilers of heating plants are exposed to demanding operational conditions that have a significant impact on the degradation of material and maintenance of facilities. Industrial boilers of heating plants use natural gas for operation. In practice, we often solve the maintenance after the failure and it does not give us the opportunity to prevent equipment failures effectively.

It seems that in term of the boilers operation, maintenance is a very effective according to the

Hutnické listy č. 3/2014, roč. LXVII
ISSN 0018-8069

technical state. This type of maintenance is connected with managing and using of technical diagnostics methods that allow continuous monitoring of the equipment technical state. These include using continuous diagnostics (remote monitoring) or periodic monitoring of technical condition for devices by external technical diagnostics methods [1].

In this study, we paid attention to the investigation of material from one part of the boiler which was degraded by corrosion. Our research was focused on pipes of the boiler. A fundamental risk parameter for the assessment of technical condition of the boiler is the extent of corrosion. Corrosion process and related damaging of the pipe occurs at the interface of the metal and the heat transfer medium.

Corrosion can damage the entire area of the metal. It may sometimes occur only at the surface or it may infringe some components of the material structure. Various forms of corrosion depend on the material (type, structure, properties, purity), the corrosive environment and the conditions to which the material is exposed in corrosive environments. In terms of operation and maintenance of the pipes in heating plants, substantial problems of corrosion are connected with gas and water environment [1, 2].

Corrosion in gases

Corrosion in the gases will depend on the character and composition of the medium.

Corrosion in oxidizing gases

During the higher temperatures occurs in the gases with a metal oxidizing effect (O_2, CO_2, SO_2) to the formation of undesirable corrosion products. The corrosion rate is influenced by the characteristics of emerging corrosion products. If there is the continuous homogeneous layer, the effect of the corrosive environment is limited by layer and character of oxides which can slow the rate of corrosion. For inhomogeneous layer (or highly porous), a metal surface could be in direct contact with corrosive environments and therefore, corrosion takes place significantly [3, 4].

Corrosion in reducing gases

The most reducing medium is hydrogen. The conditions under which the metal comes into contact with hydrogen are very different. The process of corrosion is dependent on these conditions. The hydrogen corrosion is very dangerous corrosion damage of metal in a reducing environment. Due to the reaction conditions (temperature, pressure, catalyst) and the actual surface of the metal, hydrogen can be activated to the atomic state. Hydrogen atom bonds with oxygen to form H_2O molecules that cause high stress in the structure. Cations of hydrogen are penetrated into the material surface which is systematically ruptured and it leads to its brittleness and cracking [3, 4].

Corrosion in water

The electrochemical process is the dominant degradation process in water corrosion. However, the speed of this process is influenced by a number of factors which may be applied separately. These factors include for example chemical processes in solution, mechanical contaminants, microbes or cavitation.

Corrosion characteristics of constructional carbon steel of class 12

Carbon steel is the most widely used construction material for its mechanical characteristics and good workability. Steels of class n. 12 are high-grade carbon steels which have defined the boundaries of the chemical composition. Therefore, they are suitable for refining, cementation and surface hardening [5].

From the corrosion point of view, carbon steel is the less durable material. The oxides and other corrosion products are spontaneously formed on the steel surface with a limited protective ability. Corrosion of steel occurs in most indoor and outdoor industrial environments. It occurs even at lower relative humidity in comparison to the critical humidity.

The basic reason of atmospheric corrosion of steel is hidden in humidity which together with aggressive components of the atmosphere leads to creation of the electrolyte layer on the surface and it causes corrosion. The carbon dioxide is the main stimulus for atmospheric corrosion. In electrolyte, the surface of the steel is under the rapid oxidation of sulphur dioxide into sulphur trioxide and it is connected with formation of a water sulphate ions. Then, sulphate ions are actively involved into the anodic reaction of iron and it takes place in several basic stages. The hydrated iron oxide (rust) is the final product of these processes is. The corrosion caused by chloride ions has a similar course [3, 5].

The course of the atmospheric corrosion of steel is influenced by many factors (humidity, temperature, pollution, air flow) that interact to varying degrees in each environment. The sulphur dioxide has the dominant position in relation to corrosion processes. The corrosion rate of steel is decreased during the time duration. The steady annual decrease of corrosion in low polluted outdoor atmosphere is 5-30 microns and in high polluted atmosphere, it reaches values up to 50 microns. This should be taken into consideration during the engineering design solutions [3].

Pitting corrosion

This type of corrosion is characteristic for easily passivation metals, such as iron, chromium, aluminium, nickel, stainless steel, etc. Pitting occurs because of the

presence of chlorides in the environment. This is created by local damage of the passive layer mainly in environments containing chlorine or other oxidizing agents (oxygen, chromium). The origin of these damages is caused by the inhomogeneity of the material (inclusions), the presence of surface contaminants or local violation of the passive layer. This is a very dangerous type of corrosion that can lead to penetration of the relatively thick walls thus to the elimination of the whole installations [6].

Experiment

Material and methods

In our study, the corrosion damage was observed for the membrane wall of pipe steel 12021.1. The chemical composition of this steel is provided in Tab. 1. From literature sources, it is known that the unalloyed structural steel is prone to creep and corrosion, but this type of steel is normally used for natural gas operation. Diameter of the pipe is 60 mm and the wall thickness is 4 mm. The samples in the longitudinal axis and the annulus were cut from the pipe (see Fig 1). Corrosion of these samples was observed visually and with a stereo microscope NIKON SMZ1500. The samples were grinded, polished and etched (NITAL 2%). The prepared structures were evaluated with the light microscope Neophot 32.

Tab. 1 Chemical composition of material [6]
Tab. 1 Chemické zloženie materiálu [6]

Chemical composition [wt%]			
C	**Mn**	**Si**	**Cr**
0.07-0.15	0.35-0.60	0.17-0.35	max 0.25
Ni	**Cu**	**P**	**S**
max 0.25	max 0.25	max 0.040	max 0.040

Fig. 1 Sections
Obr. 1 Řezy

Results and discussion

Microstructure of the pipe was extensively damaged by corrosion on the inner side where there is the interaction with the superheated steam (100 °C / 16 bar). Fig. 2 and 3 show the complex corrosion products and sediment throughout the inner side of the pipe. The composition of sediments is based on iron oxide with the possible presence of the other elements, e.g. chlorides which usually cause pitting. The observation of the cross-section of the etched structure (Fig. 4) confirmed the presence of the pitting corrosion.

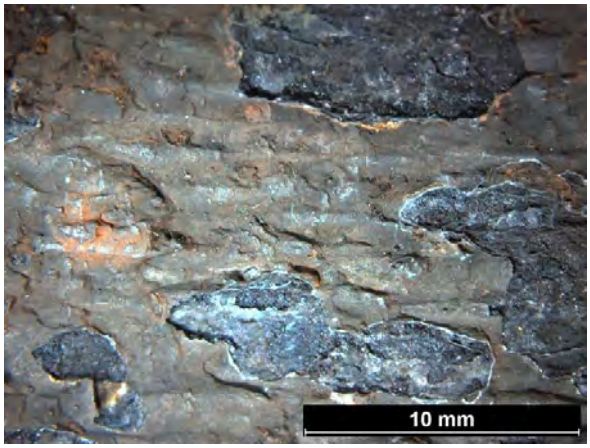

Fig. 2 Sediment, pitting corrosion, stereo microscopy
Obr. 2 Úsada, důlková koroze, stereomikroskop

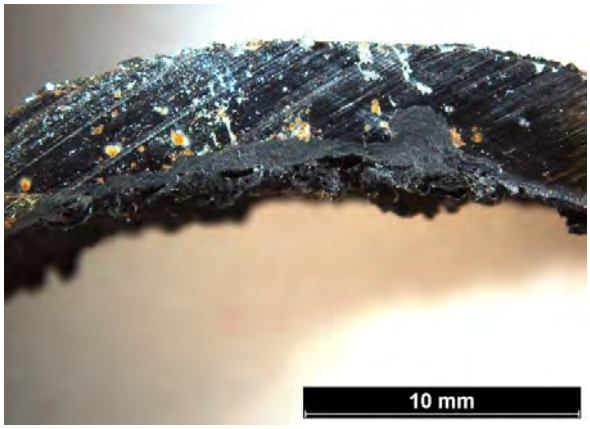

Fig. 3 Pitting corrosion, stereo microscopy
Obr. 3 Důlková koroze, stereomikroskop

Structure of the pipe material consists of ferrite-pearlite structure (Fig. 5) in which there is the occurrence of fine particles of M_nS. Detail of cut pipe in the transverse direction gives information on the character of the pit and disintegration (Fig. 6). On the basis of the etched structures, it is evident that the corrosion spreads across the boundary of ferrite but there is also loss of sulphides in the surface and subsurface area of the pipe.

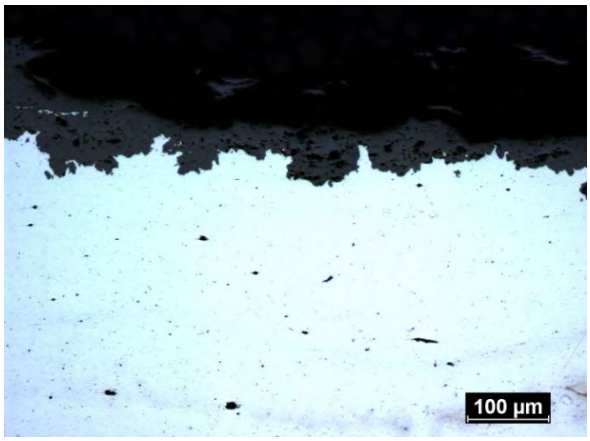

Fig. 4 Pitting corrosion, non-etched structure, light microscope
Obr. 4 Důlková koroze, neleptaná struktura, světelný mikroskop

Hutnické listy č. 3/2014, roč. LXVII
ISSN 0018-8069

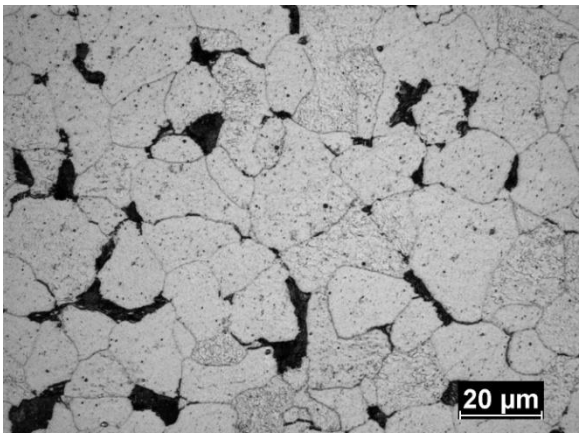

Fig. 5 Ferrite-pearlite structure, etched Nital
Obr. 5 Feriticko-perlitická struktura, leptáno Nital

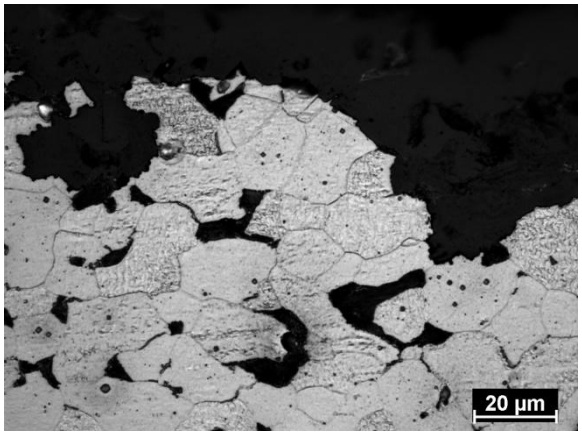

Fig. 6 Detail of pitting corrosion, etched Nital
Obr. 6 Detail důlková koroze, Leptáno Nital

The partial corrosion damage was observed for the external side of the pipe because of the combustion products of natural gas at high temperatures (800 °C).

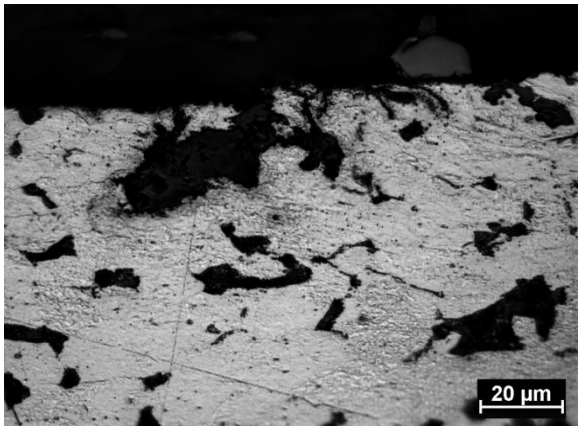

Fig. 7 External side of the pipe, etched Nital
Obr. 7 Vnější strana trubky, leptáno Nital

Conclusions

From a structural assessment, it can be stated that the pipe with ferrite-pearlite microstructure and the M_nS content will be susceptible to corrosion damage which mainly occurred on the inside part of the surface. The occurrence of sediment superposes the pitting corrosion. A consequence of pitting corrosion can lead to localized penetration of the pipe wall but it is problem if the pipe is in operation. We recommend further research for analysis of the sediments and evaluation of mass losses. It is possible to design such cleaner that could extend or replace the current cleaner for cleaning inner surfaces of pipes.

Acknowledgments

This work was supported by Innovation Centre for Diagnostics and Application of Materials No. CZ.2.16/3.1.00/21037and by the Grant Agency of the Czech Technical University in Prague, grant No. SGS13/188/OHK2/3T/12 and by the Ministry of Education, Youth and Sport of the Czech Republic, program NPU1, project No. LO1207.

Literature

[1] KADRNOŽKA, J., OCHRANA, L. *Teplárenství*. Brno, 2001, ISBN 80-7204-222-X

[2] KRBEK, J., POLESNÝ, B., FIEDLER, J. *Strojní zařízení tepelných central - Návrh a výpočet*, PC-DIR Real, s.r.o., 1999, ISBN 80-214-1334-4

[3] KUDLAČEK, J. *Degradační procesy I*, ČVUT, Praha 1994

[4] GROYSMAN, A. *Corrosion for Everybody*, New York, 2010, ISBN 978-90-481-3476-2

[5] DORAZIL, E. *Nauka o materiálu 1*, VUT Brno

[6] FURBACHER, I., MACEK, K., STEIDL, J., et al. *Lexikon technických materiálů*. Prague, 2006. ISBN 80-86229-02-5

Fatigue Lifetime of the Construction Steel under the Cyclic Loading

Únavová životnosť konštrukčnej ocele pri cyklickom zaťažení

Ing. Petra Kováčiková[1], prof. Ing. Ján Vavro, PhD.[1], Ing. Peter Kopas, PhD.[2], Ing. Marian Handrik, PhD.[2], Ing. Rudolf Valášek[1], Ing. Ján Vavro, PhD.[1]

[1]University of Alexander Dubček in Trenčín, Faculty of Industrial Technologies, I. Krasku 491/30, 020 01 Púchov, Slovak Republic
[2]University of Žilina in Žilina, Faculty of Mechanical Engineering, Univerzitná 1, 010 26 Žilina, Slovak Republic

The given paper is focused on the problems relating to the mechanical fatigue and it is also devoted to the investigation of the lifetime for the selected material which was used for preparation of samples. The given samples were investigated with help of testing device SCHENCK. The vibration stress was obtained by using of cyclic loading based on bending. The accumulation of the stress as well as change of service conditions can have the influence on the damage or rupture of the operating part. The given damage or total failure can even occur without any indication of rupture. Therefore, it is necessary to reduce or eliminate the effect of these undesired properties and moreover, there is also an effort to find solutions for prolongation of the lifetime of operating part. The given experimental work is mainly focused on performance of such tests which are closely connected with mechanical fatigue because on the basis of these tests, it is possible to determine the material parametres and characteristics which are needed for further evaluation as well as specification of material behaviour under the critical conditions. To make the mutual comparison, the two types of austenitic chrome-nickel steels were used for preparation of samples. The tests were carried out under the gradually increased loading and the selected frequency was 15 Hz. In relation to the gradually increased loading during the testing, Wöhler fatigue curve as well as the value for fatigue yield point can be acquired. Nowadays, the investigation of the fatigue is mainly based on utilisation of the numerical analysis and therefore, the results of mentioned experiments were used as input parametres for the specification of physical and material characteristics which is based on creation of the computational analysis. Using the numerical program system based on the finite element method (FEM), the given computational analysis was used for simulation of loading. In terms of FEM, the program software of ADINA 8.8.0 was used.

Keywords: *fatigue, Wöhler fatigue curve, numerical analysis, FEM*

Príspevok sa zaoberá problematikou mechanickej únavy a životnosti materiálu vzoriek, ktorých experiment bol uskutočnený na zariadení SCHENCK. Kmitavé napätie sa dosiahne ohybovým cyklickým zaťažením vzorky pri rotácii pri rôznych hladinách zaťaženia. Kumuláciou poškodenia a zmenou prevádzkových podmienok môže nastať poškodenie súčiastky bez náznaku porušenia a preto sa snažíme znižovať účinok týchto nežiaducich vlastností a hľadáme možnosti ako zvýšiť životnosť materiálu. Experiment je venovaný skúške mechanickej únavy pre stanovenie materiálových parametrov, charakteristike štrukturálnych vlastností a sledovaniu zmien materiálových vlastností, pretože zmena týchto vlastností a parametrov ovplyvňuje celkové výsledné chovanie konštrukcií a ich súčastí. Pri tejto skúške sme na porovnanie použili skúšobné vzorky s kruhovým prierezom austenitickej chrómniklovej ocele STN 17 240 a austenitickej chrómniklovej ocele STN 17 346 pri odstupňovanom zaťažení a frekvencii 15 Hz. Výsledkom skúšky na odstupňovaných hladinách zaťaženia je Wöhlerova krivka únavy a hodnota medze únavy. V dnešnej dobe sa výskum v oblasti únavy zaoberá najmä numerickou analýzou a výsledky z experimentu budú vstupnými parametrami na zadefinovanie fyzikálnych a materiálových charakteristík pre druhú časť práce, kde sa budeme zaoberať vytvorením výpočtovej analýzy, ktorá nám umožní simuláciu zaťaženia využitím výpočtového programového systému na báze metódy konečných prvkov – MKP, kde využijeme programový softvér ADINA 8.8.0. Pre zjednodušenie výpočtov bude simulácia riešená ako lineárna úloha. Táto práca bude predstavovať kombinovaný výskum experimentu v oblasti únavy namáhaním, numerickou analýzou na základe mechanických a únavových vlastností, následným vyhodnotením a komparáciou získaných výsledkov, čo prinesie nové pohľady, ale aj výsledky pre ďalší výskum a rozvoj aplikácie riešenej problematiky mechanickej únavy.

Kľúčové slová: *únava, Wöhlerova krivka únavy, numerická analýza, MKP*

Hutnické listy č. 3/2014, roč. LXVII
ISSN 0018-8069

Nowadays, the research of the fatigue lifetime is focused on comparison of experimental results to the results based on numerical analysis. The given paper is closely connected with performance of such tests which are closely connected with the mechanical fatigue because on the basis of these tests, it is possible to determine the material parametres which are needed for further evaluation as well as specification of materialbehaviour under the critical conditions. Besides the material characteristics of structural or construction properties, the changes of material properties are also investigated because all these factors have significant influence on the resulting behaviour of material constructions and their parts. The mentioned tests were preformed for the samples with the round cross-section while the two types of steels were used for their preparation in order to make comparison. The samples were prepared from austenitic chrome-nickel steels with designations: STN 17 240 and STN 17 346 (designation is based on the Slovak Technical standard). The determination of Wöhler curve and knowledge in relation to the material and geometrical data for investigated material represent the basic requirement for determination of the input parametres in relation to the numerical analysis. From the aspect of the given numerical analysis, it enables us to perform the simulations for cyclic loading while ADINA 8.8.0 program which is based on utilisation of numerical finite element method is used [1].

Characteristics of construction steels

The chemical analysis was performed with help of spectral method using spark discharge excitation and the basic mechanical properties were obtained on the basis of the static tensile test. The chemical composition for both construction steels is presented in Tab. 1 and 2. The results relating to the mechanical properties are shown in Tab. 3 [2].

Tab. 1 Chemical composition of the 17 240 material
Tab. 1 Chemické zloženie materiálu 17 240

	C	Mn	Si	P	S
Material 17 240	0.065	0.58	1.05	0.024	0.011
	Cr	**Ni**	**Mo**	**Cu**	**W**
	19.09	7.42	0.17	0.06	0.058

Tab. 2 Chemical composition of the 17 346 material
Tab. 2 Chemické zloženie materiálu 17 346

	C	Mn	Si	P	S
Material 17 346	0.042	0.50	1.50	0.028	0.014
	Cr	**Ni**	**Mo**	**Cu**	**W**
	16.70	8.96	2.05	0.36	0.065

Tab. 3 Mechanical properties of the materials
Tab. 3 Mechanické vlastnosti materiálov

Material	$R_{P0,2}$ [MPa]	R_M [MPa]	A [%]	Z [%]
17 240	263	642	65.5	77.1
17 346	255	559	66.8	77.2

The microstructure of the sample representing 17 240 steel (Fig. 1) is mainly formed by polyhedric grains of austenite and particle of delta-ferrite can be found in the surface layers.

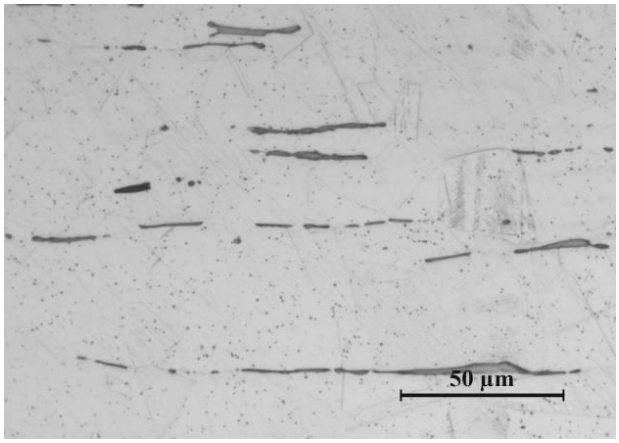

Fig. 1 Microstructure of the 17 240 steel
Obr. 1 Mikroštruktúra ocele 17 240

The microstructure of the sample representing 17 346 steel (Fig. 2) is also formed by polyhedric grains of austenite but the given austenitic structure is coarse-grained in comparison to the microstructure of 17 240 steel. Moreover, it has to be also mentioned that the occurrence of the delta-ferrite is only sporadic.

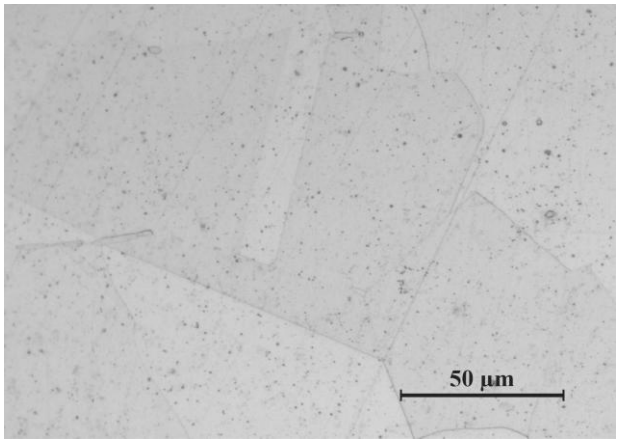

Fig. 2 Microstructure of the 17 346 steel
Obr. 2 Mikroštruktúra ocele 17 346

Mechanical fatigue test

Using testing device SCHNECK, the fatigue tests were performed. The initial stress (σ_1) for the first one tested rod with round cross-section was selected and in relation to this initial stress, it was less by 10 MPa in comparison to the highest admitted R_e for the given material. The distance (*a)* of the ballast weight was calculated for the given diameter of the rod. After the fracture of the first one rod, the gradation scale of the stress was specified for each one sample while the frequency of loading was still the same and it was 15 Hz. The test was performed in the mentioned way until the critical values of the stress were recognized. The critical

values of the stress represent the values at which the tested rod withstands the number of cycles which are selected as the basis for the determination of the fatigue yield point and therefore, it is necessary to perform also the control test at least of one rod. The given control test is performed for the same or even less loading by 15 MPa. The testing process is performed continuously (the test is not allowed to be interrupted and the end of this test is based on the occurrence of the fracture (Fig. 3) or the visible crack (Fig.4) and this fact has to be mentioned in the documentation relating to the test [3].

Fig. 3 Fatigue fracture of the material
Obr. 3 Únavový lom materiálu

Fig. 4 Fatigue crack of the material
Obr. 4 Únavová trhlina materiálu

Sample model

The basic model of the sample was created using ADINA 8.8.0 program. In relation to the fatigue tests under the cyclic loading, the smooth rod is used for preparation of the samples. The ends of the samples are wider because of better clamping and the cross-section of the thinner tested part is strictly predefined. The input parametres for analysis included Poisson ratio, modulus of elasticity for the tested austenitic chrome-nickel steels and all important values representing the critical conditions. On the basis of the mentioned input parametres, the mesh was generated (Fig. 5) [4].

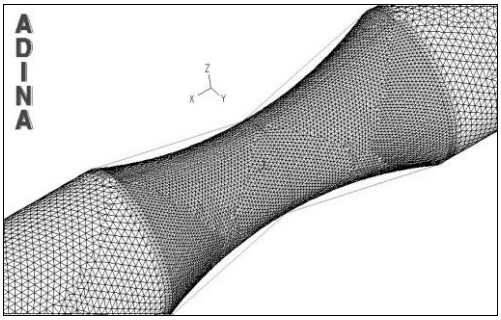

Fig. 5 Mesh of the model
Obr. 5 Sieť modelu

In relation to the analysis of the lifetime, the linear, elastic material model was selected on the basis of the created bending moment in time intervals regarding to the ends of the model [5].

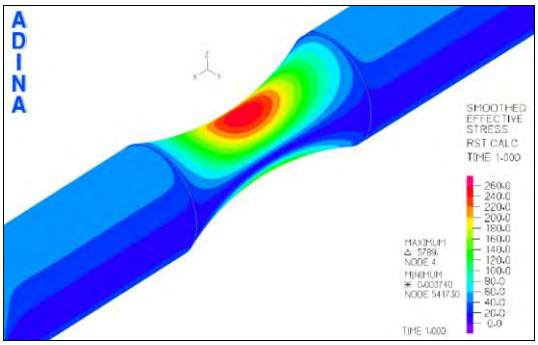

Fig. 6 Numerical analysis
Obr. 6 Numerická analýza

Results and discussion

The following tables (Tab. 4 and 5) represent the measured values (results) which were obtained on the basis of the fatigue test while the given experiment was performed with help of device SCHNECK and there are also the values which were obtained on the basis of the finite element method.

Tab. 4 The results of the fatigue test for 17 240 steel
Tab. 4 Výsledky skúšky únavy ocel'e 17 240

17 240	σ [MPa]	Number of cycles N
1	259.75	13 000
2	249.16	15 300
3	238.58	32 700
4	228.00	45 900
5	218.61	102 900
6	208.03	270 200
7	197.44	10 468 200
8	186.86	10 102 800

Hutnické listy č. 3/2014, roč. LXVII
ISSN 0018-8069

Tab. 5 The results of the fatigue test for 17 346 steel
Tab. 5 Výsledky skúšky únavy ocele 17 346

17 346	σ [MPa]	Number of cycles N
1	253.86	13 200
2	249.16	23 600
3	238.58	64 300
4	228.00	84 100
5	218.61	131 100
6	208.03	211 800
7	197.44	10 205 600
8	186.86	10 259 100

On the basis of the obtained data for gradually increased loading, Wöhler fatigue curves were created (Fig. 7).

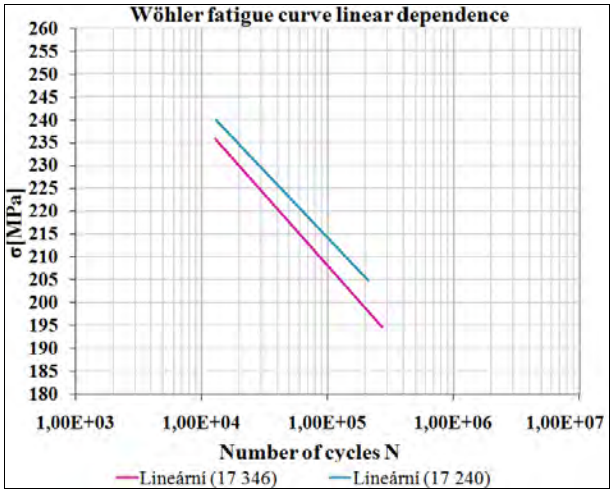

Fig. 7 Wöhler fatigue curve for the 17 240 and 17 346 materials
Obr. 7 Wöhlerova krivka únavy materiálu 17 240 a 17 346

Conclusions

The given paper is closely connected with the analysis of the fatigue lifetime for construction or structural materials which are under the cyclic loading. During the experiment as well as under the real conditions, there are complex mechanical, chemical and physical phenomena in the tested sample or in the operational part. According to the mentioned fact, it is necessary to find the way which can help us to generate or create the accurate results for verification of the results obtained on the basis of measurements. Besides the results relating to mechanical properties of material, there are chemical composition, microstructure description as well as fatigue tests for two different types of steels in the paper. All the mentioned parametres, features, properties are important from the aspect of creation of Wöhler fatigue curves for these two different types of austenitic chrome-nickel steels [6].The precise geometry is also necessary because of numerical analysis because this analysis is important for creation of the computational model. Furthermore, in relation to the numerical analysis, the physical as well as material characteristics have to be strictly defined utilizing table values as well as values based on experimental procedures and it can help us to find the most effective and accurate results. In relation to the fatigue lifetime, the numerical analysis is performed with help of ADINA 8.8.0 program and it is based on the finite element method. The main aim of the paper was to show whether there was any accordance between values based on experimental investigations and values based on the numerical analysis while the evaluation was connected with the fatigue lifetime. The created simulation was solved as the linear equation because of simplification of the calculations. In this paper, there is the combination of the experimental investigation and numerical analysis while the experimental part is connected with the occurrence of the fatigue under the cyclic loading and numerical part is based on the calculation of the mechanical as well as fatigue properties [7]. The obtained results are going to be used for specification of lifetime for glass moulds but they can be also the contribution in relation to the field of material engineering because the evaluation and comparison of the obtained results can be the stimulus for further investigation as well as development and progress of used applications with regard to the problem including mechanical fatigue.

Acknowledgements

This work has been supported by VEGA grant No.1/0385/14 and KEGA grant No. 007 TnUAD-4/2014.

Literature

[1] KOVÁČIKOVÁ, P., VAVRO, J., VALÁŠEK, R., VAVRO, J. jr. *Fatigue of Construction Steel under the Cyclic Loading*. In: Hutnické listy, vol. LXVI, is. 7, 2013, p. 22-24. ISSN 0018-8069

[2] VELES, P. *Mechanické vlastnosti a skúšanie kovov*, Bratislava: Alfa, 1985. 408 s. ISBN 63–559–85

[3] STN 420 363: *Skúšanie kovov, skúšky únavy kovov, metodika skúšania.* Vydané 1. 10. 1986

[4] SÁGA, M., KOPAS, P., UHRIČÍK, M. *Modeling and Experimental Analysis of the Aluminium Alloy Fatigue Damage in the case of Bending – Torsion* Loading. In: Procedia Engineering, Vol. 48, 2012, p. 599-606. ISSN 1877-7058

[5] NICOLETTO, G., BOKŮVKA, O., COLLINI, L., KOPAS, P. *Fatigue resistance in the very high-cycle regime.* Transaction of FAMENA, Vol. 29, No. 1, Croatia, Zagreb 2005, p. 9–16. ISSN 1333–1124

[6] JAKUBOVIČOVÁ, L., SÁGA, M., VAŠKO, M.: *Impact Analysis of Mutual Rotation of Roller Bearing Rings on the Process of Contact Stresses in Rolling Elements*. In: Manufacturing technology, Vol. 13, Issue 1, 2013, p. 50-54. ISSN 1213-2489

[7] VAŠKO, M., LEITNER, B., SÁGA, M. *Computational fatigue damage prediction of the lorry frames under random excitation.Communications.* Scientific Letters of the University of Žilina, Vol. 12, No. 4, 2010, p. 62-67. ISSN 1335-4205

Structural Changes of Selected Materials after Thermal Shocks

Štruktúrne zmeny vybraných materiálov po teplotných šokoch

Ing. Adriána Pavúčková[1], Ing. Michaela Ďurovcová[1], prof. Ing. Františka Pešlová, PhD.[1], Ing. Stanislav Krum[2]

[1]Alexander Dubček University of Trenčín, Faculty of Industrial Technologies in Púchov, I. Krasku 491/30, 020 01 Púchov, Slovak Republic
[2]Czech Technical University in Prague, Department of Materials Engineering-ICDAM, Faculty of Mechanical Engineering, Karlovo nam. 13, 121 32 Prague 2, Czech Republic

The given paper is closely connected with the investigation of the structural changes for selected material which is exposed to the thermal shocks. The investigated material was supposed to be used in such industrial sphere where it has to withstand extremely high temperatures. The heating of the selected material was simulated under the specified conditions to optimize the structure of the given material loaded thermally. On the basis of this simulation, it was possible to specify the first one initiation of the failure. Toolox 33 is the material which was the subject of our investigation and this material was compared to Dominial ZF2 which is commonly used for manufacturing of moulds in the glass industry. From the economical aspect, there was the proposal that Toolox 33 could be used as replacing material of Dominial ZF2. According to this proposal, it was necessary to perform a lot of investigations in relation to the structural changes of the given tested material. The attention was paid to the microstructure imperfections because these imperfections represent the first initiation of the failure. On the basis of the experiments and obtained results, the material Toolox 33 is not recommended to be used for manufacturing of moulds in glass industry.

Keywords: *thermal shocks, fracture surface, initiation of the failure, structural changes*

Práca sa zaoberá štúdiom štruktúrnych zmien vybraných materiálov vystavených tepelnému namáhaniu. Vzhľadom k tomu, že sa jedná o materiály využívané na súčasti, ktoré sú teplotne zaťažené v prevádzke, boli podľa toho navrhnuté experimenty. Tepelné namáhanie bolo simulované ohrevom materiálu na vysoké teploty, rýchlym ochladením toľkými cyklami, ktoré je materiál schopný vydržať do prvej iniciácie porušenia. Jedná sa o materiál Dominial ZF 2, ktorý sa bežne využíva v sklárskom priemysle pre teplotne namáhané formy alebo predformy, ktoré sú v interakcií so sklovinou. Firma z ekonomického hľadiska navrhuje nový typ materiálu, ktorý sa do súčasnej doby v sklárskom priemysle nepoužíval. Jedná sa o náhradu za Dominial ZF 2 kde je navrhovaný materiál Toolox 33. Z toho dôvodu boli sledované a porovnávané tieto vybrané materiály. Tieto materiály pri rovnakých teplotných cykloch boli následne vystavené statickej skúške v ťahu. Skúškou v ťahu boli získané lomové plochy, ktoré boli fraktograficky hodnotené. Z lomových plôch sa dá usúdiť charakter porušovania týchto materiálov aj na ich mikroštruktúre. Pozornosť bola venovaná nedokonalostiam mikroštruktúry, ktoré sú prvotnými iniciátormi porušenia hlavne v teplotných šokoch. Na základe experimentov a získaných poznatkov nedoporučujeme materiál Toolox 33 pre sklársky priemysel. Literárne rešerše potvrdzujú tento záver tým, že aj keď tieto ocele patria do skupiny koróziivzdorných materiálov ich správanie za vyšších teplôt je superponované aj koróziou a mechanickým opotrebením, čím sa skracuje ich životnosť. Z experimentov a štúdia štruktúr sa dá predpokladať, že samotný materiál, aj keď je koróziivzdorný a odolný proti korózii, bude musieť byť aj povrchovo upravený. Odporúčame navrhnúť takú povrchovú úpravu, ktorá zvýši životnosť týchto materiálov používaných v sklárskom priemysle. Konkrétne úpravy na materiáli ZF 2 odskúšať na formách a predformách priamo v prevádzke.

Kľúčové slová: *teplotné šoky, lomová plocha, iniciácia porušenia, štruktúrne zmeny*

Production of the construction and technical objects is closely connected with requirements for enhancement material quality because the final products are exposed to heavy-duty in-service conditions. These requirements include thermal, mechanical as well as chemical resistance of the given material [1]. The steels which withstand high temperatures and mechanical load are required to be used for production of such components which are under the high thermal stress. The steels used for high resistant components have to be resistant to corrosion, heat as well as fire.

The paper deals with evaluation of the material Toolox 33 which could be used as a replacing material of Dominial ZF 2. Dominial ZF 2 is the material which is used for production of components under the high thermal stress. Components under the high thermal stress can also be found in a glass industry. The moulds and pre-moulds are commonly made of Dominial ZF 2. There was the proposal to investigate any other type of

Hutnické listy č. 3/2014, roč. LXVII
ISSN 0018-8069

material in order to prolong the lifetime of the pre-mould and mould. During operation time, there is the occurrence of material degradation processes which cause large number of the undesirable factors and these are summarised in Fig. 1. The selected steels were exposed to extreme thermal loading in order to simulate critical conditions which can lead to specification of material behaviour at high temperatures. The materials were exposed to short-term thermal shocks at temperatures from 800 to 900 °C and subsequently, they were cooled quickly. To predict the occurrence of the failure of the components, it is necessary to pay attention to observations of structural changes and mechanical characteristics which can occur during the thermal shocks in materials. The mentioned prediction is related to the lifetime of the specific components and it also connected with the selection of the right material.

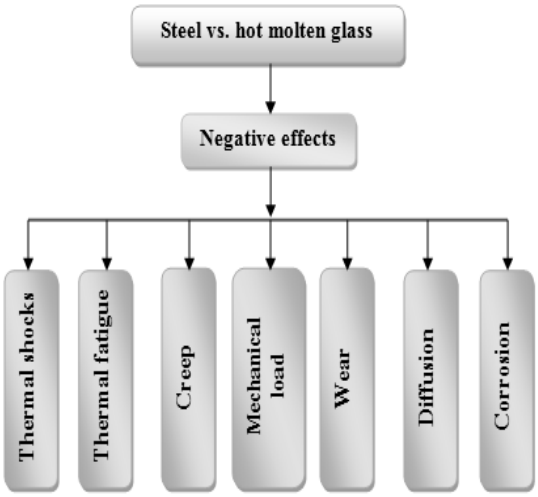

Fig. 1 Negative effects – "steel vs. hot molten glass"
Obr. 1 Negatívne vplyvy vyskytujúce sa v oceli vs. horúca sklovina

The introduced negative effects occurring during the operation time are closely connected with the reduction of the lifetime and they have great effect on production of final glass products with their imperfections [2].

Experimental part

Dominial ZF 2 is high-alloyed CrNi steel with austenitic structure and its chemical composition is shown in Tab. 1. Toolox 33 is hardened steel with extremely high hardness 300 HBW with martensitic structure. The chemical composition of the materials is given in Tab. 1. These materials have been determined by chemical composition which is given according to the standards but the materials which were investigated did not exhibit the same chemical composition in comparison to the standards which were supplied by the company. According to the mention fact, the chemical composition was inspected on the basis of the performed chemical analysis and using this supplemented chemical analysis for the specified area, the content of various elements was calculated statistically.

Tab. 1 Chemical analysis of the material ZF 2 and Toolox 33 (ICDAM-CTU, Prague)
Tab. 1 Chemická analýza materiálu ZF 2 a Tooloxu 33 (ČVUT-ICDAM, Praha)

Chemical composition [wt. %]		
Materials	**ZF 2**	**Toolox 33**
C	0.12	0.25
Al	0.26	0.15
Si	1.31	0.92
S	0.10	*
Cr	28.61	1.47
Mn	1.06	0.84
Fe	47.99	91.41
Ni	15.36	*
V	*	0.17
Mo	*	0.71

The proposal of the geometry for the sample under the thermal shocks

In relation to the testing machine, proposal of sample geometry corresponds to the methodology requirements for testing under the thermal shocks. Test equipment has been obtained by modification of the resistance spot welding machine. The middle of the sample (with diameter 8 mm) represents the critical area which is under the highest stress because of thermal shocks and these thermal shocks were simulated by the modified resistance spot welding machine. The selected temperature was in the range from 800 to 900 °C and this temperature corresponds to the temperature of the hot drops of molten glass. The temperature gradient has to be high enough to gain the simulation at the maximum load (although the mentioned maximum load has not be commonly seen during the operation). On the basis of this simulated condition, it was possible to observe the structural reaction and changes of a given material. In relation to these changes, the given material was able to be observed from the aspect of the specified thermal cycles.

The thermal loading

The researched materials were exposed to thermal shocks at temperatures from 800 to 900 ^{o}C and then, the samples were cooled for 5 sec. in the cooling the water medium and this process was repeated until the crack initiation. During the experiment, the determined conditions were the same for all tested material samples.

The structural evaluation

Before and after thermal shocks, the tested samples of Dominial ZF 2 and Toolox 33 were prepared metallographically and their microstructure was evaluated in longitudinal and cross-sectional direction. Metallographic observation was carried out for the middle of the sample because there was the largest concentration of heat. The microscopic evaluation was

performed for both materials at various magnifications. The starting microstructure of Toolox 33 consists of a martensitic structure (Fig. 2) and residual austenite. Martensitic structure is kept but there is only the change in occurrence of the residual austenite which is much more visible (Fig. 3).

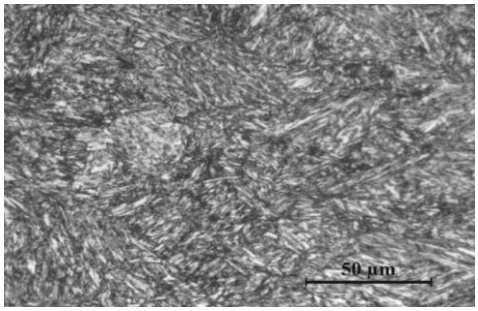

Fig. 2 Toolox 33 before thermal shocks
Obr. 2 Toolox 33 pred teplotnými šokmi

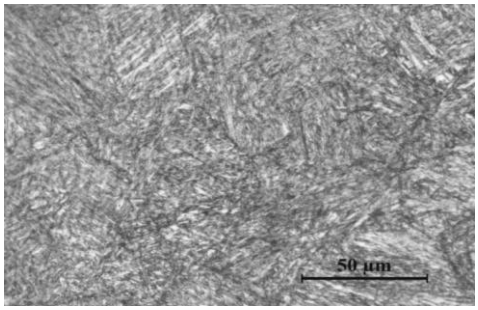

Fig. 3 Toolox 33 after thermal shocks
Obr. 3 Toolox 33 po teplotných šokoch

From the aspect of crack initiations, it is necessary to know the purity of the initial microstructure and it can be determining factor for recognition of the initiated crack. The evaluation of the micropurity of Toolox 33 sample under its surface led to specification of occurrence of carbonitrides (Fig. 4).

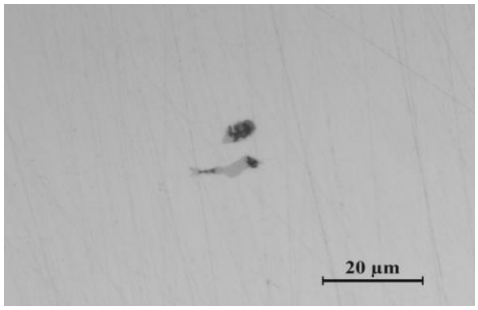

Fig. 4 Detail of carbonitrides
Obr. 4 Detail karbonitridov

The influence of thermal stress led to the formation of failure in the area of grain boundaries. Fig. 5 shows the connection of three different cracks in austenite and they were spread along the grain boundaries.

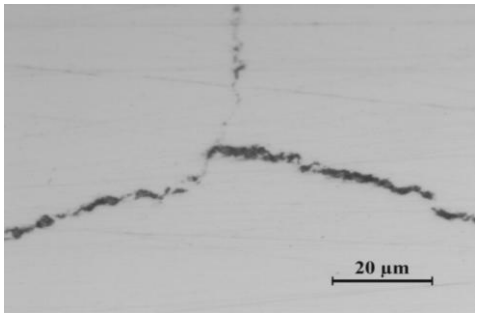

Fig. 5 Character of crack
Obr. 5 Charakter trhliny

Microstructure of Dominial ZF 2 was formed by austenitic structure with the non-uniform grain size and it is shown in Fig. 6. The twins of different sizes were observed in the austenitic grains. Character of austenitic grains after thermal shocks is shown in Fig. 7 where the occurrence of the carbide phases is much more visible.

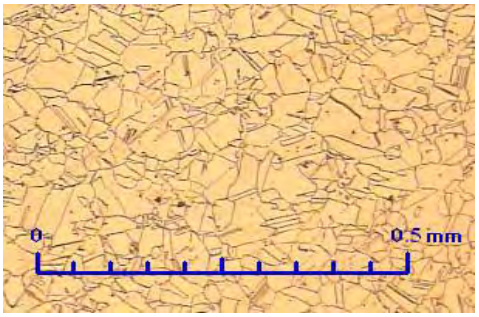

Fig. 6 Dominial ZF 2 before thermal shocks
Obr. 6 Dominial ZF 2 pred teplotnými šokmi

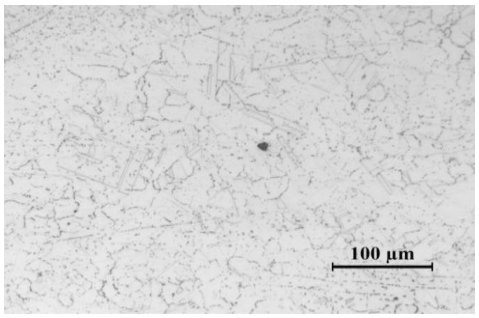

Fig. 7 Dominial ZF 2 after thermal shocks
Obr. 7 Dominial ZF 2 po teplotných šokoch

The evaluation of micropurity showed the occurrence of oxides, carbonitrides and non-formable silicates (Fig. 8).

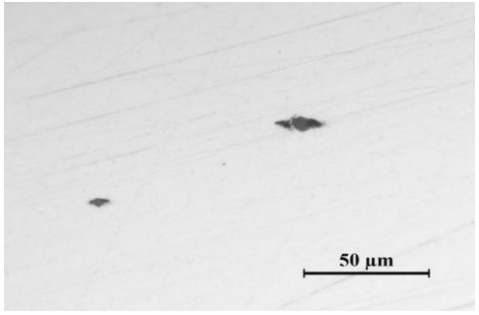

Hutnické listy č. 3/2014, roč. LXVII
ISSN 0018-8069

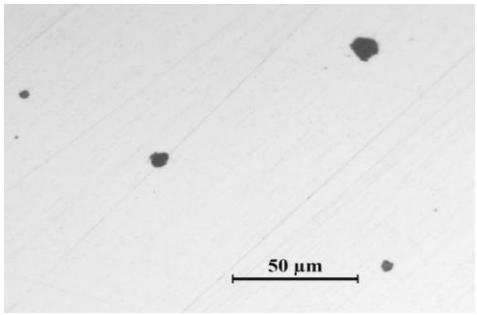

Fig. 8 Micropurity of Dominial ZF 2 - base material
Obr. 8 Mikročistota Dominialu ZF 2 - základný materiál

In fractographic terms, the fracture surfaces were evaluated and the tested samples for both materials were compared mutually after the static tensile test as well as before thermal cycling and after thermal cycling [3]. On the basis of macrofracture observation (see Fig. 9 and Fig. 10), it can be pointed out that there is a different character of fracture surfaces in relation to the observed materials. In comparison to the Dominial ZF2, visible areas of cracks in all directions were observed for Toolox 33.

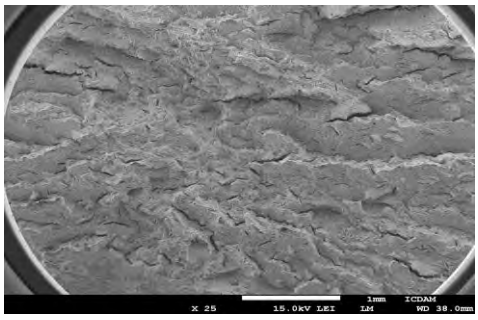

Fig. 9 Toolox 33 non-cycled
Obr. 9 Toolox 33 necyklovaný

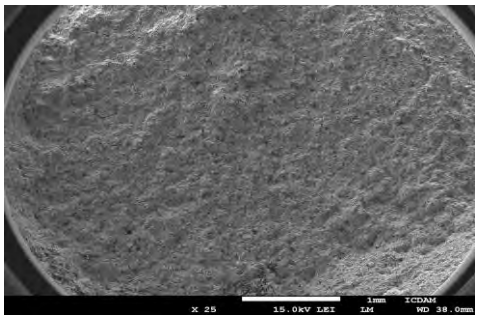

Fig. 10 Dominial ZF 2 non-cycled
Obr. 10 Dominial ZF 2 necyklovaný

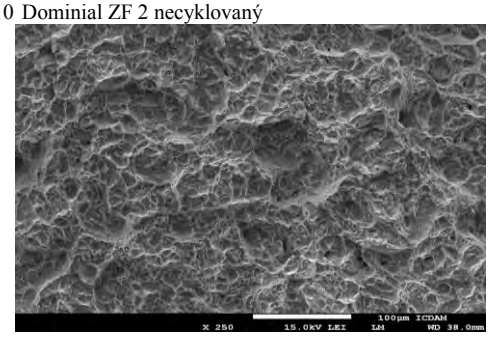

Fig. 11 Toolox 33 - 40 cycles
Obr. 11 Toolox 33 - 40 cyklov

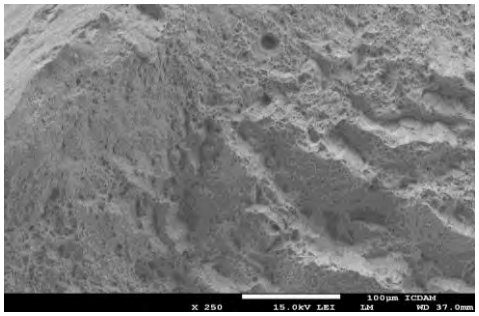

Fig. 12 Dominial ZF 2 – 40 cycles
Obr. 12 Dominial ZF 2 - 40 cyklov

On the basis of the detailed examination of the surface fracture it can be stated that there is a ductile void failure Fig. 11, Fig. 12.

After 60 cycles, the material Toolox 33 exhibited the disintegration of the grains and dendrites had the initial character (Fig. 13 and 14). It can be assumed that grains could be molten at such high temperatures. The intercrystalline failure was observed for the material Dominial ZF 2.

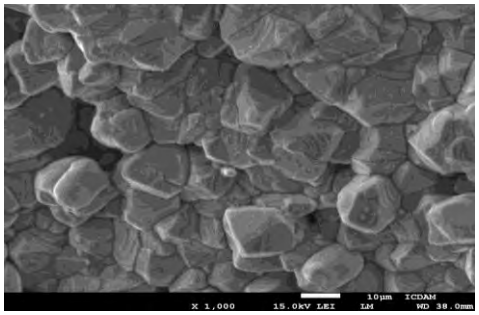

Fig. 13 Toolox 33 – 60 cycles
Obr. 13 Toolox 33 – 60 cyklov

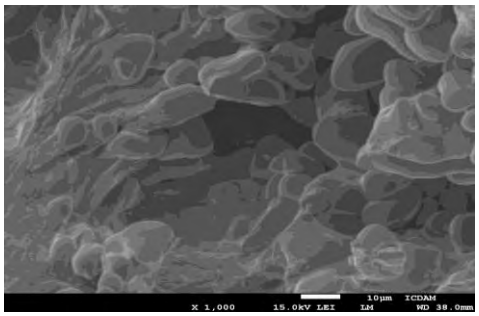

Fig. 14 Dominial ZF 2 – 70 cycles
Obr. 14 Dominial ZF 2 - 70 cyklov

After the maximum cycles (80 cycles), centralized striations were observed. These striations represented the cycles causing the layered structure around the circumference of the sample (Fig. 15).

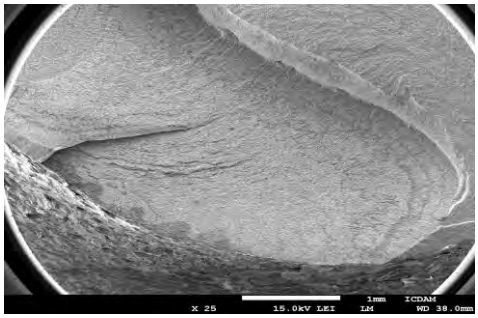

Fig. 15 Toolox 33 – 80 cycles
Obr. 15 Toolox 33 – 80 cyklov

After 80 cycles, Dominial ZF 2 (Fig. 16) exhibited two typical areas in fracture surface. The fracture surface was porous and typical with its disintegrity.

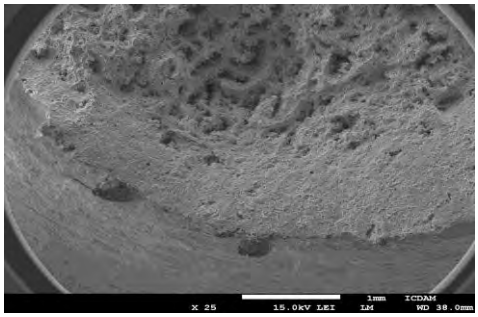

Fig. 16 Dominial ZF 2 – 80 cycles
Obr. 16 Dominial ZF 2 - 80 cyklov

Detailed views (Fig. 17 and 18) show the degradation process at high temperatures and maximum number of cycles. The selected areas for fracture surfaces have the different degree of degradation.

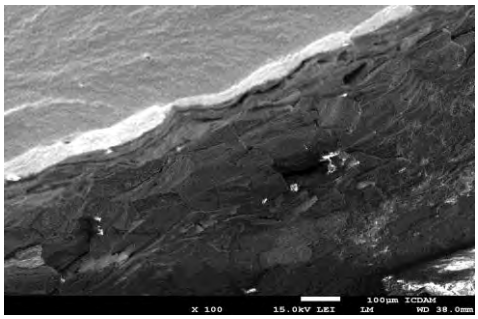

Fig. 17 Toolox 33 – 80 cycles
Obr. 17 Toolox 33 – 80 cyklov

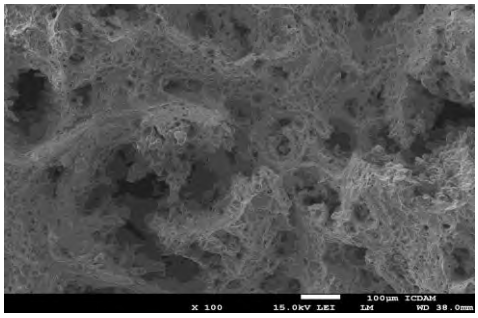

Fig. 18 Dominial ZF 2 – 80 cycles
Obr. 18 Dominial ZF 2 - 80 cyklov

Conclusions

The simulated tests of the thermal shocks were proposed because of different failure character of material during its operation. Furthermore, the degradation process is increased due to the corrosion environment. According to the evaluations of the microstructure and all obtained results, it can be concluded that the material with worse purity has higher tendency to be more susceptible in relation to the thermal loading. From the aspect of the micropurity, both types of materials seem to be the same. Toolox 33 can be considered as much more brittle in comparison to Dominial ZF 2 because it can be seen not only in fracture surfaces but also in strength characteristics. According to the obtained results, we do not recommend to use Toolox 33 for manufacturing of glass moulds and pre-moulds. In addition, we recommend the surface treatment of Dominial ZF 2 in order to prolong the lifetime of the components for processing of glass.

Acknowledgements

We would like to give our thanks the Slovak Grant Agency VEGA: 1/0385/14, KEGA: 007 TnUAD-4/2013 and Innovation Centre and diagnostics applications of materials at CTU in Prague - ICDAM (project OPPK CZ. 2 16/3 1. 00/21037).

Literature

[1] LUPTAKOVÁ, N., ANISIMOV, E., JANOTOVÁ, I., ŠVEC, P., BENÁK, M., PEŠLOVÁ. F. *Analysis of waste material in the production of zinc oxide*. In: Machine Modeling and Simulations. 17th International Slovak-Polish Conference, 2012. p. 165–172. ISBN 978-83-923315-2-0

[2] VAVRO, J., HAJSKÁ, H., VAVRO, J. Jr., VAVROVÁ, A. *Nové metódy a prístupy experimentálnej mechaniky pri identifikácii vád a porúch výrobkov*. Krakow: Spolok Slovákov v Poľsku, 2011. 264 s. ISBN 978-83-7490-461-2

[3] KOUTSKÝ, J., KAREL, V., JANDOŠ, F. *Lomy ocelových částí*. Praha: STNL, 1976. 345 s.

Hutnické listy č. 3/2014, roč. LXVII
ISSN 0018-8069

Study of the Influence of Different Transition Metal Ions on the Thermal and Spectral Properties of Materials with Biologically Important Heterocyclic Compounds

Štúdium vplyvu rôznych iónov prechodných kovov na termické a spektrálne vlastnosti materiálov s biologicky významnými heterocyklickými zlúčeninami

Ing. Zuzana Harmatová[1], prof. Ing. Eugen Jóna, DrSc.[1], Ing. Veronika Janíková[1], Ing. Róbert Janík, PhD.[1], Jozef Miklovič[2]

[1]Alexander Dubček University of Trenčín, Faculty of Industrial Technologies in Púchov, I. Krasku 491/30, 020 01 Púchov, Slovak Republic
[2]Department of Chemistry, Faculty of Material Sciences, University of St. Cyril and Methodius, 917 01 Trnava, Slovak Republic

This paper is focused on the study of the influence of different transition metal ions (Ni^{2+},Co^{2+}) on the thermal properties of materials with biologically important heterocyclic compound including $M(NCS)_2(fpy)_4$ and $M(NCS)_2(bfpy)_4$ (M = Ni, Co) where fpy is furo[3,2-C]furopyridine and bfpy is benzo[2,3-c]furopyridine (new pharmacophores with potential antipsychotic activity with the furopyridines ring system). Thermal decomposition of Ni(II)complexes consists of the three specific steps but thermal decomposition of Co(II) complexes consists of two steps. The influence of different transition metal ions on the thermal properties of studied materials is evident. The thermal stability of the studied Ni(II) complexes (the temperature of the first peak on the DTG curves) is higher than thermal stability of Co(II) complexes. Spectral measurements indicated end-bonding of NCS groups.

Keywords: *Furopyridines, Ni^{2+} and Co^{2+} ions, thiocynate anions, thermal decomposition, antipsychotic activity*

Predkladaná práca sa zaoberá štúdiom vplyvu rôznych iónov prechodných prvkov (Ni^{2+}, Co^{2+}) na termické vlastnosti materiálov s biologicky významnými heterocyklickými zlúčeninami, menovite $M(NCS)_2(fpy)_4$ a $M(NCS)_2(bfpy)_4$ (M = Ni, Co, fpy-furo[3,2-c]pyridín a bfpy - benzofuro[3,2-c]pyridín. Furopyridíny patria medzi heterocyklické zlúčeniny, ktoré sú zložkami viacerých vitamínov a liečiv (nové farmakofóry s potenciálnou antipsychotickou aktivitou obsahujú furopyridínový systém). Aj nikelnaté a kobaltnaté ióny vykazujú významné biologické vlastnosti. Nikel je stopovým prvkom v živých organizmoch. Z funkcie niklu má význam najmä aktivizovanie mnohých enzýmov, podieľajúcich sa na metabolizme sacharidov. Podporuje funkciu viacerých hormónov (napr. inzulínu). Podporuje tiež pôsobenie železa, a tak chráni organizmus pred anémiou z nedostatku železa. Vyplýva to zo skutočnosti, že pri anémii sa zistily nízke hodnoty niklu v krvi. Súvisí to s tým, že spolu s kobaltom a železom je katalyzátorom niektorých katalytických reakcií anzýmov, pričom spolupôsobí aj s vanádom. Enzýmy obsahujúce nikel katalyzujú kľúčové reakcie v energetickom a dusikovom metabolizme pri prokariotických baktériách. Izotop kobaltu ^{59}Co patrí medzi esenciálne mikroprvky. Tvorí súčasť vitamínu B_{12} a zasahuje do niektorých enzymatických reakcií. Vitamín B_{12} nahrádza dve fyziologicky dôležité funkcie: redukciu rôznych organických zlúčenín a viazanie metylovej skupiny. Kobalt sa prostredníctvom vitamínu B_{12} zúčastňuje na tvorbe krvi a urýchľuje dozrievanie erytrocytov. Pri štúdiu stechiometrie termického rozkladu skúmaných zlúčenín pomocou TG a DTG sa zistilo, že molekuly furopyridínov pri Ni(II) materiáloch sa uvoľňujú v dvoch stupňoch, zatiaľ čo pri Co(II) materiáloch len v jednom stupni. Vplyv rôznych iónov prechodných kovov na stechiometriu termického rozkladu skúmaných materiálov je zrejmý. Termická stabilita skúmaných materiálov stanovená na základe teploty prvého píku na DTG krivkách je vyššia za prítomnosti Ni^{2+} iónov, v porovnaní s Co^{2+} iónmi Spektrálne merania potvrdili koncovo viazané NCS skupiny cez atóm dusíka..

Kľúčové slová: *Furopyridíny, Ni^{2+} a Co^{2+} ióny, tiokynátové anióny, tepelný rozklad, antipsychotická aktivita*

Many authors have studied heterocyclic compounds as ligands in coordination compounds with transition metal ions understood as central atoms and they have also investigated their biological properties [1–3]. Especially six-membered ring systems are a component of several vitamins and drugs [4]. The investigation of quinoline isoesters (furopyridines), in which the benzene ring is replaced by furan ring has also resulted in discovering many biologically active compounds. New pharmacophores with potential antipsychotic activity posses the furo [3,2-c] pyridines ring system [5]. In our previous papers, we described the thermal properties of Mg(II) and Cu(II) compounds with biologically important compounds [6-10]. This work is aimed on the comparison of stoichiometry of thermal decomposition of isothiocyanato Ni(II) and Co(II)

compounds with furo[3,2-c]pyridine (fpy) and benzo-furo-[3,2-c]pyridine (bfpy) (fig. 1). 8].

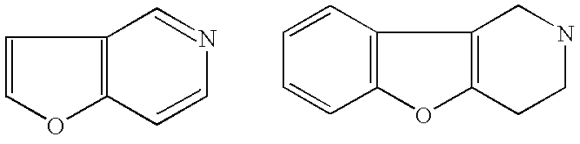

a) b)

Fig. 1 Structures of furo [3,2-c] pyridine (a) and benzo [2,3] furo [3,2-c] pyridine (b)
Obr. 1 Štruktúrne vzorce furo [3,2-c] pyridínu (a) and benzo [2,3] furo [3,2-c] pyridínu (b)

Experiment

Synthesis of Ni(II) and Co(II) complexes

Complexes $Ni(NCS)_2(fpy)_4$(I), $Ni(NCS)_2(bfpy)_4$ (II) $Co(NCS)_2(fpy)_4$ (III) and $Co(NCS)_2(bfpy)_4$(IV) and were prepared by treating (0,002 mol) fpy or bfpy with $Co(NCS)_2.6\ H_2O$ (0,001 mol) in methanol (50 ml). The solutions were kept at room temperature. The fine precipitated monocrystals were filtered off, washed with cold methanol and dried at room temperature.

Measurements

The contents of C, H, and N were determined by elemental analysis. Thermal properties were studied with a Derivatograph OD 102 (MOM Budapest) in air atmosphere with a sample mass of 150 mg, measurement temperature was from room temperature up to ~ 800°C and heating rate was 10°C.min^{-1}. These mentioned conditions were used for all measurements.

The infrared (IR) spectra were obtained on a Philips analytical PV 9800 FTIR spectrometer using KBr tablets in the range 700-1200 cm^{-1}.

Results and discussion

Presented in tab. 1, the analytical data of the studied complexes show a good agreement between the experimental and calculated data.

The data for the thermal properties of the complexes I-IV are shown in tab. 2.

Tab. 1 Analytical data of studied complexes I-IV
Tab. 1 Analytické údaje skúmaných zlúčenín I-IV

Complex	Theoretical [%]			Experimental [%]		
	C	H	N	C	H	N
$Ni(NCS)_2(fpy)_4$(I)	55.32	3.10	12.90	54.91	3.02	12.85
$Ni(NCS)_2(bfpy)_4$(II)	64.88	3.31	9.87	63.55	3.30	9.79
$Co(NCS)_2(fpy)_4$(III)	55.30	3.09	12.90	55.15	2.69	13.00
$Co(NCS)_2(bfpy)_4$(IV)	64.86	3.31	9.87	63.79	3.27	9.60

Tab. 2 Thermal decomposition data of the compounds I-IV
Tab. 2 Údaje o termickom rozklade zlúčenín I-IV

Complex	DTG		TG	
	Tmax [°C]	Temp. Interval [°C]	Δm(found/calc.) [%]	Lost component
I	180	130 - 190	36.1 / 36.6	2 fpy
	230	190 - 340	36.2 / 36.6	2 fpy
	380	340 - 450	12.5 / 12.9	SCN,CN
II	243	127 - 284	50.5 / 49.7	2,5 bfpy
	307	284 - 350	29.7 / 29.8	1,5 bfpy
	383	350 - 450	9.8 / 9.9	SCN,CN
III	178	120 - 445	73.50 / 73.12	4 fpy
	588	445 - 675	13.00 / 12.90	SCN,CN
IV	188	130 - 447	80.00 / 79.44	4 bfpy
	538	447 - 610	10.50 / 9.87	SCN,CN

Hutnické listy č. 3/2014, roč. LXVII
ISSN 0018-8069

The thermal decomposition of the complexes $Ni(NCS)_2(fpy)_4$(I) and $Ni(NCS)_2(bfpy)_4$(II) is a multi-stage process. TG and DTG curves indicate that mass loss occurs at ~130 °C (complex I) or ~127 °C (complex II) and these three mass loss steps were observed. The first step between 130-190 °C (I), or 127-284 °C (II) is accompanied by 36.1 %(I) or 50.5 %(II) mass loss and it corresponds to the release of 2 fpy (I) or 1.5 bfpy(II). The second step took place between 190-340 °C (II) or 284-350 °C (II) and it is accompanied by ~36.2 %(I) or 29.7 %(II). It is attributed to the release of the remaining 2 fpy (I) or 1.5 bfpy (II). The third step took place between 340-450 °C (I) or 350-450 °C and is accompanied by 12.5 % mass loss (I) or 9.8 % mass loss (II). It is attributed to the decomposition of the $Ni(NCS)_2$ to NiS. The thermal decomposition scheme is as follows (L = fpy or bfpy):

$$Ni(NCS)_2L_4 \rightarrow Ni(NCS)_2L_x \ (x = 2 \text{ (I) or } 1{,}5 \text{ (II)}) \quad (1)$$

$$Ni(NCS)_2L_x \rightarrow Ni(NCS)_2 \quad (2)$$

$$Ni(NCS)_2 \rightarrow NiS \quad (3)$$

The TG and DTG curves for the complex $Co(NCS)_2(fpy)_4$ (III) indicate that it is stable up to ~120 °C and complex $Co(NCS)_2(bfpy)_4$ (IV) is stable up to ~130 °C. The release of furopyridine and benzofuropyridine molecules takes place during the one step. The mass losses corresponding to the decomposition steps are ~73.5 % (complex III) or 80 % (complex IV) and they are in good agreement with the theoretical values (tab. 2). It corresponds to the presence of one intermediate decomposition product $Co(NCS)_2$. The thermal decomposition scheme is as follows (L = fpy or bfpy):

$$Co(NCS)_2L_4 \rightarrow Co(NCS)_2 \quad (4)$$

$$Co(NCS)_2 \rightarrow CoS \quad (5)$$

The modes of the NCS groups in the studied complexes have been investigated by means of IR spectra. The IR frequencies attributed to the ν_{CN} and ν_{CS} at the complexes I-IV are reported in tab. 3. In accordance with literature data [11], tab. 3 shows that for studied complexes, the NCS groups are end-bonded through the nitrogen atom (M-NCS).

Tab. 3 Some IR spectral data for complexes I-IV
Tab. 3 Niektoré údaje infračervených spektier komplexov I-IV

Assignment	Complex [cm^{-1}]			
	I	II	III	IV
ν_{CN}NCS	2072	2074	2065	2059
ν_{CS}NCS	801	802	783	775

Conclusions

All of the complexes are stable in air and soluble in water, ethanol, methanol and dimethylsulfoxide. The loss of the neutral heterocyclic ligands occur (obtained from DTG curves) in two steps (complexes I and II) or one step (complexes III and IV). The influence of different transition metal ions (Ni^{2+} or Co^{2+}) on the stoichiometry of thermal decomposition of studied materials is evident. The thermal stability of the Ni(II) compounds (on the basis of the temperature of the first peak on the DTG curves) is higher than thermal stability of Co(II) compounds.

Spectral (IR) data are in agreement with M-N(NCS) bound in studied complexes.

Acknowledgement
We would like to give our thanks the Slovak Grant Agency KEGA: 006 TnUAD-4/2014.

Literature

[1] MOJUMDAR, S.C., MELNÍK, M., JÓNA, E. *Thermo-analytical investigation of Mg(II) compound SCN and heterocyclic N-donor ligans.* J. Anal. Appl. Pyrolysis, 1999, vol. 48, p. 111-120

[2] MOJUMDAR, S.C., MELNÍK, M., JÓNA, E. *Thermal and IR properties of Mg(II) complexes with heterocyclic ligands.* Thermochim. Acta, 2000, vol. 352, p. 127-132

[3] JÓNA, E., LAJDOVÁ, Ľ., LODUHOVÁ, M., LENDVAYOVÁ, S., PAVLÍK, V., MONCOĽ, J., LIZÁK, P., MOJUMDAR, S.C. *Thermal properties of solid complexes with biologically important heterocyclic ligands. Part IV. Thermal and spectral properties of 2-chloro- and 2-bromobenzoato Cu(II) complexes with nicotinamide and different bonded water molecules.* J. Therm. Anal. Calorim. 2012, vol. 108, p. 2365-2368

[4] JÓNA, E., SIROTA, A., ŠIMON, P., KUBRANOVÁ, M. *Thermochemical investigation of Nickel (II)-nicotinamide – solvent interactions in solid halogenocomplexes.* Thermochim. Acta, 1995, vol. 258, p. 161-173

[5] NEW, J.S., CHRISTOPHER, W.L., YEVICH, J.P., BUTLER, R., FRANCIS SCHLEMER JR, R., VAHDERMAELEN, C.P. *The thienol [3,2-c] pyridine and furo [3,2-c] pyridine rings: New pharmacophores with potential antipsychotic activity.* J. Tred. Chem, 1989, vol. 32, p. 1147-1156

[6] HARMATOVÁ, Z., JÓNA, E., MEDVECKÁ, J. *Biologically important materials with Cu^{2+} ions and heterocyclic compound and their thermal properties.* Hut. Listy, 2013, roč. LXVI, ISSN 0018-8069, p. 28-30

[7] MOJUMDAR, S.C., MELNÍK, M., JÓNA, E. *Thermal and IR properties of Mg(II) and Cu(II) complexes with heterocyclic N-donorligands.* J. Anal. Appl. Pyrolysis, 2000, vol. 53, p. 149-160

[8] JÓNA, E. LAJDOVÁ, Ľ. KVASNICOVÁ, L. LENDVAYOVÁ, S. PAJTÁŠOVÁ, M. ONDRUŠOVÁ, D. LIZÁK, P. MOJUMDAR, S.C. *Thermal properties of solid complexes with biologically important ligands III. Thermal decomposition and infrared spectra of thiocyanato Mg(II) complexes with 2-hydroxypyridine, quinoline and quinoxaline*. J. Therm. Anal. Calorim., 2011, vol 10, p. 817-821

[9] MOJUMDAR, S.C., JÓNA, E., MELNÍK, M. *The thermal decomposition of magnesium (II) complexes with acetic and halogenoacetic acids.* J. Therm. Anal. Calorim., 2000, vol. 60, p. 571-676

[10] MOJUMDAR, S.C. MELNÍK, M. JÓNA, E. *Thermal decomposition of Mg(II) complexes with ronicol*. J. Therm. Anal. Calorim., 1995, vol. 56, p. 541-546

[11] NAKAMOTO, K. *Infrared spectra of inorganic and coordination compounds.* 2nd Edition. Wiley Interscience, 1970, p. 80

Numerical Analysis of Stress States for Cast Iron with the Spheroidal Shape of Graphite

Numerická analýza napäťových stavov liatiny s guľôčkovým tvarom grafitu

Ing. Ján Vavro, PhD., jr.[1], prof. Ing, Ján Vavro, PhD.[1], Ing. Petra Kováčiková[1], Ing. Peter Kopas, PhD.[2], Ing. Marián Handrik, PhD.[2], Ing. Radka Bezdedová[1]

[1]Alexander Dubček University of Trenčín, Faculty of Industrial Technologies in Púchov, I. Krasku 491/30, 020 01 Púchov, Slovak Republic
[2]University of Žilina, Faculty of Mechanical Engineering, Univerzitná 1, 010 26 Žilina, Slovak Republic

The given work is focused on numerical analysis of the stress states for cast iron with the spheroidal shape of graphite. The analysis was made with help of finite element method in the software system ADINA.v.8.6.2. On the basis of the real structure, the finite element method was used for creation of the model which was subsequently used for calculation of the stresses distribution of the structure of material. The he input data for numerical analysis were obtained on the basis of evaluation of the structure by help of image analysis. The utilisation of the numerical analysis is closely connected with the new possibilities and new opportunities of material engineer who can perform modelling of material structures and he can also make simulations for various types of loading. Moreover, the utilisation of the numerical analysis enables engineer to observe particles which have atypical microstructure shape. The given analysis proved that the graphetic particles in the matrix cause the concentration of the stress and the extension of the given stress depends on the shape of the graphetic particles.

Keywords: *numerical analysis, stress distribution, cast iron, spheroidal shape of graphite*

Rozvoj numerickej analýzy je úzko spätý s možnosťami a novými prístupy v rámci výpočtového modelovania a ich následnej simulácie pre rôzne druhy zaťaženia štruktúry materiálu. Práca sa zaoberá numerickou analýzou napäťových stavov liatiny s guľôčkovým tvarom grafitu. Analýza bola vykonaná metódou konečných prvkov v softvérovom prostredí ADINA.v. 8.6.2. V článku je stručne popísaná štruktúra tvárnej liatiny s guľôčkovým tvarom grafitu. Vstupné hodnoty pre numerickú analýzu metódou konečných prvkov sa získali z hodnotenia štruktúry obrazovou analýzou. Využitie numerickej analýzy konečných prvkov umožňuje pozorovanie častíc s atypickými mikroštruktúrnymi rozmermi, ale táto analýza sa využíva aj v rôznych oblastiach vedy a výskumu. Výpočtové modely štruktúry boli vytvorené v 2-D oblasti pomocou trojuholníkových trojuzlových elementov pre dva typy štruktúry liatiny s guľôčkovým tvarom grafitu (Obr. 1, 2). Veľkosť elementov bola stanovená na základe citlivostnej analýzy (Tab. 1). S využitím tejto analýzy bola stanovená veľkosť elementov 0,5 μm. Analyzovaná oblasť bola vo veľkosti 0,5×0,5 mm. Numerická analýza sa uskutočnila pre 750 výpočtových modelov. Na základe reálnej štruktúry materiálu bol vytvorený konečno-prvkový model, z ktorého sa vypočítalo rozloženie napätia v grafitickej štruktúre liatiny. Štruktúra grafitickej liatiny závisí od vplyvu mnohých faktorov zahŕňajúc chemické zloženie a austenitickú transformáciu. Rozmery grafitických častíc závisia od rýchlosti kryštalizácie a počtu eutektických fáz v tavenine. Z numerickej analýzy vyplýva, že grafitické častice svojou existenciou v matrici spôsobujú koncentráciu napätia a veľkosť koncentrácie napätia bude závisieť od tvaru grafitických častíc. Koncentrácia napätia sa zväčšuje nepravidelnosťou grafitickej častice. Najpriaznivejšie rozdelenie je pri ovalite tvaru gule. Ukazuje sa tu nová oblasť využitia výpočtových prostriedkov pre analýzu stavu štruktúry materiálu v oblasti napäťových, frekvenčných a tlmiacich vlastností materiálu.

Kľúčové slová: *numerická analýza, distribúcia napätia, liatina, guľôčkový tvar grafitu*

The progress of the numeric processes is closely connected with the new possibilities and new opportunities of material engineering including modelling of structures of materials and their simulations for various types of loading. The process of deformation is connected with the foreseeability and understanding of microstructure properties because it is really important for knowledge and specification of defect formations of castings during the process of their production or during the moulding processes [1, 2]. In the recent years, the microstructure modelling and its simulation has played an important role because of finding out of properties and suitability of usage of the given material before its production.

The finite element method allows us to operate with atypical parameters of microstructure. Nowadays, this method is commonly used in the various scientific fields and spheres. In addition, the most common usage can be found in mechanics, materials engineering, thermo-dynamics and biomechanics etc. [3, 4]. All types of simulations reduce the given specific construction

Hutnické listy č. 3/2014, roč. LXVII
ISSN 0018-8069

process and there is also opportunity to test or investigate the model at various working conditions and loadings.

Structure of cast iron with the spheroidal shape of graphite (SGCI)

The structure of the basic metallic microstructure of SGCI influences many factors. Two of these many factors are very important because they are connected with the differences of characteristics of austenite transformation which is carried out at unchanged conditions. Influence of chemical composition and influence of cooling speed are the given and important two factors which are mentioned hereinbefore. According to this mentioned fact, there can be the occurrence of ferritic, ferritic-pearlitic or pearlitic structure for cast irons (Fig. 1 and Fig.2).

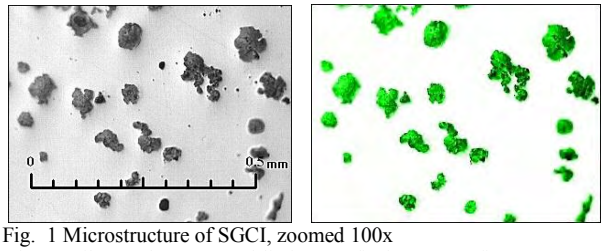

Fig. 1 Microstructure of SGCI, zoomed 100x
Obr. 1 Mikroštruktúra tvárnej liatiny s guľôčkovým grafitom, 100 násobné priblíženie

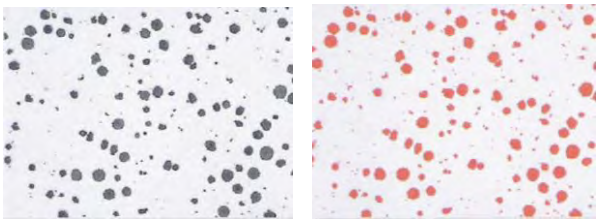

Fig. 2 Microstructure of SGCI, zoomed 100x
Obr. 2 Mikroštruktúra tvárnej liatiny s guľôčkovým grafitom, 100 násobné priblíženie

Moreover, structure as well as properties of SGCI can be influenced by alloying process and thermal treatment in some particular limiting cases. SGCI belongs to iron carbon alloys and there are also other elements. Its structure consists of basic metallic substance – matrix and the graphite can be found in this matrix. This graphite has a specific shape. It is sort of the regular granular grains. From the aspect of the shapes, this shape of graphite has the least notch or impact effect. Due to this fact, SGCI has very good mechanical properties and therefore SGCI can be included among the most common materials which are suitable for manufacturing of castings [5, 6].

Evaluation of the microstructure by image analysis

Image analysis of the microstructure (SGCI Fig. 1 and 2) is carried out for the purpose of obtaining of basic data which are needed for formation of the model that is identical with real state of cast iron. The image analysis was used for evaluation of number of graphetic particles, content of graphite and shape of graphite (via shape factor) and the content of ferrite in basic material was evaluated for etched samples. Shape factor K represents the circularity and if the value equals to number one, it means that it is circle but if the value equals to number zero, it means that it is straight line. According to the mentioned facts, the circularity can be calculated by help of equation:

$$K = \frac{4\,\pi\,A}{P^2} \tag{1}$$

where A is an area of the particle and P is a circumference of particles. The shape factor can acquire values [7]:

- for lamellar graphite: K < 0.27;
- for vermicular graphite: K = 0.27 ÷ 0.60;
- for spheroidal graphite: K > 0.65.

Selection of type of finite elements and size of element

Tab. 1 Sensitivity analysis toward the size of elements
Tab. 1 Analýza citlivosti voči veľkosti zŕn

Size of elements	σ_{yy}	σ_{zz}	σ_{yz}	σ_{HMH}
0.01	1.215	0.0516	0.012	1.042
0.009	1.209	0.0461	0.0033	1.038
0.008	1.208	0.0464	0.0055	1.036
0.007	1.225	0.0371	0.0185	1.059
0.006	1.489	0.146	0.048	1.211
0.005	1.501	0.16	0.028	1.206
0.004	1.780	0.246	0.0011	1.388
0.003	1.947	0.271	0.0060	1.510
0.002	2.385	0.384	0.013	1.819
0.001	2.800	0.310	0.0069	2.247
0.0009	2.780	0.285	0.164	2.270
0.0008	2.904	0.266	0.048	2.369
0.0007	2.861	0.237	0.0821	2.358
0.0006	2.925	0.215	0.0864	2.436
0.0005	2.931	0.180	0.0089	2.467
0.0004	2.918	0.146	0.013	2.479
0.0003	2.916	0.107	0.007	2.507

Where σ_{yy} – stress in the direction of loading, [MPa]; σ_{zz} – stress which is perpendicular to direction of loading, [MPa]; σ_{yz} – shear stress, [MPa]; σ_{HMH} – equivalent stress with reference to HMH theory, [MPa]

The designed model of SGCI material structure was connected with performance of sensitivity analysis (Tab. 1) relating to change of intensity of stress distribution around the graphetic particles. The graphetic particles are designed as cavities without finite element mesh. On the base of the sensitivity analysis, the determined size of elements was 0.5 µm. This mentioned size of elements ensures good uniformity and accuracy of resolution and the error is not higher than 2.5 %. Linear triangular elements (Fig. 3) are used for solution. Geometric model was made up for 10 % graphetic proportion in structure, the number of particles was 200 pieces per squared

millimeter and size was chosen in the interval from 30 μm to 60 μm.

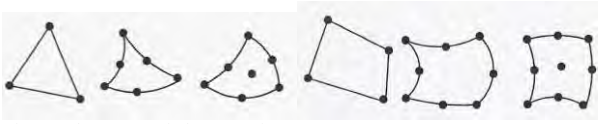

Fig. 3 The types of elements for 2-D areas
Obr. 3 Typy elementov pre 2-D oblasti

Geometric model of SGCI

The shape of the graphetic particle has a significant influence on size of eigenfrequences as well as there is the influence on state of surrounding stress. If we want to evaluate the quality of graphetic particle, we have to determine some geometric characterizations which describe the mentioned particle. The given determination is also closely connected with the method of measurement of these characterizations [8]. The precise description of boundary relating to graphetic particles can be obtained only during the process of evaluation of results of FEM analysis. This partial restriction is caused by impossibility to obtain any other description of boundary. It can be done only by help of mesh of finite elements.

The first phase of preparation of models is concerned with determination of basic model properties. Matrix could be considered to be a homogenous structure with the linear dependency deformation – stress. Graphetic particle could be the cavity which could be designed in a specific way and it means that the mesh of the finite elements would not be created in the area of this cavity. This type relating to modelling of graphetic particles is possible because of their properties: low tension and frequent decohesion from matrix. Calculation as well as statistic evaluation of results could be done only after generation of large number of geometric models and in this case, the generation should be done for approximately 750 models. During the solving of given task, we decided to create the automatic model generator which operates on the base of generating of random numbers [8].

From the point of view of materials engineering, the preparation of geometric model is closely connected with the utilization of characteristic data of SGCI (for purpose of definition of input data). The mentioned characteristic data were obtained on the base of visual image analysis of the experimental material:

- number of graphetic grains for 1 mm^2: 100 ÷ 300 units,
- average diameter of graphetic grain: 0.01 ÷ 0.08 mm,
- area proportion of graphite in the structure: 4 ÷ 12 %.

The portion of graphetic skeleton depends on crystallization rate (growth is subjected to diffusion of carbon) and amount (proportion and number) of eutectic units especially depends on number of nuclei in molten mass (treating agents). These two mentioned factors have significant influence therefore they are the determinative factors for area proportion of graphite in the structure. On the base of the given mentioned fact hereinbefore, we generated the mesh from points which were connected together and these points can be also understood as representatives of potential centres of graphetic particles. The auxiliary parameter was used for their generation. This auxiliary factor specifies minimal distance between particular graphetic particles. For determination of the given diameter of graphetic particle, we have to generate the auxiliary mesh of points with the sufficient density, for example 100×100 points and then we can specify the number of points which belong to individual centres of graphetic particles. The mentioned process is the principle for determination of area proportion for graphite and it is in relation to the individual graphetic particles with the respect to number and size. According to this fact, it is possible to determine the diameter of the individual graphetic particles. This type of change relating to generation of models is connected with the elimination of many problems including size, distribution and number of graphetic particles. On the other side, the diameter of particle can be understood as function of mutual position of graphetic particles and it means that there is not any possibility of occurrence of such particles which would be disproportional from the aspect of "largeness" or size and it also means that there is the elimination of occurrence of too "small" particles of spheroidal graphite. According to these properties, the algorithm was supplemented by control of scattering relating to size of graphetic particles. In case that the given scattering runs over the determined values, the selection relating to centres of graphetic particles is not suitable for any other analysis and therefore these unsuitable particles are not utilized for any other analysis. The algorithm which was made in this way fulfils all qualitative as well as quantitative parameters. This given algorithm is also supplemented by ability of shape variation for graphetic particles.

Software solution of algorithm is connected with software Octave (share-ware version of Matlab) which is able to generate input file for software GID where spline curves are used for solutions in the area relating to individual graphetic particles. End points of spline are identical but they are not continuous. The post editing of spline curves can help us to obtain continuous areas which represent graphetic particles. Subtraction of the area for graphetic particles from the whole area of investigated model is used for obtaining of resultant geometric model without graphetic particles whereby the boundaries of the model are continuous. This obtained geometric model is saved in IGES format. FEM in software ADINA is used for consecutive analysis because this software allows downloading of geometric data in IGES format. The results of generated "graphetic particles" in software Octave can be found in the Fig. 4. Arbitrary structure of material can be represented by graphetic particles which are randomly generated for creation of the model of various size and shape.

Hutnické listy č. 3/2014, roč. LXVII
ISSN 0018-8069

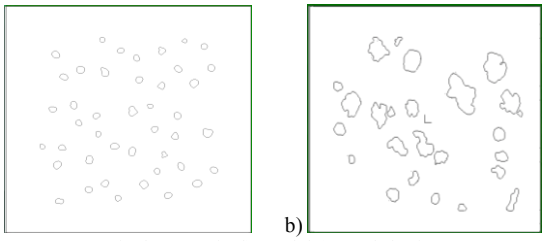

Fig. 4 Geometrical (numerical) model (a) and (b) for SGCI
Obr. 4 Geometrický (výpočtový) model (a) a (b) tvárnej liatiny s guľôčkovým grafitom

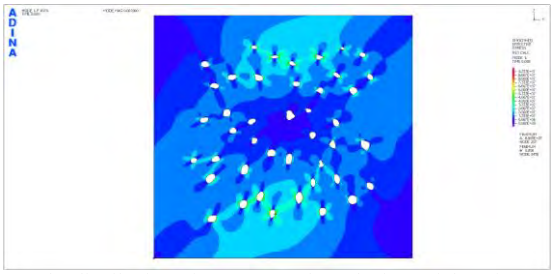

Fig. 5 The distribution of stress around graphetic particles of SGCI for model in Fig. 4a
Obr. 5 Rozloženie napätia okolo grafitických častíc tvárnej liatiny s guľôčkovým grafitom pre model na obr. 4a

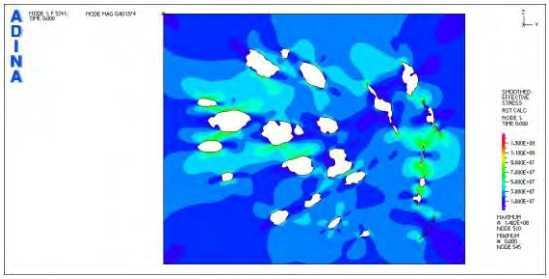

Fig. 6 The distribution of stress around graphetic particles of SGCI for model in Fig. 4b
Obr. 6 Rozloženie napätia v okolo grafitických častíc tvárnej liatiny s guľôčkovým grafitom pre model na obr. 4b

As it has been said, graphetic particle can be understood as a cavity in the structure of material with its various size and shape. The whole problem is based on the solution of the two-dimensional system. The limiting conditions can be represented by taking of degrees of freedom from the whole circumference relating to model. The linear material model with the respect to Young's modulus, also known as tensile modulus $E = 2.1 \cdot 10^5$ [MPa], Poisson's ratio $\nu = 0.3$ and mass density $\rho = 7850$ [kg/m^3] is used. The area of the resolving is determined for one or more graphetic particles with the size of 0.5×0.5 mm, while graphetic particles are generated in the area of 0.45×0.45 mm. This chosen ratio for area of resolution, where graphetic particles are generated, means elimination of influence including eigenfrequences which can be connected with the closeness of boundary for area of resolution.

The Fig. 5 and 6 represent only distribution of stress around the graphetic particles for model (Fig. 4a and 4b).

Conclusions

Existence of graphetic particles in matrix causes concentration of stress and the intensity of the given stress depends on the shape of graphetic particles. The concentration of stress is increased by irregularity of graphetic particle. The most perfect distribution is found out for spheroidal shape relating to sphere. The mentioned process relating to investigation can be used for any other types of cast iron structures. The results which are obtained on the basis of analyses represent the first information about loading and properties of the whole system or structure of material and the given results can be used as input data during the further investigation of the mentioned material.

Acknowledgement

The work presented in this paper was supported by VEGA grant No. 1/0385/14 and KEGA grant No. 007 TnUAD-4/2013.

Literature

[1] SHEN, G., ROLLINS, J., FURRER, D. Microstructure Modeling of Forged Waspaloy Discs. Superalloys 1996, KISSINGER, R.D. et al. (Ed.). TMS, 1996, p. 613–620

[2] DOBRZAŃSKI, L.A., ŚLIWA, A., TAŃSKI, T. Finite Element Method application for modelling of mechanical properties. In Computational Materials Science and Surface Engineering.2009, vol. 1, p. 25–28 [cit.2010-9-3]

[3] DUARTE, C.A., BABUŠKA, I., ODEN, J.T. Generalized finite element methods for three-dimensional structural mechanics problems. In Computers & Structures [online]. 2000, vol. 77, p. 215–232 [cit. 2010-9-3]

[4] CHAWLA, N., GANESH, V.V., WUNSCH, B. Three-dimensional (3D) microstructure visualization and finite element modeling of the mechanical behavior of SiC particle reinforced aluminum composites. In Scripta Materialia 2004, vol. 51, p. 161–165 [cit. 2010-9-3]

[5] DEKAZINCZY, F. Effect of Small Defects on the Fatigue Properties of Medium-Strength Cast Steel, Iron Steel Inst., 208,1970, p.851-855

[6] MURAKAMI, Y. Metal Fatigue : Effcts of Small Defects and Nonmetalic Inclusions, First edition, Elsevier Science, 2002

[7] NELDER, J.A., MEAD, R. A Simplex Method for Function Minimization, Computer Journal, 7, 1965, p.308-313

[8] HANDRIK, M. Algoritmizácia modelovania stavu napätosti v mikroštruktúra LGG liatin, DP, ŽU v Žiline, 2008

Recenzované výzkumné články

The Abrasive Wear of Materials for Functional Parts of Water Turbines

Abrazivní opotřebení materiálů funkčních součástí vodních turbín

Ing. Jan Holec[1], doc. Ing. Jiří Cejp, CSc.[1], Ing. Stanislav Krum[1], prof. Ing. Františka Pešlová, PhD.[2]

[1]Czech Technical University in Prague, Faculty of Mechanical Engineering, Department of Materials Engineering, Karlovo náměstí 13, 121 35 Prague, Czech Republic
[2]Alexander Dubcek University of Trencin, Faculty of Industrial Technologies in Puchov, Department of Materials Engineering, I. Krasku 491/30, 020 01 Puchov, Slovak Republic

The paper deals with the influence of abrasion which significantly contributes to the damage of material for the functional water machines parts besides the corrosion and cavitation. The striking edges of impeller and diffusion ring wheel blades belong to the areas which are the most stressed by the abrasive wear. That is the reason for a research of new materials that would allow prolonging the lifetime of blades and safety of the entire turbine besides traditional corrosion resistant steel 1.4313. At present, ductile cast iron is one of the materials suitable for the manufacture of blades for some types of hydraulic turbines. According to the mentioned aspect, these materials along with heat treated ductile cast iron ADI (Austempered Ductile Iron) were compared. Microstructural analysis was performed. Material properties (yield strength R_e / $R_{p0,2}$, tensile strength R_m , elongation A, hardness HBW and impact energy KV / KU) were measured. The abrasive wear was also simulated by help of specially constructed testing equipment.

Keywords: *water turbine, blade, abrasive wear, corrosion-resistant steel, ductile cast iron*

Příspěvek je věnován vlivu abraze, která se vedle koroze a kavitace významně podílí na porušování materiálu funkčních částí vodních strojů, a snižuje tak provozní spolehlivost především Kaplanovy, Peltonovy a Francisovy turbíny. Mezi nejvíce namáhaná místa abrazivním opotřebením patří náběžné hrany lopatek rozváděcích a oběžných kol. Dopadající tvrdé částice unášené proudem vody (písek a pod.), způsobují postupné obrušování a omílání lopatky, čímž se mění její geometrie a tím i celková účinnost a výkonnost vodní turbíny. Z tohoto důvodu je snaha najít nové materiály, které by vedle tradiční korozivzdorné oceli 1.4313, umožnily prodloužit životnost lopatek i bezpečnost celé turbíny. Mezi materiály, vhodné na výrobu lopatek pro některé typy vodních turbín, patří v současnosti i litina s kuličkovým grafitem. Proto tyto materiály, doplněné o litinu s kuličkovým grafitem, tepelně zpracovanou postupem ADI (Austempered Ductile Iron), byly podrobeny vzájemnému hodnocení. Byla provedena mikrostrukturní analýza, byly změřeny materiálové charakteristiky (mez kluzu R_e, mez pevnosti v tahu R_m, tažnost A, tvrdost HBW a rázová práce KV / KU) a na speciálně sestrojeném zkušebním zařízení bylo simulováno abrazivní opotřebení. Z metalografického hodnocení oceli 1.4313, která byla v odlitém a následně popuštěném stavu byla patrná martenzitická struktura. Litina s kuličkovým grafitem měla perliticko-feritickou mikrostrukturu (lamelární perlit, feritické dvorce kolem grafitu, podíl feritu 10 %), přičemž grafit byl rovnoměrně rozložený, dokonale i nedokonale zrnitý o velikosti 0,03 až 0,06 mm. Tato litina byla dále izotermicky zušlechtěna na stav ADI. Toto tepelné zpracování změnilo původní perliticko-feritickou matrici na stejnorodou strukturu dolního bainitu, přičemž morfologie grafitu zůstala zachována. Simulace abrazivního opotřebení probíhala na tvarově a rozměrově stejných vzorcích za konstantních podmínek (úhel natočení vzorků, rychlost otáčení, koncentrace abraziva - křemičitý písek a voda, doba vystavení vzorků abrazivnímu působní, časový interval výměny abraziva). Test abraze byl vyhodnocován zjišťováním hmotnostního úbytku po 5-ti hodinových intervalech vystavení vzorků abrazivnímu působení, maximálně však do doby 15-ti hodin. Z důvodu rozdílné hustoty zkoumaných materiálů byl hmotnostní úbytek vyjádřen jako procentuální úbytek váhy vzorku od původní váhy před testem abraze. Z výsledků je patrno, že nejmenšího úbytku po 15-ti hodinách simulované abraze je dosaženo u litiny s kuličkovým grafitem (12,34 %), poté u korozivzdorné oceli 1.4313 (13,43 %) a největší úbytek u izotermicky zušlechtěné litiny ADI (14,84 %).

Z provedených zkoušek vyplývá, že vhodnou alternativou ke klasické martenzitické oceli 1.4313 může být pro vybrané typy vodních turbín litina s kuličkovým grafitem. V případě tepelného zpracování litiny s kuličkovým

Hutnické listy č. 3/2014, roč. LXVII
ISSN 0018-8069

grafitem (ADI) bylo předpokládáno výrazné zlepšení mechanických vlastností a tím i odolnosti proti abrazivnímu opotřebení, které nebylo potvrzeno [1,2,4].

Klíčová slova: *vodní turbína, lopatka, abrazivní opotřebení, korozivzdorná ocel, litina s kuličkovým grafitem*

In addition to corrosion and cavitation, it is abrasive wear that contributes most significantly to the degradation of water turbines. The given degradation is especially connected with the impeller and diffusion ring blades. Magnitude of the abrasive effect is based on the abrasive properties (hardness, geometry of the particles impinging on the blade surface, distribution of the particles), medium characteristics (speed, incidence angle of the particles) as well as the blade material. At present, the martensitic corrosion resistant steel 1.4313 and ductile cast iron are the most used materials for the manufacture of the water turbines parts. These materials were compared and their mechanical properties and abrasion resistance were investigated. Their microstructure was also documented. In the case of the ductile cast iron with original pearlitic - ferritic matrix, there was an assumption that by the appropriate heat treatment in order to achieve ADI state (Austempered Ductile Iron) a homogeneous matrix structure consisting of lower bainite will be achieved and mechanical properties and wear resistance will be improved. Therefore, the cast iron in a state of ADI was evaluated and compared to the stainless steel 1.4313 as well as the ductile cast iron in original state [1-3].

Experimental details

Materials

The commonly used martensitic corrosion resistant steel 1.4313 and ductile cast iron in original state and in state of ADI were the materials which were subjected to the study. Their chemical composition in weight percentage is shown in Tab. 1 and 2.

Tab. 1 Chemical composition of steel 1.4313
Tab. 1 Chemické složení oceli 1.4313

	C	Si	Mn	Ni	Mo
Steel 1.4313	< 0.05	0.7	0.47	3.63	0.65
	Cr	**S**	**P**	**N**	**Fe**
	12.2	0.02	0.01	0.02	rest

Tab. 2 Chemical composition of ductile cast iron
Tab. 2 Chemické složení litiny s kuličkovým grafitem

	C	Si	Mn	Ni	Mg
Steel 1.4313	3.6	2.5	0.1	1.0	03
	Cu	**S**	**P**	**N**	**Fe**
	0.7	0.01	0.05	0.01	rest

Mechanical properties

Strength and plastic characteristics of the studied materials was measured by the tensile test at ambient temperature according to DIN EN ISO 6892-1. Toughness was determined by Charpy impact test at room temperature according to DIN EN ISO 148-1 for samples with U or V notch and hardness was based on Brinell test and it was measured in accordance to CSN EN ISO 6507.

Abrasive wear testing

Abrasive wear was simulated by help of the specially constructed equipment into which the prepared samples of studied materials with well-defined dimensions were inserted. The samples were fixed to the rotor part of the testing machine under constant angle and immersed into the abrasive medium (silica sand and water). The rotation speed of the samples in the abrasive medium was constant during the test. Based on the conditions hereinbefore, it was possible to compare the different materials from the aspect of weight losses after the same time intervals. Weight loss was recorded three times after every 5 hours (the maximum duration was 15 hours). Between the measurement cycles, the used abrasive was replaced by the new one while its concentration was maintained to be constant. Development of wear of all samples was photo-documented with a stereomicroscope as well.

Results and discussion

Steel 1.4313 showed martensitic structure in tempered state as shown in Fig. 1. Ductile cast microstructure consisted of pearlite - ferritic matrix. Ferrite content was 10 % and it was around graphite particles. Pearlite was in lamellar form. By graphite assessment according to DIN EN ISO 945-1, the graphite was uniformly distributed and the size of the graphite particles was in the range from 0.03 to 0.06 mm (Fig. 2). The presented chemical composition of the ductile cast iron (Tab. 2) shows that copper and nickel are present. They inhibit the graphite globularization and it is the reason for the imperfect form of graphite. However, these two elements increase the hardenability which was involved in isothermal transformation of the cast iron into ADI state. By the means of heat treatment, the ductile cast iron (austenitization temperature of 910 ± 3 °C, dwell of 60 minutes, rapid cooling to isothermal transformation temperature of 280 °C with a dwell time of 90 minutes followed by the additional cooling to the ambient temperature) was transformed from the initial pearlitic - ferritic matrix into a matrix consisting only of the lower bainite. The graphite morphology, i.e. size, shape and distribution remained entirely preserved - Fig. 3 [3].

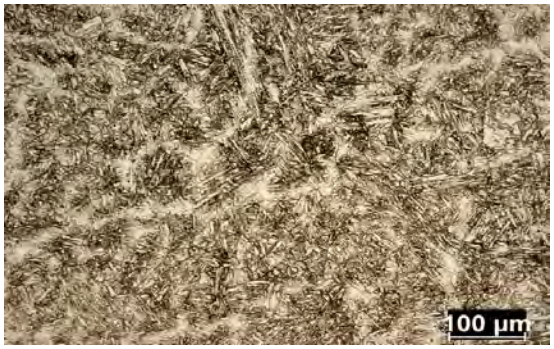

Fig. 1 Microstructure of steel 1.4313
Obr. 1 Mikrostruktura oceli 1.4313

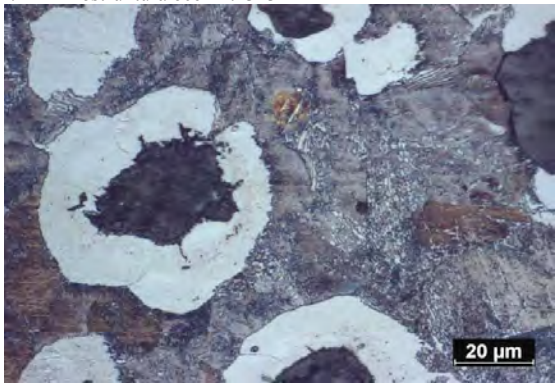

Fig. 2 Microstructure of ductile cast iron
Obr. 2 Mikrostruktura litiny s kuličkovým grafitem

Fig. 3 Microstructure of austempered ductile iron
Obr. 3 Mikrostruktura litiny s kuličkovým grafitem ve stavu ADI

The measured values of mechanical properties are shown in Tab. 3. It is apparent that the ultimate tensile strength of the heat treated cast iron has been increased more than twice in comparison to its initial state and furthermore, the hardness value of this heat treated cast iron has been increased almost by 50% in comparison to steel 1.4313. Ductility which was negligible in both states of ductile cast iron value is halved. Corrosion resistant steel had similar values in comparison to ductile cast iron in the initial state.

The results of the abrasion test are in Fig. 4 - 6 and also in the graph in Fig. 7. Visual appearance of samples for all tested materials before and after the abrasion test was documented. The samples after 15 hours testing are shown on the right side of the images.

Tab. 3 Mechanical properties of examined materials
Tab. 3 Mechanické hodnoty zkoumaných materiálů

	Unit	Steel 1.4313	Ductile cast iron	ADI cast iron
R_e	[MPa]	666	483	1469
R_m	[MPa]	766	684	1510
A	[%]	14	2.8	1.2
HBW	[-]	235	268	343
KV/KU	[J]	116 (KV)	2.9	5.4

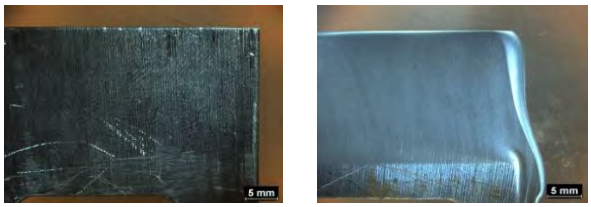

Fig. 4 Steel 1.4313 before and after the abrasion test
Obr. 4 Ocel 1.4313 před a po zkoušce abraze

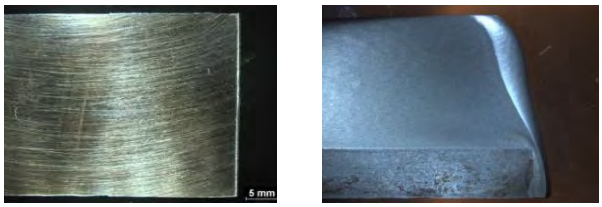

Fig. 5 Ductile iron before and after the abrasion test
Obr. 5 Litina s kuličkovým grafitem před a po zkoušce abraze

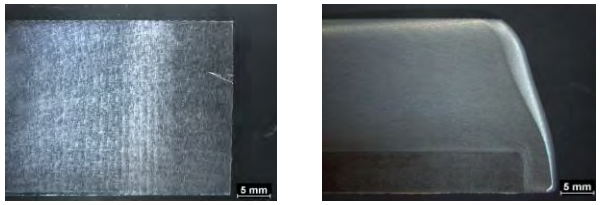

Fig. 6 Austempered ductile iron before and after the abrasion test
Obr. 6 Izotermicky zušlechtěná litina před a po testu abraze

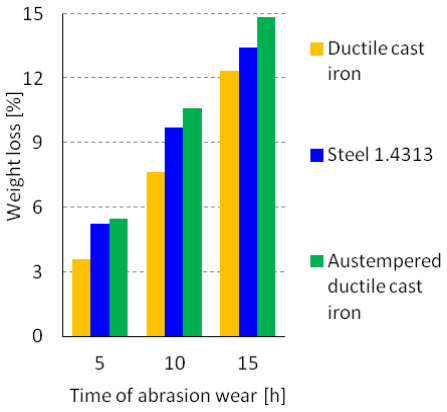

Fig. 7 Values for weight loss during the abrasion test
Obr. 7 Hodnoty hmotnostních úbytků v průběhu testu abraze

Based on the abrasion test, there is the significant change of the blade geometry and shape due to the intensive wear of the striking edge during repeated

Hutnické listy č. 3/2014, roč. LXVII
ISSN 0018-8069

interaction between abrasive particles and material. Abrasion magnitude increases approximately as a linear function with the duration of the test. The results confirm the positive effect of cast iron morphology (lamellar pearlite and its content in the ferrite-pearlite matrix of cast iron) in relation to the resistance to abrasive wear. In spite of all expectations, there was not higher abrasion resistance of the isothermally heat treated cast iron consisting of bainite and residual austenite in comparison to the cast iron which had the same chemical composition and pearlitic matrix.

Conclusions

Based on the performed experimental procedures it can be stated that the ductile cast iron attains sufficient resistance to abrasive wear. If its good corrosion properties are confirmed then it could be a suitable alternative to conventional alloyed steels for the manufacturing of parts of several types of water turbines with regard to production technology and economic demands.

Acknowledgement

This program was made possible within the framework of TACR - TA02011121 - Progressive Material-Technological Increase in Efficiency of the Turbine Blades Production and with the help of the Innovation Centre for Diagnostics and Application Materials - CZ.2.16/3.1.00/21037.

Literature

[1] MADAN MOHAN DAS, Mimi Das Saikia. *Irrigation and water power engineering*. New Delhi: PHI Learning Pvt. Ltd. ISBN 978-812-0335-875

[2] DIAS, J.F., RIBEIRO, G.O., CARMO, D.J., VILELA J.J. The effect of reducing the austempering time on the fatigue properties of austempered ductile iron, *Materials Science and Engineering: A*, Volume 556, 30 October 2012, p. 408–413, ISSN: 0921-5093

[3] BAYER, R. Mechanical wear fundamentals and testing. 2nd ed., rev. and expanded. New Delhi: M. Dekker, c2004, ix, 399 p. Mechanical engineering (Marcel Dekker, Inc.), 172. ISBN 08-247-4620-1

[4] ANDERSSON, Sören a Igor FÜRSTNER. *Advanced knowledge application in practice*. Rijeka: Sciyo, 2010. ISBN 978-953-307-141-1

Defect of Shaft Due to Occurrence of Surface Failure during Machining Process

Porušenie hriadeľa vznikom povrchových vád pri opracovaní

Ing. Mariana Janeková[1], Ing. Ľuba Hajduchová, PhD.[1], prof. Ing. Františka Pešlová, PhD.[2]

[1]Faculty of Industrial Technologies in Púchov, Alexander Dubček University of Trenčín, I. Krasku 491/30, 020 01 Púchov, Slovak Republic
[2]Czech Technical University in Prague, Faculty of Mechanical Engineering, Karlovo nám. 13, 121 32 Prague 2, Czech Republic

The main objective of the given paper is connected with the effort to find the reason of surface rupture relating to the construction surface represented by shaft which was made of material designated as 42CrMoS4. The non-metallic inclusions were recognized in the structure on the basis of microstructural investigation as well as hardness test was performed for semi-products used for manufacturing of shaft. When the heterogeneous phases are observed for the microstructure, the following manufacturing process (e.g. machining process with occurrence of chips) leads to the undesired release of particles and this release is closely connected with failure of the structure. The final part of the presented work is connected with the recommendations including permanent control of initial material to eliminate problems which occur on the basis of shaft failure.

Keywords: *finishing cutting methods, surface defects, non-metallic inclusions, microstructure, hardness, cracks*

Práca sa zaoberá hľadaním príčiny povrchového porušenia konštrukčného povrchu – hriadeľa, vyrobeného z materiálu 42CrMoS4. Pri priebežnej kontrole hriadeľov defektoskopickou skúškou boli detekované povrchové porušenia rozpracovaných výrobkov, ktoré v určených miestach boli potvrdené aj makroskopickým pozorovaním s využitím stereomikroskopu. Súčiastka, ktorá bola podrobená dôkladnému skúmaniu a analýze, bola dodaná firmou, ktorá patrí k popredným svetovým dodávateľom hydraulických sústav a komponentov pre mobilné pracovné stroje. Zmena kvality finálneho výrobku môže byť spôsobená medzioperačnými postupmi, ktoré možno odhaliť pomocou defektoskopickej skúšky. Na základe tejto skúšky boli vyznačené na rozpracovanom výrobku v stredovej oblasti hriadeľa porušenia materiálu a týmto porušeniam bola venovaná pozornosť ako z makroskopického, tak aj mikroskopického hľadiska. Odhalenie príčiny povrchového poškodenia, ako aj druh a rozsah poškodenia hriadeľa môžu byť východiskovým materiálom pre špecifikáciu možných zmien, ktoré môžu nastať v základnom materiáli ako výsledok medzioperačných postupov. Na základe odhaleného porušenia hriadeľa bolo nutné venovať pozornosť aj východiskovému materiálu, z ktorého bol hriadeľ vyrobený. K dispozícii bolo šesť odrezkov východiskového polotovaru – tyčového materiálu, z ktorého boli narezané priečne rezy pre zhodnotenie mikročistoty. U jednej z dodaných tyčí, ktorá sa použila na odber a prípravu vzoriek, boli na povrchu identifikované necelistvosti, a preto sa pristúpilo k dôkladnému metalografickému skúmaniu. Na základe mikroštruktúrneho skúmania doplneného skúškami tvrdosti je možne preukázať výskyt nekovových vtrúsenin v štruktúre. Pokiaľ sú prítomné rôzne heterogénne fázy v štruktúre, dochádza pri ďalšom spracovaní, napr. trieskovým obrábaním, k vytrhávaniu častíc a k narušeniu mikroštruktúry. V záverečnej časti predkladanej práce je odporúčanie kontroly východiskového materiálu, ktorá by eliminovala problémy, ktoré vznikajú porušením povrchu hriadeľa [1, 2].

Kľúčové slová: *dokončovacie operácie, povrchové vady, nekovové prímesky, mikroštruktúra, tvrdosť, trhliny*

Using the defectoscopy test, the continuous control led to the detection of the surface failure of the parts which were under the machining process.

The failure sites were also observed by help of stereo-microscope in more detailed way and this observation confirmed the occurrence of the mentioned defects. The given tested component part was supplied by company which belongs to the most famous and world wide suppliers of hydraulic assemblies and components for mobile operating machines and therefore the given company has to pay attention to the semi-operation problems which can be the signal for the change of product quality. The brief sketch of the final product is shown in the Fig. 1.

Based on the defectoscopy test, the central area of the tested shaft semi-product was designated as the area of the defects and therefore the given areas were subjected to the macroscopic as well as microscopic observation. The given shaft semi-product was made of the material designated as 42CrMoS4 and it can be seen in the Fig. 2.

Hutnické listy č. 3/2014, roč. LXVII
ISSN 0018-8069

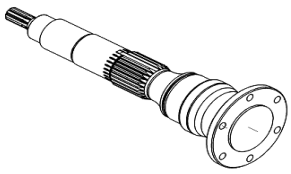

Fig. 1 The shaft
Obr. 1 Hriadeľ

Fig. 2 The failure of the shaft before the further processing operation
Obr. 2 Porušenie hriadeľa pred ďalším spracovaním

The main objective of the given work was to find out the reason of the surface rupture or failure leading to the more detailed identification of the type of failure. Furthermore, the investigation of the mentioned semi-product was performed in order to reveal the extension of the failure as well as its influence on the initial or basic material [3].

Experiment

The first one step of the experimental part was connected with the evaluation of the basic or initial material which is commonly used for production of the shafts. The detailed observation as well as analysis showed that there was the occurrence of the disintegrity in some sites and therefore, the given sites were subjected to the metallographic investigation. The given metallographic investigation can be seen in the Fig. 3.

Properties of the 42CrMoS4 steel

The shafts are commonly made of the chrome-molybdenum noble steel which, on the other hand, contains only a small amount of the given alloying elements and the higher through-hardening is the typical feature of the mentioned steel which is subsequently used for production of heavy-duty components into machines. Considering the advantages of this steel, the given steel is not susceptible to the temper brittleness.

The hardening process is carried out under the less penetrative hardening conditions because there is possibility relating to occurrence of the cracks or surface failures as the results of the hardening process while the given mentioned cracks can be commonly observed in the sites with the notch impact. After hardening process, the mentioned steel is resistant to adhesion and abrasion wearing. The chemical composition of the investigated 42CrMoS4 steel is shown in the Tab. 1.

The important material parameters representing the mechanical properties of the steel 42CrMoS4 after its ennoblement can be seen in the Tab. 2.

Tab. 1 Chemical composition of 42CrMoS4 steel
Tab. 1 Chemické zloženie ocele 42CrMoS4

Chemical composition [wt.%]						
C	**Cr**	**Mn**	**Mo**	**Si**	**S**	**P**
0.38	0.9	0.6	0.15	max.	0.02	max.
0.45	1.2	0.9	0.3	0.4	0.04	0.025

Tab. 2 Mechanical properties of the material 42CrMoS4
Tab. 2 Mechanické vlastnosti materiálu 42CrMoS4

Mechanical properties	
Proportions [mm]	$16 < d \leq 40$
Yield point [MPa]	$Re \geq 750$
Ultimate tensile strength [MPa]	Rm = 1000 - 1200
Elongation [%]	$A \geq 11$
Reduction in cross-section [%]	$Z \geq 45$ %
Notch toughness [J]	$KV \geq 35$

Metallographic analysis

On the basis of the defectoscopy test which revealed the defect of the shaft, the second step was closely connected with the investigation of the initial or basic rod material which was used for manufacturing of the shaft. The initial material was represented by 6 pieces of the rod semi-products which was used for achievement of cuttings and these cuttings were used for preparation of the samples subjected to the micropurity evaluation in their cross-section. Using the stereo-microscope, the disintegrity of the surface was detected for the investigated rod and it can be seen in the Fig. 3. The sites with the disintegrity were designated in order to pr

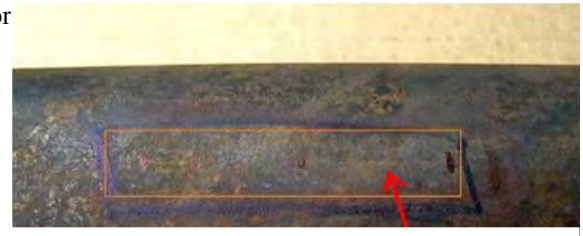

Fig. 3 Initial material – the disintegrity on the surface
Obr. 3 Východiskový materiál – necelistvosť na povrchu

The evaluation of the micropurity showed that there was the occurrence of the non-metallic inclusions in the central site as well as under the surface.

On the basis of the shaft disintegrity (grooves) which was found out by the macroscopic observation (Fig. 3), the cross-sectional cuts were prepared because of more detailed specification of the type of the internal failure. The cross-sectional area of the metallographic section exhibited the occurrence of the crack accompanied with oxide phases as well as overlapping microlayer and they are presented in the Fig. 4. The length of the crack was approximately 0.135 mm and the depth of the given crack was approximately 0.12 mm (Fig. 4a). Furthermore, the overlapping microlayer was detected under the surface around the periphery of shaft cross-section and its depth was 0.026 mm (Fig. 4b).

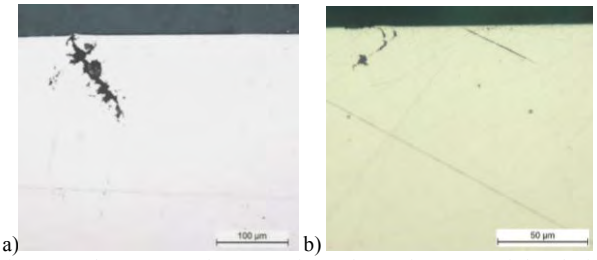

a) b)

Fig. 4 a) The cross-section – crack on the surface area of the shaft, zoomed 200x; b) Overlapping microlayer under the surface around the periphery of shaft cross-section, zoomed 200x

Obr. 4 a) Priečny rez – trhlina v mieste povrchového poškodenia, zv. 200x; b) Mikropreložka po obvode priečneho rezu hriadeľa, zv. 200x

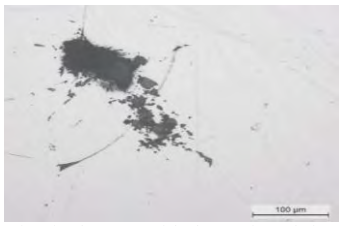

Fig. 5 Cross-section in the area with the surface defect of the shaft; zoomed 200x

Obr. 5 Priečny rez v mieste výskytu povrchového porušenia poškodeného hriadeľa; zv. 200x

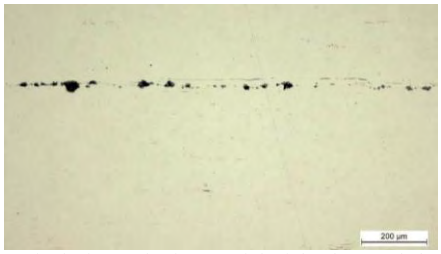

Fig. 6 Macroinclusions – basic material of the damaged shaft – cut in the longitudinal direction; zoomed 100x

Obr. 6 Makroinklúzie v základnej časti porušeného hriadeľa – pozdĺžny rez; zv. 100x

The evaluation of the rod cross-section in the central area revealed the occurrence of the accumulated impurities. Furthermore, the cavity in this central area was also recognized and these impurities as well as cavity can be seen in Fig. 5. The size of the mentioned cavity was approximately 0.33 mm. Based on the detection mentioned hereinbefore, the metallographic section relating to the longitudinal direction was prepared for the selected and specified area of the rod. The given metallographic section was used for detailed recognition of the oxide macroinclusions. The length of the area referring to the detected macroinclusions was approximately 12.5 mm and it was documented in Fig. 6 according to the specification of HMS 142 (attributing to DIN 50 602). The occurrence of sulphides was observed in relation to detailed view of micropurity corresponding to the degree of 3. According to the specifications in STN EN 10 247 standards, the detailed view of the micropurity can be seen in Fig. 7.

The microstructure of the damaged shaft in the area of the crack detection (Fig. 4) was composed of high-tempered martensite (fine sorbite) and **ε**-carbide. The microstructure of the etched as well as non-etched cross-sectional area of the sample is shown in Fig. 8. The decarbonisation of the initial or basic material was not observed.

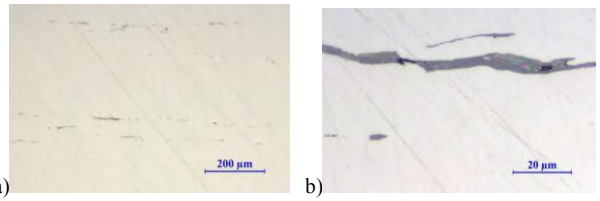

a) b)

Fig. 7 Sulphide phases – cut in the longitudinal direction: a) zoomed 80x; b) zoomed 800x

Fig. 7 Sulfidické fázy – pozdĺžny rez: a) zv. 80x; b) zv. 800x

Fig. 8 The microstructure of the damaged shaft – crack area, zoomed 400x

Obr. 8 Mikroštruktúra poškodeného hriadeľa v oblasti trhliny, zv. 400x

In relation to the base or initial material used for shaft manufacturing, the changes of the microstructure were connected only with the technology of the material forming treatment. The Fig. 9 consists of the individual selected images representing the microstructure of the basic or initial material which was cut in longitudinal direction. The given microstructure was documented for the periphery and the central area of the metallographic sample (Fig. 9a-d) at the different resolutions. According to the analysis of the mentioned structures, the semi-product used for shaft manufacturing exhibited fine arrangement of the particles in non-uniform lines under the surface in the marginal area. Much more uniform arrangement of particles was observed for the central area. The arrangement of the carbide particles is not such distinctive at resolution of 200x because arrangement of the particles is not circumscribed clearly. In relation to the further shaft manufacturing, the microstructure is still acceptable and therefore, the semi-material can be used for production of the final product – shaft. The detailed image of the given microstructure is shown in the Fig. 10.

a) marginal area – cut in a longitudinal direction; zoomed 50x

a) okraj – pozdĺžny rez, zv. 50x

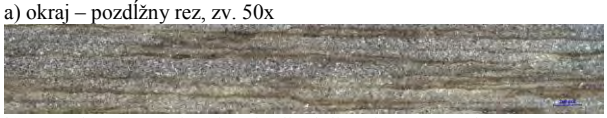

b) central area – cut in a longitudinal direction; zoomed 50x

b) stred – pozdĺžny rez, zv. 50x

c) marginal area – cut in a longitudinal direction; zoomed 200x

c) okraj – pozdĺžny rez, zv. 200x

Hutnické listy č. 3/2014, roč. LXVII
ISSN 0018-8069

d) central area – cut in a longitudinal direction, zoomed 200x
d) stred – pozdĺžny rez, zv. 200x

Fig. 9 Microstructure – cut in the longitudinal direction
Obr. 9 Mikroštruktúra okraja a stredu vzorky – pozdĺžny rez

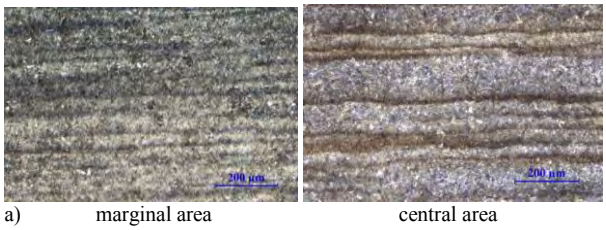

a) marginal area central area

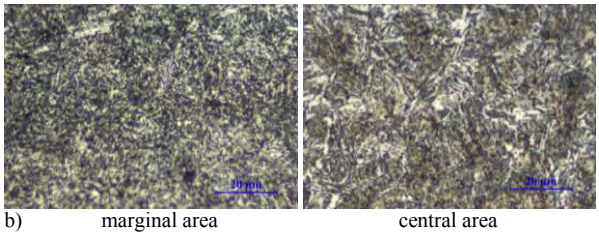

b) marginal area central area

Fig. 10 Detail of the microstructure of marginal and central area – cut in the longitudinal direction; a) zoomed 150x, b) zoomed 800x
Obr. 10 Detail mikroštruktúry okraja a stredu vzorky – pozdĺžny rez; a) zv. 150x, b) zv. 800x

Measurement of shaft hardness

Brinell Harness Test – $HB_{5/750}$ was used for the measurement of the basic or initial material along the length while the determined length corresponded to the whole length of the shaft. The results of the measurement are presented in Tab. 3. Referring to the Tab. 3, the average values for hardness together with the standard deviation of the measurement ($HB_{5/750}$ = 302.4 ± 11.3) were performed in order to compare them to the given specifications of HMS 142. According to the specification which based on MHS142, $HB_{5/750}$ = 290 – 327 is the specified hardness for material which is designed as 42CrMoS4. If the given material exhibits the mentioned values of hardness, it can be used for shaft manufacturing. The determined sites of the hardness measurement can be seen in the Fig. 2 (five areas were selected for the measurement).

Tab. 3 The measurement of the hardness $HB_{5/750}$ along the whole shaft length
Tab. 3 Meranie tvrdosti $HB_{5/750}$ po dĺžke hriadeľa

Hardness $HB_{5/750}$						
Number of measurements	1	2	3	4	5	average
$HB_{5/750}$	313	302	286	298	313	302.4 ± 11.3

Conclusions

In relation to this investigation, the given work is closely connected with specification of the reason of shaft damage. The given shaft damage was recognized with help of the defectoscopy test during the final inspection. In relation to the basic material, the areas of the surface damage were designated on the shaft after the semi-cutting operation. The given damaged areas were documented in a macroscopic way. The length of the detected and evaluated cracks was 11.5 mm. The more detailed evaluation of the shaft micropurity led to the specification of the overlapping microlayers and cracks accompanied by impurities with the size of 0.135 mm and 0.026 mm. In the central area, there was the accumulation of the impurities along with cavity and the length of this cavity was 0.33 mm. Furthermore, the uniform arrangement of the detected macroinclusions and the length of the area referring to the detected macroinclusions was approximately 12.5 mm. On the basis of the mentioned facts, the analysis had to be completed by analysis relating to the chemical composition of the shaft. In comparison to the specified chemical composition based on standards, the given chemical analysis of the damaged shaft did not confirm any change of chemical composition in relation to the individual chemical elements. The chemical composition of the tested material was suitable for the production of the shaft. The microstructure of the damaged shaft in the area of the crack detection was composed of high-tempered martensite (fine sorbite) and **ε**-carbide.

According to the specification which is based on MHS142, the value for the micropurity of the material is not allowed to be higher than K3 ≤ 40. In addition, according to the DIN 50 602, the inclusion is not allowed to be higher than the critical admitted limit while this critical admitted limit corresponds to the degree of 5. In relation to these inclusions, the important fact is that the critical limit of size was beyond the degree 5 and it is connected with the occurrence of the macroinclusions and it was the reason for shaft damage during the final cutting procedure. The microstructure and hardness of the evaluated semi-material for the shaft as well as the microstructure and hardness of the shaft as final component were in accordance with the determined specifications which are based on standards [3].

Acknowledgement

Authors would like to thank Innovation Centre for Diagnostics and Applications of Materials (CZ. 2. 16/3 1 00/21037).

Literature

[1] PULC, V., HRNČIAR, V., GONDÁR, E. *Náuka o materiáli.* Bratislava: Slovenská technická univerzita, 2004. 333 p. ISBN 80-227-2098-4.

[2] SKOČOVSKÝ, P. a kol. *Náuka o materiáli pre odbory strojnícke*. 1. vyd. Žilina: Žilinská univerzita, 2001. 381 p. ISBN 80-7100-831-1.

[3] PIROHOVA, A. *Príčina porušenia povrchových vád na hriadeli zistených defektoskopickou kontrolou*. (diplompvá práca.) Ved. d.p. Ing. Ľuba Hajduchová, PhD. Púchov: TnUAD, FPT, 2013. 63 s. Signatúra: VP 13680

Continuously Cast Round Rod of EN-GJS-700-2 Material for Servo-Cylinder Production

Kontiliata guľatina pre výrobu servovalcov z materiálu EN-GJS-700-2

Ing. Daniela Koštialiková[1], Ing. Ľuba Hajduchová, PhD.[1], prof. Ing. Františka Pešlová, PhD.[2]

[1]Faculty of Industrial Technologies in Púchov, Alexander Dubček University of Trenčín, I. Krasku 491/30, 020 01 Púchov, Slovak Republic
[2] Czech Technical University in Prague, Faculty of Mechanical Engineering, Karlovo nám. 13, 121 32 Prague 2, Czech Republic

The given paper is closely connected with the quality relating to the microstructure of round cast iron rods which are produced of material, the designation of which is EN-GJS-700-2. The mentioned round cast iron rods are produced by help of specific method which is called continuous casting method. The given round cast iron rods are used as semi-product for production of servo-piston into the servo-cylinder. In relation to this paper, from the practical aspect, there is the serious danger of surface rupture, damage or imperfection because the servo-pistons are commonly modified or treated by such methods as nitriding and hardening. EN-GJS-700-2 is a material representing cast iron which is very sensitive to processing methods. The technology of the processing methods is reflected in the final structure and therefore the paper is focused on investigation of the structures referring to the selected areas of round rod while the given areas were selected randomly. The main aim of the investigation is connected with the evaluation of the influence of the technological processing procedure on the structural properties of the round rods of cast iron.

Keywords: *cast iron, spheroidal shape of graphite, nitriding, hardening, microstructure, continuously cast rods*

Daná práca sa zaoberá riešením problematiky, ktorá je spätá s kvalitou makro a mikroštruktúry tyčí liatiny EN-GJS-700-2, ktoré slúžia ako polotovar pre výrobu piesta servovalca, pretože kvalitná výroba piesta servovalca je podmienená práve dodržaním technológie kontiliatia tyčí. Materiál EN-GJS-700-2 je tvárna liatina, čo je zliatina železa, uhlíka a ďalších prísadových prvkov, kde je grafit vylúčený prevažne v tvare guľôčkových častíc označených ako liatina – liatina s guľôčkovým grafitom. Na mechanické vlastnosti týchto grafitických liatin má vplyv nie len charakter kovovej matrice, ale aj morfológia, veľkosť a rozloženie grafitu. Tepelným spracovaním sa mení kovová matrica, ktorá ovplyvňuje celkovo materiálové vlastnosti liatiny. Skúmaný materiál sa používa na výrobu takých súčastí, ktoré sú značne mechanicky namáhané a medzi takéto súčasti patria aj piesty servovalcov. Piesty servovalcov sú povrchovo upravované nitridovaním a kalením, preto existuje veľké nebezpečenstvo, že dôjde k vzniku nedokonalostí povrchu. Keďže materiál na výrobu piestov je liatina, ktorá je veľmi náročná na voľbu povrchového spracovania, bolo potrebné zhodnotiť správnosť nitridovania a povrchového kalenia pracovnej plochy piestu servovalca. Na metalograficky pripravených vzorkách sa zmerala hĺbka nitridovania a povrchového kalenia a zároveň sa stanovila tvrdosť základného materiálu podľa Brinella a Vickersa. Technológia súvisiaca s odlievaním kontiliatych tyčí liatiny EN-GJS-700-2 sa vždy zobrazí v konečnej štruktúre. Z tohto dôvodu sa práca venuje skúmaniu štruktúry pre náhodne vybrané miesta tyčí, ktoré boli hodnotené pomocou svetelnej mikroskopie. Mikroštruktúry vybraných miest z liateho a tepelne spracovaného materiálu sa hodnotili na svetelnom mikroskope DMI 5000. Na základe tejto analýzy bol navrhnutý režim tepelného spracovania za účelom zlepšenia kvality mikroštruktúry a tvrdosti kontiliatych tyčí. Po vyhodnotení mikroštruktúry tepelne spracovaných kontiliatych tyčí podľa navrhnutého režimu tepelného sparacovania, boli z týchto uvoľnených polotovarov vyrobené piesty servovalcov a následne bola zhodnotená aj finálna súčiastka samotného piestu servovalca.

Kľúčové slová: *liatina, guľôčkový tvar grafitu, ntridácia, kalenie, mikroštruktúra, kontiliate tyče*

In relation to the servo-piston into servo-cylinder (Fig. 1), the quality of the servo-piston is subjected to the processing technology, namely continuous casting. The given processing technology has to be strictly kept in order to obtain required semi-product which is subsequently used for production of the servo-piston. According to the mentioned fact, it was necessary to evaluate the influence of the processing technology on the structural properties of the round rods. The attention was paid to the evaluation of the macrostructure (Fig. 2) as well as microstructure. Cast iron with its designation EN-GJS-700-2 is the material which is commonly used for production of servo-pistons into the servo-cylinders. This material is very sensitive from the aspect of the selection of the appropriate surface treatment and therefore, it was necessary to evaluate the processing

Hutnické listy č. 3/2014, roč. LXVII
ISSN 0018-8069

conditions in relation to the nitriding and surface hardening of the servo-piston into servo-cylinder. The samples of EN-GJS-700-2 material were prepared in order to make analysis of nitriding as well as surface hardening procedures in relation to the service areas of the servo-piston. The metallographic samples (designated 1, 2, 3) were also subjected to measurement of the depth relating to nitriding and surface hardening process. Moreover, the hardness of the initial or basic material was determined according to Brinell and Vickers hardness tests.

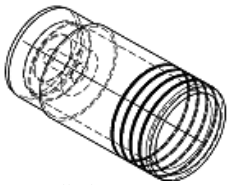

Fig. 1 Sketch of the servo-cylinder
Obr. 1 Náčrt servováľca

Fig. 2 Cross-sections of continuously cast round rods
Obr. 2 Priečne rezy kontinuálnych tyčí

Experiment

In relation to the cast iron with designation EN-GJS-700-2 which is used for production of round rods, the final microstructure is based on the used technology and in our case, the used technology is called continuous casting. According to the mentioned fact hereinbefore, the work is mainly focused on investigation of the structures. The observation of the structures was performed for the areas of round rods while the given investigated areas were selected randomly. The light microscopy was used for observation of the structures. Based on the macroscopic observation of round rod cross-sections (Fig. 2), the solidification of the material was non-uniform and on the surface, there was the layer which was expected to be etched in a different way. The given layer exhibited non-uniform thickness around the whole circumference and it means the change of the microstructure through the cross-section of the round rods. It was assumed that there was the occurrence of the cementite. Furthermore, the thickest site reached the value of 10 mm [3].

Fig. 3 shows the cut rods and there is also the designation of the parts which were used for preparation of the metallographic sections. In relation to the microstructure evaluation, the prepared metallographic sections were embedded into dentacryl in such a way to obtain the largest area for observation.

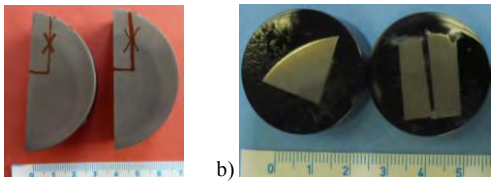

Fig. 3 Removal of the samples and prepared metallographic samples: a) cross-sections; b) etched samples
Obr. 3 Odber vzoriek a pripravené metalografické výbrusy: a) priečne rezy; b) naleptané vzorky

EN-GJS -700-2 – cast iron for servo-pistons

Material with designation EN-GJS-700-2 belongs to the class representing ductile cast irons and it means that this cast iron is the alloy of iron, carbon and other additional elements and the graphite is mainly in the shape of spheroidal particles which are designated as cast iron – cast iron with the spheroidal shape of graphite. The chemical composition is shown in Tab 1. Ductile cast iron with the spheroidal shape of graphite is commonly used for production of the servo-pistons into servo-cylinders but it is also used for manufacturing of parts which have to withstand high stress conditions. The mechanical properties of the given material are shown in Tab. 2.

Tab. 1 Chemical composition of EN-GJS-700-2
Tab. 1 Chemické zloženie materiálu EN-GJS-700-2

Chemical composition [wt.%]					
C	**Si**	**Mn**	**P**	**S**	**Mg**
3.2	1.8	0.2	max	max	0.04
4.0	3.0	0.08	0.1	0.05	0.08

Tab. 2 Mechanical properties of EN-GJS-700-2
Tab. 2 Mechanické vlastnosti materialu EN-GJS-700-2

Mechanical Properties*	
Ultimate tensile strength [MPa]	$R_m > 700$
Proof strength [MPa]	$R_{P0.2} > 420$
Elongation [%]	A >2

*According to HMS 140 and DIN EN 10204 -3.1

Metallographic evaluation

The mechanical properties of the graphitic cast irons are influenced by character of metallic matrix, morphology, size and arrangement of the graphite. Thermal treatment causes the change of the metallic matrix while this metallic matrix has significant influence on material properties of the cast iron. The microstructures for the selected areas of cast and thermally treated material were evaluated with help of DMI 5000 – light microscope. To make better evaluation of microstructure, the images of observed areas were joined together and it led to possibility to evaluate the microstructure of selected areas from the surface up to the inside central area (Fig. 4). The samples designated with numbers were removed randomly while the removal of samples included removal of three pieces form the areas selected randomly along the whole length of the round rod. The depth relating to the change of size of graphite from the surface area up to the inside

central area was approximately 6.9 mm. Regarding to the marginal area, the arrangement and the size of spheroidal graphite was VI 8 / 20 % 7 – it can be seen in Fig. 4 and 5. In relation to the mentioned fact hereinbefore, it can be seen that it is spheroidal graphite with the size corresponding to 8 / 20 % 7 specified in Slovak technical standards – STN 42 2461. In the inside central area, the shape of graphite corresponds to VI – uniformly grained and the size of graphite is 6 and it corresponds to VI 6 according to the standard mentioned above (see Fig. 5).

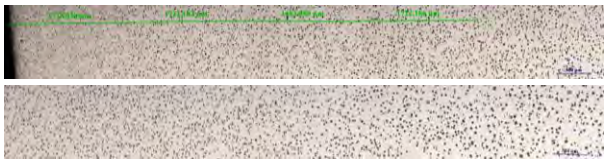

Fig. 4 Spheroidal graphite from marginal to the central area, zoomed 20x (sample n. 2)
Obr. 4 Guľôčkový grafit od okraja po stredovú oblasť, zv. 20x (vzorka označená č. 2)

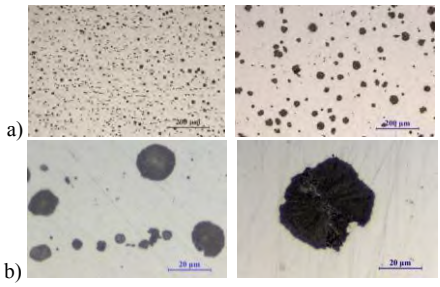

Fig. 5 Arrangement of the spheroidal graphite – detailed image (sample n. 2) – marginal area (on the left), central area (on the right); a) zoomed 90x, b) zoomed 900x
Obr. 5 Rozloženie guľôčkového grafitu – detail (vzorka č. 2) –- okrajová (vľavo) a stredová oblasť (vpravo); a) zv. 90x, b) zv. 900x

Evaluation of the material microstructure

The main aim of the work was to find out whether the all requirements for continuous casting procedure were kept in relation to the production of the servo-piston into the servo-cylinder and therefore, the evaluation of the microstructure and measurement of hardness had to be carried out. After the etching process, the microstructure was observed. In relation to the all investigated samples obtained from three round rods, the changes in microstructure were revealed from the surface area into the inside central area. For better understanding, sample designated as n. 2 (obtained from the rod designated as n. 2) was selected for demonstration in this paper because in the case of this sample, the most noticeable changes were observed from the surface area into the inside central area (see Fig. 6). The depth referring to the changes from the surface area into the central area was 8.5mm and it is almost the same as the value obtained during the measurement of the macrostructure (see Fig. 2 and part with the heading "Experiment"). In relation to the sample with n. 2, the microstructure at the marginal area is based on spheroidal graphite of P 2 – with the content of pearlite (P) beyond 98%. Dispersion was $Pd_{1.0}$ (beyond 0.8 and up to 1.3 μm) and the content of cementite was C 40 (beyond 40%) while the size of shapes for cementite was Cv 6000 (beyond 2000 and up to 10 000). According to these mentioned facts, it can be concluded that the resulting specification of the microstructure for marginal area of sample with n. 2 is: P 2 – P – $Pd_{1.0}$ – C 40 – Cv 6000 and the resulting specification of the microstructure for the central area of sample with n.2 is P 2 – P 96 – $Pd_{0.5}$

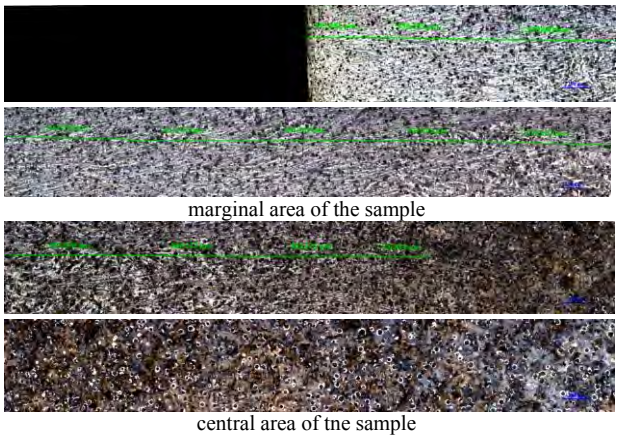

Fig. 6 Microstructure from the surface of the rods into the central area (sample n. 2); zoomed 40x
Obr. 6 Mikroštruktúra od povrchu tyčí smerom k stredovej oblasti (vzorka č. 2); zv. 40x (prvé dve zobrazennia = okraj vzorky, druhé dve zobrazenia = stred vzorky)

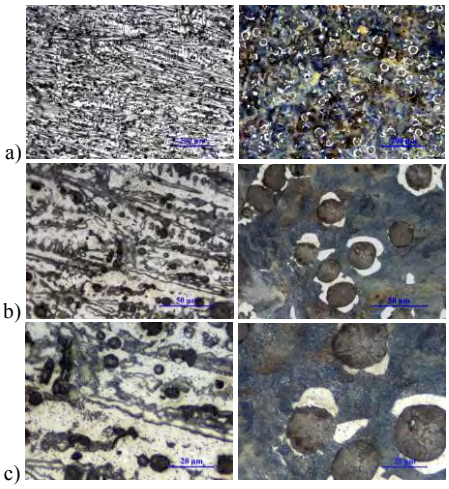

Fig. 7 Microstructure of the maginal area (sample n. 2) – from the outside (on the left) to inside (on the right); a) zoomed 90x, b) zoomed 400x, c) zoomed 900x
Obr. 7 Mikroštruktúra pri okraji (vzorka č. 2) – od okraja (vľavo) ku stredu (vpravo); a) zv. 90x, b) 400x, c) 900x

In relation to the controlled solidification for the marginal area, the detailed evaluation of the microstructure for cross-section of sample with n. 2 was connected with recognition of the higher content of ferrite and cementite (Fig. 6 and 7). In the central area of the given sample, there was not occurrence of the cementite and the macrostructure vas based on lamellar pearlite and spheroidal graphite. Moreover, discontinuous cover consisting of ferritic grains was observed around the circumference of the spheroidal graphite.

Hutnické listy č. 3/2014, roč. LXVII
ISSN 0018-8069

The reduction of the cementite as well as hardness by thermal treatment

On the basis of facts and evaluations which were mentioned hereinbefore, the regime for the thermal treatment was proposed in order to enhance the quality of the microstructure as well as hardness. The Tab. 3 shows the proposal for thermal treatment in order to modify the cementite and hardness for continuously cast round rods.

Tab. 3 The proposal for modification of the regime for thermal treatment
Tab. 3 Návrh tepelného spracovania pre úpravu obsahu cementitu a tvrdosti kontiliatych tyčí

The proposed regime for thermal treatment	
Annealing	880°C / 2 hours / Cp = 0.7 % C
	the modification of the first degree to
	855°C / 2 hours / Cp = 0.8 % C
Cooling	outside of the furnace and under the slow stream of the air

After the modified thermal treatment had been performed, the structures of continuously cast round rods were observed again. From the aspect of macrostructure observation, the bright band around the whole circumference of rod cross-section was eliminated (Fig. 8).

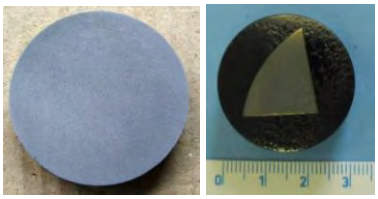

Fig. 8 The microstructure of the continuously cast rounds rods after annealing; zoomed: 1:1
Obr. 8 Mikroštruktúra kontiliatych tyčí po žihaní; zv. 1:1

After etching process, there was the reduction of the ferrite content as well as cementite during the microstructure observation (Fig. 9).

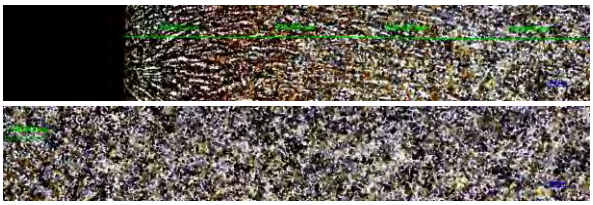

Fig. 9 Microstructure after repeated thermal treatment; zoomed 40x
Obr. 9 Mikroštruktúra po opakovanom tepelnom spracovaní; zv. 40x

After the repeated thermal treatment, the etched and non-etched microstructure was:

- for marginal area:
  VI 8 / 25% 7 - P 2 – P 96 – $Pd_{0.5}$ – C 4 – Cv6000,
- for central area:
  VI 6 - P 2 – P 96 – $Pd_{0.5}$

Thermal treatment of the servo-piston into the servo-cylinder

After the microstructure evaluation of thermally treated continuously cast round rods, the servo-pistons were made of these semi-products. Subsequently, the given produced final part was evaluated. In relation to the long time operation of the servo-pistons, the pistons are subjected to nitriding process to form the layer on the surface and the bottom of the servo-pistons is subjected to the hardening process. The microstructure for servo-piston pieces is shown in Fig. 10.

Fig. 10 The servo-piston sample
Obr. 10 Vzorka piestu servovalca

In relation to the central area, the bottom of the servo-piston (operating area) was hardened on the surface. After the evaluation of the non-etched samples (morphology, size and arrangement of graphite), the subsequent evaluation of the same sample was performed but this sample was had been etched before the observation. Regarding to the bottom of the servo-piston (operating area), the depth of the hardening process for surface is presented in the Fig. 11.

Fig. 11 The surface layer after hardening process; zoomed 40x
Obr. 11 Povrchovo kalená vrstva; zv. 40x

The total depth of the hardened layer in the thickest site (2 mm + (0.8/2) = 2.4 mm)was 2.4 mm while the depth of the basic part of the hardened layer was 2 mm and thermally influenced area of hardened layer (0.8 /2) was 0.4 mm. The cross-section which was prepared for a metallographic observation (Fig 12) can be used as demonstration of the course relating to influence of the hardening process on changes occurring from the surface to the basic material. The hardened layer on the surface (see Fig. 12) is formed with thick acicular martensite and there is also non-uniform arrangement of the residual austenite. The microstructure of the basic area of the hardened layer gets step by step into the basic or initial material trough the thermally influenced area consisting of martensite-bainite structure. The microstructure of the basic or initial material has pearlite structure with the spheroidal graphite (Fig. 12).

In relation to the nitriding process, the influence of nitridation on the basic or initial material was not observed. In Fig. 13, there is the detailed image representing the **ε** – phase of nitrided layer.

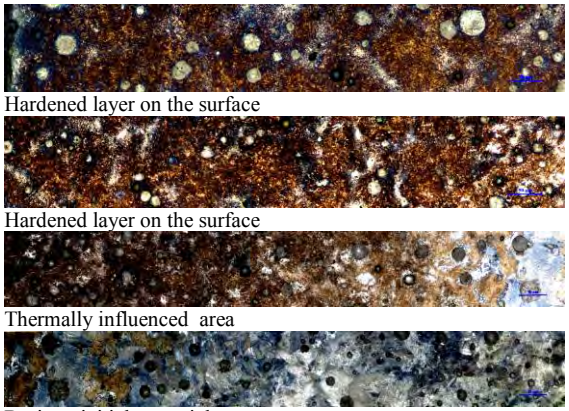

Fig. 12 Hardened layer from the surface into the basic or initial material, zoomed 200x
Obr. 12 Priebeh povrchovo kalenej vrstvy od povrchu až po základný materiál, zv. 200x – (zhora nadol – povrchovo kalená vrstva, povrchovo kalená vrstva, tepelne ovplyvnená oblasť, základný materiál)

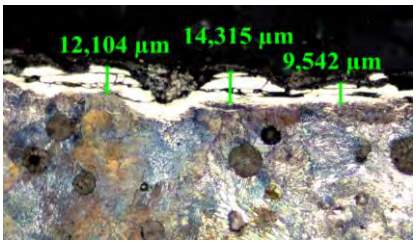

Fig. 13 Nitrided layer on the surface of the part, zoomed 500x
Obr. 13 Nitridovaná vrstva na povrchu súčasti; zv. 500x

The hardness was measured for the marginal area as well as central area using Brinell ($HB_{5/750}$) and Vickers (HV_1) hardness tests. The results of measurements are shown in Tab. 4. On the basis of the obtained values, it can be summarized that after usage of continuous casting, the round rods were not suitable for production of servo-piston because the hardness values were higher in comparison to the strictly given specification (see Tab. 4).

Tab. 4 The measured hardness values using $HB_{5/75}$ and HV_1 for sample n. 2 – before repeated thermal treatment
Tab. 4 Namerané hodnoty tvrdosti $HB_{5/75}$ a HV_1 pre vz. č. 2 - pred opakovaným tepelným spracovaním

Hardness values for sample n. 2 - obtained by measurements before the repeated thermal treatment		
Measurement method	Marginal area modified layer	The central area
$HB_{5/75}$ - average values	292	294
Individual measurements of HV_1	312, 310, 325, 305, 308	276, 267, 316, 332, 282
HV_1 – average values	312 ± 7.7	294.6 ± 27.9
According to the technical documentation, specification of HMS 140 and DIN EN 10204-3.1, the hardness of HB for the given semi-product is: $HB_{5/750}$ = 235 – 285. The obtained valued of $HB_{5/750}$ and HV_1 were controlled on the basis of conversion tables for hardness measurement in relation to DIN EN ISO 18265-13. According to the mentioned conversion tables, the admitted tolerance for suitable HV_1 is: HV_1 = 247.5 – 303.		

The occurrence of the cementite in the central area was almost the same in comparison to the occurrence of cementite in the marginal area. After the utilisation of the proposed thermal treatment modification, the microstructure became more uniform and it was also confirmed by repeated measurement of the hardness and it can be seen in Tab. 5. In relation to the modification of the thermal treatment, the round rods were suitable to be used for production of the servo-pistons into the servo-cylinders.

Tab. 5 The measured hardness values using $HB_{5/75}$ and HV_1 for sample n. 2 – after repeated thermal treatment
Tab. 5 Namerané hodnoty tvrdosti $HB_{5/75}$ a HV_1 pre vz. č. 2 – po opakovanom tepelnom spracovaní

Hardness values for sample n. 2 obtained by measurements after repeated thermal treatment		
Measurement method	Marginal area modified layer	The central area
$HB_{5/75}$ - average values	286	283
Individual measurements of HV_1	297, 315, 305, 295, 301	310, 300, 298, 295, 280
HV_1 – average values	302 ± 7.9	296.6 ± 10.9
Based on the facts relating to the admitted harness tolerance (Tab. 4), the resulting values obtained after the repeated thermal treatment show that semi-product can be used for production of the servo-piston into the servo-cylinder.		

Conclusions

According to the microstructure as well as macrostructure evaluation and hardness measurements, it can be concluded that the procedure relating to continuous casting can be used but it is necessary to change the regime of thermal treatment because when the regime of the thermal treatment is modified, the final part can be made of investigated semi-product obtained from material which is designated EN-GJS-700-2. Furthermore, the semi-products manufactured with help of continuous casting have to be subjected to annealing heat treatment before the further technological processing [3].

Literature

[1] PTÁČEK, L. a kol. *Nauka o materiálu II*. 2. vyd. Brno: Akademické nakladateľstvo EDIS, 2002. 395 p. ISBN 80–7204–247–3

[2] MORAVČÍK, R. a kol. *Náuka o materiáloch I*. Bratislava: STU, Materiálovo technologická fakulta Trnava, 2010. 250 p. ISBN 978–80–8096–123–7

[3] RYPÁKOVÁ, J. *Kontiliaté tyče pre výrobu servovalca z materiálu EN - GJS –700 – 2.* (diplomová práca.) Ved. d.p. Ing. Ľuba Hajduchová, PhD. Púchov: TnUAD, FPT, 2013. 68 s. Signatúra: VP 13683

Hutnické listy č. 3/2014, roč. LXVII
ISSN 0018-8069

Study of the Final Product in the Production of ZnO

Štúdium konečného produktu pri výrobe ZnO

Ing. Natália Luptáková, PhD.[1], **prof. Ing. Františka Pešlová, PhD.**[2]

[1]Institute of Physics of Materials, Academy of Sciences of Czech Republic, Žižkova 22, 616 22 Brno, Czech Republic
[2]Alexander Dubček University of Trenčín, Faculty of Industrial Technologies, I. Krasku 491/30, 020 01 Púchov, Slovak Republic

The given paper is closely connected with the process of ZnO manufacturing. Zinc oxide is a unique material that exhibits piezoelectric, semiconducting and multiple properties and moreover, zinc oxide represents semi-material important for many technologies. From the industrial aspect, the most of ZnO is produced by pyrometallurgical methods (e.g. the indirect process and the direct process) or by hydrometallurgical methods. European production of zinc oxide is based on the indirect method of production (so-called "French process"). The quality of the ZnO depends on the precursors which are used. In relation to the production of ZnO, the purity of zinc oxide has been the subject of several investigations, but there is still conflict among the result obtained. On the basis of the occurrence of the residual content of other elements, it is possible to make prediction about the material behavior in the metallographic process. The final residual materials were investigated and this investigation was done from the aspect of structural and chemical composition of the materials.

Keywords: *zinc oxide, zincite, production of zinc oxide, French process*

Oxid zinočnatý je dôležitou súčasťou moderných a inovačných technológií globálneho priemyslu. Jeho veľmi dobré vlastnosti majú široké uplatnenie. Využíva sa pri výrobe pneumatík, náterových látok, kŕmnych zmesí, ako prísada do zubných náhrad. Je najnovším objavom vo svete optoelektroniky, nanočastíc, laserov atď. Súčasné najpoužívanejšie spôsoby výroby oxidu zinočnatého sú priame a nepriame pyrometalurgické spracovania zinkových surovín alebo elektrolyticky upraveného kovového zinku. Rozhodujúcim faktorom, ktorý ovplyvňuje celý technologický proces, je výber vstupných materiálov, t.j. primárnych surovín. O výhodnosti ich použitia rozhodujú chemické a fyzikálne vlastnosti a primárne technologické okolnosti. ZnO sa vyrába rôznymi spôsobmi, ale najčastejší spôsob výroby používaný v Európe je priamy, t.j. pyrometalurgické spaľovanie zinku. Pary Zn pri teplote vyššej ako 906 °C reagujú s O_2, vzniká oxid zinočnatý sprevádzaný luminiscenciou. V tomto prípade vznikajú odpady, ktoré predstavujú značne množstvo prvotného materiálu. Jedná sa najmä o chemické komplexy prvkov železa, zinku a hliníka. Nebezpečenstvom výskytu týchto prvkov je ich schopnosť vytvárať potrojné eutektiká, ktoré z hľadiska deformačne napäťových stavov v štruktúre sú nevyhovujúce, lebo ich krehká štruktúra ovplyvňuje ďalší metalurgický proces. V pecnom priestore dochádza taktiež k porušeniu termodynamickej rovnováhy (je spôsobená zmenou tepelného gradientu alebo poklesom tlaku), čo vedie k sekundárnej kryštalizácii ZnO, ktorá bude ovplyvňovať ďalší priebeh. Na základe výskytu zvyškového obsahu ďalších prvkov je možné predikovať chovanie materiálu v metalografickom procese. V tejto práci bol výsledný produkt skúmaný z hľadiska morfologickej zmeny štruktúr a chemického zloženia daného oxidu. Výsledky získaných analýz budú slúžiť pre minimalizáciu nežiaduceho odpadu (zinkovej trosky), zlepšenie akosti výsledného produktu a zvýšenie produktivity výroby oxidu zinočnatého.

Kľúčové slová: *oxid zinočnatý, zinkit, výroba oxidu zinočnatého, Francúzsky proces*

In relation to the worldwide investigation results, zinc oxide (ZnO) seems to be very attractive topic for discussion in scientific community. ZnO has been widely studied since 1935 and in resent years, this compound has been even designated as „material of the future"[1]. In many cases, the current production industry providing some goods for customers is extremely dependent on this compound. ZnO has already been widely used in our society and indeed, it is key element in many industrial manufacturing processes including paints, cosmetics, pharmaceuticals, plastics, batteries, electrical equipment, rubber, soap, textiles, floor coverings and many others. With improvements in growth technology of ZnO nanostructures, epitaxial layers, single crystal and nanoparticles, we are now moving into an era where ZnO devices will become increasingly functional [2].

ZnO is composed of abundant elements; the abundances of Zn and O in the earth crust are 132 ppm and 49.4 %, respectively [3]. The renewed interest in this material has arisen out of the development of growth technologies for the fabrication of high quality single crystals and epitaxial lays, allowing for the realization of ZnO-based electric and optoelectronic devices [2].

At ambient pressure and temperature, ZnO crystallizes in the wurzite (B4 type) structure, as shown in fig. 1. This is a hexagonal lattice, belonging to the space group $P6_3mc$, and it is characterized by two interconnecting sublattices of Zn^{2+} and O^{2-} where each Zn ion is surrounded by a tetrahedral of O ions, and vice-versa. This tetrahedral coordination gives rise to polar symmetry along the hexagonal axis. This polarity is responsible for a number of the properties of ZnO, including its piezoelectricity and spontaneous polarization and it is also a key factor in crystal growth, etching and defect generation. The four most common face terminations of wurzite ZnO are the polar Zn terminated (0001) and O terminated (000**1**) faces (c-axis oriented), and the non-polar (11**2**0) (a-axis) and (10**1**0) faces which both contain an equal number of Zn and O atoms. The polar faces are known to posses different chemical and physical properties, and the O-terminated face possesses a slightly different electronic structure to the other tree faces [4].

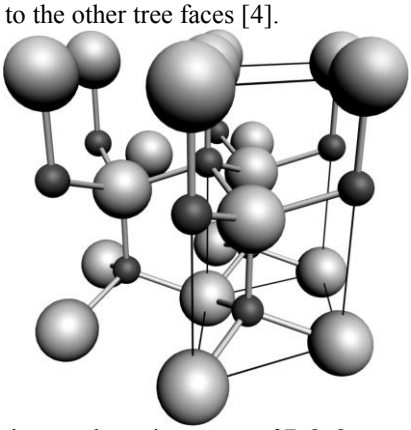

Fig. 1 The hexagonal wurtzite structure of ZnO. O atoms are shown as large white spheres, Zn atoms as smaller black spheres [5]
Obr. 1 Hexagonálna wurzitická štruktúra ZnO. Atómy O sú zobrazené ako biele gule, atómy Zn sú malé čierne gule [5]

The specific heat of a material is influenced by the lattice vibrations, free carriers and defects within the material. In crystals of high quality and purity, the specific heat is mainly influenced by the lattice vibrations. Unfortunately, there are very limited data available in the literature for specific heat measurements of ZnO. The Handbook of Chemistry and Physics [6] gives a value of the specific heat capacity of ZnO at constant pressure as $C_p = 40.3$ J.mol^{-1}K^{-1}.

Background

European production of ZnO is based on the indirect or French process. Metallic zinc/zinc alloys are melted in a crucible or furnace and vaporized at temperatures above 907 °C. Zinc vapor reacts with the O_2 in the air to give ZnO and it is accompanied by a drop in its temperature and bright luminescence. This indirect method was popularized by LeClaire (France) in 1844 and therefore, it is commonly known as French process. In relation to this process, product normally consists of agglomerated zinc oxide particles with an average size from 0.1 to a few micrometers. By weight, most of the world's zinc oxide is manufactured via French process [7, 8]. The production process is performed according to chemical reactions [7]:

$$Zn_{(s)} \rightarrow Zn_{(l)} \rightarrow Zn_{(g)} \quad (1)$$

$$Zn_{(g)} + \tfrac{1}{2}O_{2\,(g)} \xrightarrow{+CO/CO_2} ZnO_{(s)} \quad (2)$$

We have investigated the morphology, chemical composition, particle-size, some physical properties of different ZnO samples. These studies have shown interesting correlations between morphology and chemical composition of ZnO samples.

Testing methodology

The microstructures and the fracture surface of the samples were investigated by optical and scanning electron microscopy. The measurements were performed using the stereomicroscopic device NIKON SMZ 1500, SEM - JSM 7600F, AAS –AA 240 VARIAN and X- Ray diffraction Brűcker 8, KalfaCo with Co-lamp. In relation to the measurement setting, time to step is set up in different cps (counts per second).

Experimental materials

Five polycrystalline and crystalline ZnO samples with different morphologies and chemical composition have been studied. Samples of zinc oxide (fig. 2) which was prepared by French process have been chosen in the order to investigate and study the morphology and chemical composition of materials. The powders of ZnO (samples No. 1-3, tab. 1) fed by gas transport are based on the reaction (2). The ZnO crystals (samples No. 4, 5) have been grown by methods, as has been reviewed recently [8] and large-size ZnO substrates are available [9, 10]. The primary materials were zinc with additions (approx. 90 wt. % Zn). Selection of zinc oxide samples represents the given process of production and output material. The chosen samples were from crystallized minerals and their composition was corresponded to primary element of the production process. Zinc oxide is also created on the surface of metal zinc at the temperature over 419.5 °C (fig. 3) as well as by casting of molten zinc into the ingot.

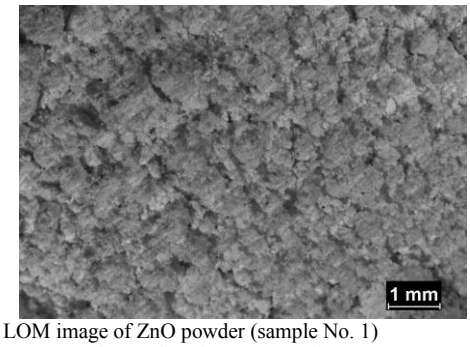

Fig. 2 LOM image of ZnO powder (sample No. 1)
Obr. 2 LOM snímka práškového ZnO (vzorka č. 1)

Hutnické listy č. 3/2014, roč. LXVII
ISSN 0018-8069

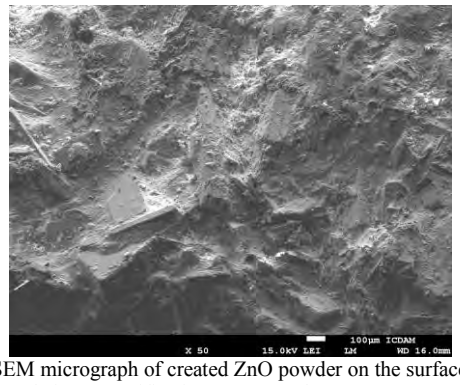

Fig. 3 SEM micrograph of created ZnO powder on the surface of metal zinc, magnification 50x (sample No. 2)
Obr. 3 SEM snímka vytvoreného práškového ZnO na povrchu kovového zinku, zväčšnie 50x (vzorka č. 2)

Tab. 1 Chemical composition of the elements of ZnO samples (wt. %) obtained by AAS
Tab. 1 Chemické zloženie prvkov vo vzorkách ZnO (hm. %) získané atómovou absorpčnou spektroskopiou (AAS)

Name of Sample	ZnO	Pb	Al	Cd	Fe
No. 1 (powder)	99.0	0.1	0.05	0.004	0.5
No. 2 (powder)	98.6	0.09	0.25	0.001	0.3
No. 3 (sintered powder)	*not detected*				
No. 4 (crystal)	90.5	0.9	0.6	-	2.1
No. 5 (crystal)	95.8	0.1	0.9	-	2.0

Result and discussion

X-ray diffraction analysis of polycrystalline ZnO has shown that all the chosen samples have the lattice parameters – a = 3.2495 ± 0.0001·10^{-9} m and c = 5.2069 ± 0.0001·10^{-9} m. Different morphology of the ZnO samples, which were investigated by the SEM and LOM method, is shown in fig. 2 - 4.

Created samples of ZnO are reduced to Zn vapor at elevated temperatures by the addition of graphite which is transported with a flow of gas (CO, CO_2). The zinc vapor is then oxidized in a region of lower temperature under the admission of oxygen or air. Needle-line crystal of ZnO can be grown with diameters up to several mm and length of several cm (fig. 4).

Fig. 4 LOM image of the needle-like single crystal of ZnO (sample No. 4)
Obr. 4 LOM snímka ihlicovitej morfológie vzorky ZnO (vzorka č. 4)

The analyzed sintered sample No. 3 was removed as a re-combusted material. That sample could not be prepared by conventional chemical method based on the evaporation of H_2SO_4 (1:3) but it was only dissolved in HCl (1:1) and heated to the boiling point of solution. After dissolution and following chemical analysis, differences were found in the results of the analysis. These differences could be caused by insufficient dissolving of the sample in boiling acid.

X-ray diffraction for the samples No. 3 showed that the sample contained about 94 wt. % of zincite (ZnO) and other compounds (or minerals), such as 5 wt. % gahnite ($ZnAl_2O_4$) and residue of PbO_2 (plattnerite). Analysis of results is shown in the diffraction diagram (fig. 5).

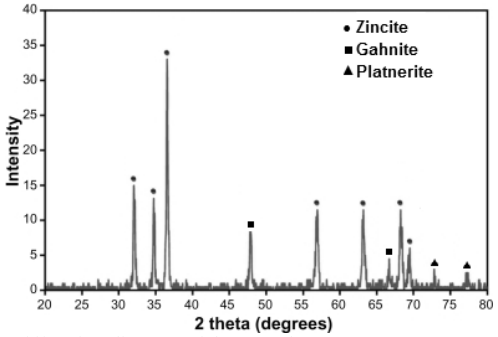

Fig. 5 Diffraction diagram of the Sample No. 3
Obr. 5 Difraktogram vzorky ZnO č. 3

Conclusions

The following conclusions can be introduced on the basis of the study of ZnO samples:

- X-ray diffraction analysis of polycrystalline ZnO has shown that all the chosen samples have the lattice parameters – a = 3.2495 ± 0.0001·10^{-9} m and c = 5.2070 ± 0.0001·10^{-9} m.
- Sintered samples of ZnO (sample No. 3) contained an enormous amount of ZnO which does not pass into the final product but it remains stuck as the slag on the lining of furnaces – more zinc, more losses in relation to final product.
- High temperature and low pressure lead to re-crystallization of some compounds, such as Zincit (ZnO), Plattnerite (PbO_2), Gahnite ($ZnAl_2O_4$) and others compounds or minerals.
- The analysis of sintered samples should not be performed by wet chemical method for performing AAS because of insufficient dissolution of the waste material in HNO_3 as well as insufficient dissolution by evaporation of H_2SO_4. Using Co lamp, the X-ray diffraction analysis was the most suitable. Usage of X-ray diffraction in crystals can be understood as the non-destructive method for determination of the internal structure of crystals and their qualitative and quantitative analyses can be done using obtained diffraction pattern.

- The resulting final product - zinc oxide in an imperfect production process of ZnO can contain Fe_2O_3 and Al_2O_3 which cause that ZnO can be yellow-brown colour.
- From the chemical analysis, the composition of the crystal was obtained. The matrix is formed by the majority of Zn and other elements, such as: Pb, Fe and one thousandth of wt. % relating to Mn, Ni and Cd and it will subsequently affect their following growth.
- As a solution, it is recommended to find a suitable method of cleaning of the furnace after three days of continuous operation as well as pure zinc (designated SHG or HG) have to be used to furnace instead of hard Zn (less than 95 wt. % of Zn) while this zinc contains such negative substances as iron, lead and aluminum and other undesired elements.

Acknowledgements

This work has been supported by the Slovak Grant Agency –VEGA: 1/0385/14, KEGA: 007 TnUAD-4/2013.

Literature

[1] BUNN, C.W. A Comparative Review of ZnO Materials and Devices. *Proceedings of the Physical Society*, 1935, Vol. 47, p. 835–841

[2] ÖZGÜR, Ü., MORKOC, H. Optical Properties of ZnO and Related Alloys. In: *Zinc Oxide Bulk, Thin Films and Nanostructures, Processing, Properties and Applications.* Ed.: C. Jagadish, S.J. Pearton, Oxford, Elsevier, 2006, pp. 175–240

[3] ELLMER, K. Transparent Conductive Zinc Oxide and Its Derivatives. *Handbook of Transparent Conductors*, Publisher Springer US, 2011, pp. 193–263, ISBN-978-1-4419-1637-2

[4] DULUB, O., BOATNER, L.A., DIEBOLD, U. STM study of the geometric and electronic structure of ZnO(0001)-Zn, (000-1)-O, (10-10), and (11-20) surfaces. *Surface Science,* Vol. 519, 2002, p. 201–210

[5] O'Neill, B. *Markets, Applications and Alternatives Minor Metals*. Lisbon, 2005

[6] LIDE, D.R. *CRC Handbook of Chemistry and Physics*. 73rd Edition, CRC Press, New York, 1992

[7] KOUDELKA, L., HORÁK, J., JARIABKA, P. Morfology of Polycrystalline ZnO and its Physical Properties. *Journal of Materials Science*, 1994, Vol. 29, p. 1497–1500

[8] PAVÚČKOVÁ, A. et al. Systematic approach of material engineer to obtain basic characteristics for computing modeling of the loaded on thermal – mechanical way. *Machine Modeling and Simulations. Slovak – Polish Scientific Conference*, 2013, Vol. 4, p. 143–146, ISSN 1337-8996

[9] LOOK, D.C. Recent advances in ZnO materials and devices. *Materials Science and Engineering*, 2001, Vol. B 80, p. 381–390

[10] OSHIMA, E. et al. Growth of the 2-in-size bulk ZnO single crystals by the hydrothermal method. *Journal of Crystal Growth*, 2004, Vol. 260, p. 166–175

[11] NTEP, J.M. et al. ZnO growth by chemical vapour transport. *Journal of Crystal Growth,* 1999, Vol. 207, p. 30–39

VOEST Alpine Tubulars uvádí do chodu novou válcovací stolici na trubky od SMS Meer

Steel Guru/Steel Trade Today 26. 3. 2014

Výrobce bezešvých trubek VOEST Alpine, sídlící v Rakousku, uvedl do chodu válcovací stolici na trubky od německé SMS Meer, a tak zlepšil svou stávající CPE válcovnu v Kindbergu. Nové zařízení umožňuje vyrábět trubky větších průměrů a větší tloušťky stěny. Výrobce již má pozitivní zkušenosti s předchozí stolicí od SMS Meer. Ale požadavky na kvalitu a materiál během let vzrostly, takže v kvalitě opět spoléhá na SMS Meer. Na instalaci stolice postačil jeden týden. Celkově byl provoz byl přerušený pouze na 15 dní. S novou stolicí na trubky je firma schopna válcovat trubky s daleko větší hmotností, maximálním průměrem až 221 mm a tloušťkou stěny až 25 mm. Stolice má svařovaný rám a obsahuje nové vodicí elementy pro stavěcí zařízení. Všechny pracovní válce mají hyperbolický profil a co do délky jsou identické. Jejich výška a úhel podávání mohou být nastaveny individuálně. Stolice je vybavena zařízením pro rychlovýměnu válců. V případě náhlého vzrůstu válcovací síly může být tlak pracovních válců okamžitě odstraněn otevřením horních válců hydraulickým systémem. Stejný hydraulický systém stavění válců také měří válcovací síly.

Hutnické listy č. 3/2014, roč. LXVII
ISSN 0018-8069

Corrosion Cracking of the Demonomerizing Column

Korózne praskanie demonomerizačnej kolóny

doc. RNDr. Ján Bezecný, CSc. [1], **Ing. Andrej Dubec**[1], **Ing. Róbert Vavrík**[1]

[1]Alexander Dubček University of Trenčín, Faculty of Industrial Technologies in Púchov, I. Krasku 491/30, 020 01 Púchov, Slovak Republic

Emulsion polyvinyl chloride (PVC E) is produced in autoclaves by emulsion polymerization of vinyl chloride (VC) in the aqueous phase solution containing the polymerization initiator, emulsifier, buffering agent, an alkaline agent and a reducing agent. Semi-product – emulsion PVC is conveyed to be subjected to a vacuum demonomerizing and then it is conveyed into containers for homogenization and stabilization and storage into the storage tanks of latex E PVC. After about 3 years operation of demonomerizing column (DC), there was the occurrence of the unexpected corrosion of the wall leading to subsequent leakage of working environment. The old one demonomerizing column had been in operation process for 20 years before it was replaced by the new one and this new one. In relation to the materials which were used for production of the new as well as old demonomerizing column, they were the same. The ruptured DC was used for preparation of the investigated samples while 3 samples were taken from the plates, 1 sample was from of pipe, 1 sample was from bolt and 1 sample represented the initial material which was used for column manufacturing. At the same time the sample was taken from suspending environment. Designation and specification of the samples is documented in Table 1 and Table 2. Operation conditions of damaged DC included loading by internal pressure, the operating temperature of the suspension were in the range from 90 to 108 °C (including) and temperature of steam was 160 ° C. According to the technical documentation, DC was made of material STN 41 7348 and during the start-up operating process (several times a year), it was loaded dynamically. When operating at lower temperatures (50-60 °C), there were not any problems. The aim of the analysis was to assess the cause of premature corrosion of the column and propose the measures in order to increase corrosion resistance. The investigation process was also connected with the verification of the chemical composition of materials, corrosion environment analysis, microstructural analysis and microfractography analysis.

Keywords: *corrosion cracking, chloride ions, austenitic steels, premature corrosion*

Emulzný polyvinylchlorid (E PVC) sa vyrába v autoklávoch emulznou polymerizáciou vinylchloridu (VC) v roztoku vodnej fázy obsahujúcej iniciátor polymerizácie, emulgátor, pufrovacie činidlá, alkalickú zložku a redukovadlo. Medziprodukt – emulzia PVC sa dopravuje na vákuovú demonomerizáciu , do zásobníkov na homogenizáciu a stabilizáciu a do skladovacích zásobných nádrží latexu E PVC. Po cca 3 rokoch prevádzky demonomerizačnej kolóny (DK) na výrobu vinylchloridu nastalo u nej k nečakanému prekorodovaniu stien s následným únikom pracovného média. K nečakanému preto, že pred jej plánovanou generálnou opravou výrobnej linky pracovala pôvodná komora 20 rokov bezproblémovo. Materiály použité pri výrobe boli pritom zhodné. Z predmetnej DK boli odobraté 3 vzorky z plechov, po 1 vzorke z rúrky, skrutky a z použitého polotovaru. Kolóna bola podľa informácie výrobcu PVC namáhaná vnútorným pretlakom, teplota suspenzie bola 90 až 108 °C a 108 °C a pary 160 °C. Podľa výkresovej dokumentácie bola vyrobená z materiálu STN 41 7348 a počas nábehu pracovného procesu (viackrát do roka) je namáhaná dynamicky. Pri prevádzke pri nižších teplotách (50 až 60 °C) sa takéto problémy nevyskytovali. Cieľom analýzy bolo posúdiť príčiny predčasnej korózie kolóny a navrhnúť opatrenia k zvýšeniu koróznej odolnosti. V rámci riešenia bolo vykonané overenie chemického zloženia materiálov, rozbor korózneho prostredia, mikroštrukturálna analýza a mikrofraktografická analýza. Bolo zistené, že príčinou predčasnej korózie bol jav korózneho praskania , na ktorého vznik vplývajú viaceré faktory. Rozhodujúcimi sú : druh použitého materiálu, druh korózneho prostredia, pôsobenie vonkajších a vnútorných napätí a tak ako aj v našom prípade výška teploty pracovného média. Už relatívne malá zmena pracovnej teploty o cca 50 °C vyvolala korózne praskanie a viedla k nutnosti nahradiť pôvodný materiál iným.

Kľúčové slová: *korózne praskanie, chloridové ióny, austenitické ocele, predčasná korózia*

The complexity of solved problems was the stimulus for decision to carry out much more detailed material analysis including the verification of the chemical composition for the analysed materials. Moreover, the analysis of operating environment, investigation and evaluation of microstructures of fracture surfaces with the specific non-integrities was also performed in order to find solutions and make recommendations or proposals in relation to the premature corrosion process of the new demonomerizing column. The mentioned corrosion process was revealed after about three years of its operation and it was unexpected phenomenon because the old one replaced demonomerizing column had been in the operation process for more than 20 years.

Experiment

Chemical analysis

The investigated individual samples were subjected to the chemical analysis and the results of this analysis can be seen in Tab. 1 and 2. The given chemical analysis shows that the investigated material, which was taken from the pipe, does not correspond to the declared designation (STN 417348) because it has a lower content of Ni and Mo in comparison to the given declared designation. The obtained results show that the given material could be designated as STN 417246 or STN 417248. Except of the mentioned pipe, the other investigated samples correspond to the declared material.

Characteristics of steel 17 348 (AKV EXTRA S9)

Steel 17 348 can be also designated as AKV EXTRA S9 with the reference to the specification based on principles which are introduced by manufacturer POLDI and it also corresponds to AISI 316L and DIN X6CrNiMoTi17-12-2, SIS 2350. According to STN 417348, the given steel can be characterized as the austenitic, weldable as well as stabilized steel which is resistant to intergranular corrosion. The given described steel is suitable from the aspect of the construction of various chemical equipment including pressure vessels. This steel is a good choice for non-oxidizing environments containing strong organic and inorganic acids at lower concentrations up to medium temperature [1]. According to the manufacturer POLDI [2], after homogenisation annealing procedure, the given CrNiMo steel has the austenitic structure with a low content of delta ferrite. Welding operation makes it be less susceptible to cracking due to additional materials as well as due to some ferrite content in the structure while this ferrite can be understood as a base material.

Tab. 1 Chemical analysis of metal plates samples
Tab. 1 Chemická analýza vzoriek plechu

Element content [mass %]	Sample		
	Plate 1	Plate 2	Plate 3
C	0.062	0.064	0.083
Mn	1.12	1.03	1.18
Si	0.313	0.283	0.350
Cr	18.54	18.54	17.22
Ni	12.46	12.48	11.76
Mo	2.24	2.23	2.10
Ti	0.445	0.457	0.411

Tab. 2 Chemical analysis of the samples
Tab. 2 Chemická analýza daných vzoriek

Element content [mass %]	Sample		
	Pipe	Bolt	Semi-product
C	0.088	0.088	0.097
Mn	1.19	1.24	1.22
Si	0.455	0.736	0.664
Cr	17.36	17.33	17.36
Ni	9.97	12.48	10.88
Mo	0.125	2.08	1.92
Ti	0.554	0.459	0.580

The mentioned processing procedure leads to increase of the strength which can cause reduction of the corrosion resistance during the forming process. The total corrosion resistance can be obtained after repeated heat treatment. It is not resistant to hydrochloric acid at the higher concentrations. When the concentration of the given acid is 0.1 % and boiling point is obtained, the corrosion rate is up to 0.11 mm per year but there is a danger of corrosion cracking and pitting corrosion [2 – 4]. In relation to the given steel, the resistance to corrosion cracking is comparable to steel AISI 316 (depending on temperature and concentration of chloride ions) and it is shown in figure 1 [5].

The analysis of the corrosion environment

In relation to the corrosion environment, it is represented by suspension PVC where suspension of PVC is about 30 %, vinyl chloride is about 0.7 % and there is also presence of xylene and trichloroethylene. In addition, the given corrosion environment exhibited pH 2.1. Measuring the pH of model solutions of various concentrations of HCl, we discovered that the HCl content is 0.05 %. Titration was used for determination of the HCl content which was 0.04%. The results of these tests showed that the approximate content of HCl in the working environment was in the range from 0.03 to 0.05 %. At this mentioned concentration and ambient temperature around 55 °C, initiation of corrosion cracking can occur and it is shown in figure 1.

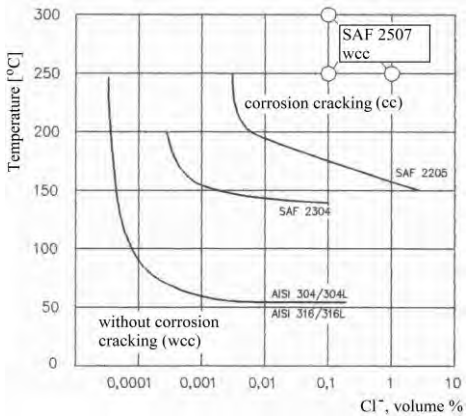

Fig. 1 Resistance of duplex steels to corrosion cracking in solutions containing chloride ions [5]
Obr. 1 Odolnosť duplexných ocelí proti koróznemu praskaniu v roztokoch obsahujúcich chloridové ióny [5]

Microstructural analysis

The bolt shank, as well as metal plates exhibited large number of radial cracks (fig. 2, 3). In order to perform evaluation of the structure for the selected areas of the tested material, the representative samples were prepared. Marble was used as the etching agent. The microstructure of all samples was austenitic, with bands of delta ferrite and these bands were in the accordance with the direction of forming process. The grain size was evaluated according to the standards STN 420462 with the degree from 7/8 up to 8. The microstructure consists of little amount of delta ferrite (fig. 4). The

Hutnické listy č. 3/2014, roč. LXVII
ISSN 0018-8069

sharp-edged inclusions, probably titanium carbonitride, are arranged uniformly in the investigated material. The two basic principles relating to crack propagation were found out for samples of metal plates. The first principle of crack propagation was based on the occurrence of the side cracks which are further branched to sides and they are quite thin (fig. 5, 6).

Fig. 2 Cracks on the bolt, zoomed 2.1x
Obr. 2 Trhliny na skrutke, zväčšenie: 2,1x

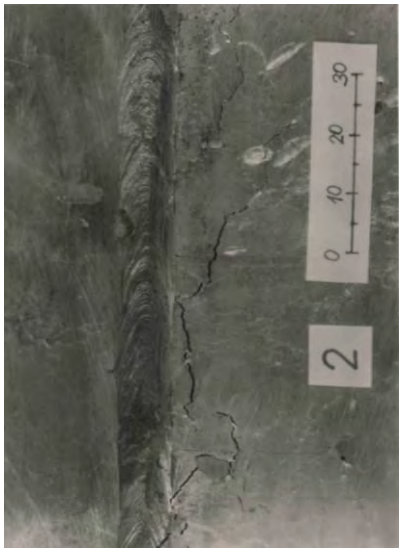

Fig. 3 Cracks on the metal plate 2, zoomed 1.1x
Obr. 3 Trhliny na plechu 2, zväčšenie: 1,1x

The second principle of the crack propagation is connected with the corrosion attack where the direction of the main crack is parallel with the direction of the metal plate surface. The corrosion process attacks mainly the lines of delta ferrite and the corrosion effect increases length and width until it forms the continuous area which is full of corrosion products (fig. 7). In both principles, there is the main crack, which is propagated vertically into the material penetrating to different depths. There was not any propagation of cracks in relation to the titanium carbonitride. The corrosion attack observed for the other metal plates is comparable to the metal plate 1. The given crack propagation has mainly the transgranular and local intergranular character. In connection with the bolt, the cracks propagate perpendicularly to the axis of the bolt. The surface of cracks is not covered by the same amount of the corrosion products in comparison to the metal plates and pipe. The first one principle of the crack propagation is predominant and it is based on the occurrence of the side cracks which are further branched to sides.

Fig. 4 Microstructure of the metal plate semi-product, zoomed 400x
Obr. 4 Mikroštruktúra polotovaru plechu, zväčšenie: 400x

Fig. 5 Branching of the crack, zoomed 400x
Obr. 5 Vetvenie trhliny, zväčšenie: 400x

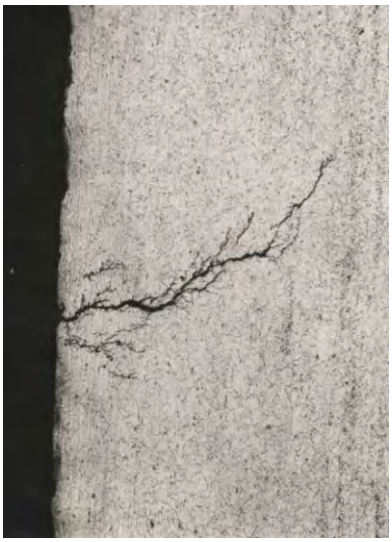

Fig. 6 Propagation of the main crack and lateral cracks, zoomed 100x
Obr. 6 Šírenie hlavnej trhliny a bočných trhlín, zväčšenie: 100x

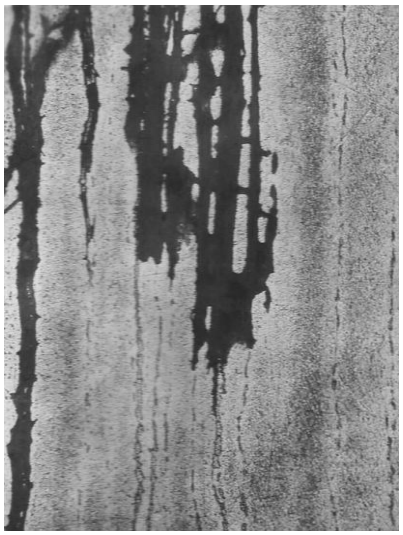

Fig. 7 Corrosion attack of the delta ferrite, zoomed 400x
Obr. 7 Korózne napadnutie feritu delta, zväčšenie: 400x

Microfractography analysis

Micromorphology of fracture surfaces was evaluated using SEM TESLA BS 301. Fracture surfaces were totally covered by corrosion products. The transgranular, crystallographic fracture with microrelief of facets corresponding to corrosion cracking (fig. 8) was observed for the cleaned fracture surfaces of all samples of metal plates and pipe. According to literature data, the interaction of hydrogen can not be excluded. The absence of intergranular facets also indicates the activity of relatively low stress. In the case of the bolt, in the area of the final fracture a striation can be observed in a direction which perpendicular to some fan-shaped facets (fig. 9). It is evident that the external cyclic stress had effect on the crack propagation while mechanical and corrosion component was almost the same. Laboratory fracture of material semi-product showed significant toughness without any evidence of the embrittlement. On the basis of fractographic analysis of fracture surfaces, it can be concluded that the majority of the cracks was formed by corrosion cracking mechanism. Significant influence of the external cyclic stress was observed in the case of the bolt.

Results and discussion

Based on the results obtained from material expertise and information about the operation of the device, it can be pointed out that the column was made of a material according to STN 17 348 417 348 and the pipe was made of material 17 246 or 17248.

Additional internal stresses in the material were caused by forming process (curling) and welding. These internal stresses have participated in the crack propagation and it is also called the mechanism of stress corrosion cracking. Based on the assessment of the effect of external factors and specific microstructural as well as microfractographic features, it is possible to make a conclusion that all samples were broken by corrosion cracking. In terms of the bolt corrosion cracking, it was accompanied by corrosion fatigue. Some differences between the bolt and the other samples can be explained by various ratios between the internal stresses, cyclic stress and corrosion environment activity. This type of corrosion is extremely harmful and dangerous case of damage in relation to metals and alloys and it can be commonly observed for environments which are not very aggressive. In case of the stainless steels, chlorides or hydroxides represent the harmful as well as dangerous components of environments.

The corrosion cracking which is also called the stress corrosion cracking can be observed for environment with chlorides while the concentration of the chloride ions is only several ppm. Moreover, this corrosion process is also accompanied by increased temperature. For instance, the transgranular corrosion cracking of austenitic chrome-nickel steels occurs in chloride environments and intergranular corrosion cracking of soft carbon steel can be recognized in alkali nitrates [6]. Detailed analysis of the obtained results showed that there was not only the replacement of old DC but the working temperature was also increased and it was changed from the initial operating temperature 50-60 °C to the operating temperature 90-110 °C in order to increase product purity.

Based on the introduced graphs hereinbefore, it is evident that with increased operating temperature, the given concentration of chloride ions caused that material AISI 316L was in area of corrosion cracking.

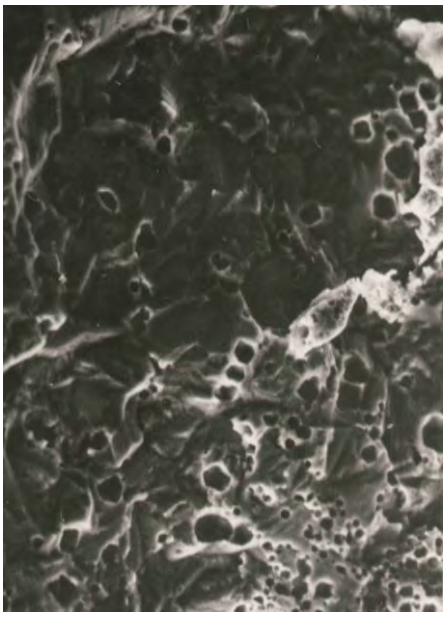

Fig. 8 Micromorphology of fracture surface, the metal plate, REM, zoomed 1000x
Obr. 8 Mikromorfológia lomovej plochy, plech, REM zväčšenie: 1000x

Hutnické listy č. 3/2014, roč. LXVII
ISSN 0018-8069

Fig. 9 Micromorphology of bolt fracture surface, REM, zoomed 1000x
Obr. 9 Mikromorfológia lomovej plochy skrutky, REM zväčšenie: 1000x

Proposals for measures

Elimination of corrosion cracking phenomenon is primarily based on the choice of a suitable material. If the selection of the suitable material is not possible, it is necessary to reduce the stress by appropriate heat treatment. If the appropriate heat treatment can not be provided, it is necessary to remove the aggressive component from the environment or modify this environment by lowering the temperature or by adding an inhibitor. In relation to the proposals and resolution of this problem, there is only one solution and it is connected with change of material. Based on international as well as national experiences, there is the recommendation for application of austenitic-ferritic stainless steels. SAF steel 2205 with its designation DIN X2CrNiN22 5 3 was recommended (especially in terms of price) to be used. Company Sandvik produces other suitable duplex steels with equivalent designation which is shown in the tab. 3.

Tab. 3 Equivalents of Sandvik materials [5]
Tab. 3 Ekvivalenty materiálov Sandvik [5]

Sandvik	SAF2507	SAF2205	SAF2304
W.-Nr.	-	1.4462	1.4362
DIN	X 2 CrNiMoN 25 7 4	X 2 CrNiMoN 22 5 3	X 2 CrNiN 23 4
AFNOR	-	Z 2 CND 22-05-03	Z 2 CN 23-04AZ
SS	2328	2377	2327

From the aspect of the resistance to stress corrosion cracking (in solutions containing chloride ions), stress corrosion cracking in dependence on time as well as the stress / tensile strength ratio, the mutual comparison of these duplex steels provided by company SANDVIK is shown in figure 10 [3].

Tab. 4 Chemical composition of the materials SAF [5]
Tab. 4 Chemické zloženie materiálov SAF [5]

SANDVIK	SAF2507	SAF2205	SAF2304
Cr	25	22	23
Ni	7	5.5	4.5
Mo	4	3.2	-
N	0.3	0.18	0.1
C	<0.02	<0.03	<0.03
Si	<0.8	<1	<0.5
Mn	<1.2	<2	<1.2
P	<0.03	<0.03	<0.035
S	<0.015	<0.015	<0.015

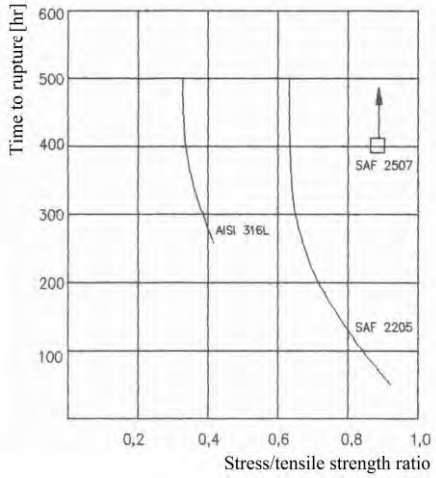

Fig. 10 Resistance of duplex steels to stress corrosion cracking in a solution of 40 % $CaCl_2$, pH 1.5, 100 °C [5]
Obr. 10 Odolnosť duplexných ocelí proti koróznemu praskaniu v roztoku 40 % $CaCl_2$, pH 1,5, 100 °C [5]

From the mutual comparison of the graphs and resistance to stress corrosion cracking, the stainless steel AISI 316 is the most suitable in relation to the operating conditions in company NCHZ Nováky but all types of the investigated steels can be used by this company. In addition to the investigation, the steel SAF 2507 exhibits the minimum susceptibility to stress corrosion cracking.

Conclusions

Based on the results of material expertise, it can be concluded that premature failure of DC was based on stress corrosion cracking which was caused by the inappropriate choice of material from the aspect of the operating conditions and working temperatures. The prevention of similar failures is hidden in the usage of the mentioned austenitic-ferritic duplex steels for operating temperatures about 100 °C. The material SAF 2507 seems to be the most optimum in terms of resistance to stress corrosion cracking. The specific choice of material depends also on the other factors (produced assortment, delivery conditions, price, processing technology and welding, providing additional materials, etc.). Furthermore, the given choice also needs subsequent laboratory, technological

and operational verification and therefore, the material SAF 2205 was proposed to be used for DC.

Literature

[1] ČSN, Ocel 17 348 Cr Ni Mo Ti. Praha: ÚNM, 1974

[2] PŘIBIL, E. : *Korozivzdorné a žáruvzdorné oceli Poldi a jejich použití*, Poldi Kladno, 1989

[3] ČÍHAL, V. *Korozivzdorné oceli a slitiny,* Ostrava, Academia, Praha, 1999 ISBN 80-7204-248-3

[4] ČÍHAL, V. Korozivzdorné oceli a slitiny. *Zborník prednášok medzinárodného seminára*. Ostrava: VŠB, s. 171-201, 1992

[5] Prospektový materiál fy SANDVIK, 1996

[6] PITTER, J. et al. Fraktografie korozního praskání austenitických nerezavějících ocelí. *Fraktografia* '83, Vysoké Tatry, 1983

Hutnické listy č. 3/2014, roč. LXVII
ISSN 0018-8069

Functional PVD Coatings for Tool Steels

Funkční PVD povlaky pro nástrojové oceli

Ing. Jakub Horník, PhD.[1], Ing. Stanislav Krum[1], Ing. David Tondl[1], prof. Ing. Františka Pešlová, PhD.[2]

[1]Czech Technical University in Prague, Faculty of Mechanical Engineering, Department of Materials Engineering, Karlovo náměstí 13, 121 35 Prague, Czech Republic
[2]Alexander Dubček University of Trenčín, Faculty of Industrial Technologies in Púchov, I. Krasku 491/30, 020 01 Púchov, Slovak Republic

The paper deals with evaluation of single layer PVD coatings based on Cr, Ti and Al widely used in tool application and it is also closely connected with W and WN based functionally graded coatings. In the case of functionally graded coatings, the diversity of composition was due to content of N varying with the depth from the surface. The nitridation process was also used as an "interlayer" in several cases in order to obtain the further improvement of the adhesion. The coatings were evaluated from the point of view of hardness and adhesion. The hardness measuring was carried out using nanoindentation and microindentation methods. The scratch test and „Mercedes" test for qualitative adhesion measurement was performed for adhesion testing. The results of scratch test showed the presence of the nitrided layer and it is connected with the significant increase of the adhesion values of CrN coating. Moreover, the presence of metallic interlayer in functionally graded materials further increases coating adhesion by gradually approaching its composition to the substrate. Coatings consisting of W and WN have showed very good adhesion too. With regard to results of the scratch test and their relative higher values of the hardness, for the coatings of WN, CrAlN and duplex TiN, it can be assumed that they have a good protective function. Results will be applied in development of functionally graded layers for functionally graded materials.

Keywords: *PVD coatings, tool steel, adhesion, nanoindentation*

Tenké povlaky jsou důležitou a stále se rozvíjející oblastí povrchového inženýrství. Povlakování má v technických aplikacích účel především ochranný a funkční. Jednou z metod vytváření tenkých povlaků na nástrojových ocelích je nanášení odpařením z pevné fáze (PVD). Výhodou této metody je nízká teplota depozice, což je důležité pro zachování vlastností dosažených předcházejícím tepelným zpracováním. Nevýhodou je pak relativně nízká adheze povlaku k základnímu materiálu. Zlepšení adheze je pak dosaženo co největším přiblížením fyzikálních vlastností povlaku k vlastnostem základnímu materiálu. Pokud mají oba materiály porovnatelnou tvrdost, dochází k výraznému navýšení adheze. V práci byly hodnoceny PVD povlaky nanesené metodou magnetronového naprašování (CrN, TiN, AlTiN, WN). Zkoušené vzorky povlaků byly připraveny v zařízení Flexicoat 850 (Hauzer). Před procesem depozice proběhla optimalizace depozičních parametrů všech typů povlaků. Tloušťka hodnocených povlaků byla přibližně 2 µm. V rámci hodnocení vlastností povlaků bylo provedeno měření adheze. Za tímto účelem bylo použito scratch testu indentorem dle Rockwella. Kromě toho byl proveden rychlý standardizovaný „Mercedes" test pro kvalitativní hodnocení adheze. Dále byla na připravených povlacích měřena nanotvrdost. Za účelem zhodnocení mikrostruktury a měření tloušťky povlaku bylo provedeno pozorování za použití skenovacího elektronového mikroskopu vybaveného EDS detektorem. Hodnocené povlaky mají ve všech případech homogenní sloupcovitou strukturu bez trhlin. Výsledky scratch testu ukazují, že vytvořením povrchové nitridované vrstvy na základním materiálu výrazně zlepšuje adhezi povlaku. Povlaky W a WN vykazují velmi dobrou adhezi a to i přes vysokou tvrdost VN. Výsledky scratch testu a poměrně vysoké tvrdosti povlaků WN, CrAlN a duplexní TiN zřejmě plní povlaky dobře ochrannou funkci v tribologických aplikacích. Výsledky budou využity ve vývoji funkčně gradientních vrstvách pro funkčně gradientní materiály.

Klíčová slova: *PVD povlak, nástrojová ocel, adheze, nanoindentace*

Thin coatings are an important area of surface engineering nowadays, experiencing rapid progress. Coatings have a protective or functional purpose in a wide range of technical applications. They increase substrate resistance against oxidation, heat transfer, wear and corrosion [1]. PVD (physical vapour deposition) is the one of the ways for deposition them onto tool steels substrate. The low deposition temperature is significant advantage of this method. However, such coatings show relatively low adhesion to substrate. Improvement of adhesion may be achieved by modifying the substrate or adjusting physical properties of the coating to it as much as possible in order to achieve similar mechanical properties like hardness [2]. Amongst the most used coatings, there are the PVD coatings based on Cr-N, Ti-N, Al-Ti-N, and W-N. However, tungsten or its nitrides and carbides are not widely used alternatives [3, 4], in spite of the good

abrasive resistance comparable to Mo_2N which has significantly lower wear loss than commercially used TiAlN or TiCN [5]. WN based coatings suffer from rapid formation of oxides over the temperature of 500 °C. These oxides occur also in surface microcracks and their growth contributes to crack propagation and coating destruction process [4]. Presented paper deals with characterization of PVD coatings types based on Cr, Ti and W nitrides deposited on a tool steel substrate. The scratch test [6, 7], "Mercedes" test [6, 8], microindentation and nanoindentation [9, 10] were used for investigation. The results will be used for development of functionally graded layers for functionally graded materials.

Experiment

As a substrate, tool steel X40CrMoV5-1 (ČSN 41 9554, Orvar Supreme) was selected. Its chemical composition in [wt. %] is in Tab. 1.

Tab. 1 Chemical composition of X40CrMoV5-1
Tab. 1 Chemické složení X40CrMoV5-1

Element	C	Si	Mn	Cr	Mo	V
Content	0.39	1.0	0.4	5.2	1.4	0.9

According to the work objective, *W, Al, Ti and Cr* based coatings were deposited (Tab. 1). All samples were prepared using the same deposition parameters. The reason for that was to eliminate effects potentially arising from different deposition parameters (among different coatings cycles) and to compare behaviour of different substrates or different coating systems. All the parameters (Bias voltage, coil current, gas flow etc.) were previously optimized by test cycles. Gas flows were optimized in case of WN coating in order to reach majority of β phase. Deposition parameters are presented in Tab. 2. The deposition time was set to reach approximately 2 μm of coatings thickness for all samples. In relation to the prior deposition, all substrates were polished to mirror-like surface then cleaned in an ultrasonic cleaning machine in acetone bath. The coating procedure was carried out with Flexicoat 850 (Hauzer) device in a single process. In several cases, duplex coating underlayer was created by plasma nitriding process (temperature of 510 °C, duration of 4 h and Ar/N_2 flow = 50/50) and it was applied in order to improve adhesion.

Adhesion measurements were performed using the Revetest Xpress + (CSM instruments) device with Rockwell indenter (tip angle = 120°, tip radius = 0.2 mm). A linearly increasing load was set from 1 to 100 N with the loading rate of 49.5 N/min. The length of each scratch was 10 mm. Velocity of the indentor was 5 mm/min. Additionally, quick standardized "Mercedes" test [8] was performed using a Rockwell hardness tester with a load of 1500 N. Nanotest (Micro Materials Ltd.) device was used to determine the hardness of the coatings. 10 indentations were made to each sample with the load of 200 mN and the loading times of 10 sec/5 sec/10 sec (load / dwell / unloading) were used. The hardness values were calculated from the results of nanoindentation $H_{IT.}$ For the evaluation of microstructure and coating thickness, the scanning electron microscope designated as Jeol JSM 7600F with EDS detector was used. Samples were prepared according to standard metallographic procedure and fractography samples were broken after the 20 minutes dwell in liquid nitrogen bath.

Tab. 2 Deposition parameters, coil current 3A
Tab. 2 Depoziční parametry, proud na cívkách 3A

Coating	Bias [V]	Ar/N_2 [sccm]	Cathode power	Substrate temperature
W	80	90/0	1*4 kW	300 °C
WN	75	90/60	1*4 kW	300 °C
Cr	75	90/0	2*3 kW	350 °C
CrN	85	90/20	2*3 kW	350 °C
CrN*	85	90/20	2*3 kW	510/450 °C
CrAlN	75	90/40	1*4 kW	450 °C
TiN	75	90/35	2*4 kW	450 °C
AlTi	75	90/0	1*3 kW	450 °C
AlTiN	75	90/20	1*3 kW	450 °C
TiN*	75	90/35	2*4 kW	510/450 °C

*Duplex coating (nitrided underlayer)

Results and discussion

Mechanical properties of the coatings are summarized in Tab. 3. It represents the values of nanohardness (H_{IT}), hardness (HV) and reduced Young's modulus of elasticity (E_r). Tab. 4 shows the results of the scratch test as a force when the coating chipping occurs and the values of "Mercedes" HRC adhesion test. The measured values of hardness and modulus of elasticity correspond well to the available data [1, 4, 5, 10].

Tab. 3 Mechanical properties of the coatings
Tab. 3 Mechnické vlastnosti povlaků

Coating	Nanohardness H_{IT} [GPa]	Hardness [HV]	Er [GPa]
W	16.4	1631	301
WN	28	2855	258
Cr	7.6	670	278
CrN	16.2	1652	248
Duplex CrN	18.1	1846	250
CrAlN	24.1	2457	262
TiN	24.4	2488	252
AlTi	11.2	1142	155
AlTiN	26.8	2733	240

The values of nanohardness of the Cr and AlTi coatings were quite low. W, CrN and duplex CrN showed mediocre nanohardness values when compared to other coating types. The nanohardness values of AlTiN, TiN and CrAlN coatings were relatively high. The highest hardness was measured in case of WN coating. WN coating modulus of elasticity is comparable to CrN, CrAlN, TiN and AlTiN. In the case of CrAlN and

Hutnické listy č. 3/2014, roč. LXVII
ISSN 0018-8069

AlTiN, the comparable and the highest hardnesses were achieved. The highest modulus of elasticity was achieved in case of the W coating. Hardness is comparable to the common CrN coatings.

Tab. 4 Adhesion tests for the coatings - scratch and "Mercedes" test
Tab. 4 Adheze povlaku zjištěná scratch testem a "Mercedes" testem

Process	Coating thickness [µm]	Lc-edge chipping [N]	HRC [1-6]
Duplex CrN	<5	73	2
CrN	<5	28	4
CrAlN	<5	34	4
W	<2	>100N	1
WN	<2	>100N	2-3
Duplex TiN	<3	>100N	1

Performed scratch test showed a wide range of adhesion values of different coatings. In the case of W, WN and duplex TiN, the maximum loading force was not sufficient to initiate coating delamination. Duplex CrN coating showed relatively high value of adhesion force (73 N). On the other hand, in case of non-duplex CrN and CrAlN coatings, delamination occurred at the noticeably lower values of the loading force.

Results of adhesion tests using scratch test and HRC test correspond well. The best adhesion was measured for duplex/TiN, W and WN coatings. The best results of HRC test were indicated in case of W coating and duplex TiN and CrN coatings. Improvement of the adhesion with rising hardness of the substrate surface layer by plasma nitriding is evident.

Evaluation of microstructure

The documentation of coatings was performed after breaking of samples in liquid nitrogen (Fig. 1 - 3). The surface quality and tendencies to delamination were evaluated. All deposited coatings revealed a columnar structure according to its growth pattern. In the Fig. 1, there is a microphotograph of PVD relating to W coating and patterns after HRC adhesion test. WN coating deposited on the Orvar tool steel is documented in Fig. 2. The thickness measurements were performed along with the examination of coatings in relation to assumed stoichiometry using EDS mapping and linear analysis (Fig. 3). Chemical composition of the coating (spectrum 1), subsurface layer of the substrate (spectrum 2) and substrate (spectrum 3) is shown in the Tab. 5.

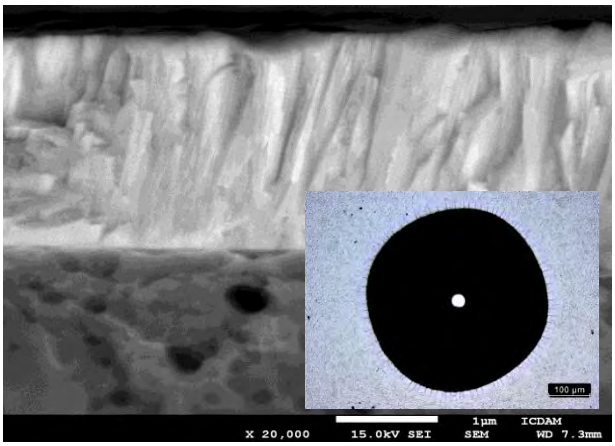

Fig. 1 W coating structure on Orvar steel and "Mercedes" test
Obr.1 Struktura W povlaku na oceli Orvar a „Mercedes" test

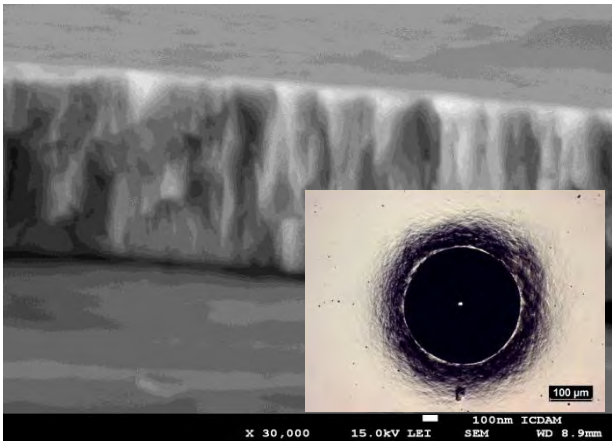

Fig. 2 WN coating structure on Orvar steel and Mercedes test
Obr. 2 Struktura WN povlaku na oceli Orvar a Mercedes test

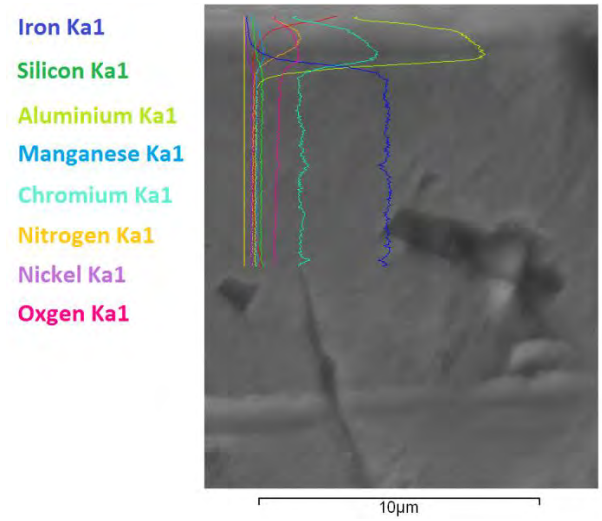

Fig. 3 Linear EDX analysis of chemical composition for duplex CrAlN coating
Obr. 3 Lineární EDX analýza chemického složení duplexního CrAlN povlaku

Tab. 5Chemical composition in [wt. %] for different locations of duplex CrAlN coating
Tab. 5Chemické složení v různých místech duplexního CrAlN povlaku v [hm. %]

Element	Coating	Interface	Base
N	29.48	10.79	0
O	0	0.67	0.66
Al	24.89	19.90	0.22
Si	0	0,34	0.75
Cr	44.26	35.43	18.18
Mn	0	0.36	0.85
Fe	2.18	30.66	76.95
Ni	0	1.86	4.35

Conclusions

All deposited coatings are approx. 2 µm thick and have homogeneous columnar structure without the cracks.

The results of scratch test showed that the presence of the nitrided layer significantly increases the adhesion values of the CrN coating. Furthermore, from the HRC adhesion test results, it can be summarized that the presence of the nitrided layer also improves the adhesion of the TiN coating, since any delamination was not observed up to the load force of 100 N. Coatings consisting of W and WN have also shown very good adhesion, despite to the high hardness. With regard to results of the scratch test and their relative higher values of the hardness, the coatings of WN, CrAlN and duplex TiN have a good potential for protective function in tribological applications.

The application of pure metals as a material of "interlayers" improves the adhesion of the coatings by gradually approaching their composition to the substrate. The results will be used for further FGM research.

Acknowledgment

The research was supported by Czech Science Foundation project GAP108/12/1872 Complex functionally graded materials.

Literature

[1] GRAINGER, S., BLUNT, J. *Engineering Coatings (second ed..)* Woodhead Publishing LLD, Abingdon 1998

[2] JURČI, P. et al. *Využití PVD povlaků na ledeburitických ocelí*. Metal 2009

[3] HORNIK, J., TONDL, D., SACHR, P., ANISIMOV, E., PUCHNIN, M., CHRASKA, T. *The Effect of PVD Tungsten-Based Coatings on Improvement of Hardness and Wear Resistance*. Key Engineering Materials Vol. 606, 2014, p. 163-166

[4] POLCAR, T., PARREIRA, N.M.G., CAVALEIRO, A. *Structural and tribological characterization of tungsten nitride at elevated temperature*. Wear, Vol. 265, 2008, p. 319-326

[5] KUTSCHEJ, K., MAYRHOFER, P.H., KATHREIN, M., POLCIK, P., TESSADRI, R., MITTERER, C. *Structure, mechanical and tribological properties of sputtered Ti1-xAlxN coatings with 0,5<x<0,75*. Surf. Coat. Technology, Vol. 200, 2008, p. 2358-2368

[6] KADIOGLU et al. *Crack problem for functionally graded layer on elastic foundation.* International Journal of Fracture 94(1) 1998, p. 66-77

[7] SOSNOVÁ, M. *Kluzné vrstvy a metody hodnocení adhezivně-kohezního a tribologického chování*. [online]. Pilsen : West bohemia university in Pilsen, 2006. URL: <http://ateam.zcu.cz/FRVS_zprava_dalsi_studium_sosnova.pdf>

[8] VDI 3198, Verein Deutscher Ingenieure Normen, VDI-Verlag, Dusseldorf, 1992.

[9] EN 1071-3 *Adraned technical ceramics, Determination of adhesion and mechanical failure.*

[10] OLIVER, W.C., PHARR, G.M. *An improved technique for determining hardness and elastic modulus using load and displacement sensing indentation experiments.* J. Mater. Research 7 (6), 1992, p. 1564-1583

Huta Labedy objednává HF linku na svařování trubek

Steel Guru/Steel Trade Today 26. 3. 2014

Pro své ocelárny v Gliwicích v Polsku objednala Huta Labedy vysokofrekvenční svařovací linku na trubky s API finalizujícím zařízením od německého firmy SMS Meer. Tato firma je jediným dodavatelem veškerého technologického vybavení a je rovněž zodpovědná za jeho instalaci a uvedení do chodu. Vzhledem k systému rychlé horizontální změny bude Huta Labedy schopna zvýšit svou produktivitu ve srovnání s konvenčními systémy rychlých změn o 30 %. Nové zařízení má roční kapacitu 270 tis. t a může vyrábět trubky o průměru 4 1/2 – 12 3/4 inch, tloušťce stěny 3.0 až 12.7 mm a v délkách až 18 m. Maximální rychlost výroby je 60 m/min. Všechny stolice jsou vybaveny individuálním pohonem. Počítačem řízený CSS Quicksetting systém zajišťuje, že válce jsou po změně velikosti automaticky stavěny do svých pracovních pozic.

Hutnické listy č. 3/2014, roč. LXVII
ISSN 0018-8069

Evaluation of Interaction of Steel Cord – Elastomer in Tire Casing

Zhodnotenie interakcie oceľový kord – elastomér v plášti pneumatík

Ing. Peter Vido[1], Ing. Jozefína Panáčková[1], doc. Ing. Jan Krmela[1], PhD., Ing. Rudolf Valášek[1]

[1]Alexander Dubček University of Trenčín, Faculty of Industrial Technologies in Púchov, I. Krasku 491/30, 020 01 Púchov, Slovak Republic

The given paper deals with determination of mechanical properties of specific composites with elastomeric matrix and steel reinforcement. Furthermore, design of computational model of composite system is also involved in this paper. A finite element method (FEM) will be applied for computational modeling for chosen parts of tires. For stress-strain analysis of tires, experimental procedures have to be performed because it is necessary to determine individual material parameters relating to the steel reinforcement, elastomeric matrix as well as entire specific composite structure. These parameters will be determined from the aspect of material characteristics of the individual components constituting the composite. In the paper, there are presented partial results of experiments used to obtain the material characteristics of cord – elastomer composites which are used as input data for the calculations and they are also necessary for verification of computational models.

Keywords: *composites, tire casing, steel cord, elastomeric matrix, computational modeling*

Článok sa zaoberá stanovením mechanických vlastností jednotlivých zložiek kompozitného systému oceľový kord–elastomér využitých ako vstupné údaje do výpočtov. Tieto kompozity tvoria prevažne oceľokordové nárazníky a kostru plášťa pneumatiky pre osobné automobily. Jednotlivé konštrukčné časti plášťov pneumatík sú reprezentované špecifickými experimentálnymi vzorkami v zastúpení od nánosových zmesí, oceľových výstužných kordov až po vzorky, kde sú v interakcii oceľové kordy a elastomérové matrice. Pre hodnotenie mechanických vlastností hotových gumárenských výrobkov, ale aj pre ich vysokú vypovedaciu schopnosť o kvalite prípravy gumárenských zmesí a oceľových výstuží sú dôležité statické skúšky v ťahu. Pomocou týchto skúšok možno overiť výrobcom stanovené materiálové parametre (napr. pevnosť v ťahu), ale aj určiť dôležité parametre, potrebné pre výpočtový model systému kord–elastomér. Výpočtové modelovanie vybraných častí plášťov pneumatík bude realizované s využitím metódy konečných prvkov. Pri vytváraní výpočtových modelov je dôraz kladený na materiálové charakteristiky a parametre jednotlivých konštrukčných častí pneumatík ako dôležitých vstupných materiálových údajov do modelov, ktoré možno stanoviť pomocou vybraných experimentov. Pre deformačno-napäťové analýzy plášťov pneumatík je potrebné experimentálne stanoviť materiálové parametre ako pre samotné oceľové výstuže a elastomérovú matricu, tak aj pre celistvý kompozitný systém kord–elastomér. Tieto parametre budú získané z materiálových charakteristík jednotlivých komponentov tvoriacich plášť pneumatiky. Dôležitými faktormi, ktoré môžu značne ovplyvniť presnosť výpočtov vybraných častí plášťov pneumatík, sú počiatočné a okrajové podmienky, reflektujúce zaťaženie, geometriu a materiálové parametre každej konštrukčnej a materiálovej časti plášťa. V článku sú prezentované vybrané výsledky z experimentov potrebných na získanie materiálových charakteristík kordovo-elastomérových kompozitov, ktoré sú nevyhnutné aj pre verifikáciu údajov z výpočtov s experimentálne získanými údajmi.

Kľúčové slová: *kompozit, plášť pneumatiky, oceľový kord, elastomér, výpočtové modelovanie*

In relation to the utilisation of the computational model outputs, it is necessary to perform a whole range of experiments to determine the input parameters for the computational models of the tire for passenger cars as well as their parts.

From the aspect of creation of computational models for the tires, the attention is paid to the investigation of the mechanical properties and characteristics of the various parts of the tire because the obtained results are the important input material data for creation of these models. Using selected experiments, we can determine the mechanical properties of individual components of the tire casing.

Material parameters of individual parts of the tire casing

Individual constructional parts of tire for passenger car are represented by specific experimental samples obtained from alluvial mixtures and the investigation is connected with the interaction of steel, textile, polymer cords and elastomeric matrix. Static tensile tests are important for the evaluation of material parameters of finished rubber products and they also give evidence whether the individual mixtures were selected for the application correctly. Division of experiments that are needed to obtain the material characteristics of individual components of the tire casing is shown in scheme presented in Fig. 1.

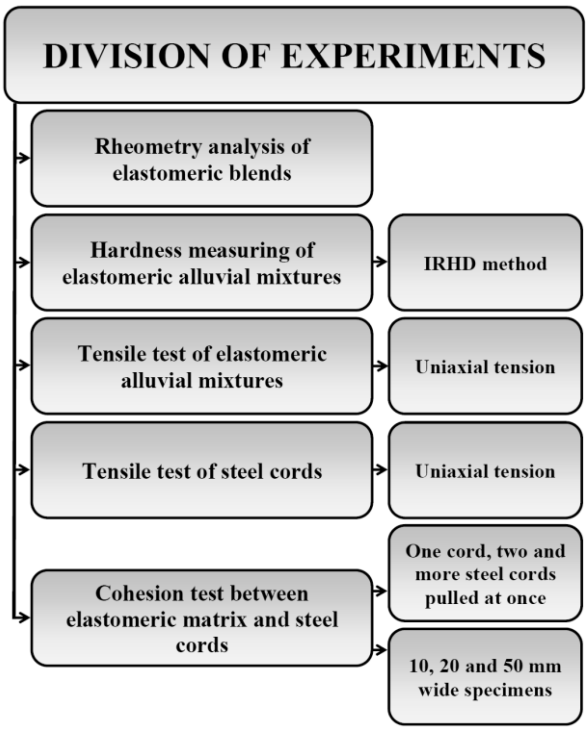

Fig. 1 Division of experiments
Obr. 1 Rozdelenie experimentov

Alluvial elastomeric mixtures

It is necessary to perform rheometric analysis of given rubber mixtures which are used for subsequent vulcanization of the elastomeric mixtures. We can determine the vulcanisation characteristics of the alluvial mixtures by using rheometric analysis performed in accordance to ISO 3417 [1].

From the results of rheometric analysis of given rubber mixture, the most important obtained data involve the time of vulcanization (30 minutes), temperature (150 °C) and pressure of vulcanizing press (20 MPa) [2]. The static universal testing machine Hounsfield H20K-W was used for the static tensile test using uniaxial load. The setting of loading rate was 25 mm/min and setting of the initial distance between the clamps was 80 mm [3, 4]. The tested samples of elastomeric alluvial mixture in form of the double sided blade before and after tensile test are shown in Fig. 2. Test samples after tensile test remained permanently deformed.

The measurement of hardness by IRHD method was also performed. Average value of hardness is 82.7 in relation to the all measurements performed for elastomeric alluvial mixtures.

Graphic dependency of loading force on elongation was transformed into diagram of tension dependence on elongation and it is shown in Fig. 3.

Fig. 2 Elastomeric samples: before tensile test (upper sample) and after rupture
Obr. 2 Elastomérne vzorky: pred ťahovou skúškou (hore) a po pretrhnutí

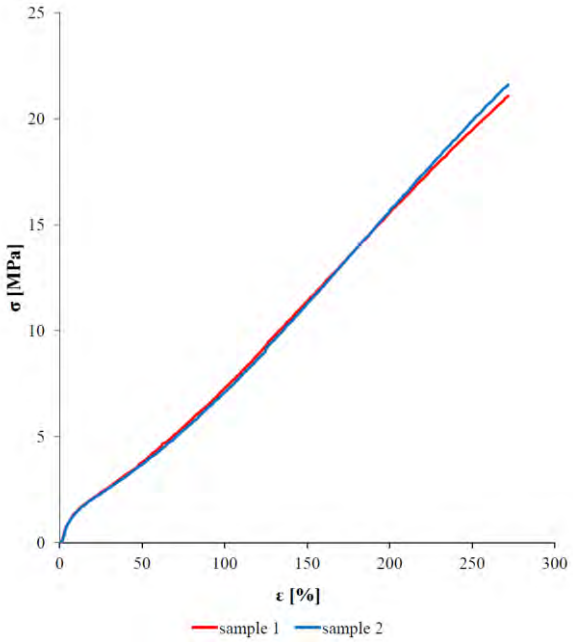

Fig. 3 Dependency of tension stress on elongation for alluvial mixtures
Obr. 3 Závislosť napätia od pomerného predĺženia pre nánosov zmesí

The graphic dependency of tensile force on the elongation was as a result of the tensile test and it was closely connected with the evaluation of the dependency of stress on relative elongation. Consequently, according to Mooney Rivlin two-parameter equation (1), the relationships for the calculation of the material parameters C_{10} and C_{01} were derived.
The Mooney-Rivlin two-parameter equation has the form [5]:

$$\sigma = \frac{F}{A_0} = 2C_{01}\left(\alpha - \alpha^{-2}\right) + 2C_{10}\left(1 - \alpha^{-3}\right) \qquad (1)$$

where σ – inside stress in the sample [MPa], F – loading force [N], A_0 – cross section of tested sample [mm^2], C_{10} and C_{01} – Mooney-Rivlin parameters [MPa], α – relative length [mm].
The simple modification of the equation (1) led to linearized form (2) hereinafter:

$$\frac{\sigma_i}{2\left(1 - \frac{1}{\lambda_i^3}\right)} = C_{01}\lambda + C_{10} \qquad (2)$$

where λ_i – relative deformation for individual values of λ [-].
Acquired Mooney-Rivlin parameters for alluvial mixtures used for rubberizing of steel cords in steel belts of tire casing are shown in the tab. 1.

Hutnické listy č. 3/2014, roč. LXVII
ISSN 0018-8069

Tab. 1 Values for alluvial mixtures for rubberizing of steel cords
Tab. 1 Hodnoty pre nánosové zmesi na pogumovanie oceľových kordov

Measured values				
sample	**F [N]**	**Δl [mm]**	**A_0 [mm^2]**	**l [mm]**
1	305.6	217.8	14.5	80.0
2	316.3	217.7	14.6	80.0
Calculated values				
sample	**σ [MPa]**	**ε [%]**	**C_{10} [MPa]**	**C_{01} [MPa]**
1	21.09	272.18	3.321	-1.965
2	21.62	272.16	3.583	-2.667

Examination of steel cords

The steel cords in form of the wire with construction 2×0.30 that are rubberized and used as steel reinforcements in the buffers of tire casings for passenger cars were examined by a static tensile test. Setting of the loading rate was 2 mm/min and the initial distance between the clamps was 200 mm. Dependencies of tension on the elongation for the steel cords are shown in Fig. 4.

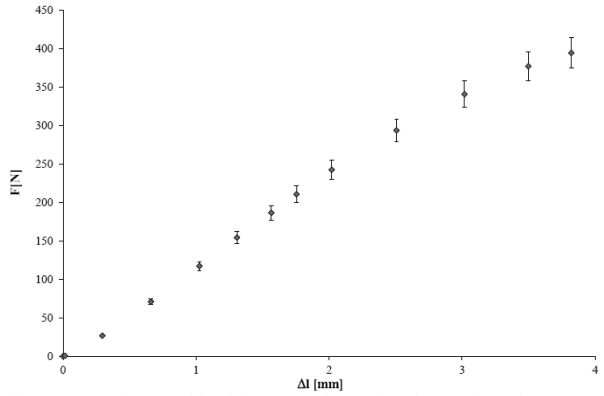

Fig. 4 Dependency of load force on elongation for steel cords
Obr. 4 Závislosť zaťažovacej sily od predĺženia pre oceľové kordy

Cohesion test for steel cords and elastomeric matrix

For the cohesion test relating to the elastomeric matrix and steel cords, modification had to designed and manufactured allowing performing this test by help of the device Hounsfield H20K-W because this device is not primarily assigned to perform such a test [6].

Fig. 5 shows cord – elastomeric samples in specific clamps manufactures for performance of the cohesion test relating to the steel cords and elastomeric matrix. The designation „A" represent single cord pulled from matrix, "B" represent two cords pulled from matrix at once and "C" represents three cords pulled from matrix at once. The length of steel cords pressed in the elastomer matrix was 10 mm, loading rate was 20 mm/min and initial length was 100 mm.

Fig. 5 Chosen samples of steel cord and elastomeric matrix
Obr. 5 Vybrané vzorky oceľových kordov a elastomérovej matrice

Dependencies of the force on elongation for chosen elastomeric samples are shown in Fig. 6. Curve "a" represents single cord pulled from matrix, curve "b" represents two cords pulled from matrix at once and curve "c" represents three cords pulled from matrix at once.

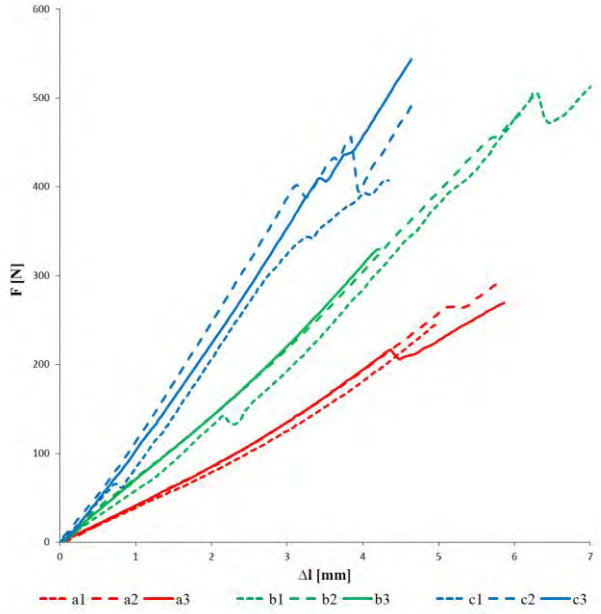

Fig. 6 Dependency of load force on elongation from cohesion test between steel cords and elastomeric matrix
Obr. 6 Závislosť zaťažovacej sily od predĺženia zo skúšky súdržnosti medzi oceľovými kordmi a elastomérom

Due to better knowledge on the behavior of system cord – elastomer, the samples with a length of steel cord pressed in a matrix with 20 mm and 50 mm were also subjected to the static test of cohesion.

Comparison of dependency of the force on elongation for chosen elastomeric samples with length 10, 20 and 50 mm of steel cord which was pressed into matrix is shown in Fig. 7. Curve "a" represents the cord pressed 10 mm into matrix, curve "b" represents the cord pressed 20 mm into matrix and curve "c" represents cord pressed 50 mm into matrix.

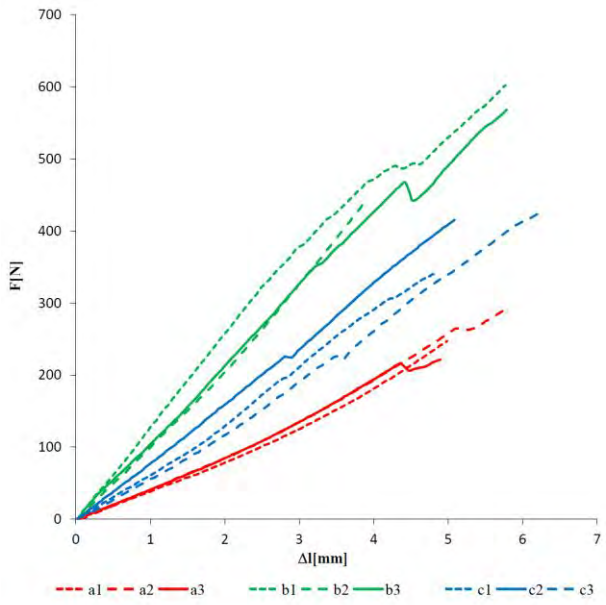

Fig. 7 Dependency of load force on elongation from cohesion test for various length of molding
Obr. 7 Závislosť zaťažujúcej sily od predĺženia zo skúšky súdržnosti pre rôzne dĺžky zálisu

Computational modeling of cord – elastomeric composites

Experimental data obtained from tensile test of steel cords and elastomeric blends and also from cohesion tests are used as input data for characterization of material parts in relation to the computational models. Except the basic model which is simplified untwisted model based on real model (Fig. 8), there are also few types of steel cord models including model of the same diameter and model of the same perimeter.

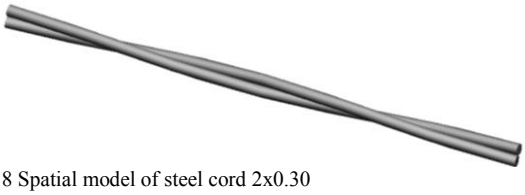

Fig. 8 Spatial model of steel cord 2x0.30
Obr. 8 Model oceľového kordu 2x0.30

Based on the simplification for fast response of calculations computational model was designed for the untwisted cord (Fig. 9). At the same time computational models are designed with usage of the several cords. The search for opportunity to shorten the calculation time in relation to the reduction of the number of finite elements led to utilization of symmetry with reference to the computational model planes.

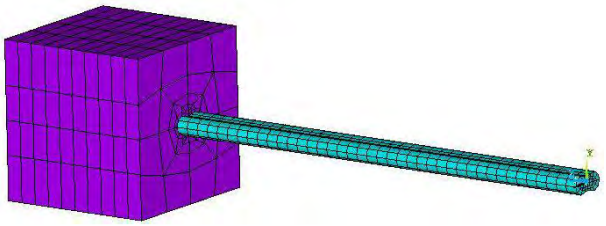

Fig. 9 Computational model of steel cord in elastomeric matrix
Obr. 9 Výpočtový model oceľového kordu v elatomérovej matrici

Conclusions

Selected elastomeric samples represent the alluvial mixtures for rubberizing of steel cords and these mixtures are commonly used in the production of steel cord belts for tire casings for passenger cars.
For the test of cohesion between the elastomeric matrix and steel reinforcement, it is necessary to know the tensile strength of steel cords so that we are able to specify whether there is the destruction of the adhesive bond in the system cord – elastomer or whether there is the rupture of reinforcement.
The results mentioned in the paper are the part of research including computational modeling relating to pulling of cords. The given research is also connected with verification of data based on experiments with the data based on computational modeling. Therefore, the obtained results will be used as verification parameters for the calculation of car tire casings or specific parts of tires, such as steel cord buffers and many others.

Literature

[1] International standard ISO 3417, Rubber – Measurement of vulcanization characteristics with the oscillating disc curemeter

[2[VIDO, P. et al. Investigation of Mechanical Properties of Composite System Cord-elastomer for Use of Computational Modeling of Tire Casing, In: Hutnické listy. 2013, vol. LXVI, issue 7, p.130-133. ISSN 0018-8069

[3] DRDÁKOVÁ, J., KRMELA, J. Mikrolokalita degradovaných oceľokordových nárazníkov v plášti radiálnych pneumatík. In: Preveda - interaktívna konferencia mladých vedcov, Slovak Republic, 2012, p. 75, [cited 10.9.2012]. http://www.preveda.sk/conference/viewer/id=518/presentation/, ISBN 978-80-970712-3-3

[4] STRUHARŇANSKÁ, M., PAJTÁŠOVÁ, M., KRMELA, J. Vybrané fyzikálno-mechanické vlastnosti polymérnych materiálov s plnivami na báze kremičitanov. In: Preveda - interaktívna konferencia mladých vedcov, Slovak Republic, 2012, p. 76, [cited 4.4.2012] <http://www.preveda.sk/conference/article/id=456/>, ISBN 978-80-970712-3-3

[5] ŠIMEK, I. Fyzika polymérov. Bratislava: CHTF-SVŠT, 1987, s.230

[6] VIDO, P. Systém kord – elastomér pri výrobe plášťa a jeho vplyv na životnosť pneumatiky. [diploma work]. University of Alexander Dubček in Trenčín, Faculty of Industrial Technologies, Slovak Republic, 2011, 68 p., (in Slovak)

Hutnické listy č. 3/2014, roč. LXVII
ISSN 0018-8069

Study of Mechanical Properties of NR/Biopolymer Blends

Štúdium mechanických vlastností zmesí NR/biopolymér

doc. Ing. Petra Skalková[1], PhD., Ivan Labaj[1]

[1]Alexander Dubček University of Trenčín, Faculty of Industrial Technologies in Púchov, I. Krasku 491/30, 020 01 Púchov, Slovak Republic

In recent years, bio-based materials have attracted much attention because there is pollution expansion by non-renewable resources in environment.. Cellulose is the most abundant natural polymer with very attractive properties, such as high mechanical strength, chemical stability and biodegradability. However, cellulose has some drawbacks. It is a very brittle and displays very low elongation even under dry conditions and it limits its applications. Blending solves this problem by offering a simple and relatively cheap way to develop novel materials with a number of valuable properties. Natural rubber (NR) displays multiple functions, such as good wet grip, excellent flexibility and high damping characteristics. There is the possibility of hydrogen bonding between the complementary binding sites of cellulose and NR and could affect the blend properties.

Keywords: *polymer blends, mechanical properties, cellulose, natural rubber*

Syntetické polymérne materiály sú dnes široko využívané v mnohých oblastiach priemyslu. Popri výhodách, ktoré sú dané ich vlastnosťami, spôsobujú aj nemálo problémov. Platí to najmä o obalových materiáloch vyrobených z polymérov, ktoré zaťažujú životné prostredie. Ako odpad sú veľmi odolné klimatickým vplyvom a biologickým procesom, a preto tieto odpady často trvalo končia v životnom prostredí. Problémy aspoň čiastočne riešia materiály, ktoré podliehajú biologickému rozkladu, teda sú biodegradovateľné. Takéto materiály je možné po použití zlikvidovať bezpečne a relatívne rýchlo biologickou cestou na prírodné zložky. Biodegradovateľné polyméry poskytujú kvalitatívne nové možnosti zneškodňovania resp. využitia produktov z polymérov ako druhotnej suroviny. Pre ich výrobu môžu byť použité poľnohospodárske produkty a odpady alebo obnoviteľné suroviny z biomasy. Práca sa zaoberá prípravou zmesí prírodného kaučuku (NR) a celulózy (CEL) v množstvách od 0 do 55 dsk za a bez prítomnosti tenzidu, dodecyl sulfát sodný (SDS). Množstvo tenzidu SDS v zmesi bolo 0 a 3 dsk. Na pripravených zmesiach sa študoval vplyv celulózy a tenzidu SDS na mechanické vlastnosti, ako je pevnosť v ťahu, ťažnosť a tvrdosť pred a po termooxidačnom starnutí. Najvyššie hodnoty pevnosti v ťahu a ťažnosti dosahovali neplnené zmesi NR/0 dsk CEL/3 dsk SDS a NR/0 dsk CEL/0 dsk SDS pred termooxidačným starnutím. Po termooxidačnom starnutí sa pevnosť v ťahu a ťažnosť neplnených zmesí znížila skoro o polovicu. Z plnených zmesí mala najvyššiu pevnosť v ťahu pred termooxidačným starnutím zmes NR/27,6 dsk CEL/3 dsk SDS. Po termooxidačnom starnutí sa pevnosť v ťahu plnených zmesí zvyšovala s množstvom plniva v zmesi. Tvrdosť zmesí sa so zvyšujúcim množstvom plniva za a bez prítomnosti tenzidu SDS zvyšovala. Najvyššiu tvrdosť dosahovali zmesi s najväčším obsahom plniva NR/55 dsk CEL/0 dsk SDS a NR/55 dsk CEL/3dsk SDS.

Kľúčové slová: *polymérne zmesi, mechanické vlastnosti, celulóza, prírodný kaučuk*

The use of fillers in rubber is almost as old as the use of rubber itself. As soon as the rubber-mixing machinery was developed, fillers were added to natural rubber with the aim to improve certain properties and to reduce the price of the rubber compound [1]. Carbon black is the most important reinforcing agent used in the rubber industry, but because of its origin from petroleum, this filler causes pollution and gives black color to rubber. As a result, in the last two decades, the research was focused on the development of other reinforcing agents derived from inorganic [2] and natural organic [3] materials to replace carbon black in rubber compounds. The level of reinforcement of the particulate fillers depends on the shape of the hard domains as well as on the fillers – elastomeric matrix interactions, the principal requirements for filler reinforcement – sufficiently small particle size and a good homogeneous dispersion [4].

In recent years, biopolymers have attracted more and more interest due to increasing environmental concern and decreasing fossil resources. This evolution motivates academic and industrial researchers to develop novel materials labelled as "environmentally-friendly", i.e., materials produced from alternative resources, with lower energy consumption, bio-degradability and non-toxicity. Since biopolymers are biodegradable and the main products are obtained from renewable resources, such as agro resources, they represent an interesting alternative route to common non-degradable polymers for short-life range applications (packaging, agriculture, biomedical etc.). Nevertheless, until now, some of the biopolymers are

costly compared to conventional thermoplastic and they are sometimes too weak for practical use. Therefore, it is necessary to extend the search for fully biodegradable polymers which are economically accessible and industrially accepted. In the accordance with the current environmental concerns, the researchers are interested in biocomposite area which is a solution for various industrial as well as ecological problems. Moreover, since industry is concerned with sustainable developments, the production cost of biocomposites is reduced and it could allow strong developments of biopolymers-based materials [5].

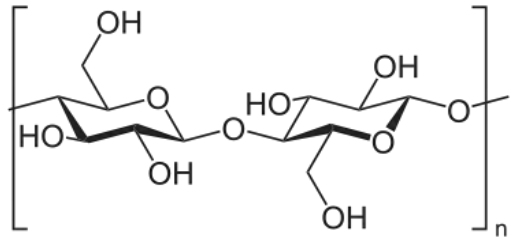

Fig. 1 Structure of cellulose
Obr. 1 Štruktúra celulózy

Natural and synthetic polymers containing hydroxyl groups, such as cellulose or poly (vinyl alcohol), have a great affinity for water owing to the formation of hydrogen bonding that swells the polymers and eventually even can dissolve them. The presence of a small quantity of water in the NR–Cell composites can also plasticize the cellulose and this effect markedly affects the mechanical properties of the blends as a result of the increase of the mobility of the cellulose chains [6].

Experiment

Materials

Natural rubber SMR 10 (NR) was purchased from Kuala Lumphur, Malaizia. Sodium dodecyl sulfate (SDS) was supplied from Aldrich. Greencel GW 600, cellulose fibres – Cellulose (CEL) 99.5 %, bulk density 70 – 90 $g.l^{-1}$ was supplied from Bukóza Invest, Ltd.

Preparation of NR/CEL blends

Cellulose was melt-blended with NR in Brabender Plasti – Corder PLE 331. Mixing was performed at 80 and 90 °C and 50 rpm. The contents of CEL were from 0 to 55 parts per hundred rubber (phr), respectively. SDS was used at two different amounts, namely 0 and 3 phr. Blends were vulcanized on the basis of the following formula: stearic acid, ZnO, Flavex, N-tert-Butyl-2-benzothiazolesulfenamide and sulphur. The temperature of vulcanization was 150 °C.

Mechanical properties

Measurements of the mechanical properties, such as tensile strength and elongation at break, were performed by the Instron Corporation Material Testing System 1.04, at 5 $mm.min^{-1}$ crosshead speeds, before and after thermo-oxidative ageing. Five measurements of each sample were performed, the average obtained values are reported in Fig. 4 to 7. The maximum percentage error did not exceed 8.2 %.

Results and discussion

Prepared blends of NR/CEL/SDS were tested to obtain the mechanical properties (tensile strength, elongation at break), hardness before and after thermo-oxidative ageing. Amount of filler (CEL) in natural rubber was 27.5; 30; 35; 40; 45; 50; 55 phr. Sodium dodecyl sulfate (SDS) was used in 0 and 3 phr.

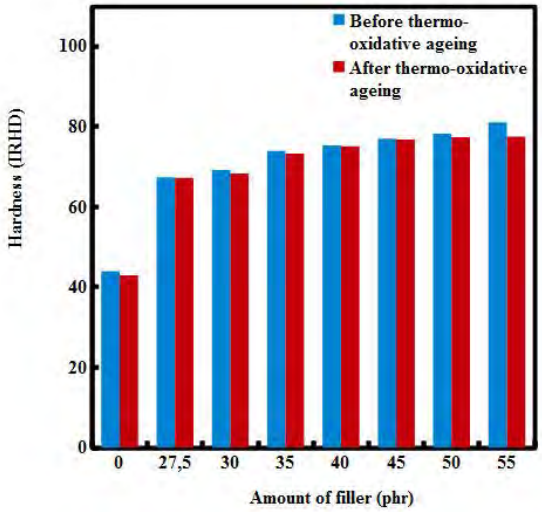

Fig. 2 Hardness values of NR/CEL blends without SDS, before and after thermo-oxidative ageing
Obr. 2 Hodnoty tvrdosti zmesí NR/CEL bez SDS pred a po termooxidačnom starnutí

From Fig. 2 can be seen that the hardness of elastomeric blends was increased with increasing amount of filler (cellulose) in NR. The filler in blends causes higher stiffness which is expressed by higher hardness of the blends. The lowest value of hardness was exhibited by unfilled blend without SDS (44 IRHD). The hardness of filled blend NR/27.5 phr CEL/0 phr SDS was increased by 23 IRHD in comparison to unfilled blend. The highest value of hardness before thermo-oxidative ageing was observed for NR blend with 55 phr cellulose and 0 phr SDS (81 IRHD), it was increased by almost 40 IRHD compared to unfilled blend. Hardness of the blends was decreased slightly after thermo-oxidative ageing. It can be caused by the effect of temperature on filler and on blend too. Temperature may evocate the break down of the inter-chains in cured systems. From Fig. 2, we can see that thermo-oxidative ageing did not have a strong effect on hardness of the blends. Hardness is affected by amount of filler.

In Fig. 3 we can see comparison of hardness of blends with different amount of filler and 3 phr of SDS, before and after thermo-oxidative ageing. Hardness of blends filled with cellulose and 3 phr of SDS was increased in comparison to blends without SDS. Unfilled blend with

Hutnické listy č. 3/2014, roč. LXVII
ISSN 0018-8069

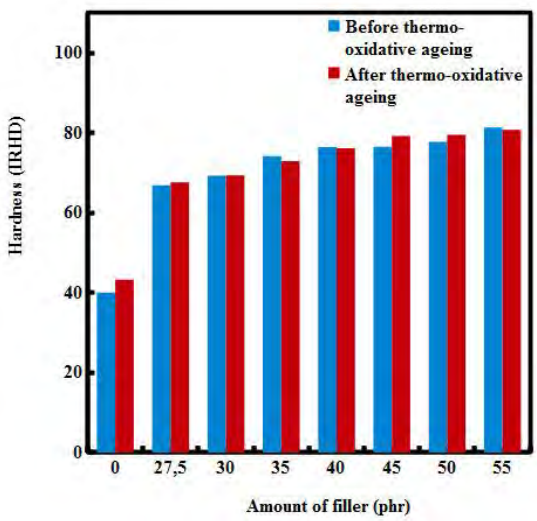

Fig. 3 Hardness values of NR/CEL blends with 3 phr of SDS, before and after thermo-oxidative ageing
Obr. 3 Hodnoty tvrdosti zmesí NR/CEL s 3 dsk SDS pred a po termooxidačnom starnutí

3 phr of SDS had 40 IRHD hardness. In NR blend with lowest amount of filler (27.5 phr of CEL) and 3 phr of SDS, the hardness increased by 20 IRHD. The highest hardness (81 IRHD) is exhibited by NR blend with 55 phr of CEL and 3 phr of SDS, before thermo-oxidative ageing. During curing process, the filler interacts with the curing system analogously to accelerator and it causes shorter inter-chains and their higher density. From Fig. 3 can be seen that presence of SDS in blend NR/CEL did not affect hardness before thermo-oxidative ageing. Tenside SDS plays an important role during thermo-oxidative ageing. In Fig. 2 and 3 we can see that hardness of blends without SDS, after thermo-oxidative ageing, was decreased in comparison to blends with 3 phr of SDS. Oxidative degradation of polymers can be in progress by two mechanisms [7]. In the first mechanism, polymers chains are broken down and it causes softening and overall decrease in strength of blend. In the second mechanism, random inter-chains are created in elastomer. It causes stiffening and brittleness. Presence of SDS probably causes oxidative degradation by the second mechanism in blends of NR/CEL/ 3 phr of SDS. Increase of hardness after thermo-oxidative ageing in blends NR/CEL/3 phr SDS is caused by random inter-chains. The blends are harder and more brittle. Hardness of blend NR/35 phr CEL/3 phr SDS after thermo-oxidative ageing was decreased. It can be caused by insufficient dispergation of tenside SDS. Thermo-oxidative ageing of this blend was progressed by first mechanism.

Fig. 4 can exhibits tensile strengths for NR blends containing various amounts of filler and SDS before thermo-oxidative ageing. The highest tensile strength was observed for unfilled blend without SDS (14.1 MPa). Unfilled blend has higher elasticity than blends filled with cellulose. The tensile strength of blends was decreased with increasing amount of filler. The elasticity was decreased by adding cellulose into the NR blends. According to Fig. 4, the highest tensile strength was observed blend NR/30 phr CEL/0 phr SDS (6.1 MPa). The tensile strength was decreased in blends with higher filler content than 30 phr.

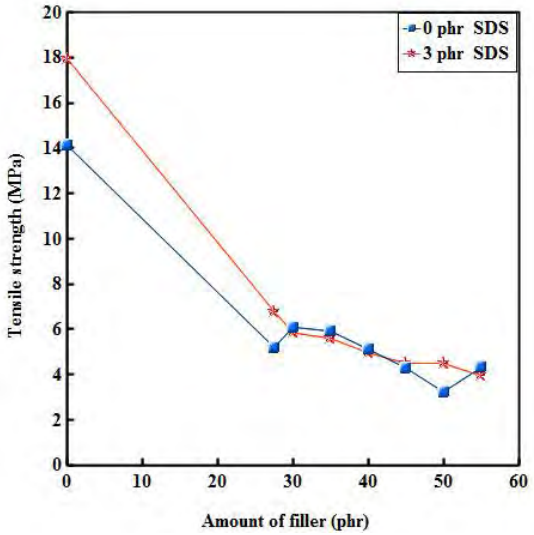

Fig. 4 Tensile strength of NR/CEL/SDS blends before thermo-oxidative ageing
Obr. 4 Pevnosť v ťahu NR/CEL/SDS zmesí pred termooxidačným starnutím

The filler blended with NR has a function of barrier at diffusion of microfissures. Blend NR/27.5 phr CEL/0 phr SDS had lower tensile strength than blend with 30 phr of cellulose. In comparison to unfilled blend without SDS (tensile strength 14.1 MPa), unfilled blend with 3 phr of SDS displays higher tensile strength (17.9 MPa). It is probably caused by tenside SDS. Tenside SDS extends inter-chains created during the curing and they support higher deformation. For NR blends filled with different amounts of cellulose and 3 phr of SDS, the tensile strength was decreased. Blend NR/27.5 phr CEL/3 phr SDS exhibits tensile strength 6.8 MPa. From Fig. 4 can be seen that SDS does not have distinct influence on tensile strength of filled blends. The tensile strength of blends NR/CEL/SDS after thermo-oxidative ageing can be seen in Fig. 5. The lowest value of tensile strength (2.2 MPa) after thermo-oxidative ageing was observed for unfilled NR blend without SDS.

Thermo-oxidative ageing effects degradation of natural rubber in blend. Inter-chains in curing system are broken down. Blends have lower tensile strength than the blends before thermo-oxidative ageing. Blends filled with cellulose have higher tensile strength values than unfilled blend. Filler in network of vulcanisates acts as barrier at deformation. Filler present in blend causes enhancing of crosslink density but it shortens it. Therefore, probably blends filled with cellulose degrade slower than unfilled blend. In comparison to filled blends before thermo-oxidative ageing, tensile strength of blends after thermo-oxidative ageing was increased with increasing of amount of filler. The highest tensile strength after thermo-oxidative ageing was observed for blend NR/55 phr CEL without SDS (3.9 MPa). It can becaused by effect of filler in blend during hermo-oxidative a geing (mentioned above). Blends NR/CEL

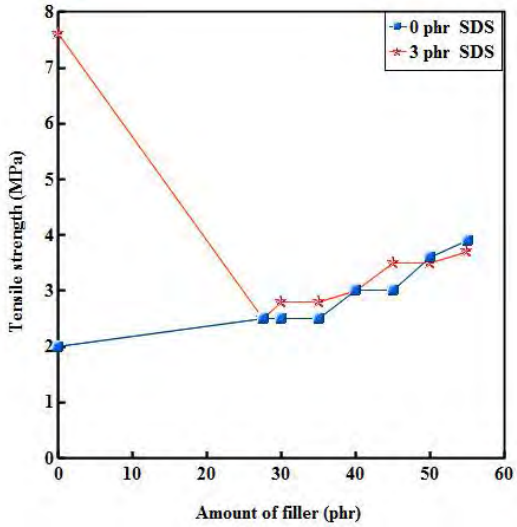

Fig. 5 Tensile strength of NR/CEL/SDS blends after thermo-oxidative ageing
Obr. 5 Pevnosť v ťahu NR/CEL/SDS zmesí po termooxidačnom starnutí

without SDS with lower cellulose content than 55 phr exhibit lower values of tensile strength in comparison to blend NR/55 phr CEL without SDS. Unfilled blend with 3 phr of SDS had the highest value of tensile strength (7.6 MPa) after thermo-oxidative ageing. In comparison to unfilled NR blend without SDS after thermo-oxidative ageing, NR blend with 3 phr of SDS had higher tensile strength after thermo-oxidative ageing, as can be seen in Fig. 4 and 5. Presence of SDS in NR/CEL blends causes that oxidation progresses by the second mechanism (mentioned above). There is the occurrence of random inter-chains in the elastomer during thermo-oxidative ageing. Inter-chains created by curing in unfilled NR blend without SDS were broken down during ageing. The highest value of tensile strength was observed for NR/55 phr CEL/3 phr DSS blend (3.7 MPa). From Fig. 5 can be seen, that the presence of SDS in blend had significant effect only on unfilled blends. Filled bends with 3 phr of SDS have similar values of tensile strength as filled blends without SDS.

The elongation at break of blends NR/CEL with 0 and 3 phr of SDS before and after thermo-oxidative ageing can be seen in Fig. 6 and 7. The highest elongation at break as well as high elasticity was observed for unfilled blend without SDS (589.4 %). Addition of filler into NR blends decreases elasticity and it causes decrease in elongation at break. In relation to filled blends, the blend NR/30 phr CEL/0 phr SDS had the best elongation at break (293.4 %). At this amount of filler, it indicates stiffening effect but blend is elastic sufficiently. Before thermo-oxidative ageing, unfilled blend with 3 phr of SDS had higher elongation at break (629.8 %) than unfilled NR blend without SDS. Tenside SDS is accountable for creation of longer NR-sulfur inter-chains during curing process which causes higher elasticity. By adding filler to blend with 3 phr of SDS, the elongation at break decreases similarly in comparison to blends without SDS. Filled blends with 3 phr of SDS exhibited higher values of elongation at break before thermo-oxidative ageing than blends without SDS. This was probably caused by presence of tenside SDS and its effect on inter-chains length. The lowest value of elongation at break was observed for filled blend NR/55 phr CEL/3 phr SDS (193.4 %).

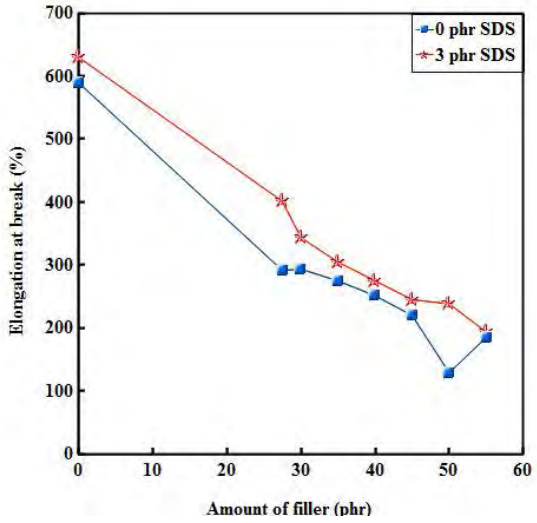

Fig. 6 Elongation at break of NR/CEL/SDS blends before thermo-oxidative ageing
Obr. 6 Ťažnosť NR/CEL/SDS zmesí pred termooxidačným starnutím

In comparison to blend NR/55 phr CEL/0 phr SDS, elongation at break of blends before thermo-oxidative ageing is almost identical. The elongation at break for NR/CEL/SDS blends after thermo-oxidative ageing can be seen in Fig. 7. The highest elongation at break after thermo-oxidative ageing was observed for unfilled blend without SDS. Thermo-oxidative ageing causes degradation, break down of polymer chains, but the blend keeps its elasticity. The elongation at break of blends filled by cellulose was decreased. Blend NR/35 phr CEL/0 phr SDS exhibits increase in elongation at break after thermo-oxidative ageing. It can be caused by part of filler amount which was not surrounded by inter-chains in vulcanizate after thermo-oxidative ageing.

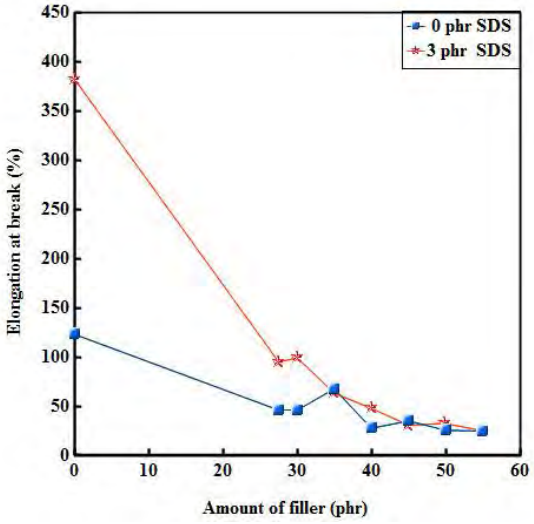

Fig. 7 Elongation at break of NR/CEL/SDS blends after thermo-oxidative ageing
Obr. 7 Ťažnosť NR/CEL/DSS zmesí po termooxidačnom starnutí

Hutnické listy č. 3/2014, roč. LXVII
ISSN 0018-8069

The highest value of elongation at break (382 %) was observed for unfilled blend with 3 phr of SDS after thermo-oxidative ageing. Effect of SDS after thermo-oxidative ageing caused that blend kept its elasticity. Elongation at break of blends was decreased by adding of hydrophilic filler. In filled blends, the best value of elongation at break was obtained in the case of NR/30 phr CEL/3 phr SDS blend. Amount of filler (30 phr) along with SDS (3 phr) partially limits the effect of filler against deformation. Blends with 3 phr of SDS and amount of filler up to 35 phr have higher values of elongation at break than blends without SDS.

Conclusions

The following conclusions can be drawn for the effectiveness of using cellulose and sodium dodecyl sulfate in natural rubber blends. Decreases of tensile strength and elongation at break were observed due to the insifficient interphase formation between cellulose and NR matrixes in order to obtain a poor interfacial adhesion. Overall, the tensile strength and elongation at break was decreased with cellulose loading before thermo-oxidative ageing, whereas the hardness was increased for all types of rubber blends. After thermo-oxidative ageing, tensile strength was increased with cellulose loading.

Literature

[1] ARROYO, M., LÓPEZ-MACHADO, M.A., HERRERO, B. Organo-montmorillonite as substitute of carbon black in natural rubber compounds. *Polymer* 44, 2003, p. 2447–2453

[2] MEERA, A.P., SAID, S. Nonlinear Viscoelastic Behavior of Silica-Filled Natural Rubber Nanocomposites. *Journal of Physical Chemistry C* 113, 2009, p. 17997–18002

[3] ANGELLIER, H., MOLINA-BOISSEAU, S., DUFRESNE, A. Mechanical properties of waxy maize starch nanocrystal reinforced natural rubber. *Macromolecules* 38(22), 2005, p. 9161–9170

[4] DUFRESNE, A. Comparing the mechanical properties of high performances polymer nanocomposites from biological sources. *Journal of Nanoscience and Nanotechnology* 6, 2006, p. 322–330

[5] ŠTURCOVA, A., DAVIES, G.R., EICHHORN, S.J. Elastic modulus and stress-transfer properties of tunicate cellulose whiskers. *Biomacromolecules* 6, 2005, p. 1055–1061

[6] MOHANTY, A.K, MISRA, M, HINRICHSEN, G. Biofibres, biodegradable polymers and biocomposites: an overview. *Macromolecular Materials and Engineering* 276, 2000, p. 1–24

[7] MALÁČ, J. *Gumárenská technologie*, FT, UTB, Zlín, 2005

Utilization of Natural and Ca-clinoptilolite in the Function of Sorbent of Zinc from Technological Wastewater – Effect of Time and pH

Využitie prírodného a Ca-klinoptilolitu vo funkcii sorbenta zinku z technologickej odpadovej vody – vplyv času a pH

Ing. Lenka Špániková[1], Ing. Michaela Ďurčeková[1], prof. Ing. Darina Ondrušová[1], PhD., Ing. Slavomíra Domčeková[1], Ing. Katarína Holcová[1]

[1]Alexander Dubček University of Trenčín, Faculty of Industrial Technologies in Púchov, I. Krasku 491/30, 020 01 Púchov, Slovak Republic

The given paper is focused on the study of the removal of zinc from technological wastewater using natural clinoptilolite and modified Ca-clinoptilolite depending on time and pH. Samples of technological wastewater came from rubber industry, specifically from cooling baths of rubber products. Adsorbents were characterized by FTIR spectroscopy. The samples of wastewater were analyzed to determine the exact concentration of zinc by atomic absorption spectrometer. Efficiency of sorption was calculated on the basis of the results of concentration before and after sorption. Obtained results of effect of time on sorption show the high efficiency of sorption (more than 90%) after 1 hour of removal of zinc. Based on results of effect of pH, it can be concluded that sorption process can be effectively carried out not only at certain pH value but also in wide range of pH. Higher efficiency for Ca-clinoptilolite can be also observed. Thus, clinoptilolite from Nižný Hrabovec is excellent sorbent for zinc from technological wastewater and it can be applied in industrial wastewater treatment.

Keywords: *zinc, technological wastewater, clinoptilolite, sorption process, FTIR spectroscopy*

Ťažké kovy ako zinok, meď, olovo sú toxické, preto ich produkcia a vypúšťanie do životného prostredia sú neprípustné. Tieto prvky sa však často využívajú pri rôznych činnostiach v priemysle, pričom vznikajú odpady a odpadové vody s obsahom týchto prvkov. V gumárenskom priemysle vznikajú odpadové vody obsahujúce zlúčeniny zinku. Bežné metódy čistenia odpadových vôd sú v prípade zinku málo efektívne, preto sú skúmané nové možnosti riešenia problému odstraňovania zinku z odpadových vôd. Prezentovaná práca sa zaoberá znižovaním obsahu zinku z odpadových technologických vôd pochádzajúcich z chladiacich vaní gumárenských výrobkov s využitím sorbentov na báze prírodného zeolitu. V práci bol vo funkcii sorbentu zinku použitý prírodný klinoptilolit a pripravený Ca-klinoptilolit. Klinoptilolit je prírodný materiál patriaci medzi zeolity. Jeho dutinová štruktúr, pozostávajúca zo vzájomne prepojených tetraédrov SiO_4 a AlO_4, obsahuje slabo viazané a ľahko vymeniteľné katióny alkalických kovov a kovov alkalických zemín. Mnohé štúdie a výskumy preukázali jeho výborné iónovýmenné a sorpčné vlastnosti, ktoré súvisia práve s jeho unikátnou štruktúrou a s prítomnosťou vymeniteľných katiónov. V práci sme sledovali vplyv času sorpcie, ako aj vplyv pH odpadovej vody na účinnosť sorpcie. Na základe koncentrácie zinku vo vzorkách odpadovej vody pred a po sorpcii stanovenej atómovou absorpčnou spektrometriou boli vypočítané účinnosti sorpcie. Prírodný i modifikovaný klinoptilolit boli charakterizované IČ spektrometriou. Výsledky účinnosti sorpcie zinku v závislosti od času poukazujú na vysokú účinnosť sorpcie už po prvej hodine sorpčného procesu. Na základe výsledkov vplyvu pH na účinnosť sorpcie, možno konštatovať, že sorpčný proces prebieha veľmi efektívne v širšom rozmedzí pH. Z hľadiska porovnania sorpčných vlastností prírodného a Ca-klinoptilolitu možno pozorovať vyššiu sorpčnú účinnosť pre Ca-klinoptilolit.

Kľúčové slová: *zinok, technologická odpadová voda, klinoptilolit, sorpčný proces, FTIR*

Environmental problems have acquired a worldwide significance with increasing pollution of the air, soil and water. Heavy metals from industrial activities are the frequent source of water pollution. Heavy metals such as zinc, copper, lead are toxic elements for human beings and animals, however, their concentrations in the surface waters increase as a result of industrial activities from day to day [1 – 3].

Heavy metals are not biodegradable and tend to accumulate in living organisms causing various disease and disorders [4].

Zinc is an essential mineral that is naturally present in some foods and it is involved in numerous aspects of cellular metabolism. Permanent overdoses may negatively influence human and animal health and if the concentrations of zinc are beyond the permitted limit,

Hutnické listy č. 3/2014, roč. LXVII
ISSN 0018-8069

zinc may even be toxic. Toxicity is low for humans and animals, but phytotoxicity may not be negligible.

The physicochemical and biological methods are among many methods which are available for removal of heavy metals. These methods are not cost effective for removal of heavy metals because of the non-degradability properties of heavy metals.

Therefore, wastewater contaminated by heavy metals needs an effective and affordable technological solution [2, 5]. The adsorption has been shown to be good method when low-cost materials are used as adsorbents [4 – 6]. This process can reduce the concentration of metal ions very effectively. In the last years, there was the increase observed in relation to utilization of natural zeolites for control of the pollution with heavy metal ions. Zeolites have high sorption capacity, large surface areas and selectivity to remove unwanted metal ions and these properties make zeolites favourable for wastewater treatment. Zeolites are crystalline aluminosilicates. There are about 80 natural zeolites and 100 synthetic zeolites which are known so far. There are zeolite deposits in more than 50 countries. The clinoptilolite is the well-know natural zeolite. Clinoptilolite belongs to heulandite group of minerals and its fundamental building block is tetrahedron of four oxygen atoms surrounding a relatively small silicon or aluminum atom [7, 8]. Clinoptilolite carries a negative charge in the structure and it originates from substitution of silica (Si^{4+}) with aluminium (Al^{3+}). These negative charges are balanced by exchangeable alkaline and alkaline earth metal cations (such as Na^{+}, K^{+}, Ca^{2+} and Mg^{2+}). The physical structure is porous while the pores are enclosed by interconnected cavities in which the metal ions and water molecules are contained [1, 8].
The results of many researchers indicated that the clinoptilolite can be used for the removal of the heavy metals (such as zinc, cooper, nickel, chromium) from industrial wastewater [1, 2, 4, 9]. Other author found out that clinoptilolite can be used in wastewater purification in order to remove toxic and radioactive nuclides (such as Cs, Sr, U) [10 – 12].

Rakic et al. investigated affinity of clays and clinoptilolite for the adsorption of salicylic acid, acetylsalicylic acid, atenolol (pharmaceuticals) from aqueous solutions [13].

In this study, there is the investigation of the zinc sorption by natural and Ca-clinoptilolite depending on time of sorption as well as on pH value of technological wastewater.

The zeolite used in this study is clinoptilolite from deposits in Nižný Hrabovec in Slovakia. Deposit contains from 40 to 70 % of this zeolite mineral. Slovak zeolite has very good thermal properties and radiation stability. Composition of natural clinoptilolite was investigated by electron microanalysis (tab.1) [14, 15].

Tab. 1 Composition of clinoptilolite sample
Tab. 1 Zloženie klinoptilolitu

Composition [%]	
SiO_2	73.94
Al_2O_3	12.31
Na_2O	0.5
K_2O	3.98
CaO	5.24
Fe_2O_3+FeO	3.48
TiO_2	-
MgO	0.75

Experiment

The clinoptilolite in natural form and its chemically modified form were used for experiments. Calcium chloride was used for the chemical treatment. The technological wastewater originated from cooling baths in rubber industry. Initial concentration of zinc in samples of wastewater was determined by atomic absorption spectrometer (AAS) using the air-acetylene flame.

Adsorbent treatment

At first, clinoptilolite was processed by crushing and sieving to obtain the particle size 0.063-0.16 mm.

Exchanged form (Ca^{2+}) of clinoptilolite was prepared by ion-exchange between 1M calcium chloride solution and natural clinoptilolite. Process of ion-exchange took 24 hours at determined rate of speed of 250 rpm. After filtration, the exchanged form was washed with distilled water to a negative reaction for Cl^{-1} and then, it was dried at 100°C for 3 hours.

Adsorbents characterization

The infrared spectra of natural clinoptilolite and Ca-clinoptilolite were recorded by FTIR Spectrometer Tensor 27 for the region 400-4000 cm^{-1}. Infrared spectrum of natural clinoptilolite is presented in fig. 1 and selected bands of the IR spectra of natural and Ca-clinoptilolite are shown in tab. 2

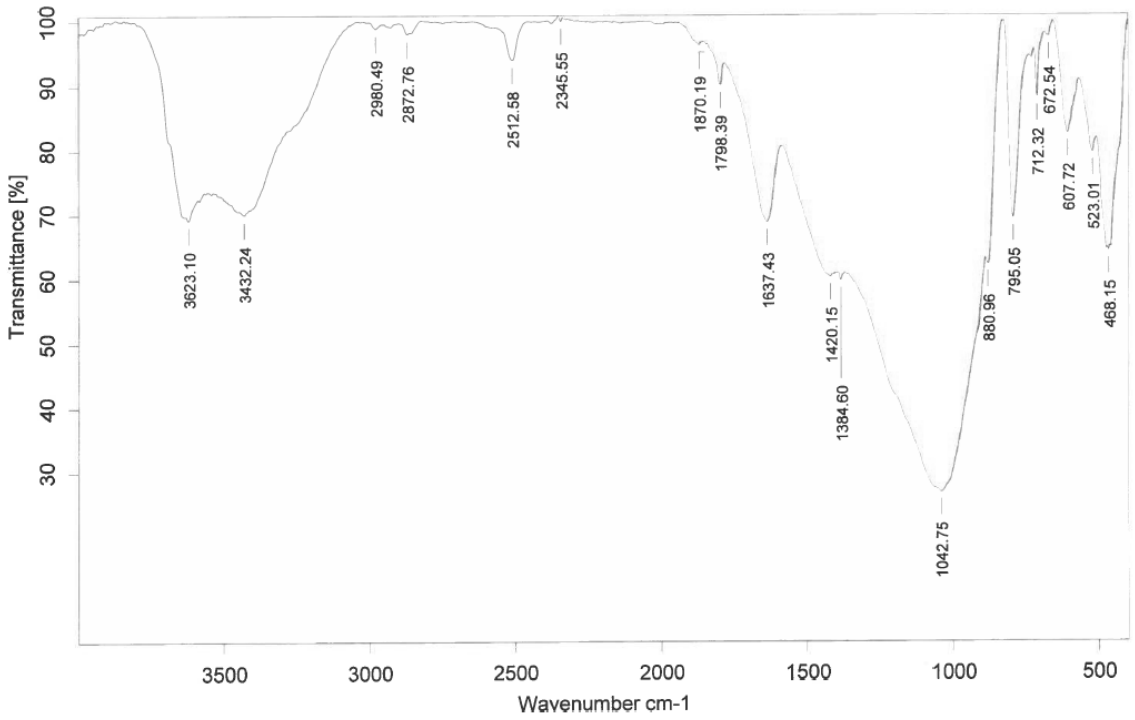

Fig. 1 Infrared spectrum of natural clinoptilolite
Obr. 1 Infračervené spektrum prírodného zeolitu

Tab. 2 Selected bands/vibrations of FTIR spectra of natural and Ca-clinoptilolite
Tab. 2 Vybrané typy vibrácií/skupín prírodného a Ca-klinoptilolitu

Type of vibration/band [cm^{-1}]	Natural clinoptilolite [NC]	Ca-clinoptilolite [CaC]
ν (O-H)	3623.10 3432.24	3653.49 3400.51
δ(H-O-H)	1637.43	1639.03
ν(Si-O) as.	1042.75	1048.87
ν (T-O) s.	795.05 712.32	797.22 -
δ (T-O)	672.54 523.01 468.15	673.43 521.39 474.35

*T = Si, Al

Infrared spectroscopy showed presence of typical bands which can be commonly observed for natural clinoptilolite. Bands in the region 3400-3700 cm^{-1} correspond to asymmetric and symmetric OH stretching vibrations (3623 cm^{-1}, 3432 cm^{-1} NC, 3653 cm^{-1}, 3400 cm^{-1} CaC) [16]. The FTIR bands (1637 cm^{-1} NC, 1639 cm^{-1} CaC) belong to the bending mode of the water [17]. The adsorption peaks at 1040-1070 cm^{-1} correspond to Si-O asymmetric stretching vibrations (1042 cm^{-1} NC, 1048 cm^{-1} CaC) and symmetric stretching vibrations of SiO_4 and AlO_4 tetrahedra are presented by peaks at 795 cm^{-1}, 712 cm^{-1} for NC and 797 cm^{-1} for CaC. Bending vibrations of SiO_4 and AlO_4 tetrahedra are represented by adsorption peaks at 672 cm^{-1}, 523 cm^{-1} and 468 cm^{-1} for NC and 673 cm^{-1}, 521 cm^{-1} a 474 cm^{-1} for CaC, respectivelly [18, 19].

The experiments of sorption – effect of time

The effect of time on zinc removal from technological wastewater was investigated in the range 1, 2, 4, 6, 12 hours. For zinc removal depending on time, 300 ml of wastewater sample containing zinc was mixed with 4g of natural clinoptilolite for specified time interval at rate of speed of 300 rpm and pH of samples was 5.56.
The same procedure was used for zinc removal in relation to prepared Ca-clinoptilolite.

The experiments of sorption – effect of pH

The effect of pH on zinc removal from wastewater was investigated in the range 2 - 6. The pH of wastewater samples containing zinc was adjusted by appropriate amount of H_2SO_4. Exact pH of the solutions was determined using the pH meter. For zinc removal depending on pH, 50 ml of sample was mixed with 0.8 g of natural clinoptilolite (or Ca-clinoptilolite) for 4 hours at rate of speed of 300 rpm.

After each experiment, the adsorbent was removed by filtration while the exact metal concentration was determined in the filtrate by AAS.

Results and discussion

The efficiency of sorption process was calculated on the basis of the measured results using the following equation:

Hutnické listy č. 3/2014, roč. LXVII
ISSN 0018-8069

$$efficiency\ of\ sorption\ (\%) = \frac{c_0 - c_t}{c_0} \cdot 100 \qquad (1)$$

where c_0 – initial zinc concentration in sample (mg/l), c_t – concentration of zinc in time t (mg/l)

Results of efficiency of zinc sorption in relation to the natural and modified clinoptilolite depending on time

Figs. 2 and 3 illustrate the effect of sorption time on removal of zinc in relation to the natural clinoptilolite and modified Ca-clinoptilolite. Efficiency of sorption process was calculated using eq.1. The conditions of sorption are given in the figure legends.

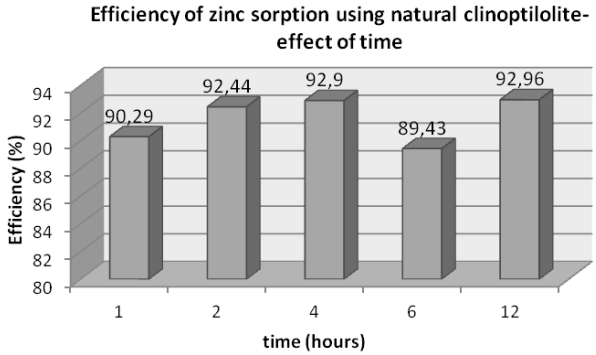

Fig. 2 Effect of time on zinc sorption using natural clinoptilolite (initial zinc concentration = 334 mg/l, pH = 5.56, rpm = 300)
Obr. 2 Vplyv času na sorpciu zinku na prírodný klinoptilolit (počiatočná koncentrácia zinku = 3,34 mg/l, pH = 5,56, rpm = 300)

As can be seen, in the case of evaluation of sorption using natural clinoptilolite, high efficiency of sorption occurred within the first one hour of contact. This result shows high effectiveness of process.

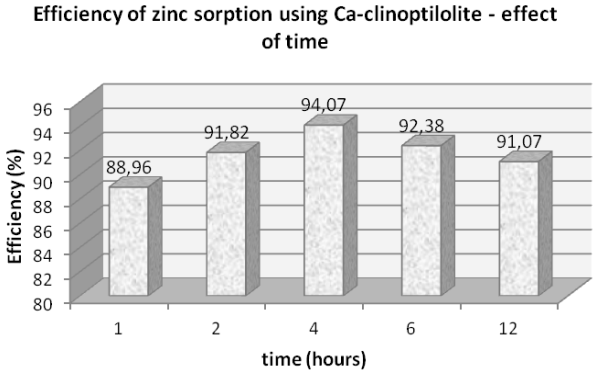

Fig. 3 Effect of time on zinc sorption using modified Ca-clinoptilolite (initial zinc concentratrion = 3.34 mg/l, pH = 5.56, rpm = 300)
Obr. 3 Vplyv času na sorpciu zinku na modifikovaný Ca-klinoptilolit (počiatočná koncentrácia zinku = 3,34 mg/l, pH = 5,56, rpm = 300)

Using Ca-clinoptilolite as sorbent, the concentration of zinc decreases significantly after the first hour but the highest efficiency of sorption was reached after 4 hours.

Short adsorption times are preferred for the minimum energy consumption and it leads to fact that natural and modified clinoptilolite can be accepted as an efficient adsorbent for zinc removal.

Results of efficiency of zinc sorption in relation tot he natural and modified clinoptilolite depending on pH of solution

Figs. 4 and 5 illustrate the effect of pH sample on removal of zinc using natural clinoptilolite and modified Ca-clinoptilolite.

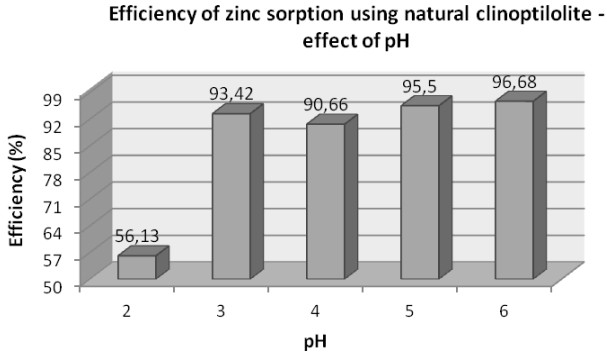

Fig. 4 Effect of pH sample on zinc sorption using natural clinoptilolite (initial zinc concentration = 3.34 mg/l, t = 4h, rpm=300)
Obr. 4 Vplyv pH vzorky na sorpciu zinku na prírodný klinoptilolit (počiatočná koncentrácia zinku = 3,34 mg/l, t = 4 h, rpm = 300)

As can be seen in fig. 4 and fig. 5, efficiency of sorption is low at pH = 2. The value of efficiency is increased by increasing the pH value. It is apparent that using solutions at pH values between 3 and 6 gives the highest values of efficiency. Thus, the sorption process can be carried out not only at a certain pH value, but also in the wide range of pH values (initial pH of wastewater is 5.56 and it is inside this mentioned range therefore, there is not need to change it). These results are in agreement with several previous investigations of metal removal by a variety of materials which revealed that the sorption capacity is low at pH values below 4 because of the competition between the protons and metals ions for the exchange sites of the zeolite particles. Thus, increased external H^+ concentration (due to lowered pH) can have effect on metal ion removal via ion-exchange by direct competition effects between the protons and metal ions for the exchange sites of the zeolite [8].

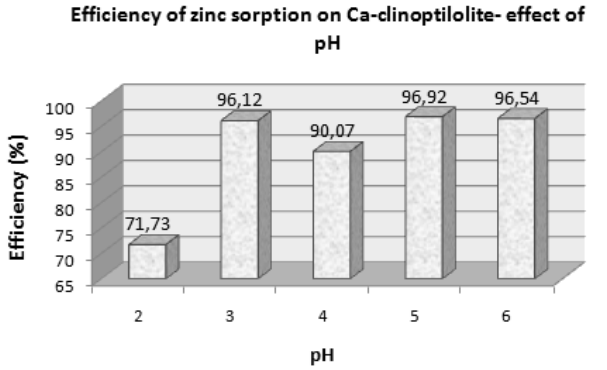

Fig. 5 Effect of pH sample on zinc sorption in relation to the modified Ca-clinoptilolite (initial zinc concentration = 3.34 mg/l, t = 4h, rpm = 300)
Obr. 5 Vplyv pH vzorky na sorpciu zinku na modifikovaný Ca-klinoptilolit (počiatočná koncentrácia zinku = 3,34 mg/l, t = 4 h, rpm = 300)

Conclusions

In this study, the interaction between zinc and natural and Ca-clinoptilolite has been investigated. The effect of time and pH on efficiency of sorption process has been studied. Based on obtained results, it can be concluded:

- minimum difference in sorption capacity between natural and modified clinoptilolite
- high efficiency of sorption after the first one hour of process
- the sorption process can be effectively carried out in range of pH values from 3 to 6

Finally, it can be summarized that clinoptilolite from the locality Nižný Hrabovec is suitable for the significant decrease of zinc content from technological waste water from rubber industry. The obtained results confirmed the great sorption capacity of clinoptilolite and this statement is presented by many researches.

Acknowledgments

This work has been supported by and KEGA No.007 TnUAD – 4/2013, KEGA No.006 TnUAD – 4/2014 and VEGA No. 1/0385/14.

Literature

[1] KORKMAZ, M. ÖZMETIN, C., ÖZMETIN, E. Copper sorption by clinoptilolite: equilibrium and thermodynamic investigation, *Sixteenth International Water Technology Conference*, IWTC 16 2012, Istanbul, Turkey

[2] SEKOMO, CH., ROUSSEAU, D., LENS, P. Use of ginesenyi volcanic rock for adsorptive removal of Cd(II), Cu(II), Pb(II), and Zn(II) from wastewater. *Water Air Soil Pollution 223,* 2012, p. 533-547

[3] KOCASOY, G., GÜVENER, Z. Efficiency of compost in the removal of heavy metals from the industrial wastewater. *Environ Geol.* 57, 2009, p. 291-296

[4] KOCAOBA, S., ORHAN, Y., AKYÜZ, T. Kinetics and equilibrium studies of heavy metal ions removal by use of natural zeolite. *Desalination 214*, 2007, p. 1-10

[5] AL-ANBER, M., AL-ANBER, Z.A. Utilization of natural zeolite as ion-exchange and sorbent material in the removal of iron. *Desalination 225*, 2008, p. 70-81

[6] TILMAN, F. Jr, BARTELT—HUNT, S., SMITH, J., ALTHER, G. Evaluation of an organoclay, an organoclay-anthracite blend, clinoptilolite, and hydroxy-apatite as sorbents for heavy metal removal from water. *Bull. Environ. Contam. Toxicol. 72,* 2004*,* p. 1134-1141.

[7] SMART, L., MOORE, E. Solid state chemistry: an introduction. 3rd edition, CRC Press, 2005. 407s. ISBN 0-7487-7516-1

[8] AKGÜL. M., KARABAKAN, A., ORHAN, A., YÜRÜM, Y. Removal of silver (I) from aqueous solutions with clinoptilolite. *Microporous and Mesoporous Materials 94*, 2006, p. 99-104

[9] FAGHIHIAN, H., BOWMAN, R. Adsorption of chromate by clinoptilolite exchanged with various metal cations. *Water Research 39*, 2005, p. 1099-1104

[10] RAJEC, P., DOMIANOVÁ, K. Cesium exchange reaction on natural and modified clinoptilolite zeolites. *J Radioanal. Nucl. Chem 275,* 2008, *p.* 503-508

[11] GALAMBOŠ, M., SUCHÁNEK, P., ROSSKOPFOVÁ, O. Sorption of anthropogenic radionuclides on natural and synthetic inorganic sorbents. *J. Radioanal. Nucl. Chem. 293*, 2012, p. 613-633

[12] AKYIL, S., ASLANİ, M.A.A., ERAL, M. Sorption characteristics of uranium onto composite ionexchangers. *J. Radioanal. Nucl. Chem. 256*, 2005, p.45-51

[13] RAKIC, V., RAJIC, N., DAKOVIC, A., AUROUX, A. The adsorption of salicylic acid, acetylsalicylic acid and atenolol from aqueous solutions onto natural zeolites and clays: clinoptilolite, bentonite and kaolin. *Microporous and Mesoporous Materials 166*, 2013, p. 185-194

[14] FÖLDESOVÁ, M., HUDEC, P. Štúdium povrchových vlastností slovenského prírodného zeolitu-klinoptilolitu fyzikálnou adsorpciou dusíka. *Petroleum&Coal 49*, 2007, s.34-40

[15] NAGYOVÁ, S. Štúdium vplyvu etyléndiamínu na nameranú ^{1}H NMR rezonančnú čiaru klinoptilolitu z Nižného Hrabovca. *Acta Montanistica Slovaca 6*, 2001, s. 221-224

[16] UNALDI, T., MIZRAK, I., KADIR, S. Physicochemical characterization of natural K-clinoptilolite and heavy-metal forms from Gördes (Manisa, wester Turkey). *Journal of Molecular Structure 1054-1055*, 2013, p. 349-358

[17] CHIMEDTSOGZOL, A., FRIESE, K. PÖLLMANN, H. Mercury sorption on clinoptilolite. *9. International Congress for Applied Mineralogy*, 2008, p. 497- 502

[18] BYRAPPA K., SURESH KUMAR, B.V. Characterization of zeolites by infrared spectroscopy. *Asian Journal of Chemistry 19*, 2007, p. 4933-4935

[19] PECHAR, F., RYKL, D. Infrared spectra of natural zeolites of the stilbite group. *Chemické zvesti 35*, 1981, p. 189-202

ArcelorMittal investuje 18 mil. Eur do Charleroi

Stahl Aktuell 28. 3. 2014

Investice je plánována do modernizace kontinuálního odlévání oceli v belgickém závodě Charleroi Industeel Belgium. Zrekonstruovaný závod umožní lepší rozměry litých bram na míru. Maximální tloušťka je zvýšena na 300 – 355 mm a maximální délka dosahuje 2,10 – 2,20 m. Bramy pak budou válcovány na tlusté plechy o tloušťce do 125 mm pro použití ve výrobě parních a tlakových nádob. Práce budou probíhat během roční odstávky v červenci a srpnu 2015, spuštění je naplánováno na první čtvrtletí 2016.

Hutnické listy č. 3/2014, roč. LXVII
ISSN 0018-8069

Removal of Fe(III) and Pb(II) from Aqueous Solutions Using Natural and Modified Zeolite

Odstraňovanie Fe(III) a Pb(II) z vodných roztokov pomocou prírodného a modifikovaného zeolitu

Ing. Michaela Ďurčeková[1], **Ing. Lenka Špániková**[1], **prof. Ing. Darina Ondrušová, PhD.**[1]

[1] Alexander Dubček University of Trenčín, Faculty of Industrial Technologies in Púchov, I. Krasku 491/30, 020 01 Púchov, Slovak Republic

The presented work deals with the preparation of modified forms of natural zeolite and it is also focused on environmental application of these investigated modified forms in the process of Fe and Pb removing from water solutions. The environment including water is exposed to heavy metals from the long term aspect. It is the general truth that industrial activities represent one of the many sources in relation to heavy metals penetrating the environment. The use of natural minerals based on zeolite is the one of the possibilities relating to partial solution of the problem. Due to their physico-chemical properties arising from their unique three-dimensional cavity structure, these natural nanomaterials are suitable for all partial detoxification of the environment. Enriching the zeolite surface with particles (for example Fe_3O_4 – magnetit) can improve its adsorption capacity and thus it is possible to use it for the wide spectrum of substances. Natural zeolite was modified by magnetic particles of magnetit in such amount to make possible to remove it from water solutions by magnetic separation.

Keywords: *zeolite, heavy metals, sorption, magnetic modification*

Práca je zameraná na prípravu modifikovaných foriem prírodného zeolitu obohatených časticami magnetitu a ich využitie v procese odstraňovania železa a olova z vodných roztokov. Prírodné a syntetické zeolity majú unikátne štruktúrne, fyzikálne a chemické vlastnosti, ktoré ich predurčujú pre využitie v mnohých technologických, poľnohospodárskych a ekologických procesoch. V mnohých prípadoch je výhodné obohatiť povrch zeolitu iónmi a časticami, ktoré zvýšia jeho adsorpčnú kapacitu, resp. umožnia jeho použitie aj pre látky, ktoré sa na neupravený zeolit neadsorbujú. Modifikácia pomocou magnetických častíc, okrem zvýšenej kapacity pre adsorpciu, obohatí zeolit aj o magnetické vlastnosti. Takto modifikovaný zeolit ponúka výhodu jednoduchej separácie v magnetickom poli, čo má veľký význam z hľadiska regenerácie adsorbenta. Výhodou použitia oxidov železa, magnetitu (Fe_3O_4), ako magnetického modifikačného prvku je okrem magnetických vlastností aj jeho termická a chemická stabilita. V štúdii sa prírodný a modifikovaný zeolit o rôznych zrnitostiach použil na odstraňovanie iónov ťažkých kovov z vodných roztokov. V prvej časti sa odstraňoval ión Fe(III) z odpadovej vody, výsledná koncentrácia sa stanovovala spektrofotometricky. V druhej časti experimentu sa odstraňoval katión Pb(II) z pripravených modelových roztokov v závislosti od času sorpcie. Vypočítala sa účinnosť odstraňovania Pb(II) v percentách a znázornila sa grafickými závislosťami v závislosti od času sorpcie. V prípade prírodného zeolitu o zrnitosti 0,063-0,125 mm sa experiment rozšíril o výpočet a grafické znázornenie adsorpčnej kapacity v rovnováhe. Získané výsledky budú použité v ďalšej štúdii, ktorá by sa mala zaoberať odstraňovaním katiónov ťažkých kovov z popolčeka v úložiskách, ktoré sú nebezpečné pre životné prostredie. Prírodný zeolit je vhodnou možnosťou pre použitie na tieto účely vzhľadom na jeho nízku cenu a vysokú absorpčnú schopnosť.

Kľúčové slová: *zeolit, ťažké kovy, sorpcia, magnetická modifikácia*

Zeolites are widespread and their wealth is based on the crystal shapes, colours for one mineral type and incidence of very diverse group of minerals. Zeolites are hydrated silicates of spatial structure. They belong to a group of tectosilicates [1]. The $[SiO_4]^4$ tetrahedron is the basis of the crystal structure and the common oxygen ions are there to provide the mutual interconnection. Silicon tetrahedron tends to be partially replaced by aluminium ions (Fig. 1).

The general chemical formula of zeolites can be expressed as follows:

$$M_xD_y[Al_{x+2y}Si_{n-(x+2y)}O_{2n}] \cdot mH_2O$$

where M_x and D_y are important cations of monovalent $[M_x]$ and divalent $[D_y]$ elements which offset negative charge arising due to substitution of Si^{4+} by Al^{3+}. Including Na, the monovalent elements are frequently present but K is occasionally present too. In relation to the divalent elements, Ca is present rarely, Ba and Sr as well as Mg and Mn are present occasionally.

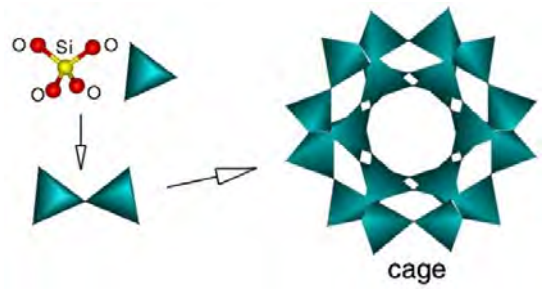

Fig. 1 Structure of zeolites[2]
Obr. 1 Štruktúra zeolitov [2]

Natural zeolite channel diameters vary from 0.2 nm to 0.7 nm.

The voids may be given only to those substances whose molecules have a diameter smaller or equal to the diameter of duct inlet openings. Molecules which are larger than the diameter of the channels do not pass through cavities [3].

Quantity and selectivity of cations bound to zeolite dependent on a number of factors while the most important factor is pH but the structure of zeolite, electrolyte, the presence of other ions and the time of adsorption are also very important factors.

In many cases, it is advantageous to enrich the surface of the zeolite particles and ions in order to increase the adsorption capacity and then, it allows us to use it for such substances that are not commonly adsorbed by zeolite. Modification which is based on usage of the magnetic particles leads to the increase of the adsorption capacity of zeolite and it is also connected with enhancement of the magnetic properties. Thus, the modified zeolite offers the advantage in relation to the easy separation in a magnetic field and it is very important from the aspect of regeneration of adsorbent [4].

The zeolite surface treatment based on magnetic metal nanoparticles (Fe, Co, Ni) is one of the most popular ways for modification of zeolites by magnetic particles. The addition of magnetic particles, such as iron oxide – magnetite (Fe_3O_4) or maghemite (γ-Fe_2O_3) has good influence on modification of the magnetic properties as well as thermal and chemical stability [5].

Experiment

In relation to the experiment, the natural zeolite – clinoptilolite from site of Nižný Hrabovec was used. Crushing and sieving process led to preparation of the following fractions of clinoptilolite:

- 0.25 – 0.40 mm
- 0.40 – 0.63 mm
- 0.63 – 1.00 mm.

We modified natural zeolite particles by magnetite Fe_3O_4. The natural zeolite was added to water solution of $FeCl_3$ and $FeSO_4$ with the ratio Fe^{3+} : Fe^{2+} = 2. After heating the mixture to 70 °C, magnetite was precipitated by solution NH_4OH according to the equation:

$$FeSO_4.7H_2O + 2FeCl_3.6H_2O + 8NH_4OH \rightarrow$$
$$Fe_3O_4 + (NH_4)_2SO_4 + 6NH_4Cl + 23H_2O$$

The mixture was decanted until the pH = 6.5 was obtained and then it was filtered and dried. The procedure was applied for all three investigated particle sizes of zeolite.

The samples based on modified zeolite were used for the removal of iron ions from the aqueous solution by adsorption. The concentration of iron in aqueous solution before and after sorption of the zeolite was determined by spectrophotometric method of calibration lines.

The next one step of the experiment was connected with the study of sorption of Pb(II) from model solutions of $Pb(NO_3)_2$ for the exact concentration. The natural as well as modified zeolite was prepared and used in such a way as it is described above. We used these fractions of zeolite:

- 0.063 – 0.125 mm
- 0.125 – 0.2 mm

In relation to the sorption, 1 g of zeolite and 75 ml solution of $Pb(NO_3)_2$ were used for the exact concentration [16.5 g Pb(II) / dm^3]. The sorption time was monitored and determined for 0.5, 1, 2, 3 and 5 hours. After the lapse of the determined sorption time, the solid phase was separated from the liquid by filtration. Concentration of Pb(II) in the filtrate was determined by titration – chelatometric way. From the resulting concentrations, the removal efficiency was calculated according to the equation:

$$Removal\ \% = \frac{\gamma_0 - \gamma_e}{\gamma_0} \cdot 100 \qquad (1)$$

where γ_0 and γ_e represent the initial and equilibrium contrentration of Pb(II) in aqueous solution [mg Pb(II)/dm^3]. The course of the removal efficiency in dependency on time of sorption is shown in Figs. 5-6.
For a sample of natural zeolite with a grain size of 0.063 – 0.125 mm, the adsorption capacity at equilibrium [mg Pb(II) / g] was determined using following equation:

$$q_e = \frac{(\gamma_0 - \gamma_e) \cdot V}{m} \qquad (2)$$

where V is the volume of the $Pb(NO_3)_2$ [dm^3] and m is the amount of sorbent [g]. The course of adsorption capacity at equilibrium in dependency on time of sorption is shown in Fig. 7.

Results and discussion

The zeolite, modified by magnetite particles, was used for the removal of iron cations from aqueous solution. Aqueous solution of iron was mixed with factions of modified and the natural zeolite in order to gain the sorption of iron ions in the structure of zeolite. The time

Hutnické listy č. 3/2014, roč. LXVII
ISSN 0018-8069

intervals: 0.5, 1, 2, 3, 5, 8 and 24 hours were used for determination and designation of samples and the aqueous solution was determined by the concentration of iron sorption of the zeolite. The original Fe concentration in aqueous solution was $10.7181.10^{-5}$ mol.dm^{-3}. The final iron concentration in the aqueous solutions for each time of sorption relating to the three studied fractions is shown by help of graphs in Figs. 2-4.

The mentioned graphical dependencies show that sorptive capacity of modified zeolite decreases with increasing particle size of zeolite and it is caused by reduction of the specific surface of the zeolite. The highest sorption efficiency was observed for a modified zeolite with grain sizes of 0.25 – 0.4 mm. The measurement results show that the concentration of Fe decreases with increasing initial sorption time. After eight hours of sorption, the concentration of Fe in solution increases transiently but then, it decreases to a value of $1.3444.10^{-5}$ mol.dm^{-3} after 24 hours of sorption. In relation to the zeolite containing magnetite Fe ions, the results confirmed the ability of sorption from aqueous solutions.

The experiment was also focused on investigation of sorption efficiency of the zeolite which was modified with magnetite particles and the values were compared to the values which were obtained for the sorption efficiency of natural zeolite – clinoptilolite.

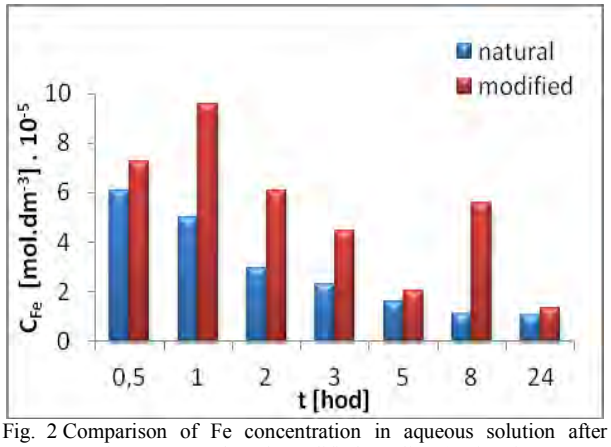

Fig. 2 Comparison of Fe concentration in aqueous solution after sorption – natural and modified zeolite (grain size 0.25 - 0.4 mm)

Obr. 2 Porovnanie výslednej koncentrácie Fe vo vodnom roztoku po sorpcii s využitím prírodného a modifikovaného zeolitu (zrnitosť 0,25 - 0,4 mm)

The graphical dependencies in Figs. 2 - 4 show that natural zeolite exhibited higher sorption capacity than modified zeolite for all assessed sorption time when the grain size was from 0.25 to 0.4 mm. In relation to the larger grains of zeolite where the grain sizes were from 0.4 to 0.63 mm and from 0.63 to 1 mm, the modified zeolite exhibited greater sorption efficiency than natural zeolite with regard to the sorption after 24 hours.

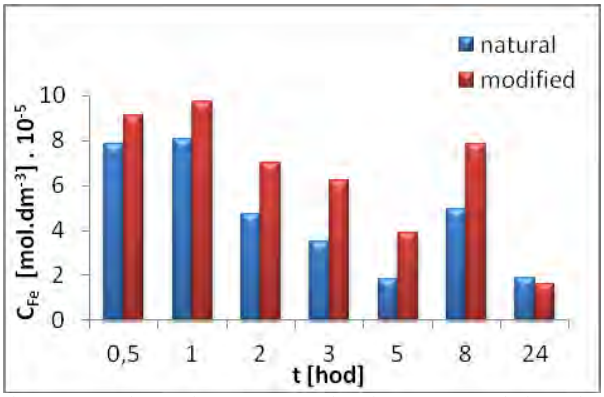

Fig. 3 Comparison of Fe concentration in aqueous solution after sorption – natural and modified zeolite (grain size 0.4 - 0.63 mm)

Obr. 3 Porovnanie výslednej koncentrácie Fe vo vodnom roztoku po sorpcii s využitím prírodného a modifikovaného zeolitu (zrnitosť 0,4 - 0,63 mm)

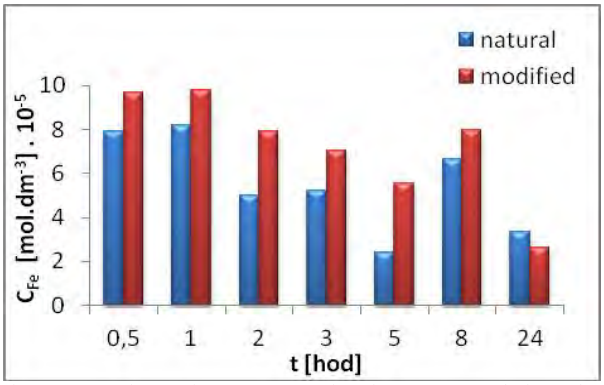

Fig. 4 Comparison of Fe concentration in aqueous solution after sorption – natural and modified zeolite (grain size 0.63 - 1 mm)

Obr. 4 Porovnanie výslednej koncentrácie Fe vo vodnom roztoku po sorpcii s využitím prírodného a modifikovaného zeolitu (zrnitosť 0,63 - 1 mm)

The removal efficiency by the natural and modified zeolite is shown in graphs in Figs. 5 and 6.

The obtained data show that the efficiency of sorption of Pb(II) from aqueous solutions by natural zeolite is in the range of 71 – 75 % while the efficiency of sorption of Pb(II) by modified zeolite is in the range of 69 – 72 %. Zeolites with smaller particle size show the increase in the mentioned efficiency.

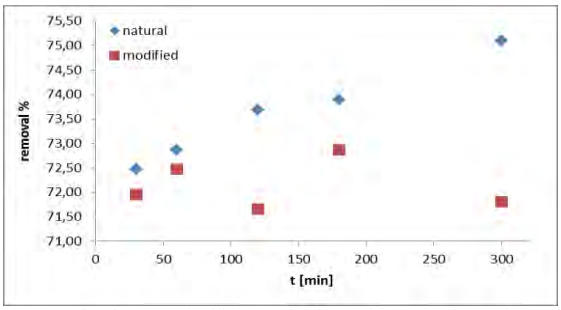

Fig. 5 Graph of removal efficiency in dependency on time of sorption – natural and modified zeolite with a grain size of 0.063 - 0.125 mm

Obr. 5 Grafická závislosť účinnosti sorpcie od času sorpcie – prírodný a modifikovaný zeolit o zrnitosti 0,063 – 0,125 mm

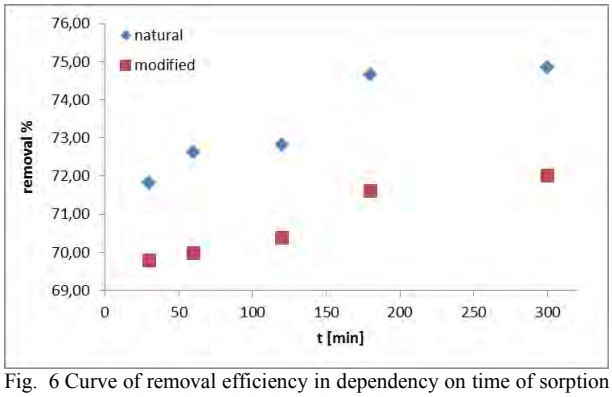

Fig. 6 Curve of removal efficiency in dependency on time of sorption – natural and modified zeolite with a grain size of 0.125 - 0.2 mm

Obr. 6 Grafická závislosť účinnosti sorpcie od času – prírodný a modifikovaný zeolit o zrnitosti 0,125 – 0,2 mm

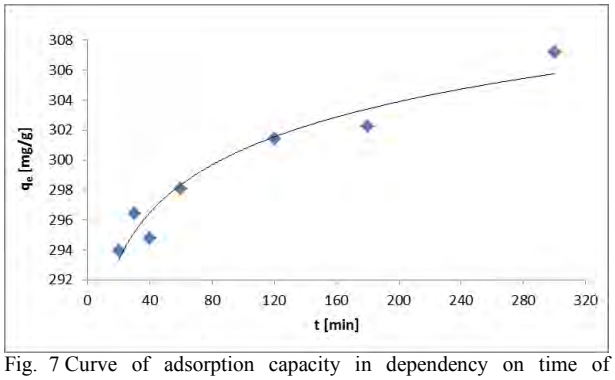

Fig. 7 Curve of adsorption capacity in dependency on time of sorption – natural zeolite with a grain size of 0.063 - 0.125 mm

Obr. 7 Krivka adsorpčnej kapacity v závislosti od času – prírodný zeolit so zrnitosťou 0.063 - 0.125 mm

Conclusions

Three samples of modified zeolite enriched by particles of magnetite with different grain size were prepared and they used for removal of Fe(III) from aqueous solution. Sorption capacity of modified zeolite was compared with the sorption capacity of natural zeolite – clinoptilolite. The results of the measurements show that there is the possibility to apply the modified zeolite with particles of magnetite in the process of iron ions removal from aqueous solutions. The highest efficiency was detected after 24 hours of sorption in the case of grain size from 0.25 to 0.4 mm. It can be concluded that sorption properties of modified zeolite at certain time intervals are comparable to sorption properties of the natural zeolite. The magnetic properties of modified zeolite with magnetite particles allow its easier separation from aqueous solutions using magnetic field. The results obtained from the experimental study of Pb(II) removal from model water solutions indicate a high sorption capacity of both studied types of zeolites – natural as well as modified. The obtained results show that zeolite can be used as an excellent sorbent for recultivation of the ponds polluted by fly ash because this type of waste represents a danger for environment. However, this application of zeolite requires further study in order to eliminate the harmful effects of fly ash in the various storage sites to a minimum.

Literature

[1] *Zeolity*. Dostupné na: http://www.zeolity.brych.cz

[2] *Štruktúra zeolitov*. Dostupné na: http://www.bza.org/zeolites.html

[3] DOMARACKÝ, D., RYBÁROVÁ, L. *Obohatené prírodné zeolity – minerálne hnojivo*. Acta Montanistica Slovaca. Roč. 6, č.5, 2001

[4] INGLEZAKIS, V.J., LOIZIDOU, M.D., GRIGOROPOULOU, H.P. *Journal of Colloid and Interface Science*, 2003

[5] NIKASHINA, V.A., SEROVA, I.B., RUDENKO, B.A. *Composition for the preparation of ferromagnetic ion-exchanger*. Patent of RF N 2081846, priority from 01. 04. 1994

[6] KORINEKOVA, M., HAVLÍK, T. *Odstraňovanie ťažkých kovov z roztokov sorpciou na zeolit*. Acta Metallurgica Slovaca, č. 12, 2006.

[7] MATIK, M. a kol. *Možnosti modifikácie zeolitu oxidmi železa a jeho využitia pri odstraňovaní Pb(II) z vodných roztokov*. Acta Montastica Slovaca, Roč. 9, č. 4, 2004

[8] KOCAOBA, S., ORHAN, Y., AKYÜZ, T. *Kinetics and equilibrium studies of heavy metal ions removal by use of natural zeolite*. ScienceDirect, Desalination 214, 2007. Dostupné na: http://www.sciencedirect.com

Výzkum a průmysl v souladu

Focus Rostfrei 17. 3. 2014

Na konci února se konalo setkání Hospodářského senátu Andrease Rimkuse (SPD) a zástupců Max Planck Institutu pro výzkum železa (MPIE). MPIE je příkladem partnerství veřejného a soukromého výzkumu financovaného prostřednictvím VDEh a Max Planck Society. Vědci z institutu sdělili hostům, že nové materiály jsou vyvíjeny na atomární úrovni a počítačové simulace šetří čas a náklady, a vývoj materiálů a různých povrchů tak může být optimalizován. Institut ukazuje spojení sociálního a politického zájmu prostřednictvím průmyslu a výzkumu. Hospodářský senát je sdružení významných osob z podnikatelské, vědecké, politické a občanské sféry. Ve společném dialogu vyvíjí strategie a řešení aktuálních problémů doby. Podobně se tématu věnuje i Forscherschaffen Werkstoffe am Computer.

Hutnické listy č. 3/2014, roč. LXVII
ISSN 0018-8069

Experimental Study of Filler Influence on Mechanical Properties of HDPE

Experimentálne štúdium vplyvu plnív na vybrané mechanické vlastnosti HDPE

Ing. Dana Bakošová, PhD.[1]

[1]Alexander Dubček University of Trenčín, Faculty of Industrial Technologies in Púchov, I. Krasku 491/30, 020 01 Púchov, Slovak Republic

The works deals with a study of fillers influence on chosen mechanical properties of high density polyethylene (HDPE) and the given influence was investigated by using of atomic force microscopy (AFM). Moreover, the used method as well as equipment relating to atomic force microscopy (AFM) is also described in this paper. In presented measurements by using of spectroscopic curve, the homogeneity and ratio of Young's modulus for HDPE samples were evaluated. The HDPE samples were prepared in standard way as well as they were modified by adding of silver and gold pigment. For each sample, the curve was created by using of five different places – points. We employed the general approximation and Snedonn's formula for analysis of data and calculation of Young's modulus off complete rake curve. On the basis of the spectroscopy curves and following calculations, it can be concluded that Young's modulus of the HDPE sample with silver is the 1.197 times higher than Young's modulus of standard HDPE and the HDPE sample with gold is 0.822 times lower in comparison to standard. We can conclude that the HDPE pigmented with silver has the reinforcing effect. From these surface topography and spectroscopic curve inclination, it is possible to point out that all used samples are homogeneous.

Keywords: *AFM, HDPE, polyethylene, filler*

Práca sa zaoberá štúdiom vplyvu plnív na mechanické vlastnosti HDPE použitím AFM. Porovnávali sme modul pružnosti v ťahu HDPE bez plnív a HDPE s prídavkom strieborného a zlatého pigmentu. Použili sme atómový silový mikroskop NT-206, ktorý spolu s riadiacim programovým zabezpečením a prostriedkami spracovania AFM-zobrazení je určený na meranie mikro a submikroreliefu povrchov, objektov mikro a nanometrových rozsahov s vysokým rozlíšením. Oblasti použitia AFM NT-206 sú fyzika pevných materiálov, tenkovrstvové technológie, nanotechnológie, mikro a nanotribológia, mikroelektronika, optika, výskum precíznej mechaniky, magnetické nahrávanie, vákuová technika atď. Použitím AFM NT-206 je možné snímať krivky zobrazujúce závislosť sily spolupôsobenia sondy a povrchu vzorky od vzdialenosti medzi nimi – sú to krivky priblíženia/oddialenia. Tieto krivky sú dôležité na meranie vertikálnej sily prikladanej k povrchu zo strany hrotu v procese skenovania. Z krivky môžeme okrem sily vyhodnotiť viskozitu zašpineného povrchu, hrúbku vrstvy pokrytia a tiež miestne variácie pružných vlastností povrchu. Krivka priblíženia/oddialenia je grafickou závislosťou odklonu meracej konzolky od predĺženia skenovacieho zariadenia. Spektroskopickú krivku sme zosnímali na piatich rôznych miestach každej vzorky. Krivky sme v požadovanom úseku aproximovali na priamku, za účelom získania smernice priamky k, pri každej vzorke sme urobili aritmetický priemer získaných smerníc. Pre výpočet pomeru modulov pružnosti jednotlivých vzoriek sme použili Snedonnov vzťah, ktorý udáva závislosť medzi záťažovým gradientom dP/dh, ktorý zodpovedá smernici priamky a Youngovým modulom pružnosti E. Zo spektroskopických kriviek a výpočtov sme zistili, že vysokohustotný polyetylén HDPE so strieborným pigmentom má 1,197krát väčší modul pružnosti ako HDPE bez plnív. Modul pružnosti HDPE so zlatým pigmentom je 0,822krát menší ako modul pružnosti HDPE bez plnív. Výsledky ukazujú, že strieborný pigment má v HDPE spevňujúce účinky. Z topografie povrchu a zo sklonu spektroskopických kriviek je vidieť, že vzorky sú homogénne.

Kľúčové slová: *AFM, HDPE, polyetylén, plnivo*

The Properties of Polyethylene

Polyethylene is a thermoplastic commodity made by the chemical industry and it is often used in consumer everyday products. Polyethylene is a polymer consisting of long chains of the ethylene monomers. Polyethylene is produced through polymerization of ethene. It can be produced through radical polymerization, anionic addition polymerization, ion coordination polymerization or cationic addition polymerization. This is because ethene does not have any substituent groups which influence the stability of the propagation head of the polymer. Each of these methods results in a different type of polyethylene [1].

Polyethylene is classified into several different categories based mostly on its density and branching.

The mechanical properties of PE depend significantly on variables such as the extent and type of branching, the crystal structure, and the molecular weight. The various types of polyethylene are produced and they era described hereinafter. UHMWPE (ultra high molecular weight PE) exhibits outstanding toughness, resistance to cut, wear and it has also excellent chemical resistance and due to these properties, UHWMPE is used in a wide variety of applications including production of can and bottle handling machine parts, moving parts of weaving machines, bearings, gears, artificial joints, edge protection of ice rinks, butchers' chopping boards. HMWPE (high molecular weight polyethylene) or HDPE (high density PE) is commonly used for such products and packaging materials as milk jugs, detergent bottles, margarine tubs, garbage containers and water pipes. In addition to the mentioned types of polyethylene, there are also HDXLPE (high density cross-linked PE), PEX (cross-linked PE), MDPE (medium density PE) and they are commonly used in gas pipes and fittings, sacks, shrink film, packaging film, carrier bags, screw closures. LDPE (low density PE), LLDPE (linear low density PE) are predominantly used in film applications due to good toughness, flexibility, and relative transparency. VLDPE (very low density PE) is used for hose and tubing, ice and frozen food bags, food packaging and stretch wrap.

Atomic-force microscope

Atomic-force microscope (AFM NT-206 - Fig. 1) in a complex with control and image processing software is intended for measurement and analysis of surface micro- and submicrorelief, objects of the micro- and nanometer range with high resolution [1].

Fields of application of the AFM include physics of solids, thin-film technologies, nanotechnologies; micro- and nanotribology, microelectronics, optics, testing systems of the precision mechanics, magnetic record, vacuum engineering etc.

The AFM can be used in scientific and industrial laboratories.

The image of a surface by the AFM is obtained through scanning of a sample in a horizontal plane by a tip attached to the cantilever and this tip has the curvature radius about tens–hundreds of nanometers. A control system traces the probe position relative to the sample surface in every measurement point and it also adjusts the tip to sample separation at constant level set by the operator. The changes of the probe vertical position in every point lead to the AFM data matrix which is recorded in a file and then can be used for further processing, visualization and analysis [2].

The scanning unit (Fig. 1) is designed for work in open air and gives convenient access for sample installation and change of scanning probe. The instrument employs measuring scheme with stationary probe over the movable sample. During measurements, precision movements of the sample are provided by a tube piezoscanner on which the sample is placed. Before measurements, the position of the probe has to be adjusted over sample to target necessary area using motorized positioning stage.

The scanning unit comprises base platform (case) (1) and detachable measuring head (8). All mechanisms are assembled on the case upper plate that serves as a base plate. On lower side (inside the case), there is a mechanism of the piezoscanner vertical motion on the base plate. The mechanism provides the approach (lifting) and the withdrawal (lowering) of the piezoscanner in relation to the sample placed on sample platform established on the tube top (16) relating to the probe (Z or vertical motion). Range of the mechanism motion is from 20 mm with the step down to about 200 nm.

On the upper side of the base plate, the XY positioning stage is mounted and it is used for preparatory motion of the measuring head over the sample (coarse XY positioning) to target necessary area on it. The positioning stage consists of Y stage (2) with its driving stepper motor (3) and X stage (4) with own driving stepper motor (5). The XY positioning stage motion range is 10 mm in both directions with step 2.5 micron.

From above, the X positioning stage, a dove tale (6) is mounted for installation of the measuring head (8). The measuring head (8) is installed by moving it forward from the front in horizontal plane. Screw (7) serves for tight fixing of the measuring head on base platform. To switch the measuring head into the general circuit, it is necessary to plug its cable (20) into socket on the rear side of the case. Additionally, it is necessary to plug the USB cable (21) of the video camera (18) into free USB socket on the host computer. To detach the measuring head from the base platform (case), the connectors (from measuring head and from video camera) have to be unplugged, the fixing screw has to be unscrewed (7) and the head off the dove tail has to be pulled (6).

Measuring head (8) represents a high-precision system comprising mechanical, optical and electronics equipped with specially designed video camera (18). In the lower part of the measuring head, a removable probe holder (12) is installed. Screw (13) is used for locking the probe holder after installation it in the measuring head. Knobs (9) and (10) serve for targeting the laser beam on to the probe at tuning. It is important to say that laser source and video camera optics are integrated in one system and therefore video camera (18) moves with the laser source adjustment. This scheme provides permanent targeting of the video camera on to the area around the laser beam center. Knobs (14) and (15) are used for tuning the photodetector on to the beam reflected from the rear side of the probe cantilever. Axis (11) turns a mirror reflecting the bounced beam on to the photodetector

Hutnické listy č. 3/2014, roč. LXVII
ISSN 0018-8069

and can be used for additional tuning of the measuring system (it is, however, recommended to keep this axis as it was established by the manufacturer and use this option in extreme cases).

Ring (19) on the video camera tube (17) serves for fine focusing of the video system in the range about 1 mm along vertical axis. The video camera module (18) can be detached from the system by unfixing special screw on the tube and pulling it then up. The video system contains fine optical elements inside and therefore it is strongly recommended to protect the opened ends of the tubes against dust and dirt.

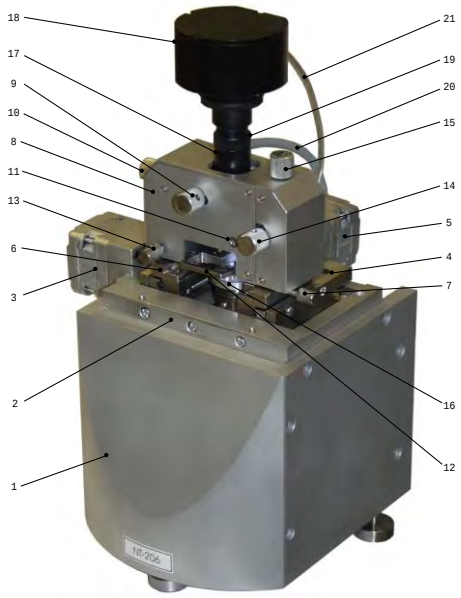

Fig. 1 Scanning unit of atomic force microscope NT-206. 1
Obr. 1 Základné časti skenovacieho bloku AFM NT – 206

Utilization of atomic-force microscope

Using AFM, it is possible to scan curves that show dependence of interaction of the probe composite force and surface of the sample relating to distance between them – they are curves of approach/moving off. These curves are very important for measurements of vertical force attached to the surface from the side of the tip in the process of scanning. Besides the force, it is also possible to evaluate viscosity of dirty surface, thickness of the covering layer and also local variations of elastic properties of the surface from the curve.

The curves of approach/moving off that are obtained seem to be specific for each sample enough and at the same time we can separate general characteristic sections in them, as shown in Fig. 2.

Section A–B: In the left part of the curve there is a scanning device completely moved off and the cantilever is not bent because the tip is not in the contact with the sample. By approaching the surface, the cantilever is not bent until the Van der Waals forces start to act (point B). In this part the curve does not contain any useful information.

Section B–C: In point B, the cantilever suddenly starts to move towards the surface and the tip starts to be in a contact with the surface (point C). This part of the curve is known as "leap to contact". Besides Van der Waals attractive forces and electrostatic forces, there is a compound influence of the surface moisture capillarity as well as impurities and grease on the tip during the working in air environment. Change of the force in the part B–C of the curve can be related to the tip shrinkage in accordance with the Hook law ($F = -k\Delta x$) and it allows to evaluate the thickness of absorbed layer on the sample surface.

Section C–D: This part characterizes further approach of the probe to the sample and it is accompanied by driving needle tip to the surface and moreover there is nearly linear curve of the cantilever towards the surface. From the shape of the C–D section, we can evaluate modulus of elasticity of the system probe–surface. In the case that, for example, the measuring probe is much softer than the surface of the sample, the curve inclination presents mostly elastic constant of the cantilever itself. Contrariwise, if the hardness of the cantilever is much harder than the surface of the sample, inclination of the section C–D allows us to study elastic features of the sample. Section C–D does not have to be straight line at all, the inclination change of this curve part shows differences in surface reactions to different attached force [3, 4].

Section D–E: Point D refers to the end of the approaching phase and the beginning of moving-off phase from the surface. If there is not hysteresis of the scanning device, the section D–E is practically the same as the section of the curve C–D, which we obtained during the approach. In the case that both of these sections are straight and parallel they do not give us any additional information (besides above mentioned). In the case that they are unparallel it allows us to determine plastic and elastic deformation of the sample (if the speed of recovery of surface geometrical features is slower than moving-off of the probe).

Section E–F: Point E refers to the neutral divergence of the cantilever. During further moving-off of the probe from the surface, the cantilever starts to incline to the sample because adhesive or gravity force affects the tip. The shape of the section E–F is influenced by presence of absorbing layers on the sample surface. In the case of the work in vacuum, Van der Waals and electrostatic forces affect the tip of the needle. If we work at the air conditions, quite strong capillary force of moisture on surface layer, grease and impurities are added to these forces. Thickness of the surface layer influences the length of the section E–F and its inclination, which is different to inclination caused by hardness of the sample, and points to moving up absorbing layers together with the moving-off probe. When the elastic

response of the cantilever outruns gravity forces of the surface side and its layers, the probe separates from the sample surface. Point F, known as the point of separation, refers to this action in the curve of approach/moving off.

Section F–G: When the elastic response of the cantilever outruns the gravity force of the surface and its layers, the probe separates from the sample. In the curve of approach/moving-off there is a point F, known as the point of separation, referring to this mentioned above. The size of straining in the point F is equal to the total maximum adhesive force between the probe and sample and provides key information on observation of adhesion. If the moisture layer is covered enough with grease layer or other impurities, it is the case when we can observe not only one point of separation (F_1 and F_2). Position of the points F_1 and F_2 depends on viscosity and thickness of these layers. Transition between the sections E–F and F–G does not necessarily have to have steep ascent. In the case that the absorbing layer has equal viscosity, the probe can move off from the surface gradually and the transition E–F - F–G will have round shapes.

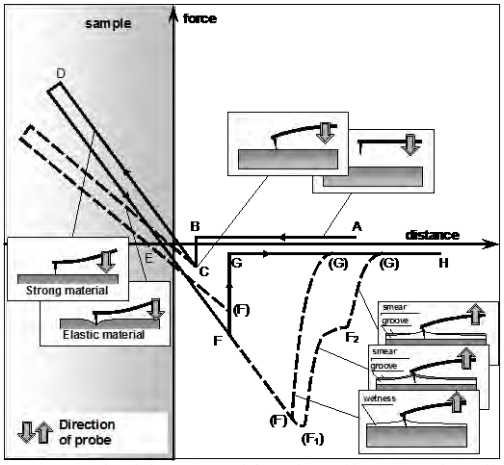

Fig. 2 Nomograph of the approach/moving-off curves. The solid lines are schematic presentation of curves obtained in vacuum. Dashed lines show variations of curves of approach/moving-off subjected to elastic features of the sample as well as presence of surface layers of moisture and impurities

Obr. 2 Krivky priblíženia/oddialenia. Plnou čiarou sú schematický zobrazené krivky získané vo vákuu. Čiarkované čiary ukazujú variácie kriviek priblíženia/oddialenia podmienené pružnými vlastnosťami vzorky a prítomnosťou povrchových vrstiev vlhkosti a šmúh (nečistôt)

Experiment

In presented measurements by using of spectroscopic curve, the homogeneity and ratio of Young's modulus were evaluated for HDPE samples. The HDPE samples were prepared in a standard way as well as they were modified by adding of silver and gold pigment. For each sample, the curve by using of five different places – points was created. In Fig. 3-5, the surface topography of investigated samples is presented.

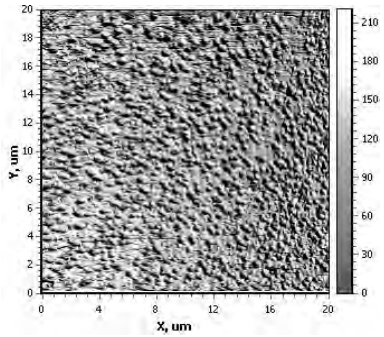

Fig. 3 Topography of microsurface of sample - standard HDPE

Obr. 3 Topografia mikropovrchu vzorky - štandardný HDPE

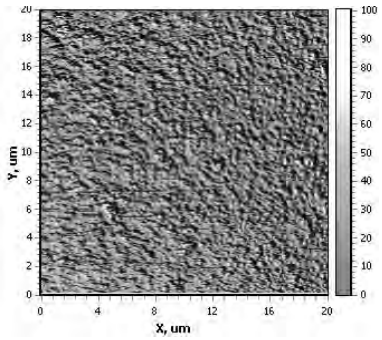

Fig. 4 Topography of microsurface of sample - HDPE with silver pigment

Obr. 4 Topografia mikropovrchu vzorky - HDPE so strieborným pigmentom

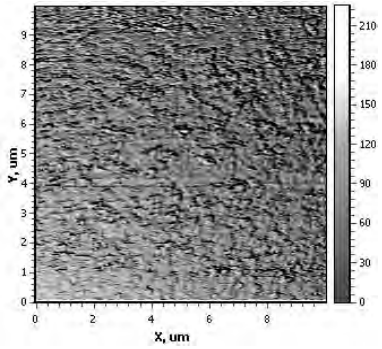

Fig. 5 Topography of microsurface of sample - HDPE with gold pigment

Obr. 5 Topografia mikropovrchu vzorky - HDPE so zlatým pigmentom

We employed the general approximation and Sneddon's formula for analysis of data and calculation of Young's modulus of complete rake curve. The Sneddon's model gives the relationship between load gradient, dP/dh, and Young's modulus, E, in the form [3, 4]:

$$\frac{dP}{dh} = \frac{2A^{1/2}}{\pi^{1/2}} E \qquad (1)$$

where $$E = \left\{\left[\left(1-\nu_m^2\right)/E_m\right] + \left[\left(1-\nu_c^2\right)\right]/E_c\right\}^{-1}, \qquad (2)$$

is the compound elastic modulus, (E_m, E_c, ν_m, ν_c Young's modulus and Poisson's ratio of a material and a cantilever, respectively), P is normal load, A is contact area, h is the indentation depth.

Hutnické listy č. 3/2014, roč. LXVII
ISSN 0018-8069

The following formula *1* represents the modulus of two different samples

$$\frac{dP_1}{dh_1} = \frac{2A^{1/2}}{\pi^{1/2}} E_1 \Rightarrow E_1 = \frac{dP_1}{dh_1}\frac{\pi^{1/2}}{2A^{1/2}}, \quad (3)$$

$$\frac{dP_2}{dh_2} = \frac{2A^{1/2}}{\pi^{1/2}} E_2 \Rightarrow E_2 = \frac{dP_2}{dh_2}\frac{\pi^{1/2}}{2A^{1/2}}. \quad (4)$$

The relation of modulus of elasticity:

$$\frac{E_1}{E_2} = \frac{\frac{dP_1}{dh_1}\frac{\pi^{1/2}}{2A^{1/2}}}{\frac{dP_2}{dh_2}\frac{\pi^{1/2}}{2A^{1/2}}} \Rightarrow \frac{E_1}{E_2} = \frac{\frac{dP_1}{dh_1}}{\frac{dP_2}{dh_2}}. \quad (5)$$

The linear equation is:

$$y = kx + q, \qquad k = \frac{dP}{dh}, \quad (6)$$

$$\frac{dP_1}{dh_1} = k_1 \quad \text{and} \quad \frac{dP_2}{dh_2} = k_2, \quad (7)$$

$$\Rightarrow \frac{E_1}{E_2} = \frac{k_1}{k_2}. \quad (8)$$

The equations of line were obtained from spectroscopic curves by approximation and resulting values are presented in the tab. 1.

Tab. 1 The values of k_1 and k_2 obtained by approximation of spectroscopic curves by assignation of line
Tab. 1 Hodnoty k_1 a k_3 z aproximácie spektroskopických kriviek na priamku

k_{1-1}	k_{1-2}	k_{1-3}	k_{1-4}	k_{1-5}	k_1
-1.7111	-1.7322	-1.7023	-1.6998	-1.7325	**-1.7156**
k_{2-1}	k_{2-2}	k_{2-3}	k_{2-4}	k_{2-5}	k_2
-2.0599	-2.0545	-2.0452	-2.0612	-2.0501	**- 2.0542**
k_{3-1}	k_{3-2}	k_{3-3}	k_{3-4}	k_{3-5}	k_3
-1.4110	-1.4102	-1.4088	-1.4063	-1.4123	**- 1.4097**

By using of average values
$k_1 = -1.7156$ standard HDPE
$k_2 = -2.0542$ HDPE with silver pigment
$k_3 = -1.4097$ HDPE with gold pigment

They are presented for the comparing of sample moduli

$$E_2 = \frac{k_2 E_1}{k_1} \quad (8)$$

$$E_3 = \frac{k_3 E_1}{k_1} \quad (9)$$

where
E_1 – Young's modulus – standard HDPE
E_2 – Young's modulus – HDPE with silver pigment
E_3 – Young's modulus – HDPE with gold pigment

$$\Rightarrow E_2 = \frac{k_2 E_1}{k_1} = \frac{-2{,}0542}{-1{,}7156} E_1 \qquad \underline{E_2 = 1{,}197 E_1}$$

$$\Rightarrow E_3 = \frac{k_3 E_1}{k_1} = \frac{-1{,}4097}{-1{,}7156} E_1 \qquad \underline{E_3 = 0{,}822 E_1}$$

Conclusions

From spectroscopy curves and following calculations, it can be concluded that Young's modulus of the HDPE sample with silver is the 1.197 times higher than Young's modulus of standard HDPE and the HDPE sample with gold is 0.822 times lower in comparison to standard. We can allege that the HDPE with silver pigment has the reinforcing effect. From these surface topography and spectroscopic curve inclination, it is possible to say that all used samples are homogeneous.

Literature

[1] WIESENDANGER, R. *Probe Microscopy and Spectroscopy: Methods and Applications.* Cambridge University Press, 1994

[2] WEISENHORN A.L., HANSMA P.K., ALBRECHT T.R., QUATE C.F. *Forces in Atomic Force Microscopy in Air and Water*. Appl. Phys. Lett. 54 (26), (1989), 2651–2653

[3] HUTTER J.L., BECHHOEFER J. *Measurement and manipulation of Van der Waals forces in atomic force microscopy*. Journal of Vacuum Science and Technology B, 12 (1994), 2251–2253

[4] СУСЛОВ А.А., ЧИЖИК С.А. *Сканирующие зондовые Микроскопы*. Материалы технологии, инструменты, 1997, №3, 78-79

Analysis of the Temperature Dependence of Thermophysical Parameters of Hardened Polyurethane

Analýza teplotnej závislosti termofyzikálnych parametrov tvrdeného polyuretánu

doc. Mgr. Ivan Kopal, PhD. [1], **Ing. Karol Kováč**[1], **Ing. Leoš Polka**[1]

[1]Alexander Dubček University of Trenčín, Faculty of Industrial Technologies in Púchov, I. Krasku 491/30, 020 01 Púchov, Slovak Republic

The work is focused on the analysis of the temperature dependence of thermophysical parameters of hardened polyurethane. Temperature dependence of thermal conductivity, thermal diffusivity and specific heat of hardened polyurethane was analysed in the range from -25 °C to +75 °C. Identified regression models of experimental data have shown that the temperature dependence of thermal conductivity can be analytically described with cubic polynoma while the temperature dependence of specific heat can be described with bilinear model and the temperature dependence of the thermal diffusivity is based on two third degree polynomials. Functional dependency of thermal conductivity and diffusivity on temperature shows inflection point corresponding to the temperature of secondary transitions identified by dynamic mechanical analysis. Temperature dependence of specific heat indicates a secondary relaxation transition at the sharp change in slope of the bilinear regression line confirmed by dynamic mechanical analysis.

Keywords: *polymers, thermophysical parameters, pulse transient method, secondary transitions*

Štúdium termofyzikálnych parametrov polymérov pri rôznych teplotách zohráva dôležitú úlohu pri chápaní prakticky všetkých procesov, ktoré sú sprevádzané teplotransportnými javmi prebiehajúcimi v týchto materiáloch. V prezentovanej práci sa venujeme vyšetrovaniu teplotnej závislosti teplotnej a tepelnej vodivosti, ako aj hmotnostnej tepelnej kapacity tvrdeného polyuretánu v teplotnom intervale od -25 °C do +75 °C. Práve polyuretány totiž poskytujú širokú bázu pre vývoj veľkého počtu konštrukčných materiálov s vlastnosťami cielene modifikovanými pre potreby širokého okruhu rôznych aplikácií. Bez poznania ich termofyzikálnych parametrov by takáto cielená modifikácia nebola možná. Študovaný tvrdený polyuretán bol výrobený reakciou polyolu s obchodným označením PX 522/HT POLYOL a diizokynátu s obchodným označením PX 521-522 HT ISO ISOCYANATE. Funkčné závislosti teplotnej vodivosti, tepelnej vodivosti, ako aj hmotnostnej tepelnej kapacity pri stálom tlaku boli získané pulznou prechodovou metódou. Identifikované regresné modely experimentálnych dát ukázali, že teplotnú závislosť teplotnej vodivosti je možné dobre analyticky popísať kubickým plynómom, teplotnú závislosť hmotnostnej tepelnej kapacity dvojlineárnym modelom a teplotnú závislosť tepelnej vodivosti dvoma polynómami tretieho stupňa, čo korešponduje s výsledkami uvádzanými vo svetovej odbornej literatúre. Náš výskum navyše preukázal, že funkčné závislosti teplotnej, ako aj tepelnej vodivosti od teploty vykazujú inflexný bod, ktorý korešponduje s teplotou sekundárneho relaxačného prechodu identifikovaného v skúmanom polymérnom materiáli dynamickou mechanickou analýzou. Teplotná závislosť hmotnostnej tepelnej kapacity indikuje sekundárny relaxačný prechod pri teplote prudkej zmeny sklonu dvojlineárnej regresnej krivky, čo potvrdzuje aj dynamická mechanická analýza viskoelastických vlastností skúmaného polyuretánu.

Kľúčové slová: *polyméry, termofyzikálne parametre, pulzná prechodová metóda, sekundárne relaxácie*

Thermophysical parameters of materials belong to the phenomenological characteristics that quantitatively describe their thermal properties. They are part of all processes involving transport of heat transfer phenomenon. Therefore, they play a crucial role in the production and study of contemporary materials, in their desired modification as well as in research and development of new advanced materials. There is not practical application which could exist without the knowledge of the thermal properties of the materials, determined just by their physical parameters. They also belong among the basic criteria for determining the level of material degradation and loss of their original characteristics. Basic thermophysical parameters are also necessary for verification of microstructural models of new materials as well as targeted modification of existing materials. The pulse transient method is one of the most effective methods for investigation of physical parameters of solids (the polymers, in our case). We applied this method in our study of the temperature dependence of thermophysical parameters of hardened polyurethane in a relatively wide temperature range from -25 °C to 75 °C. This dynamic method allows determining three basic thermophysical parameters of solids, namely thermal

Hutnické listy č. 3/2014, roč. LXVII
ISSN 0018-8069

diffusivity, thermal conductivity and specific heat at constant pressure from a single measurement.

Experiment

Functional dependence of thermal conductivity, thermal diffusivity and specific heat at constant pressure were acquired by transient pulse method [1] implemented in an experimental apparatus *Thermophysical Transient Tester 1.02* which is closely described in [2]. Pulse transient method is described in our former paper [3]. Polyurethane was prepared in reaction of polyol, trade name PX 522/HT POLYOL, and diisocyanate, trade name PX 521-522 HT ISO ISOCYANATE.

Results and discussion

Experimental functional dependence of thermal diffusivity on temperature and the regression model are shown in Fig. 1. It can be seen that the thermal diffusivity α with increasing temperature decreases rapidly while the change in the observed temperature range from -25 °C to 75 °C represents 26.1 percent decrease. There is also linear regression line in addition to experimental values of thermal conductivity. The relative proximity of the appropriateness of the statistical parameters of the applied linear model R2 = 0.993 and Adj-R2 = 0.9922 to the unit and parameters SSE = 1.713•10-5 and RMSE = 13.79•10-4 to zero indicates that the functional dependence of α (T) has a linear tendency.

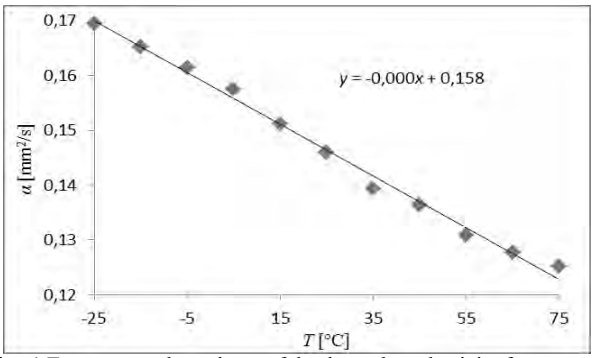

Fig. 1 Temperature dependence of the thermal conductivity for hardened polyurethane and its linear regression model
Obr. 1 Teplotná závislosť teplotnej vodivosti tvrdeného polyuretánu a jej lineárny regresný model

The appropriateness of the applied linear regression model, however, is disputed by the analysis of residues that exhibit relatively strong functional relationship. This fact can be quite sufficiently described with the third degree polynomial (Fig. 2) and it is evident from the values of the statistical parameters R^2 = 0.8152, Adj-R^2 = 0.7359, SSE = $3.165 \cdot 10^{-6}$ and RMSE = $6.725 \cdot 10^{-4}$. The temperature dependence of the thermal conductivity was analysed by polynomial regression curve of the third degree (Fig. 3) which provides much better description as evidenced by the values of the statistical parameters R^2 = 0.9987, Adj-R^2 = 0.9982, SSE = $3.166 \cdot 10^{-6}$ and RMSE = $6.725 \cdot 10^{-4}$.

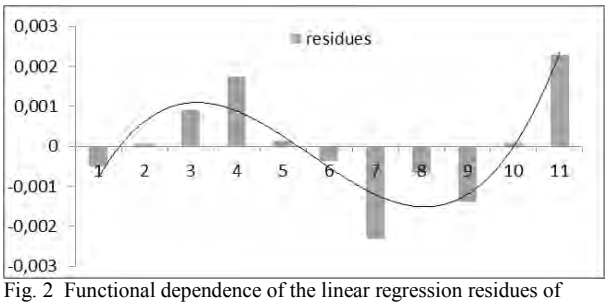

Fig. 2 Functional dependence of the linear regression residues of temperature dependence of thermal conductivity for hardened polyurethane
Obr.2 Funkčná závislosť rezíduí lineárnej regresie teplotnej závislosti teplotnej vodivosti tvrdeného polyuretánu

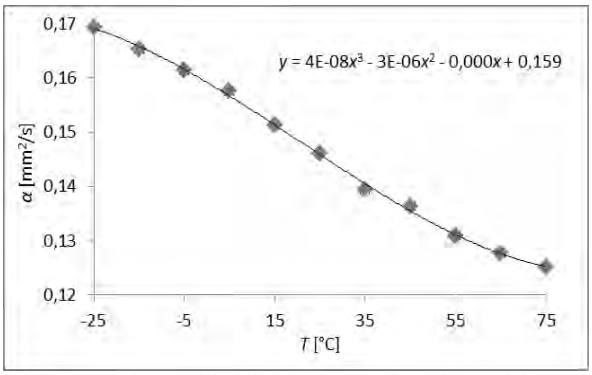

Fig. 3 Regression model of the temperature dependence of thermal conductivity for hardened polyurethane in third degree polynomial form
Obr. 3 Regresný model teplotnej závislosti teplotnej vodivosti tvrdeného polyuretánu v tvare polynómu tretieho stupňa

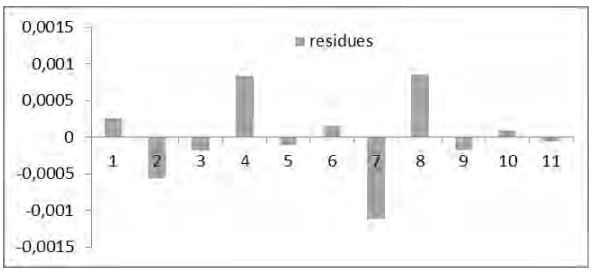

Fig. 4 Regression model residues of temperature dependence of thermal conductivity for hardened polyurethane in third degree polynomial form
Obr. 4 Rezíduá regresného modelu teplotnej závislosti teplotnej vodivosti tvrdeného polyuretánu v tvare polynómu tretieho stupňa

Model residues shown in Fig. 4 are distributed randomly with no apparent functional dependence and they are substantially lower than linear regression residues. Lilliefors normality test of distribution of residues with *p-value* 0.3462, calculated by Monte Carlo method, and statistics *ltest* = 0.1842 which is less than the critical value of the test *cv* = 0.2526 on a significance level β = 0.05 does not reject the null hypothesis H_0 that the regression residues in the third degree polynomial form have required normal distribution and therefore accept the alternative hypothesis H1 that they do not have a normal distribution [4]. Based on the analysis above, we can say that the third degree polynomial is much better regression model of temperature dependence of thermal conductivity for studied hardened polyurethane as a

linear model. There is an inflection point presented on α(T) dependency at 20.98 °C. This corresponds with the temperature of the secondary transitions confirmed by dynamic mechanical analysis of studied polymeric material.

The temperature dependence of specific heat as well as the linear regression model can be seen in Fig. 5. Values of statistic parameters R^2 = 0.9845, $Adj\text{-}R^2$ = 0.9982, *SSE* = 3297 and *RMSE* = 19.14 show that the linear regression model is not suitable for the analytical description of the experimental data curve which increase by 26.55 percent in the temperature range from -25 °C to 75 °C.

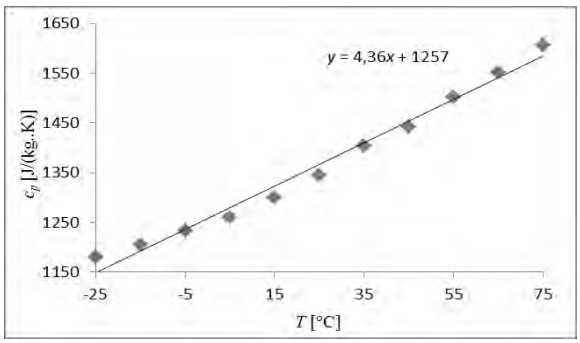

Fig. 5 Linear regression model of temperature dependence of specific heat for hardened polyurethane
Obr. 5 Lineárny regresný model teplotnej závislosti hmotnostnej tepelnej kapacity tvrdeného polyuretánu

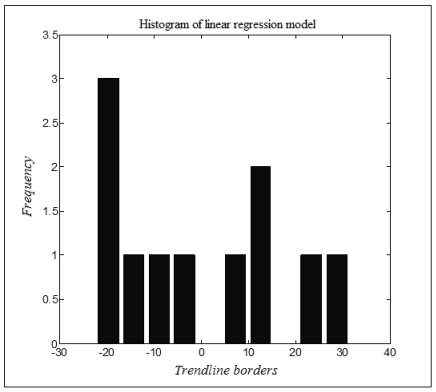

Fig. 6 Histogram of linear regression model residues of temperature dependence of specific heat for hardened polyurethane
Obr. 6 Histogram rezíduí lineárneho regresného modelu teplotnej závislosti hmotnostnej tepelnej kapacity tvrdeného polyuretánu

Histogram of linear regression model residues shown in Fig. 6 has two peaks and it leads to assumptions that residues (Fig. 7) originate from two different distributions. Therefore, the temperature dependence of specific heat for studied material was analysed by two linear regression lines. Bilinear regression model of experimental data is shown in Fig. 8. Statistical parameters R^2 = 0.9915, $Adj\text{-}R^2$ = 0.9887, *SSE* = 75.35 and *RMSE* = 5.012 for left part of regression curve and R^2 = 0.9984, $Adj\text{-}R^2$ = 0.998, *SSE* = 120.4 and *RMSE* = 4.906 for its right part give sufficient evidence about its suitability for the analytical description of the measured data.

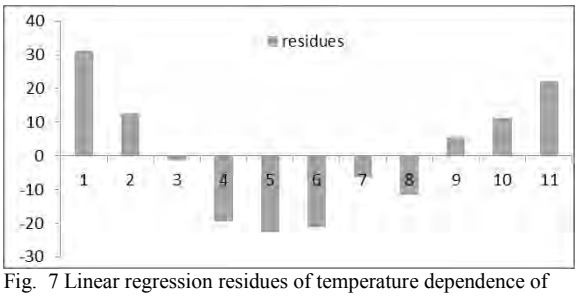

Fig. 7 Linear regression residues of temperature dependence of specific heat for hardened polyurethane
Obr. 7 Rezíduá lineárnej regresie teplotnej závislosti hmotnostnej tepelnej kapacity tvrdeného polyuretánu

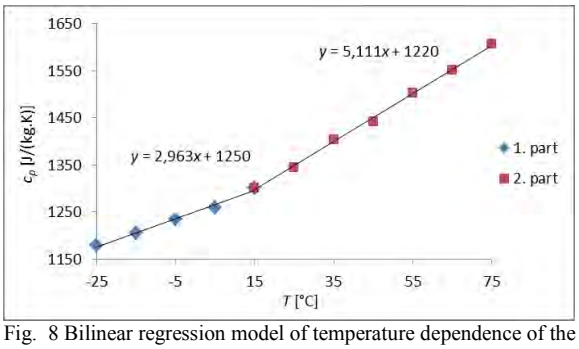

Fig. 8 Bilinear regression model of temperature dependence of the specific heat for hardened polyurethane
Obr. 8 Dvojlineárny regresný model teplotnej závislosti hmotnostnej tepelnej kapacity tvrdeného polyuretánu

Bilinear regression residues of the experimental data presented in Fig. 9 do not show a functional dependency and they are distributed randomly. Their Lilliefors normality test with parameters *p-value* = 0.3112, *ltest* = 0.1738 and *cv* = 0.2231 for left part of the curve and *p-value* = 0.3448, *ltest* = 0.1822 and *cv* = 0.2537 for its right part demonstrated that on a chosen significance level β = 0.05 residues can be considered as random variables with normal distribution. Bilinear regression model with residues parameters R^2 = 0.9944, $Adj\text{-}R^2$ = 0.9896, *SSE* = 1.35 and *RMSE* = 0.12 for left part of the regression curve and R^2 = 0.9987, $Adj\text{-}R^2$ = 0.9977, *SSE* = 0.4 and *RMSE* = 0.906 for the right part is suitable for the analytic description of the temperature dependence of specific heat for studied hardened polyurethane and it is better regression model than a simple linear model. Bilinear nature of the regression line indicates the existence of a secondary relaxation transition in the vicinity of the temperature 15 °C as it was confirmed by dynamic mechanical analysis for the material. It is clear from the gradient of the regression line that the first part has a lower level of slope while the second part exhibit that the temperature about 15 °C has a steeper character. Analytically, this finding is expressed by the first coefficients in the equations pertaining to individual parts of the temperature dependence of c_p *(T)* which are shown in the graph in Fig. 8. In the first part of functional dependence, there is an increase in the value of specific heat 2.9636 $J.kg^{-1}.K^{-1}$ with an increase in temperature by 1 °C while in the second part this value with an increase in temperature by 1 °C is 5.1112 $J.kg^{-1}K^{-1}$ - significantly higher in comparison to the first part.

Hutnické listy č. 3/2014, roč. LXVII
ISSN 0018-8069

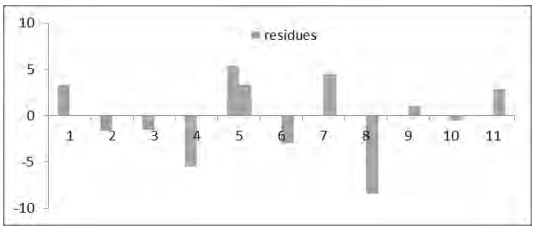

Fig. 9 Bilinear regression model residues of temperature dependence of specific heat for hardened polyurethane
Obr. 9 Rezíduá dvojlineárneho regresného modelu teplotnej závislosti hmotnostnej tepelnej kapcity tvrdeného polyuretánu

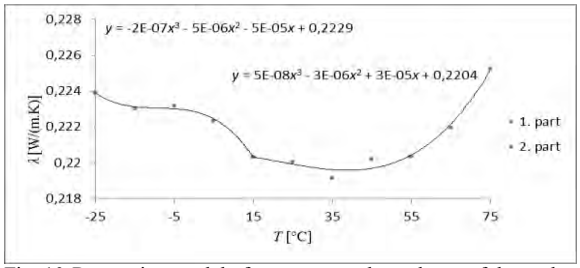

Fig. 10 Regression model of temperature dependence of thermal conductivity for hardened polyurethane
Fig. 10 Regresný model teplotnej závislosti tepelnej vodivosti tvrdeného polyuretánu

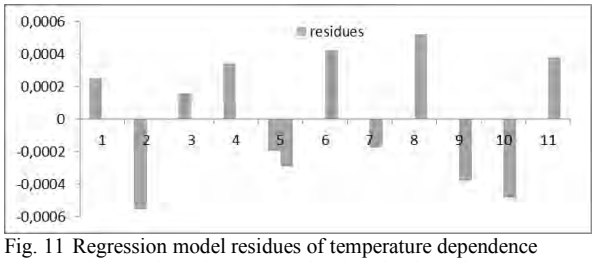

Fig. 11 Regression model residues of temperature dependence of thermal conductivity for hardened polyurethane
Fig. 11 Rezíduá regresného modelu teplotnej závislosti tepelnej vodivosti tvrdeného polyuretánu

The temperature dependence of thermal conductivity and a linear regression model is shown in Fig. 10. Since the thermal conductivity is calculated as the product of thermal diffusivity, specific heat and density of the material, experimental dependence of λ (T) was analysed by two third degree plynomials. It is assumed that in the observed temperature range, the density is a linear decreasing function of temperature.

Double cubic regression residues of the experimental data shown in Fig. 11 do not show a functional relationship and they are distributed randomly. Their Lilliefors normality test with parameters *p-value* = 0.3337, *ltest* = 0.1744 and *cv* = 0.2526 for left part of the regression curve and *p-value* = 0.3554, *ltest* = 0.1842 and *cv* = 0.2526 for the right part on the significance level β = 0.05 residues can be considered as random variables with normal distribution. Listed regression model with residues parameters R^2 = 0.9911, *Adj-*R^2 = 0.9844, *SSE* = 0.35 and *RMSE* = 1.012 for left part of the regression curve and R^2 = 0.9984, *Adj-*R^2 = 0.998, *SSE* = 0.48 and *RMSE* = 4.918 for the right part is suitable for the analytical description of temperature dependence of thermal conductivity for hardened polyurethane. Inflection point at about 15 °C indicates the secondary transitions confirmed by dynamic mechanical analysis.

Conclusions

The paper presents the results of study of the temperature dependence of thermal diffusivity, thermal conductivity and specific heat for hardened polyurethane in a temperature range from -25 ° C to 75 ° C. It has been shown that the temperature dependence of the thermal diffusivity with temperature decreases according to a cubic model, specific heat increases on the basis of bilinear regression model and the thermal conductivity with increasing temperature varies in accordance with the double cubic model. Functional dependence of thermal diffusivity and thermal conductivity on temperature exhibits inflection point corresponding to the temperature of the secondary relaxation transition identified in the examined materials by dynamic mechanical analysis. The temperature dependence of specific heat shows a secondary relaxation transition at the sharp change in slope of the bilinear regression line and it was also confirmed by dynamic mechanical analysis.

Literature

[1] BOHÁČ, V., DIEŠKA, P, KUBIČÁR, Ľ. *The Heat Loss Effect at the Measurements by Transient Pulse Method.* Measurement Science Review, 2007, vol. 7, sec 3, No. 2, ISSN 1335-8871

[2] KUBIČÁR, Ľ., BOHÁČ, V., VRETENÁR, V. *Application of the transient methods for measuring thermophysical properties in technology*. Proceedings of 10th International Symposium: Processing and Fabrication of Advance Materials, Materials Solutions, Indianapolis 2001

[3] KOPAL, I, BAKOŠOVÁ, D., ŠIŠÁKOVÁ, J., KOVÁČ, K. *Temperature Dependency of Thermal Properties of Polyurethane*. Hutnické listy, 2011, vol. LXIV, No. 7, pp. 69-72

[4] EADIE, W., T., et al. *Štatistické metódy v experimentálnej fyzike*. Amsterdam, 1971, pp. 269-271. ISBN 0-444-10117-9

Electrical Properties of Hardened Polyurethane Filled by Single Walled Carbon Nanotubes with Different Purity

Elektrické vlastnosti tvrdeného polyuretánu plneného jednostennými uhlíkovými nanorúrkami s rôznou čistotou

Ing. Karol Kováč[1], doc. Mgr. Ivan Kopal, PhD.[1]

[1]Alexander Dubček University of Trenčín, Faculty of Industrial Technologies in Púchov, I. Krasku 491/30, 020 01 Púchov, Slovak Republic

In this paper we present our study about electrical properties of hardened polyurethane filled by single walled carbon nanotubes. The object of our research is closely connected with nanocomposites synthesized from hardened polyurethane and single walled carbon nanotubes with different amount of nanotubes and different purity of nanotubes. The electrical dc conductivity was measured by using device Novocontrol Concept 90 and Keithel 6517B. The electrical ac conductivity was measured by using the device Hioki 3522-50. The temperature dependencies were both measured in the temperature range from 25 °C up to 100 °C. Electrical dc conductivity of polyurethane had an increasing character in dependency on temperature. The results have shown that higher amounts of nanotubes increase electrical conductivity. Nanotubes with purity 90 % increase electrical conductivity more than nanotubes with purity 60 %.

Keywords: *electrical dc and ac conductivity, single walled carbon nanotubes, hardened polyurethane*

Tento článok je zameraný na štúdium elektrických vlastností tvrdeného polyuretánu plného jednostennými uhlíkovými nanorúrkami s rôznou čistotou. Práca sa zameriava na vplyv určitého množstva plniva vo forme nanorúrok na perkolačný jav či už striedavej elektrickej vodivosti alebo jednosmernej elektrickej vodivosti. Skúmaný nanokompozit bol vyrobený v Žiline zmiešaním dvoch chemicky rozdielnych zložiek: polyolu a izokyanátu a uhlíkových nanorúrok s čistotou 60 % a 90 %. Následne bol vytvrdený použitím vysokého tlaku, aby dosiahol tlakový modul pružnosti a koeficient stlačiteľnosti v rozsahu 20 - 60 MPa. Jednosmernú elektrickú vodivosť sme zisťovali meraním veľkosti pretekajúceho elektrického prúdu pri stálom napätí 10 V pomocou zariadenia Novocontrol Concept 90. Meranie veľkosti prúdu bolo uskutočnené pomocou prístroja Keithley 6517B. Na meranie striedavej elektrickej vodivosti bol použitý prístroj Hioki 3522-20. Pre použité metódy merania jednosmernej a striedavej elektrickej vodivosti uvádzame v práci schémy zapojenia. Pri meraní obidvoch elektrických vodivostí sa urobila teplotná závislosť týchto elektrických parametrov v rozsahu teplôt od 25 °C do 100 °C, pričom hodnoty sme zaznamenávali s krokom 1 °C. Získané výsledky ukázali, že perkolačný jav pri obidvoch zisťovaných elektrických vodivostiach spôsobuje pridanie čistých uhlíkových nanorúrok už pri 0,5 hm. %. K takmer rovnakému zvýšeniu obidvoch elektrických vodivostí dochádza pri pridaný 1,5 hm % nanorúrok s čistotou len 60 %, čo je výborné zistenie z hľadiska ceny použitého nanoplniva. Najvyšší nárast jednosmernej elektrickej vodivosti pri 25 °C bol nameraný pri nanokompozite s obsahom 1,5 hm. % čistých nanorúrok. V porovnaní s čistým tvrdeným polyuretánom sa jednosmerný elektrická vodivosť zvýšila $7{,}7.10^{11}$ krát. Pri rovnakom nanokompozite sa v porovnaní s tvrdeným polyuretánom zvýšila striedavá elektrická vodivosť $1{,}03.10^{6}$ krát.

Kľúčové slová: *elektrická jednosmerná a striedavá vodivosť, jednostenné uhlíkové nanorúrky, tvrdený polyuretán*

Polyurethanes consist of two chemically different compounds and therefore, it gives us many possibilities for mixing polyurethane. According to the mentioned fact, we can get polyurethanes with a wide range of desired properties. Polyurethanes are synthesized from diisocyanates and polyalcohols and belong to the chemical group of polyester-amides. This is the reason, why polyurethanes are more used as matrix in nanocomposites. Carbon nanotubes used in these nanocomposites are usually multi-walled or single-walled but single-walled nanotubes are the more expensive [1]. Electrical properties, such as electrical conductivities of ac or dc are the most important characterizations of material. Nowadays, we make new materials which should be used as biomaterials or semiconductors obtained from polymers. Information about the influence of carbon nanotubes on percolation behavior is one of the most important. In the work [2] researchers examined influence of multi-walled carbon nanotubes on percolation behavior in different types of hard segments in relation to the polyurethane. They identified percolation threshold in the material at amount of nanotubes under 1 percentage. The similar research work [3] concludes the percolation threshold at amount of multi-walled carbon nanotubes under 1 percentage while these nanotubes were fillers in polyurethane matrix.

Hutnické listy č. 3/2014, roč. LXVII
ISSN 0018-8069

Material

In this investigation work, we study the hardened polyurethane filled by single walled carbon nanotubes. This material was prepared in Žilina. Polyurethane was synthesized from PX 522/HT POLYOL and PX 521-522 HT ISO ISOCYANATE. Our investigated polyurethane carbon nanocomposites were prepared in two stages. The single walled carbon nanotubes with purity 90 % and 60 % were stirred in the reaction component PX 522/HT POLYOL for approximately two minutes by the ultrasound mixer WELDER. These nanotubes are commonly produced by the company Nanocyl^{TM} and they were filled to the matrix in three different amounts: 0.5 wt. %, 1.0 wt. % and 1.5 wt. %. The mixing was implemented in a vacuum chamber to degas the polymerization mixture in the next ten minutes. After adding the isocyanate with its trade name PX 521-522 HT ISO ISOCYNATE, the mixture was stirred by ultrasound technique for two minutes. Subsequently, the curing process was carried out for 4 hours at 80 °C and 16 hours at 100 °C. Each sample was pressed by the displacement speed of 2 mm/min to a force value of 100 kN. The pressure modulus and the coefficient of compressibility were in the range of tension from 20 to 60 MPa [4].

Measurement of electrical conductivity

The direct method is used to measure the thermal dependence of dc conductivity. In Fig. 1 we have shown the connection scheme according to the direct method.

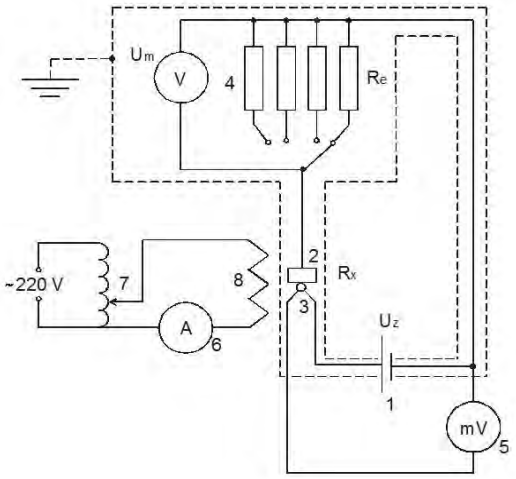

Fig. 1 The connection scheme for measurement of temperature dependency of dc electrical conductivity according to the direct method (1-source of dc voltage, 2-sample, 3-thermocouple, 4-voltmeter, 5-milivoltmeter, 6-ampermeter, 7-autotransformer, 8-heating windings) [4]

Obr. 1 Schéma zapojenia podľa priamej metódy pre meranie teplotnej závislosti jednosmernej elektrickej vodivosti vo vákuu (1-zdroj jednosmerného napätia, 2-vzorka, 3-termočlánok, 4-voltmeter, 5-milivoltmeter, 6-ampérmeter, 7-autotransformátor, 8-vinutie ohrevu) [4]

Usage of the direct method limits the accuracy of the mA meter. For the sample resistance R_x, the relationship hereinafter is valid:

$$R_x = \frac{U_z}{I} \qquad (1)$$

where U_z is the voltage at the source of dc voltage and I is the electric current through the sample.

In Fig. 2, there is the connection scheme for measurement of ac electric conductivity.

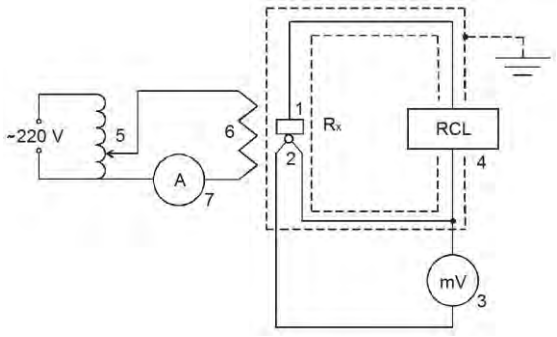

Fig. 2 The connection scheme for measurement of temperature dependency of ac electrical conductivity according to the direct method (1-source of ac voltage, 2-sample, 3-thermocouple, 4-voltmeter, 5-milivoltmeter, 6-ampermeter, 7-autotransformer, 8-heating windings) [4]

Obr. 2 Schéma zapojenia pre meranie teplotnej závislosti striedavej elektrickej vodivosti vo vákuu (1-vzorka, 2-termočlánok, 3-milivoltmeter, 4-RLC mostík, 5-autotransformátor, 6-vinutie ohrevu, 7-ampérmeter) [4]

The measurements of electrical conductivity were made in MTF STU in Trnava. The thin discs with thickness about 1.2 mm and with diameter 30 mm were prepared from the basic material by cutting. The disc samples were coated with a conductive graphite layer DAG 580 on contact surfaces.

After evaporation of the isoamyl alcohol, samples were subjected to measurement. For determination of the dc conductivity, electric current was measured at a constant voltage of 10 V using Novocontrol Concept 90, in the temperature range from 25 °C up to 100 °C. The current was determined by Picoammeter Keithley 6517B. The temperature was measured using a Pt 100 temperature sensor with an accuracy of ±1 °C. For ac measurements (from 25 °C up to 100 °C), LCR Hi-tester Hioki 3522-50 was used.

Results and discussion

In the Fig. 3, there is the temperature dependency of dc conductivity for pure polyurethane, nanocomposites with 90 % purity of nanotubes and nanocomposites with 60 % purity of nanotubes. Temperature dependency of dc conductivity has significantly increasing character for hardened polyurethane and nanocomposite with 0.5 wt. % of nanotubes of 60 % purity. At this amount, there is not occurrence of extreme changes in relation to values of electrical dc conductivity. Influence of the amount of nanotubes is significant for nanocomposites

with nanotubes of 60 % purity but these nanocomposites do not exhibit achievement of high values for electrical conductivity in comparison to the nanocomposites with nanotubes of 90 % purity. The nanotubes with purity 90 % at amount 1.5 wt. % increase electrical dc conductivity by $7.7 \cdot 10^{11}$ times in comparison to the pure hardened polyurethane at temperature 25 °C. Nanotubes with purity 90 % cause percolation even at amount 0.5 wt. %. Nanotubes with purity 60 % cause percolation at amount 1.5 wt. % but these nanotubes are cheaper. Temperature dependencies of electrical dc conductivity for nanocomposites with 90 % purity of nanotubes do not have any significant increasing character.

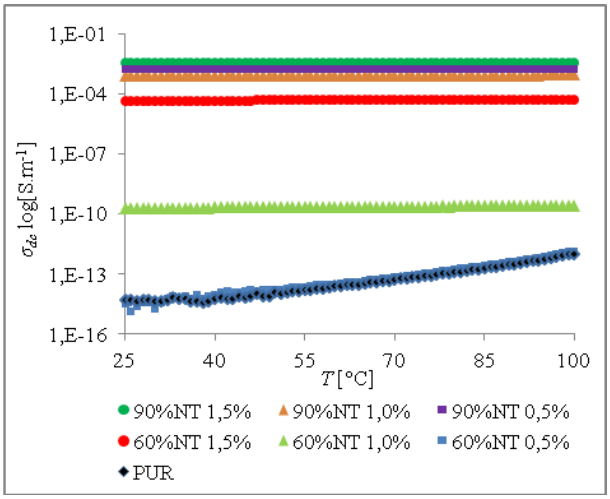

Fig. 3 Temperature dependency of dc conductivity for hardened polyurethane, nanocomposites with 90 % purity of nanotubes and nanocomposites with 60 % purity of nanotubes

Obr. 3 Teplotná závislosť jednosmernej vodivosti pre tvrdený polyuretán, nanokompozity s 90 % čistotou nanorúrok a nanokompozity s 60 % čistotou nanorúrok

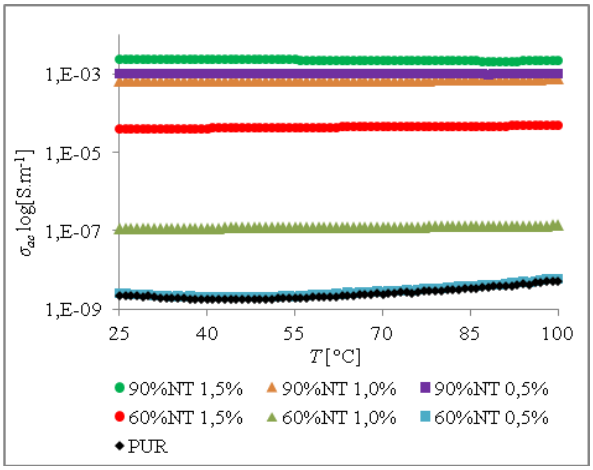

Fig. 4 Temperature dependency of ac conductivity for hardened polyurethane, nanocomposites with 90 % purity of nanotubes and nanocomposites with 60 % purity of nanotubes

Obr. 4 Teplotná závislosť striedavej vodivosti pre tvrdený polyuretán, nanokompozity s 90 % čistotou nanorúrok a nanokompozity s 60 % čistotou nanorúrok

In Fig. 4, we present the temperature dependency of the ac conductivity for hardened polyurethane, nanocomposites with 90 % purity of nanotubes and nanocomposites with 60 % purity of nanotubes. The electrical ac conductivity was measured at frequency 1 kHz. The temperature dependencies are very similar to the previous described dependences. The nanocomposite with amount 0.5 wt. % with 60 % purity of nanotubes has approximately the same values of electrical ac conductivity as hardened polyurethane. Increasing of electrical ac conductivity is very significant in dependency on amount of nanotubes with purity 60 %. Amount 1.5 wt. % of nanotubes with purity 90 % increases electrical ac conductivity approximately 10^6 times in comparison to the pure hardened polyurethane. Percolation of electrical ac conductivity occurs in the case of all nanocomposites with 90 % purity of nanotubes.

Conclusions

The paper presents the results of our study focused on the temperature dependency of electrical ac and dc conductivity of nanocomposites with polyurethane matrix filled by single walled carbon nanotubes with different amount and purity of nanotubes in a temperature range from 25 °C to 100 °C. Addition of single walled carbon nanotubes with 90 % purity causes percolation of electrical dc and ac conductivity even at amount 0.5 wt. %. The addition of 1.5 wt. % of carbon nanotubes with 60 % purity causes also the percolation of electrical ac and dc conductivity. On the other side, nanotubes with 1.5 wt. % and with 90 % purity increase the electrical dc conductivity by $7.7 \cdot 10^{11}$ times and electrical ac conductivity by $1.03 \cdot 10^6$ times in comparison to pure hardened polyurethane at temperature 25 °C.

Literature

[1] DROBNY, J. G. *Handbook of Thermoplastic Elastomers: 9 - Thermoplastic Polyurethane Elastomers.* Elsevier, ISBN 978-0-8155-1549-4, 2007, p. 215-234

[2] YUN, S., IM, H., KIM, J. *The effect of different hard segments in polyurethane on the electrical conductivity of polyurethane grafted multi-walled carbon nanotube/polyurethane nanocomposites.* Synthetic Metals. 2011, vol. 161 (13-14), p. 1361-1367

[3] BOUCHARD, J., CAYLA, A., DEVAUX, E., CAMPAGNE, C. *Electrical and thermal conductivities of multiwalled carbon nanotubes-reinforced high performance polymer nanocomposites.* Composites Science and Technology. 2013, vol. 86, p. 177-184

[4] LALUHA, D. *Elektrické vlastnosti polymérnych materiálov.* Diplomová práca. Trenčín, Slovenská Republika: Trenčianska univerzita Alexandra Dubčeka v Trenčíne, Fakulta priemyselných technológií. 2012. 49 p. (in Slovak)

Hutnické listy č. 3/2014, roč. LXVII
ISSN 0018-8069

Verification of the Colloidal Silica Influence in Rubber Compounds

Overenie vplyvu koloidnej siliky v kaučukových zmesiach

Ing. Slavomíra Domčeková[1], **prof. Ing. Darina Ondrušová, PhD.**[1], **Ing. Lenka Špániková**[1], **Ing. Zuzana Jankurová, PhD.**[1]

[1]Alexander Dubček University of Trenčín, Faculty of Industrial Technologies in Púchov, I. Krasku 491/30, 020 01 Púchov, Slovak Republic

The main aim of the given paper is to verify the colloidal silica influence by using of dynamic-mechanical thermal analysis. In relation to the dynamic-mechanical thermal analysis (DMTA), the mechanical response of a viscoelastic material is studied as a function of temperature and time, while it is subjected to sinusoidal strain. This technique applies a very small sinusoidally varying strain to test the sample at a constant frequency whilst the temperature is increased at a constant rate. The stress is measured and three different modules are calculated: storage modulus E´, loss modulus E´´, complex modulus E and loss factor (tan δ). DMTA measurements were done for identification of the resistance against the traction on the snow, the traction on the ice and on the water. The given work is also focused on the identification of the rolling resistance. The work is devoted to mechanical and dynamic characteristics of elastomer compounds which are filled with various types of precipitated silica, colloidal silica, and their combinations with carbon black.*

Keywords: *colloidal silica, precipitated silica, carbon black, dynamic-mechanical thermal analysis,*

Prezentovaná práca je zameraná na skúmanie a preverenie vplyvu koloidnej siliky v kaučukových zmesiach. Skúmanie bolo zamerané na dynamicko - mechanické vlastnosti zmesí. V praxi nie je väčšina materiálov namáhaná len staticky, ale aj vplyvom rôznych vibrácií a rázov, pričom dochádza k opakovaným deformáciám. Z toho dôvodu je dobré vzorku vystavovať dynamickým skúškam. Pri dynamickom namáhaní je potrebná menšia hodnota napätia ako je napätie pri statickom namáhaní. Táto hodnota je nastavená tak, aby nedošlo k porušeniu alebo k zmenám štruktúry vzorky. Dynamicko-mechanická analýza DMA, sa zaraďuje medzi najcitlivejšie techniky, ktorá je schopná interpretovať a charakterizovať mechanické chovanie materiálu. Princípom DMA je pozorovanie viskoelastickej ododzvy materiálu, ktorý je vystavený malému oscilačnému napätiu. Dynamicko-mechanická termická analýza DMTA prebieha podobne ako dynamická mechanická analýza DMA, vlastnosti materiálu sa však merajú ako funkcia teploty. DMTA merania sa robili za účelom zistenia odolnosti zmesi voči trakcii na snehu, ľade a za mokra, ako aj za účelom zistenia valivého odporu. Rozdiel v zložení pripravených a skúmaných zmesí spočíval v použitom type a množstve siliky: Ultrasil, Aktisil, Koloidná silika, ktorá bola varená 0 hodín, 3 hodiny a 5 hodín. Označenie pre tieto zmesi bolo SU, SA, S0h, S3h, S5h. Zmesi ktoré boli v kombinácií silika - sadze, mali označenie SSU, SSA, SS0h, SS3h, SS5h. Obsah sliky tvoril 40 dsk v piatich zamiešaných zmesiach a ďalších päť zmes bolo pripravených s obsahom 20 dsk siliky a 20 dsk sadzí. Zmesi sa pripravovali dvojstupňovým miešaním v laboratórnom hnetacom stroji Plastograph - Brabender s obsahom komory 70 ml. Následne zmesi z prvého stupňa boli homogenizované na dvojvalci a zrelaxované 24 hodín. Po relaxácií zmseí sa v druhom stupni pridával vulkanizačný systém. Takto pripravené zmesi sme podrobili dynamicko - mechanickej termickej analýze DMTA. Zo získaných výsledkov možno konštatovať, že typy použitej koloidnej siliky ako plniva nedosahújú úplne porovnatelné výsledky ako zrážaná silika, ale ďalšou úpravou siliky by bolo možné dosiahnuť výsledky, ktoré by boli schopné konkurovať zrážanej silike.

Kľúčové slová: *koloidná silika, zrážaná siliky, zmesi, dynamicko - mechanická termická analýza*

Dynamic-Mechanical Thermal Analysis (DMTA) allows to estimate the transformations occurring in the polymer during its loading in the broad range of temperature and frequency of load changes (load time) [1]. Dynamic-Mechanical Thermal Analysis (DMTA) is one of the most powerful methods used to investigate the viscoelastic properties of polymeric materials [2]. In relation to the dynamic-mechanical thermal analysis (DMTA) in torsion, the physical and thermo-dynamical properties of a sample are measured as a function of the temperature. The deformation load is kept low to avoid destroying or changing the structure of the substance (the deformation is always kept within the linear viscoelastic range) [3, 4]. The Thermomechanical Analyzer (TMA) is an analytical instrument used to test the physical properties of many different materials. The instrument is capable of heating or cooling samples while applying a predetermined force on the material. The TMA instrument consists of the following components (Fig. 1) [5]:

- *The balance enclosure* surrounds the TMA balance mechanism, which exerts a specified force on the sample

- *The probe assembly* is interchangeable for making several different measurements on various sample materials.
- *The stage* is an interchangeable component that supports the sample during measurement.
- *The furnace assembly* surrounds the stage to heat the sample; it contains the integral cooling container and the furnace monitor thermocouple.
- The weight tray, located behind *the weight tray door*, holds the weights to exert an additional known force on the sample [5].

The samples are analyzed using the TMA varying widely. The DMTA mode of TMA is able to give information on Storage Modulus, Loss Modulus, and Tan Delta data by the application of a sinusoidal force profile [5].

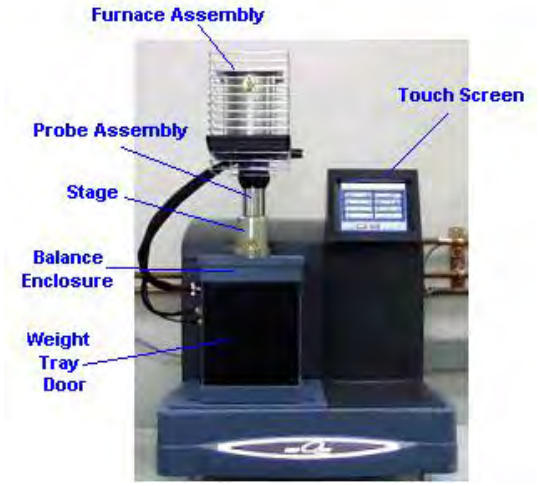

Fig. 1 The TMA instrument
Obr. 1 TMA prístroj

Experiment

The ten model rubber compounds were prepared for the testing procedures. These compounds were prepared by mixing in Brabender, the mixer with chamber volume of 70 cm^3 and it was mixed according to standard of STN 62 1425 [6]. In the first mixing step, we added natural rubber, activator ZnO, filler and plasticizer. The compounds were filled with various types of precipitated silica and colloidal silica as well as these individual types of silica were combined with carbon black (tab. 1). The temperature of 100 °C and 50 revolutions per minute represent the condition relating to the first mixing step. The sample SA and SSA were mixing at temperature of 125 °C. In the second mixing step, we added curing agent (sulfur) and accelerator to the compound. The temperature of 90 °C and 50 revolutions per minute represent the condition relating to the second mixing step. After mixing process, rubber compounds were left for 24 hours. Prepared rubber compounds were investigated by using The Thermomechanical analyzer (TMA Q400). The main aim was to verify the colloidals silica influence by using dynamic-mechanical thermal analysis. This technique applies a very small sinusoidally varying strain to the tested sample at a constant frequency whilst the temperature is increased at a constant rate. The stress was measured and three different modules were calculated: storage modulus *E´*, loss modulus *E´´*, complex modulus *E** and loss factor (tan *δ*) [2]. DMTA measurements were done for identification of the resistance against the traction on the snow as well as the traction on the ice and on the water. Furthermore, the rolling resistance was investigated too.

Tab. 1 Labelling for compounds with various types of fillers
Tab. 1 Označenie zmesí plnených rôznym druhom plnív

Sample	Filler used
SA	Silica Aktisil
SU	Silica Ultrasil
S0h	Colloidal silica stabilized 0 h
S3h	Colloidal silica stabilized 3 h
S5h	Colloidal silica stabilized 5 h
SSA	Silica Aktisil and carbon black combination
SSU	Silica Ultrasil and carbon black combination
SS0h	Colloidal silica stabilized 0 h and carbon black combination
SS3h	Colloidal silica stabilized 3 h and carbon black combination
SS5h	Colloidal silica stabilized 5 h and carbon black combination

Results and discussion

The measurements were performed by help of the instrument TMA Q400 and thin film/fiber probe was used for determination of the sample shape with dimensions of 20×4×0.3 mm.

From the aspect of the determined conditions for measurements, the force used for loading was 0.01 N, temperature range was from +20 °C to -70 °C and the frequency was 0.05 Hz. The following graphs (fig. 2 – 7) and tables (tab. 2, 3) represent the evaluation of DMTA compounds measurements.

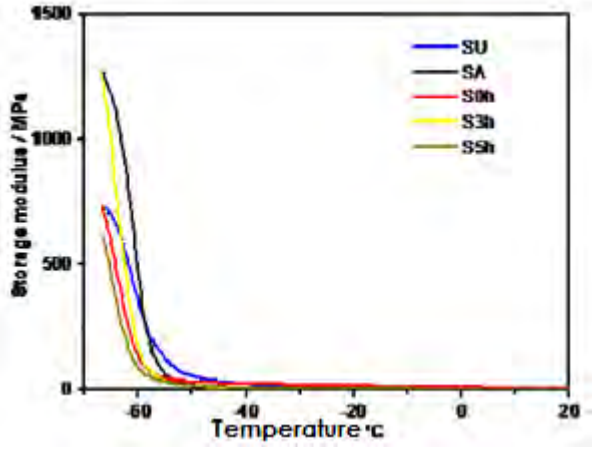

Fig. 2 DMTA measurement of compounds with silica - The dependence of storage modulus *E´* on temperature
Obr. 2 DMTA merania zmesí so silikou - závislosť šmykového modulu *E´* od teploty

Hutnické listy č. 3/2014, roč. LXVII
ISSN 0018-8069

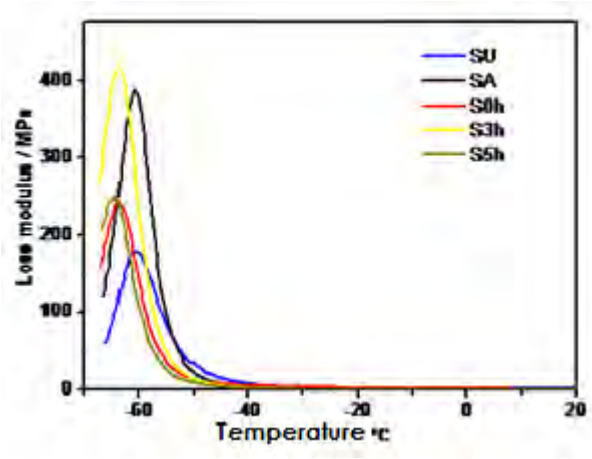

Fig. 3 DMTA measurement of compounds with silica - The dependence of loss modulus E'' on temperature
Obr. 3 DMTA merania zmesí so silikou - Závislosť loss modulu E'' od teploty

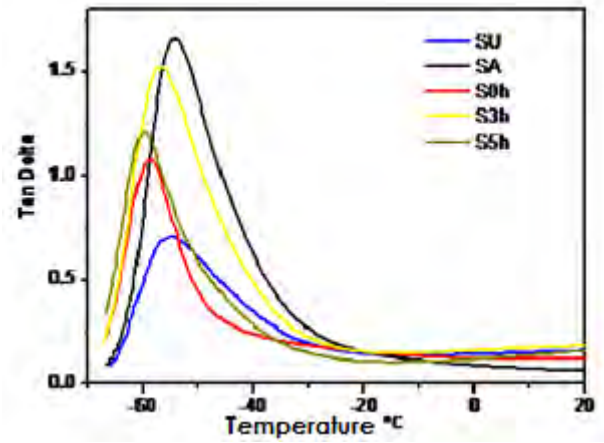

Fig. 4 DMTA measurement of compounds with silica - The dependence of tan δ on temperature
Obr. 4 DMTA merania zmesí so silikou - Závislosť tan δ od teploty

Tab. 2 Tan δ result for compounds with silica
Tab. 2 Výsledky tan δ zmesí so silikou

Samples	SU	SA	S0h	S3h	S5h
tan δ for - 25°C	0.16	0.22	0.19	0.20	0.11
tan δ for 0°C	0.15	0.09	0.11	0.17	0.11
tan δ for 60°C	0.14	0.05	0.10	0.15	0.14

Tan δ for -25 °C represents the traction on the snow and the ice. This value has to be high. On the basis of the measurements, the SA and S3h samples showed the highest values and it means that the precipitated silica Aktisil and colloidal silica which were stabilized for 3 hours could be the most suitable for preparation of compound for the winter tires.

Tan δ for 0 °C stands for the traction on the water. In relation to the behaviour of the tire on the wet road, the higher value of tan δ is necessary for 0 °C. In relation to this mentioned parameter, the highest value was achieved in the case of S3h sample, while the SA sample showed the lowest value of tan δ for 0 °C.

Tan δ for 60 °C stands for the rolling resistance of compound. If the values of rolling resistance of compound are the lowest at 60 °C, the tire made of such compound is the most suitable to be used on the dry road. All of the tested samples exhibited quite low values but the lowest values were achieved in the case of the SA sample.

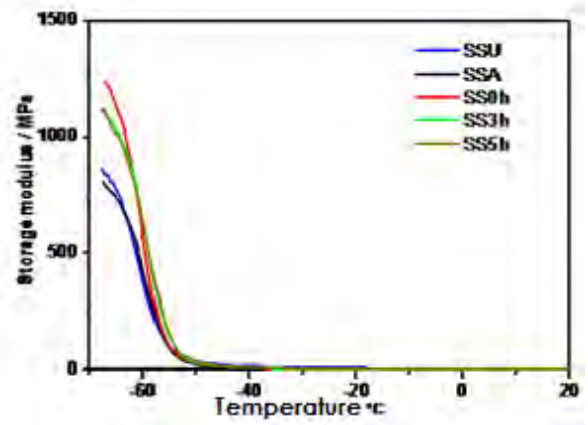

Fig. 5 DMTA measurement of compounds with silica and carbon black - The dependence of storage modulus E' on temperature
Obr. 5 DMTA merania zmesí v kombinácii siliky a sadzí - Závislosť storage modulu E' od teploty

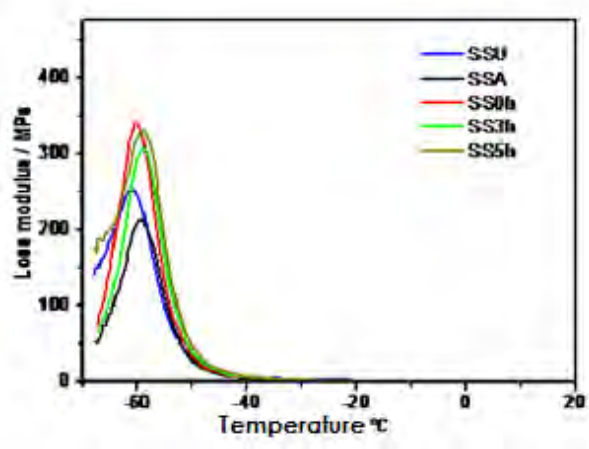

Fig. 6 DMTA measurement of compounds with silica and carbon black - The dependence of loss moduli E'' on temperature
Obr. 6 DMTA merania zmesí v kombinácii siliky a sadzí - Závislosť loss modulu E'' od teploty

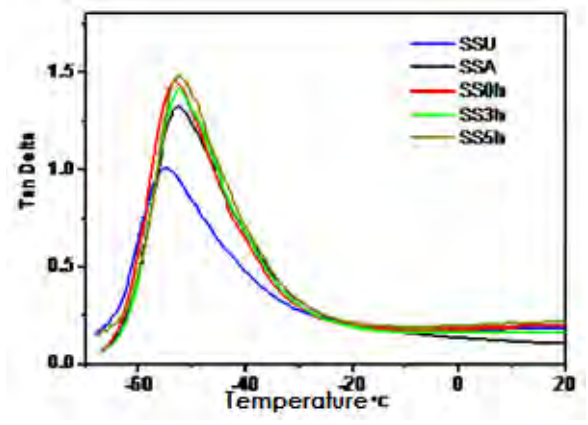

Fig. 7 DMTA measurement of compounds with silica and carbon black - The dependence of tan δ on temperature
Obr. 7 DMTA merania zmesí v kombinácii siliky a sadzí - Závislosť tan δ od teploty

In relation to the results for the compounds containing the different types of silica and carbon black, values of tan δ for -25 °C were almost the same for all samples. The highest value of tan δ for 0°C was achieved in the case of the SS5h sample which was filled with colloid silica and carbon black (the given colloidal silica was stabilized for 5 hours and then, it was added into compound together with carbon black).

Tab. 3 Tan δ results for compounds with silica and carbon black
Tab. 3 Výsledky tan δ zmesí so silikou a sadzami

Samples	SSU	SSA	SS0h	SS3h	SS5h
tan δ for - 25°C	0.24	0.25	0.24	0.24	0.25
tan δ for 0°C	0.19	0.12	0.19	0.16	0.20
tan δ for 60°C	0.19	0.10	0.20	0.16	0.21

In comparison to the other samples which showed almost the same values, the lowest value tan δ for 60 °C was observed for the SSA sample filled with silica Aktisil and carbon black.

Conclusions

In relation to the achieved result based on the measurement of dynamic-mechanical properties, it can be concluded that values relating to tan delta for -25, 0, 60 °C characterising the traction on the snow, ice and the water as well as the rolling resistance were evaluated. On the basis of the obtained values, it can be stated that colloid silica does not achieve the same values in comparison to the precipitated silica in rubber compounds. From the aspect of the influence of colloidal silica on properties of rubber compounds, the resolution and recommendation is hidden in reduction of pH of colloid silica extract.

Acknowledgements

The authors are grateful to the Slovak Grant Agency KEGA No 006 TnUAD - 4/2014 KEGA No. 007 TnUAD - 4/2013 and VEGA No. 1/0385/14 for financial support.

Literature

[1] GANTOWSKI, A., PALUTKIEWICZ, P., BOCEĄGA, E. Numerical analysis of stress state during single point bending in DMTA examination. *Journal of Achievements in Materials and Manufacturing Engineering*, 2008, vol. 28 (1), p. 47-50.

[2] SANDLUND, A.B. *A study of wood adhesion and interaction using DMTA*. Swedwn: Luleå University of Technology. 2004. p. 50. ISSN: 1402-1544.

[3] Anton Paar Germany GmbH: *Measuring the glass temperature of a polyethylene HDPE sample*. [online]. 3 p. [cit. 2014.02.19.]. Dostupné na: <http://www.anton-paar.com/us-en/footer/search/?tx_solr[q]=measuring+the+glass+temperature+of+a+polyethylene+HDPE+sample&store_context=>.

[4] Anton Paar Germany GmbH: *Comparison of a polypropylene reinforced with glass fibers and a pure polypropylene over a temperature range from -150°C to +180°C* [online]. 7 p. [cit. 2014.02.19.]. Dostupné na: <http://www.anton-paar.com/us-en/footer/search/?tx_solr[q]=Comparison%20of%20a%20polypropylene%20reinforced%20with%20glass%20fiber%20and%20a%20pure%20polypropylene%20over%20a%20temperature%20ranfe%20from%20-150%20%20to%20%2B%20180&store_context=>.

[5] *Introduce the TMA G400* [online]. [cit. 2014.02.19.]. Dostupné na: <file:///F:/QTMA/Introducing_the_TMA_Q400.htm#TMA%20Components>

[6] STN 62 1425: *Kaučuky. Príprava a vulkanizácia kaučukových zmesí. Zariadenia, 1983.*

Dillinger Hütte se může hnout z červených čísel

www.saarbruecker-zeitung.de 26. 3. 2014

S ohledem na další úspory nemusí být přijaté roční úspory v Dillinger Hütte ve výši 130 mil. Eur dostatečné, aby vyvedly závod z krize. Rok 2013 byl pro společnost nejtěžší za celá desetiletí. Konsolidované výsledky EBIT činily ztrátu 167 mil. Eur. O rok dříve vykázala společnost zisk 161 mil. Eur. Prodej se propadl o 20,8 % na 1,98 mld. Eur. Situace je napjatá a ředitel společnosti nevyloučil další možný úsporný program. Úsporný program běžíza cenu ztrátoy 450 pracovních míst. Přičemž 150 zaměstnanců přejde do Saarstahl na 24 měsíců za obdobných podmínek na podobné úrovně dovedností. Pro ostatní zaměstnance jsou dohodnuta sociálně přijatelná řešení. Program však musí být realizován rychle. Podmínkou je, aby 90 % úsporného programu bylo realizováno do konce roku a aby se tržní podmínky také změnily k lepšímu. Ve druhém čtvrtletí roku 2014 již očekává Dillinger Hütte růst cen. Navíc se společnost musí stát pružnější a citlivější na reakce zákazníků.

Hutnické listy č. 3/2014, roč. LXVII
ISSN 0018-8069

Fillers for SBR Nanocomposites Based on Organically Modified MMT and Starch

Plnivá na báze organicky modifikovaného MMT a škrobu pre SBR nanokompozity

Ing. Ladislav Janek, PhD.[1], Ing. Vladimíra Krmelová, PhD.[1], doc. Ing. Iva Sroková, PhD.[1], Ing. Jaroslava Janíčková, PhD.[1], RNDr. Vlasta Sasinková[2]

[1]Alexander Dubček University of Trenčín, Faculty of Industrial Technologies in Púchov, I. Krasku 491/30, 020 01 Púchov, Slovak Republic
[2]Slovak Academy of Sciences, Institute of Chemistry, Center for Glycomics, 845 38 Bratislava, Slovak Republic

Organically modified montmorillonite MMT (Nanofil 2, Nanofil 5) were used as the nanofillers for the preparation of the styrene-butadiene rubber (SBR) composites. The starch oleates as well as carboxymethylstarch oleates were used as compatibilizers to the SBR blends filled with modified MMT. The better dispersion of the fillers in the rubber matrix can be achieved through the compatibilizer. The physico-mechanical properties (tensile strength and tensibility) and hardness of the prepared composites were evaluated using classical methods and some of them have been even higher or comparable to the properties of the composites filled with traditional filler - carbon black. The prepared SBR blends were submitted to measurements of vulcanizing characteristics too. Optimal vulcanization time (t_{90}) was shorter in comparison to the blend containing only carbon black.

Keywords: *styrene-butadiene rubber, starch oleate, carboxymethylstarch oleate, nanofillers, organically modified montmorillonite*

Príspevok sa zaoberá prípravou polymérnych zmesí na báze styrén-butadiénového kaučuku (SBR), kde sa vo funkcii plnív použil ako čiastočná náhrada komerčného plniva – sadzí, organicky modifikovaný montmorilonit (MMT) a vo funkcii kompatibilizátora modifikovaný škrob a jeho deriváty (karboxymetylškrob). V tejto práci sa pripravili polymérne zmesi s čiastočnou náhradou komerčných sadzí, s rôznym obsahom organicky modifikovaného nano MMT ako plniva konkrétne Nanofil 2 a Nanofil 5. Zároveň súčasťou zmesí boli aj modifikované polysacharidy (modifikovaný škrob a karboxymetylškrob) vo funkcii kompatibilizátora. Zámerne sa škrob a karboxymetylškrob hydrofobizovali za vzniku oleátu škrobu a oleátu karboxymetylškrobu s vyšším stupňom substitúcie. Celkovo sa pripravilo 10 zmesí s rôznym obsahom anorganického plniva ako aj s dvomi koncentráciami hydrofobizovaného škrobu ako kompatibilizátora a rovnaký počet zmesí s oleátom karboxymetylškrobu ako druhého kompatibilizátora. Vulkanizačné charakteristiky sa stanovili pre všetky gumárenské zmesi z vulkanizačných kriviek. Sledovanými reometrickými vlastnosťami boli: M_L - najmenší krútiaci moment, M_H - najvyšší krútiaci moment, rozdiel maximálneho krútiaceho momentu a minimálneho krútiaceho momentu ($\Delta_M = M_H - M_L$), t_{90} - optimálna doba vulkanizácie. Použitie modifikovaného MMT ako i modifikovaného polysacharidu vo všetkých zmesiach viedlo k pozitívnemu zníženiu času vulkanizácie oproti štandardu. U SBR vulkanizátov sa následne stanovili ich vybrané mechanické vlastnosti a to pevnosť pri pretrhnutí (MPa) a ťažnosť pri pretrhnutí (%). Zistilo sa, že pevnosť pri pretrhnutí je porovnateľná so štandardnou zmesou, plnenou len sadzami. Ale ťažnosť vulkanizátov pri pretrhnutí sa podstatne zvýšila. Tvrdosť hodnotených polymérnych zmesí je porovnateľná so štandardnou zmesou plnenou len čistými sadzami.

Kľúčové slová: *styrén-butadienový kaučuk, oleát škrobu, oleát karboxymetylškrobu, nanoplnivá, organicky modifikovaný MMT*

Utilization of the fillers as reinforcement into rubber vulcanizates was studied in former time but nowadays, the utilisation of these fillers is studied much more extensively. Fillers improved physico-mechanical properties, such as tensile strength, elongation, hardness, resiliency, etc. of the rubber vulcanizates as well as rubber blends. Various properties of vulcanizates or polymeric rubber mixture depend on the size of the filler particles (the smaller particles have greater reinforcing effect) and furthermore, these properties also depend on the particle shape, specific surface, chemical composition, structure and content of impurities. Carbon Black (CB) belongs to the mostly used fillers and it has excellent properties in relation to the rubber blends, but they have some disadvantages including monotonous colour of the prepared blends. Moreover, the considerable environmental pollution resulting from production of CB as well as the liquidation of used products has to be mentioned [1]. Therefore, various light fillers, such as silica, clay,

caoline, lignin, starch, cellulose and different types of layered clays (montmorillonite – MMT) have been applied. Employment of montmorilonites or other layered clays into rubber mixtures and vulcanizates has considerable economical and ecological importance. The preparation of the rubber mixture from natural rubber and polypropylene, filled with layered clays, is connected with improvement of some mechanical, thermo-mechanical and barrier properties as well as flammability is reduced [2].

Utilization of MMT (bentonite type) in natural rubber and styrene-butadiene rubber was tested and studied. It was found out that there was improvement in mechanical properties, thermal stability as well as barrier properties [3]. The hydrophilic character is the disadvantage of these mentioned clays. Some years ago, three different types of lignin into rubber mixtures based on natural rubber and SBR were applied. It was found out that the lignin was able to improve the physico-mechanical properties because of compatibility of lignin and rubber matrix [4, 5].

This paper presents the preparation and properties of the SBR nanocomposites using organically modified MMT nanofillers (Nanofil 2, Nanofil 5, and NaMMT) as well as starch oleates and carboxymethyl starch oleates which were tested as the modifiers or compatibilizers.

Experimental

Materials

Styrene-butadiene Rubber Kralex SBR 1500, from Kralupy (Czech Republic) was used as a matrix. Starch oleates (S-O) and carboxymethylstarch oleates (CMS-O) were prepared as it is described in [6, 7] and applied as compatibilizers of fillers. Nanofil 2, Nanofil 5 and sodium salt of MMT were employed as inorganic fillers and they were from Süd Chemie (Germany). Carbon black (CB), which is commonly used used as a commercial filler, was from Chezacarb A-conducting (Czech Republic).

Preparation of the rubber composites

SBR composites were prepared using plasti-Corder Brabender (volume 75 cm^3), with constant rpm (50 rpm/min), at temperature of 110 °C in the first step and at temperature of 100 °C in the second step.

Glycerine as plasticizer (20 %) and S-O as well as CMS-O as compatibilizers (1 % or 5 %) have been added mechanically into model rubber mixture during the first step of the mixing. The compositions of the SBR mixtures are given in Tab. 1.

Methods

The prepared model SBR composites were submitted to measurements of vulcanizing characteristics and physical-mechanical properties.

The vulcanization characteristics of SBR blends was measured using a vulcameter Monsanto 100 at the temperature of 150 °C during 60 min and some results are shown in Tab. 2. The specimens with a shape of double-sided blades were mechanically cut out from the vulcanized slabs [8].

Physico-mechanical properties of the prepared mixtures (tensile strength and tensibility) were measured at room temperature using Monsanto 100 testing machine [9]. The hardness of vulcanized rubber was determined at room temperature by a hardness tester IRHD [10].

Tab. 1 Composition of classical polymeric rubber blends
Tab. 1 Zloženie gumárenskej zmesi

Component	Content in the mixture [phr][a]
rubber KRALEX SBR 1500	100
ZnO	5
stearin – Conti flake	2
sulfur 1 % (milling oiled)	2
CBS[b] accelerator	1
Filler (CB, NaMMT, Nanofil2, Nanofil5)	25
rapeseed oil NKO	5

[a] Parts hundred parts of rubber),
[b] N-cyclohexyl-2-benzothiazyl sulphenamide

Results and discussion

Organically modified montmorillonite (Nanofil 2, Nanofil 5 and sodium salt of MMT) as nanofiller together with commercial filler CB were employed for the preparation of nanocomposites based on the SBR. Starch oleates (S-O) and carboxymethylstarch oleates (CMS-O) were prepared as it is given in literature [6, 7] and they were applied as compatibilizers between the filler and rubber.

Vulcanization characteristics of the SBR/CB/MMT/S-O (CMS-O) mixture confirmed that the polysaccharide content of S-O and CMS-O (used as modifiers) had positive effect on the optimal cure time (Tab. 2 and 3). In comparison to CB, torque M_L of all samples decreased with increasing content of nano-fillers using compatibilizer CMS-O. In the case of sample containing 15 % of nanofiller content, compatibilizer and S-O, the reduction of torque M_L was observed and it is in contrast, to sample containing 10 % of nanofiller content and S-O because the partial increase of torque M_L was observed. Torque M_L is proportional to the viscosity of the rubber mixture heated at cure temperature and this temperature was characteristic feature of its stiffness. Maximum torque M_H showed that increasing content of inorganic filler led to increase of the shear modulus in relation to the rubber mixtures. M_H is the characteristic feature of stiffness of rubber at the end of the vulcanization process. Lower values of M_H refer to lower stiffness as well as the viscosity of the mixture at the end of the cure. The optimal vulcanization time (t_{90}) of rubber mixtures is reduced and it implies that the compatibilizer (S-O, CMS-O) affect vulcanization characteristics.

Hutnické listy č. 3/2014, roč. LXVII
ISSN 0018-8069

Based on classical methods, evaluation of the physico-mechanical properties (the tensile strength at break and tensibility) of the prepared nanocomposites provides general information on the material properties of rubber mixture. Evaluation of these characteristic features is very important for each polymer mixture. The physico-mechanical properties as well as hardness of the prepared SBR/CB/MMT/polysaccharide composites are summarized in Tab. 4.

Tab. 2 Cure characteristics of SBR composites with compatibilizer CMS-O (1 % and 5 %)
Tab. 2 Vulkanizačné charakteristiky SBR zmesí s kompatibilizátorom oleátom karboxymetylškrobu (1 % and 5 %)

Samples	Min. torque M_{min} [Nm]		Max. torque M_{max} [Nm]		Extent of cure ΔM [Nm]		Optimum cure time t_{90} [min]	
	1 %	5 %	1 %	5 %	1 %	5 %	1 %	5 %
5 % Nano2	30.0	31.0	74.0	73.0	44.0	42.0	30.5	27.5
10 % Nano2	29.8	28.0	71.2	72.0	41.4	44.0	21.5	21.0
15 % Nano2	28.2	19.0	72.2	61.5	44.0	42.5	18.5	18.0
5 % Nano5	32.3	30.0	77.2	75.0	44.9	45.0	23.5	26.0
10 % Nano5	29.0	27.0	74.0	71.0	45.0	44.0	20.3	22.5
15 % Nano5	28.0	25.0	72.2	69.5	44.2	44.5	18.8	18.0
100 %CB	32.5		91.0		58.5		37.5	

Nano2 – Nanofil 2. Nano5 – Nanofil 5

Tab. 3 Cure characteristics of SBR compostes with compatibilizer S-O (1 % and 5 %)
Tab. 3 Vulkanizačné charakteristiky SBR zmesí s kompatibilizátorom oleátom škrobu (1 % and 5 %)

Samples	Min. torque M_{min} [Nm]		Max. torque M_{max} [Nm]		Extent of cure ΔM [Nm]		Optimum cure time t_{90} [min]	
	1%	5%	1%	5%	1%	5%	1%	5%
5 % Nano2	25.7	27.0	70.8	71.0	45.1	44.0	26.5	25.0
10 % Nano2	28.5	24.5	80.0	67.5	51.5	43.0	27.5	21.5
15 % Nano2	24.0	23.2	68.5	68.5	44.5	45.3	20.5	19.5
5 % Nano5	24.8	27.0	72.0	72.0	47.2	45.0	27.0	25.0
10 % Nano5	27.0	25.0	74.0	71.0	47.0	46.0	22.5	20.5
15 % Nano5	24.0	21.0	68.5	65.0	44.5	44.0	20.5	16.0
100 % CB	32.5		91.0		58.5		37.5	

As can be seen from Tab. 4, utilisation of three types of nanofillers (NaMMT, Nanofil 2, Nanofil 5) showed a higher or comparable properties to the standard mixture properties. Using plasticizer GL and modifier CMS-O, the comparable results in tensile strength at break were obtained only by two samples (B3-1, C3-1) but using higher concentration of CMS-O (5 %) better results were obtained and it was about 20 MPa of the tensile strength (A1-5, A2-5, B1-5, B2-5, C1-5). Compared to the tensibility of standards, tensibility of the mixtures was increased in the case of all samples except one (C2-5). The hardness was comparable to the hardness of standard blend too. In relation to the three types of nanofillers, the better properties were observed at higher concentration value (10 and 15 %) and it was comparable to the standard mixture. Higher mechanical properties were achieved at higher percentage of nanofillers in the rubber mixtures. When changing the modifier CMS-O for S-O and maintaining the same percentages of the components, there was an improvement in physical-mechanical properties (Tab. 4a), especially in samples of D2-1, D3-1, F1-1, D1-1, E1-5, F2-5. These samples show higher or comparable properties to the properties of standard blend. As can be seen, a small amount of modifier S-O (1 %) is sufficient to achieve comparable physical-mechanical properties in comparison to larger quantities of modifier S-O (5 %).

Conclusions

The preparation of the SBR rubber nanocomposites was performed because of partially substitution of classical filler CB using various amounts of nanofillers (5–15 %) Moreover, two types of modifiers including starch oleate and CMS-oleate (with 1 and 5 %). MMT and organically modified MMT (Nano 2 and Nano 5 with 5 up to 15 %) were used as nanofillers and oleate esters of starch and carboxymetylstarch (S-O, CMS-O) were employed as modifiers. The investigated modified mixtures were compared to a standard mixture which was prepared from SBR filled with Carbon black.

Vulcanization characteristics of the prepared nanocomposites confirmed that the polysaccharide content of S-O and CMS-O modifiers had positive effect on the optimal cure time.

From the results of physico-mechanical properties, it can be concluded that a mixture with three types of nanofiller and with oleate esters of starch and CMS have comparable tensile strength and hardness to the standard mixture filled only with CB. Tensibility of some of these tested mixtures showed the higher values in comparison to the standard blend.

The physico-mechanical properties were better after using 1 % of S-O modificator whereas 5 % of CMS-O modificator has to be used for achievement of the same values representing the mentioned properties.

It was found out that the presence of inorganic nanofiller (organically modified MMT) with derivative of starch (S-O, CMS-O) partially adjusts mechanical properties.

Tab. 4 Physico-mechanical properties and hardness of the SBR/CB nanocomposites with various content of nanofillers and compatibilizer (%)
Tab. 4 Fyzikálno - mechanické vlastnosti SBR/CB vulkanizátov s rôznym obsahom nanoplnív a kompatibilizátora (%)

a) with CMS-oleate
a) s oleátom karboxymetylškrobu

Blends SBR/ CB partially substitued with MMT/CMS-O			**Tensile strenght [MPa]**		**Tensibility [%]**		**Hardness [IRHD]**	
	1 %	**5 %**	**1 %**	**5 %**	**1 %**	**5 %**	**1 %**	**5 %**
5 % Nano2	A1-1	A1-5	19	20	367	435	75	74
10 % Nano2	A2-1	A2-5	19	20	421	435	75	73
15 % Nano2	A3-1	A3-5	19	16	402	429	72	64
5 % Nano5	B1-1	B1-5	18	20	396	400	75	72
10 % Nano5	B2-1	B2-5	16	20	340	433	74	71
15 % Nano5	B3-1	B3-5	20	19	444	420	73	70
5 % NaMMT	C1-1	C1-5	18	20	369	414	75	75
10 % NaMMT	C2-1	C2-5	19	14	404	348	71	71
15 % NaMMT	C3-1	C3-5	20	18	427	408	73	70
100 % CB (standard)			22		365		75	

b) with Starch-oleate
b) s oleátom škrobu

Blends SBR/ CB partially substitued with MMT/S-O			**Tensile strenght [MPa]**		**Tensibility [%]**		**Hardness [IRHD]**	
	1 %	**5 %**	**1 %**	**5 %**	**1 %**	**5 %**	**1 %**	**5 %**
5 % Nano2	D1-1	D1-5	19	20	386	397	75	74
10 % Nano2	D2-1	D2-5	20	19	356	431	75	72
15 % Nano2	D3-1	D3-5	21	18	411	412	74	73
5 % Nano5	E1-1	E1-5	19	20	340	403	76	74
10 % Nano5	E2-1	E2-5	19	17	397	373	70	72
15 % Nano5	E3-1	E3-5	13	17	363	402	73	70
5 % NaMMT	F1-1	F1-5	22	17	425	391	72	71
10 % NaMMT	F2-1	F2-5	19	20	386	382	75	74
15 % NaMMT	F3-1	F3-5	17	19	379	379	70	73
100 % CB (standard)			22		365		75	

Acknowledgement

This work has been supported by project SK-PL-0044/09 and VEGA grant No. 2/0085/13.

Literature

[1] LÓPEZ MANCHADO, M.A., ARROYO, M. Short Fibers as Reinforcement of Rubber Compounds. *Polymer Composites*. 2002. Vol. 23 (4). p. 666–673.

[2] SHARIF, J., ABU BAKAR, N., AQILAH FASIHAH, R. Radiation effect on polypropylene/natural rubber/clay nanocomposites. *Enabling science and nanotechnology (EScinano)* 2010. ISBN 978-1-4244-8853-7. p. 1–2.

[3] ZHENG, G., GUOJUN, S., WEISHENG, I., PEIYAO, L., GAO, L., Li, M., HU, X. Preparation and properties of styrene butadiene rubber / natural rubber / organo-bentonite nacomposites prepared from latex dispersions. *Applied Clay Science.* 2009. Vol. 46. p. 241–244.

[4] ALEXY, P., FERANC, J., KRAMÁROVÁ, Z., HAJŠOVÁ, M., ĎURAČKA, M., MOŠKOVÁ,. D., CHODÁK, I., ILISCH, S. Application of lignins in rubber compounds. *KGK Kautschuk Gummi Kunststoffe*. 2008. Vol. 61(1-2). p. 26–32.

[5] KRAMÁROVÁ, Z., ALEXY, P., CHODÁK, I., ŠPIRK, E., HUDEC, B., GREGOROVÁ, A., ŠÚRI, P., FERANC, J., BUGAJ, P., ĎURAČKA, M. Biopolymers as fillers for rubber blends. *Polymers for Advanced Technologies.* 2007. Vol. 18(2). p. 135-140.

[6] JANÍČKOVÁ, J., SROKOVÁ, I., PAGACZ, J., CHROMČÍKOVÁ, M., PIELICHOWSKI, K. Preparation. Characterization and Properties of HEC/CMS - esters Blends. In : *Book of contribution on the 16th International Slovak – Polish Conference „Machine. Modeling and Simulations*". 2011. Terchová. Slovak Republic. ISBN 978-80-8075-494-5. p. 299–304.

[7] KEBÍSKOVÁ, J., SROKOVÁ, I., JANEK, L., CHROMČÍKOVÁ, M., CSOMOROVÁ, K. Preparation. Characterization and Properties of PLA/Starch Oleates Blends. In : *Book of contribution on the 16th International Slovak – Polish Conference „Machine. Modeling and Simulations*". 2011. Terchová. Slovak Republic. ISBN 978-80-8075-494-5. p. 315–322.

[8] STN 62 1425 – A preparation of rubber compounds.

[9] STN 62 1436 (ISO 37) – A determination of tensile properties.

[10] STN 62 1431 – A determination of hardness by pressing of point of hardness tester Shore A.

Hutnické listy č. 3/2014, roč. LXVII
ISSN 0018-8069

Determination of Selected Material Characteristics for Chosen Parts from Variously Aged Tire Casings

Stanovenie vybraných materiálových charakteristík vybraných častí z rôzne starých plášťov pneumatík

Ing. Michal Pastorek[1], **doc. Ing. Jan Krmela, PhD.**[1]

[1]Alexander Dubček University of Trenčín, Faculty of Industrial Technologies in Púchov, I. Krasku 491/30, 020 01 Púchov, Slovak Republic

The paper is focused on determination of selected material characteristics for samples from different areas in relation to passenger tire casings which are old variously. These characteristics serve as input data for computational modeling of tire casings. It was necessary to carry out various types of experiments to obtain these material characteristics. In this paper, we present the values of the modules of elasticity calculated from the results of DMA tests and static tension tests of treads, sidewalls and alluvial mixtures of variously old tire casings. From the experimental results, we were also able to determine the Mooney-Rivlin parameters which are necessary input data for computational models of tire casings and their parts. In addition, there are also presented the results which are based on the hardness tests of the given tire casing parts measured by the IRHD method. Computational models will be designed to be able to include the effect of aging of the individual tire casing parts. Knowledge on degradation processes can lead to design and material changes that can increase the resistance of casings against certain forms of degradation.

Keywords: *tire casing, degradation, hardness, Mooney-Rivlin parameters, modulus of elasticity*

Článok sa zaoberá stanovením vybraných materiálových charakteristík vzoriek z rozdielnych častí rozlične starých plášťov osobných pneumatík. Tieto charakteristiky slúžia ako vstupné dáta pre počítačové modelovanie plášťov pneumatík. Pre získanie týchto materiálových charakteristík na účely výpočtov bolo nutné vykonať rôzne druhy experimentov, najmä dynamické skúšky pomocou metódy DMA, statické skúšky v ťahu, merania tvrdosti a radiálnych deformačných charakteristík. V článku sú prezentované hodnoty modulov pružnosti vypočítané z výsledkov DMA testov a statických skúšok v ťahu behúňov, bočníc a nánosových zmesí rôzne starých plášťov pneumatík. Z experimentálnych výsledkov boli určené aj Mooney-Rivlinove parametre, ktoré patria medzi dôležité vstupné dáta do výpočtových modelov plášťov pneumatík a ich častí. Výpočtové modely musia byť navrhnuté tak, aby bolo možné zahrnúť vplyv starnutia jednotlivých častí plášťa. V článku sú uvedené aj výsledky meraní tvrdosti daných vzoriek pomocou metódy IRHD. Uvedený výskum je zameraný na vybrané rôzne staré plášte pneumatík výrobcu Continental. Skúšobné vzorky pre statické ťahové skúšky boli vyrezané z rôznych častí vybraných troch rôzne starých plášťov pneumatík. Statické skúšobné zariadenie pre skúšku ťahom Hounsfield H20K-W bolo použité pre mechanické statické ťahové skúšky v jednoosovom silovom pôsobení zaťažujúcej sily až do pretrhnutia. Rýchlosť zaťažovania bola 20 mm / min a počiatočná vzdialenosť medzi čeľusťami bola 20 mm. Testovacie zariadenie PYRIS Diamond od firmy Perkin Elmer bolo použité pre merania pomocou dynamicko-mechanickej analýzy. Teplotný rozsah bol -70 až 110 °C pri frekvencii 1 Hz. Na meranie tvrdosti bol použitý ručný tvrdomer využívajúci metódu IRHD. Z výsledkov bolo možné stanoviť mieru degradácie vzoriek jednotlivých častí daných plášťov pneumatík. Poznanie degradačných procesov môže viesť k dizajnovým a materiálovým zmenám, ktoré môžu slúžiť k zvýšenie odolnosti plášťov proti niektorým formám degradácie, k zlepšeniu bezpečnostných indikátorov a zvýšeniu životnosti.

Kľúčové slová: *plášť pneumatiky, degradácia, tvrdosť, Mooney-Rivlinove parametre, modul pružnosti*

Tires are one of the most important products used in the automobile industry. Therefore, it is important to recognize the principles and reasons of the degradation process based on ageing and furthermore, it is also important to specify the influence of ozone on mechanical properties of tires and behavior after several years with reference to their service.

For the input parameters in computational models of tires and tire parts, as well as for its own verification purposes in order to compare the results of calculations with experimental data, it is necessary to perform a whole set of experiments. Tire casings are most often modeled using the finite element method and therefore, it is necessary to determine the material characteristics of the individual casing parts accurately [1].

Research is focused on chosen selected old tire casings of the manufacturer Continental. The article is focused on the experimental determination of dynamic and static moduli of elasticity, M-R parameters and IRHD hardness of selected parts of these tire casings. These data are important material input data for computational models in relation to the natural degradation of tire casings.

Performed experiments

Experimental tests were performed in order to obtain material characteristics and parameters of the selected parts of the tire casing as important material input data with regard to the calculations for verification and analysis of computer models with experimental data.

Samples were prepared from treads, alluvial mixtures and sidewalls of tree tire casings aged in a various way. Dynamic DMA tests were performed with PYRIS Diamond test device from Perkin Elmer in the temperature range from -70 to 110 °C at frequency 1 Hz. Static test device Hounsfield H20K-W was used for the mechanical static tensile test in uniaxial force influence of the load force until the breakage. Loading rate was 20 mm/min and initial distance between the clamps was 20 mm [2]. Temperature was 20 °C.

Hardness tests were performed using a hand IRHD hardness tester at temperature 20 °C.

Modules of elasticity

Dependencies of dynamic modules of elasticity on temperature obtained from DMA tests are shown in Figures 1 – 3.

The static modules of elasticity were calculated from the dependencies of load force on elongation. Their values for each sample are shown in Tab 1 [3].

In Tab. 2, there are the values of the dynamic modulus E^* for the temperature 20 °C.

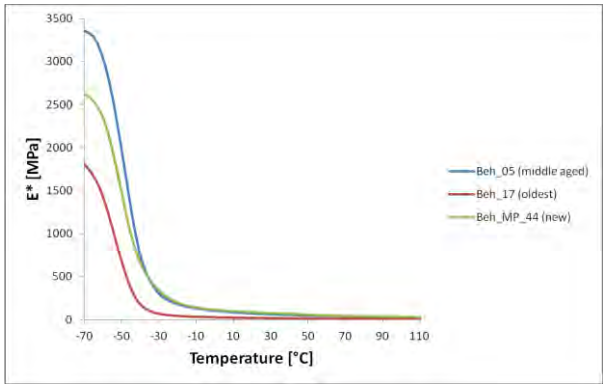

Fig. 1 Dependency of elastic modulus E^* of treads on temperature
Obr. 1 Závislosť modulu E^* behúňov od teploty

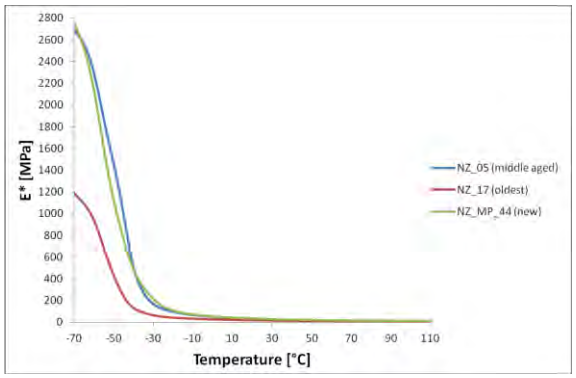

Fig. 2 Dependency of modulus E^* of alluvial mixtures on temperature
Obr. 2 Závislosť elastického modulu E^* nánosových zmesí od teploty

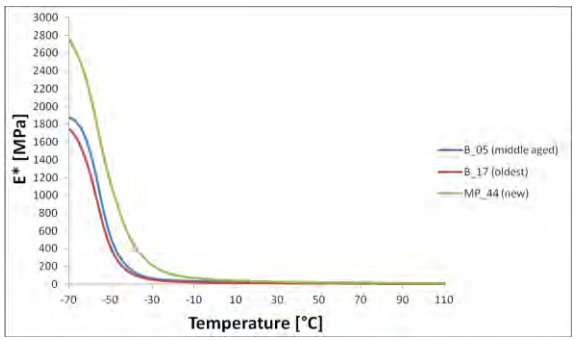

Fig. 3 Dependency of modulus E^* of sidewalls on temperature
Obr. 3 Závislosť modulu E^* bočníc od teploty

Tab. 1 Values of E for the samples at temperature 20 °C
Tab. 1 Hodnoty E vzoriek pre teplotu 20 °C

Sample	E 05 (mid. aged) [MPa]	E 17 (oldest) [MPa]	E MP44 (new) [MPa]
tread	5.34	11.22	20.07
sidewall	1.02	1.52	0.65
Alluvial mixture	2.73	2.01	1.34

Tab. 2 Values of dynamic modulus E^* at 20 °C
Tab. 2 Hodnoty dynamického modulu E^* pri 20 °C

Sample	E^* 05 (mid. aged) [MPa]	E^* 17 (oldest) [MPa]	E^* MP44 (new) [MPa]
tread	72.70	18.21	86.74
sidewall	21.06	13.98	33.01
Alluvial mixture	34.79	19.70	33.01

Figures 4 – 6 show the comparison of the values of the dynamic and static modules of elasticity.

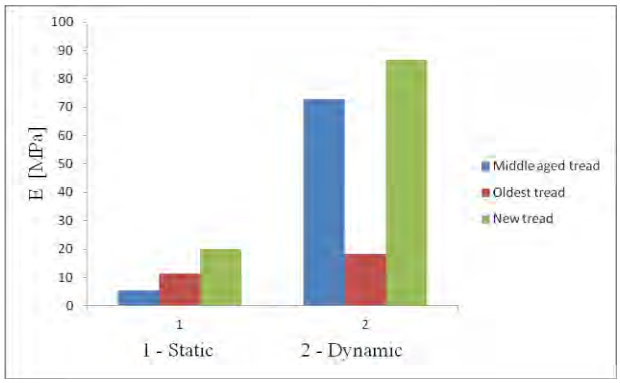

Fig. 4 Comparison of modules of elasticity for treads
Obr. 4 Porovnanie modulov pružnosti behúňov

Hutnické listy č. 3/2014, roč. LXVII
ISSN 0018-8069

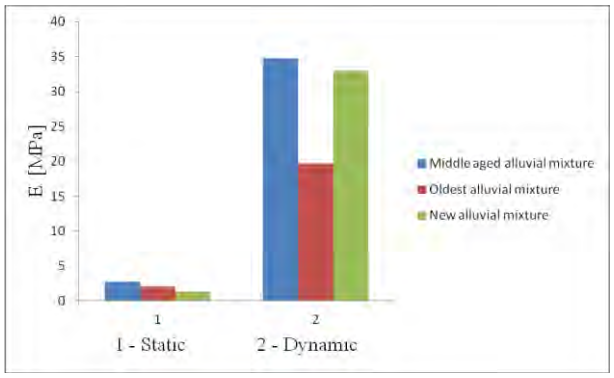

Fig. 5 Comparison of modules of elasticity for alluvial mixtures
Obr. 5 Porovnanie modulov pružnosti nánosových zmesí

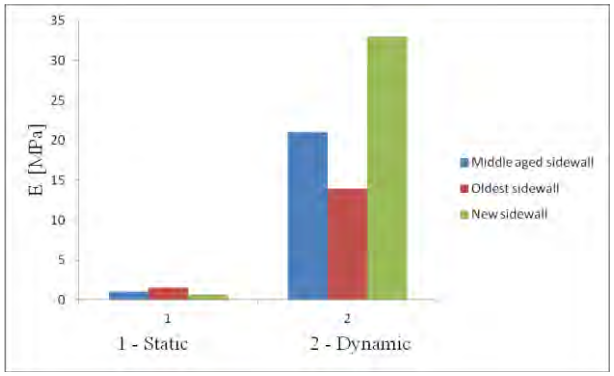

Fig. 6 Comparison of modules of elasticity for sidewalls
Obr. 6 Porovnanie modulov pružnosti bočníc

From the results can be seen that the dynamic modules have much higher values than the static ones. This is caused by dynamic stress which has always higher values than dynamic stress.

On the basis of dynamic and static tests, it can be concluded that the samples taken from the oldest tire are significantly degraded.

Mooney-Rivlin parameters

Figures 7 – 9 show the Mooney-Rivlin dependencies of each tire casing sample with the calculated values of the M-R parameters C01 and C10.

These dependencies were obtained by calculation relating to the dependencies of stress δ on elongation ε and these dependency values were obtained which on the basis of static tensile tests [4].

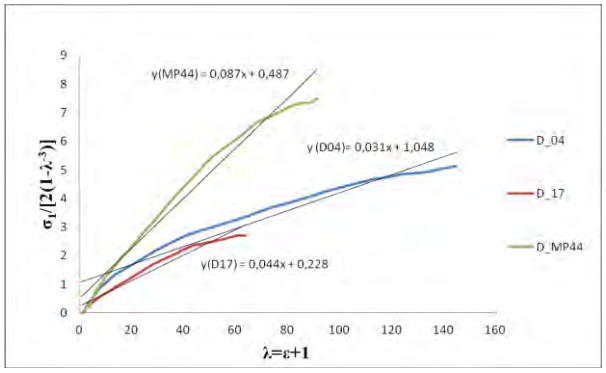

Fig. 7 M-R parameters for tire casing treads
Obr. 7 M-R parametre behúňov plášťov pneumatík

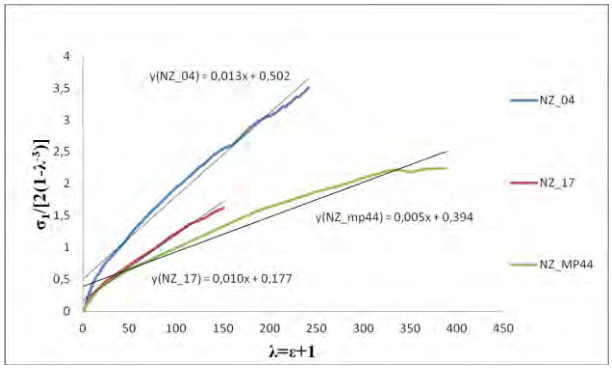

Fig. 8 M-R parameters for tire casing alluvial mixtures
Obr. 8 M-R parametre nánosových zmesí plášťov pneumatík

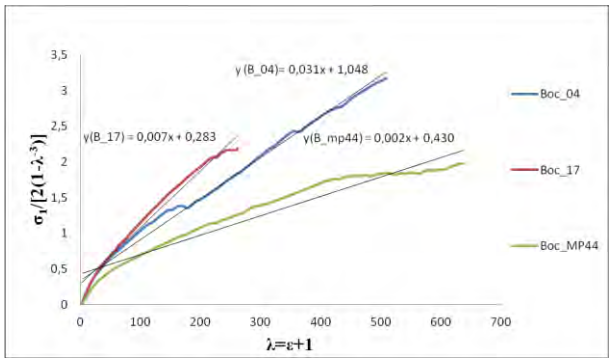

Fig. 9 M-R parameters for tire casing sidewalls
Obr. 9 M-R parametre bočníc plášťov pneumatík

These parameters are very important because they will serve as input data for computational models of tire casing degradation.

Hardness tests

Using the IRHD hardness tester, the hardness of the selected variously aged tire casing parts was determined. In Tab. 3, there are the values of hardness in relation to the given samples [5].

Tab. 3 Values of IRHD hardness
Tab. 3 Hodnoty tvrdosti IRHD

Sample	*IRHD* MP44 (new) [-]	*IRHD* 05 (mid. aged) [-]	*IRHD* 17 (oldest) [-]
tread	72.83	73.5	79.33
sidewall	43.17	56.67	65
Alluvial mixture	44	51.5	62.17

Figures 10 – 12 show the comparison of the measured values of hardness for each sample.

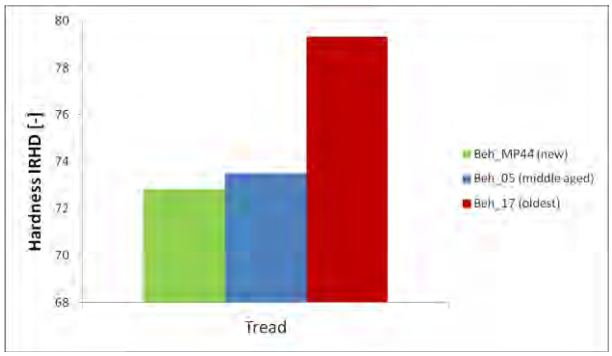

Fig. 10 IRHD hardness for tread samples
Obr. 10 Tvrdosť IRHD vzoriek behúňov

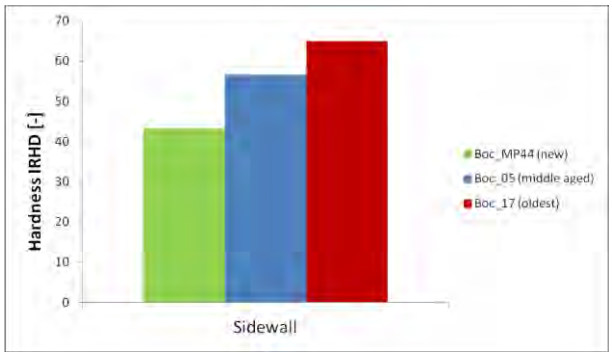

Fig. 11 IRHD hardness for sidewall samples
Obr. 11 Tvrdosť IRHD vzoriek bočníc

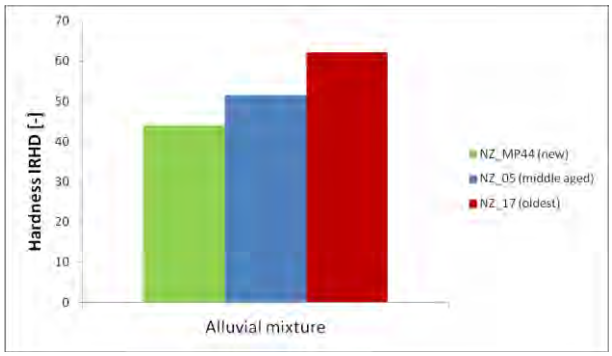

Fig. 12 IRHD hardness for alluvial mixture samples
Obr. 12 Tvrdosť IRHD vzoriek nánosových zmesí

From the results can be seen that harness increases with age. This is most significant recognition from the aspect of the results for tread samples where the the oldest tread has significantly higher values of hardness than the new treads. This mentioned fact gives a clear evidence of the level of degradation of the oldest tire casing.

Conclusions

From the dynamic and static experiments, modules of elasticity of tread, sidewall and alluvial mixture samples were determined and compared. The results show that the dynamic modules have much higher values than the static ones. This is caused by dynamic stress which has always higher values than dynamic stress.

From both dynamic and static tests can be concluded that the samples from the oldest tire casing are significantly degraded.

Mooney- Rivlin dependencies and parameters were obtained by calculation relating to the dependencies of stress δ on elongation ε while these dependencies were obtained on the basis of the static tensile tests.

From the results of the IRHD hardness test can be clearly seen that hardness increases with age. This is most significant fact in relation to the results for tread samples. From all of the results can be concluded that the oldest tire casing is degraded significantly.

Literature

[1] KRMELA, J. *Systémový přístup k výpočtovému modelování pneumatik I*., 1st ed., Czech Republic 2008, 102 p., ISBN 978-80-7399-365-8

[2] VIDO, P., PASTOREK, M., KRMELA, J. *Vybrané experimentálne skúšky kompozitov s elastomérovou matricou pre overenie výpočtových modelov pneumatík*. In: SEMDOK 2013 : 18th International of PhD. student´s seminar, Slovak Republic, Žilina, 2013, pp. 152-155, ISBN 978-80-554-0629-9

[3] VIDO, P., PASTOREK, M., DRDÁKOVÁ, J., STRUHARŇANSKÁ, M., KRMELA, J. *Determination of material characteristics for verification of computational models of tires*. In: Interdisciplinární mezinárodní vědecká konference doktorandů a odborných asistentů QUAERE 2013. Czech Republic, Hradec Králové: MAGNANIMITAS, 3rd ed., 2013, pp. 2611-2616, ISBN 978-80-905243-7-8

[4] KRMELA, J., DRDÁKOVÁ, J., KOVÁČ, I., VIDO, P., PASTOREK, M., STRUHARŇANSKÁ, M. Determination of Mooney-Rivlin Parameters of Alluvial Mixtures of Steel cords as an Input for FEM Models of Tire. In: *Hutnícke listy*. - ISSN 0018-8069, pp. 104-106.

[5] PASTOREK, M., VIDO, P., KRMELA, J. *Selected experiments of composites with elastomers for computational modelling of a tire*. In: ARSA2012: Proceedings in advanced research in scientific areas, The 1st virtual international conference. Slovak Republic, Žilina: EDIS, 2012, pp.1554-1559, ISBN 978-80-554-0606-0

Hutnické listy č. 3/2014, roč. LXVII
ISSN 0018-8069

Effect of Filler on Curing Characteristics of NR/Cellulose Blends

Vplyv plniva na vulkanizačné charakteristiky zmesí NR/celulóza

doc. Ing. Petra Skalková, PhD.[1], Ing. Katarína Kostelanská, PhD.[2], Pavol Boško[1]

[1]Alexander Dubček University of Trenčín, Faculty of Industrial Technologies in Púchov, I. Krasku 491/30, 020 01 Púchov, Slovak Republic
[2]Bukóza Invest, s r.o. Hencovská 2073, 093 02 Hencovce, Slovak Republic

Rubber blends have gained wide acceptance in industry due to ability to customize their properties to fit particular needs. Sulphur vulcanization process is the predominant method employed in the crosslinking of unsatured elastomers. This system is composed of sulphur, metal oxide (ZnO) and one or more organic accelerators. Natural rubber has been studied and reported extensively because of its superior performance in tire applications. The vulcanization of elastomeric materials has a high impact on the properties of the final product. Therefore, it is important to monitor and control this crosslinking process. The objective of the presented work is to evaluate the effect of biopolymer as reinforcing filler and sodium dodecyl sulphate as plasticizer on the curing characteristics of natural rubber blends.

Keywords: *elastomeric blends, vulcanization, scorch time, crosslinking density*

Vlastnosti polymérnych zmesí sú silne ovplyvňované druhom a obsahom jednotlivých typov polymérnych zložiek. Vzájomné miešanie polymérov je zložitý proces, pri ktorom vznikajú dvoj- alebo viaczložkové polymérne systémy. Prírodný kaučuk je obnoviteľný prírodný zdroj, ktorý má mnoho vynikajúcich vlastností, ako napr. vynikajúcu odolnosť všeobecne, vysokú pevnosť, ťažnosť a dobrú spracovateľnosť. Nevýhodou nenasýteného polyméru je malá odolnosť voči vysokým teplotám, vplyvu kyslíka, ozónu, ultrafialovému žiareniu, ktoré spôsobujú postupnú degradáciu polyméru a má negatívny vplyv na ich aplikáciu. Na prekonanie týchto obmedzení NR a rozšírenie použitia je nevyhnutná jeho modifikácia pre zlepšenie vlastností. Vytváranie nových zmesí polymérov prináša isté úskalia, pretože väčšina polymérov je vzájomne nemiešateľná. Vzájomná nemiešateľnosť spôsobená ich odlišnou štruktúrou, má negatívny dopad na úžitkové vlastnosti materiálov získaných ich miešaním. Negatívne tendencie sa potláčajú tzv. kompatibilizáciou, pridaním vhodného kompatibilizátora, alebo tenzidu. Práca sa zaoberá štúdiom vulkanizačných charakteristík zmesí prírodného kaučuku (NR) a celulózy (CEL) v množstvách od 0 do 55 dsk, za a bez prítomnosti tenzidu, dodecylsulfát sodný (SDS). Množstvo tenzidu SDS v zmesi bolo 0 a 3 dsk. Sledoval sa vplyv polysacharidu celulózy a tenzidu SDS na vulkanizačné charakteristiky, ako je minimálny krútiaci moment (M_L) a maximálny krútiaci moment (M_H), spracovateľská bezpečnosť zmesi (t_{s02}), počiatočný čas vulkanizácie (t_{c90}). Najvyššie hodnoty maximálneho krútiaceho momentu dosahovala najviac plnená zmes NR/55 dsk LBG bez SDS. Najvyššie hodnoty minimálneho krútiaceho momentu mala neplnená zmes a zmes NR/55 dsk LBG bez SDS. Podobný jav možno pozorovať aj u zmesí s rovnakým zložením a 3 dsk SDS. So zvyšujúcim obsahom celulózy do 40 dsk v zmesi s NR bezpečnosť zmesi a optimálna doba vulkanizácie klesali. Najvyššiu hodnotu optimálnej doby vulkanizácie mali neplnené zmesi s a bez SDS a zmes NR/55 dsk LBG/3 dsk DSS).

Kľúčové slová: *elastomérne zmesi, vulkanizácia, spracovateľská bezpečnosť zmesi, sieťová hustota*

Elastomers represent one of the most widely used material classes today. Their typical material properties, such as high elasticity and high damping, make these materials very important. The fields of application are manifold including vehicles parts, tires, tubing, shoes, gloves, seals, adhesives, drive and conveyor belts. In engineering applications, materials are subjected to a complex combination of manufacturing and in-service loadings. Filled elastomers are usually used both in the large strain and small strain regions and their viscous properties play an important role in their structural applications [1]. To reach the unique material properties of the raw material which is generally a mixture of rubber, crosslinking agent, fillers and several additional ingredients, this raw material must be crosslinked to an insoluble form and permanent material shape. Due to the chemical crosslinking, a thermoset material with a low crosslinking density, compared to e.g. epoxy resins, is formed. The crosslinking or vulcanization of elastomeric materials is a complex process which is crucial to obtain the final material properties. During vulcanization, "the properties of a rubber compound are changed" and therefore, "the vulcanization characteristics can be determined by measuring properties as a function of time and temperature" [2]. After vulcanization, rubber loses its tackiness, becomes insoluble in solvent and becomes more resistant to heat, light and aging processes [3, 4]. It is a common technique to measure vulcanization isotherms with a curemeter according to ISO 6502 and it leads to the

determination of the typical characteristic times for the compound curing process. The scorch time t_{s2} can be mentioned as and example and it represents the time at which the crosslinking reaction shows an influence on the measured torque and 2% of the total increase in torque is reached. The scorch time can be used as a measure of the processing safety of the compound. Other important characteristic values attained from a curemeter test are M_L minimum torque, M_H maximum torque, χ reached percentage of full cure, t_x time to reach a defined percentage x of full cure. The reached percentage of full cure can be calculated according to the following equation:

$$x = \frac{M_{(t)} - M_L}{M_H - M_L} . 100\%$$

A drawback of these measurements is that they are performed under the determined laboratory conditions which do not correspond to the processing conditions within the mould and moreover, samples shape does not represent the actual product geometry. The direct measurement of the crosslinking process within the production mould has not been performed yet.

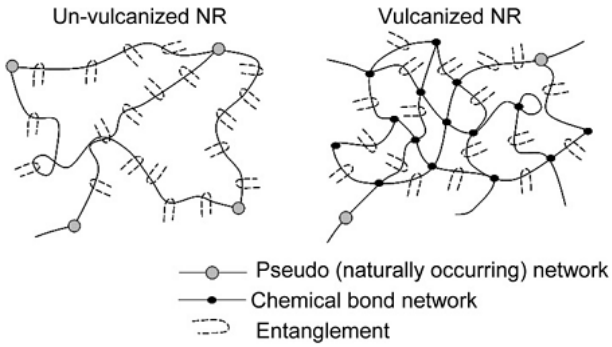

Fig. 1 Structure of network and entanglements in vulcanized and un-vulcanized NR
Obr. 1 Štruktúra siete a zauzlenia vulkanizovaného a nevulkanizovaného prírodného kaučuku

Further studies on the mechanical and curing properties of these systems showed that the cellulose improves the physicochemical as well as the technological properties of pure NR. The presence of cellulose decreases the vulcanization time and induces a significant increase in the crosslinking density presumably as a consequence of favourable polymer–filler interactions which cause an increment of the NR reactivity [5, 6].

Experiment

Materials

Natural rubber SMR 10 (NR) was purchased from Kuala Lumphur, Malaizia. Sodium dodecyl sulfate (SDS) was supplied from Aldrich. Greencel GW 600, cellulose fibres – Cellulose (CEL) 99.5 %, bulk density 70 – 90 $g.l^{-1}$ was supplied from Bukóza Invest, Ltd.

Preparation of NR/CEL blends

Cellulose was melt-blended with NR in Brabender Plasti – Corder PLE 331. Mixing was performed at 80 and 90 °C and 50 rpm. The contents of CEL were from 0 to 55 parts per hundred rubber (phr), respectively. SDS was used at two different amounts, namely 0 and 3 phr. Blends were vulcanized with the following formula: stearic acid, ZnO, Flavex, N-tert-Butyl-2-benzothiazolesulfenamide and sulphur. The temperature of vulcanization was 150 °C.

Determination of curing characteristics

Curing characteristics, such as scorch time (ts_2), cure time (tc_{90}), maximum and minimum torque (M_H, M_L) of filled NR blends were determined using a curemeter RHEOMETER 100 MONSANTO with rotor and software Daisy, 60 minutes at 150 °C.

Results and discussion

This study deals with curing characteristics of elastomer blends consisting of natural rubber filled with biopolymer, with and without presence of tenside represented by sodium dodecyl sulfate. Amount of cellulose used as a filler in the blends with NR was 0; 27.6; 30; 35; 40; 45; 50; 55 phr and content of tenside SDS was 0 and 3 phr.

Fig. 2 shows that blends filled with cellulose without SDS had lower values of minimal torque than unfilled blend without SDS. However, they had a higher maximum torque and it leads to assumptions that there isn't a strong adhesion between the rubber and filler surfaces. Generally, presence of nanoparticles of filler should increase the values of torque. Lower values of minimal torque can be a result of lower density of the blend filled with cellulose without SDS. Compared to unfilled blend, the higher stiffness of filled blends during curing is probably due to interaction of organic cellulose as well as accelerator with NR during curing process. Final thickening of the blend is a result of shorter and denser inter-chains created during accelerated curing process [7]. In comparison to the unfilled blend, the higher value of minimum torque was only measured for blend NR/55 phr CEL/0 phr SDS. Minimal torques of NR blends with different content of filler without SDS did not exhibit any kind of increasing or decreasing tendency based on the filler amount.

Hutnické listy č. 3/2014, roč. LXVII
ISSN 0018-8069

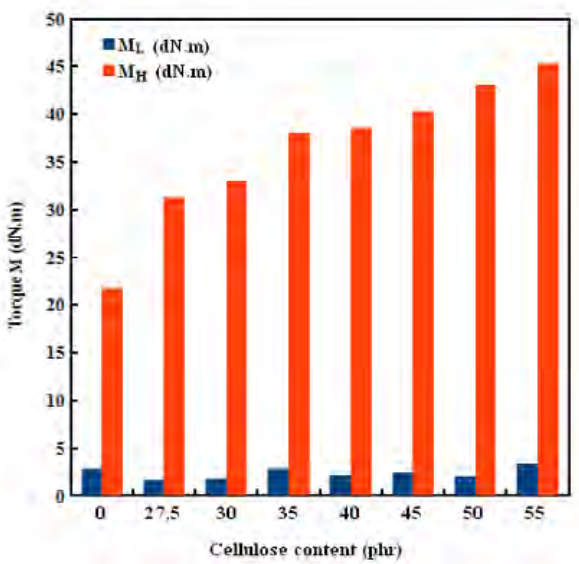

Fig. 2 Comparison of torque M_H and M_L in NR blends with different amounts of cellulose, without SDS
Obr. 2 Porovnanie krútiaceho momentu M_H a M_L zmesí prírodného kaučuku s rôznym obsahom celulózy, bez DSS

The biggest difference between minimum and maximum torque was exhibited by blend NR/55 phr CEL/0 phr SDS. The smallest difference was observed for unfilled blend without SDS. Value of maximum torque for NR/55 phr CEL/0 phr SDS blend (43 dN.m) was double higher than value of maximum torque of unfilled blend without SDS (22 dN.m).

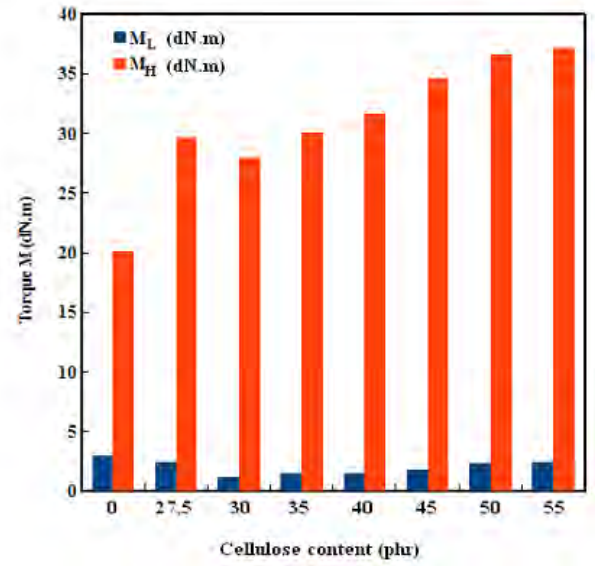

Fig. 3 Comparison of M_H and M_L torque in NR blends with different amounts of cellulose and with 3 phr SDS
Obr. 3 Porovnanie krútiaceho momentu M_H a M_L zmesí prírodného kaučuku s rôznym obsahom celulózy s 3dsk SDS

From Fig. 2 and 3 can be seen that unfilled NR blend with 3 phr of SDS exhibited slight refinement in comparison to unfilled blend without SDS. Values of minimum and maximum torque were lower. Blends with different amount of cellulose and 3 phr of SDS had higher maximal torque but it was a bit less significant than in filled blends without SDS. The increasing of maximum torque is linear with increasing of amount of cellulose filler in the blends with 3 phr of SDS and the same course is fulfilled for filled blends without SDS. The blend of NR/27.5 phr CEL/3 phr SDS is an exception because it exhibits higher value of maximum torque than the blend NR/30 phr CEL/3 phr DSS. The linear increase of M_H was observed for NR blends with higher content of cellulose than 30 phr and 3 phr of SDS. Value of maximum torque for NR/55 phr CEL/3 phr SDS blend was double higher than value of maximum torque for unfilled blend with 3 phr of SDS. The highest value of minimum torque (3 dN.m) was observed for unfilled blend of NR with 3 phr of SDS.

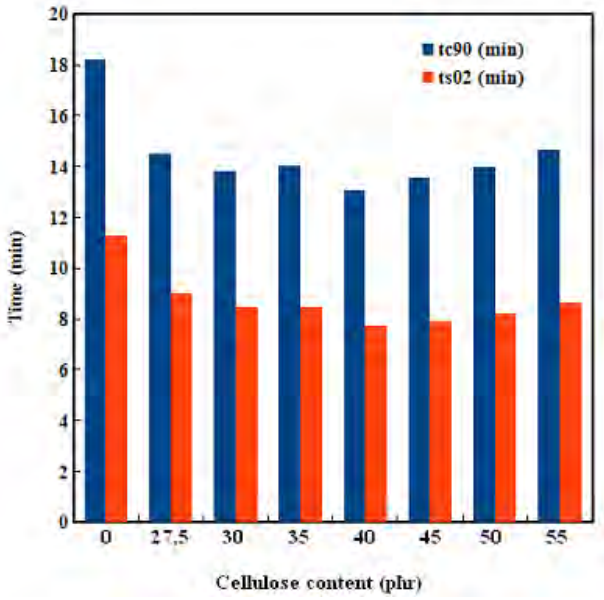

Fig. 4 Comparison of scorch time and optimal curing time of NR/CEL blends without SDS
Obr.4 Porovnanie spracovateľskej bezpečnosti a optimálnej doby vulkanizácie zmesí NR/CEL bez SDS

From Fig. 4 can be seen, that the highest value of optimal curing time and scorch time was observed unfilled blend without SDS (18.22 and 11.31 minutes). In all blends filled with cellulose, the values of optimal curing time and scorch time were reduced. This effect is probably caused by cellulose which acts as an accelerator in NR blends as mentioned in work [7]. The lowest values of optimal curing time and scorch time were observed for blend NR/40 phr CEL/0 phr SDS (13.08 and 7.75 minutes). These values present the limit amount of cellulose (40 phr) in NR. Further increasing of values of scorch time and optimal curing time in blends with higher cellulose content than 40 phr is probably caused by interaction of cellulose polymeric inter-chains. It is connected with the fact, that the blends were much stiffer with higher amount of cellulose in NR. The blend with highest cellulose amount (55 phr) without SDS does not have such long optimal curing time or scorch time as unfilled NR blend without SDS.

From Fig. 5 can be seen that unfilled NR blend with 3 phr of SDS content exhibited slightly increasing optimal curing time and scorch time in comparison to the unfilled NR blend without SDS. Tenside SDS probably acts as cure inhibitor. In filled blends with 3 phr of SDS, we could observe decrease in optimal curing time and scorch time again, but it is less significant than in the case of filled blends without SDS. Optimal curing time and scorch time were decreased up to 35 phr of cellulose content. Blend NR/35 phr CEL/3 phr SDS had almost the same value of optimal curing time and scorch time (14.83 and 8.96 minutes) as blend NR/40 phr CEL/3 phr SDS (14.8 and 8.81 minutes). Optimal curing time and scorch time were increased with the filler content higher than 40 phr in NR blends as well as in blends without SDS. The values of optimal curing time and scorch time for blend NR/55 phr CEL/3 phr SDS were 17.41 and 9.76 minutes. It was still less in comparison to unfilled NR blend with 3 phr of SDS (18.95 and 12.43 minutes).

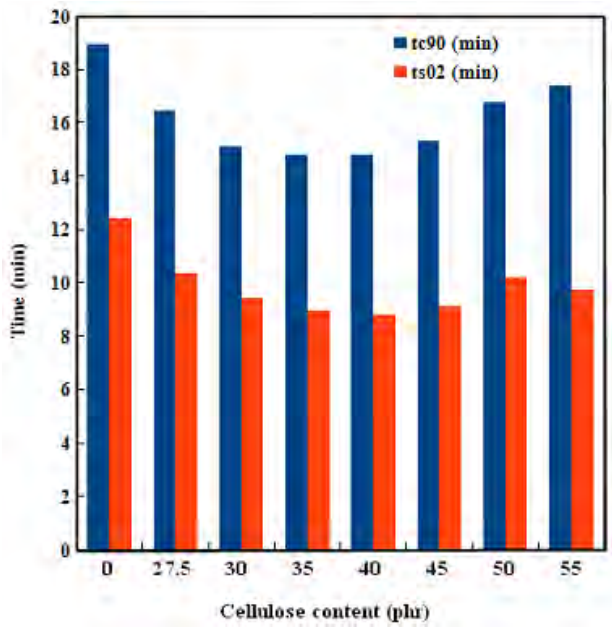

Fig. 5 Comparison of scorch time and optimal curing time of NR/CEL blends with 3 phr of SDS
Obr. 5 Porovnanie spracovateľskej bezpečnosti a optimálnej doby vulkanizácie zmesí NR/CEL s 3 dsk SDS

Conclusions

According to the obtained results, the scorch time and curing time was decreased with cellulose loading, whereas the maximum torque (M_H) was increased for all types of rubber blends. NR blend with the highest content of the cellulose but without tenside exhibited highest value of minimum torque (M_L). The increasing cellulose-NR compositions and the presence of SDS improve the processability and maximum torque of the NR/CEL blends. The scorch time and curing time are decreased with the increase composition of cellulose up to 40 phr in NR blends.

Literature

[1] SAE-OUI, P., SIRISINHA, C., THAPTONG. P. Utilization of limestone dust waste as filler in natural rubber. *Journal of Material Cycles and Waste Management* 11 (1), 2009, p. 166–171

[2] ZHANG, W., ZHANG, X., LIANG, M., LU, C. Mechanochemical preparation of surface acetylated cellulose powder to enhance mechanical properties of cellulose filler reinforced NR vulcanizates. *Composites Science and Technology* 68(12), 2008, p. 2479–2484

[3] FAN, R.L., ZHANG, Y., LI, F., ZHANG, Y.X., SUN, K., FAN, Y.Z. Effect of high-temperature curing on the crosslink structures and dynamic mechanical properties of gum and N330-filled natural rubber vulcanizates. *Polymer Testing* 20, 2001, p. 925–36

[4] AKINLABI, A.K., OKIEIMEN, F.E., EGHAREVBA, F., MALOMO, D. Investigation of the effect of mixing schemes on rheological and physico-mechanical properties of modified natural rubber blends. *Materials and Design* 27 (1), 2006, p. 783–788

[5] ISMAIL, H., SHAARI, S.M. Curing characteristics, tensile properties, and morphology of palm ash/halloysite nanotube/ethylene-propylene-diene monomer (EPDM) hybrid composites, *Polymer Testing* 29, 2010, p. 872−878

[6] ISMAIL, H., OSMAN, H., ARIFFIN, A. A comparative study on curing characteristics, mechanical properties, swelling behaviour, thermal stability, and morphology of feldspar and silica in SMR L vulcani-zates, *Polymer-Plastics Technology and Engineering*. 43 (5), 2005, p. 1323–1344

[7] MARTINS, A.F., VISCONTE, L.L.Y. NUNES, R.C.R. Evaulation of Natural Rubber and Cellulose II Compositions by Curing and Mechanical Properties, RAW Materials and Applications, *KGK Kautschuk Gummi Kunststoffe* 55. Jahrgang 12, 2002

Hutnické listy č. 3/2014, roč. LXVII
ISSN 0018-8069

Evaluation of Experimental Results for Selected Rubber Compounds before and after Aging Degradation

Vyhodnocovanie experimentálnych výsledkov vybraných materiálových charakteristík gumárenských zmesí pred a po zostarnutí

Ing. Monika Struharňanská[1], doc. Ing. Jan Krmela, PhD.[1]

[1]Alexander Dubček University of Trenčín, Faculty of Industrial Technologies, I. Krasku 491/30, 020 01 Púchov, Slovak Republic

The paper is focused on the investigation of the tire rubber compounds and influence of degradation on their mechanical properties. The aging of rubber compounds may occur in their production, but it can be also connected with the technological process in the production. One of the ways how to simulate the selected degradation processes of rubber compounds is to use software systems based on the finite element method as computer numerical methods. The selected degradation process of alluvial compounds is evaluated by computational modeling in combination with experimental investigations. The new alluvial compounds in comparison to degraded one are evaluated in the paper. The tensile strength obtained from static tensile tests in uniaxial tension is evaluated and compared. The Mooney-Rivlin parameters are set on the basis of dependencies mentioned hereinbefore. Using simulations, we can find the potential modifications in technological production processes of the tire in order to minimize the aging degradation.

Keywords: *tire, rubber compounds, degradation, experiment, cyclic loading*

Príspevok je orientovaný na problematiku gumárenských zmesí plášťov pneumatík. V plášťoch pneumatík sú gumárenské zmesi v interakcii s výstužnými materiálmi. Ku starnutiu gumárenských zmesí môže dochádzať pri ich vlastnej výrobe, ale aj v technologickom procese vo výrobe. Na degradáciu gumárenskej zmesi má vplyv mnoho faktorov (skladovanie, vplyv okolitého prostredia a i.). Pre vyhodnotenie je potrebné poznať chemické zloženie gumárenskej zmesi, ako aj ich mechanické vlastnosti. Jednou z možností, ako simulovať vybrané degradačné procesy gumárenských zmesí a ich vplyv na mechanické charakteristiky vyrobených elastomérov, je využitie programových systémov na báze metódy konečných prvkov. Skúšobné vzorky boli vyrobené z gumárenských zmesí zamiešaných pred 1-7 rokmi. Výrazným faktorom, ovplyvňujúcim degradáciu, je vplyv vzdušného ozónu. Bude zhodnotený vybraný degradačný proces nánosových zmesí výpočtovým modelovaním v kombinácii s experimentmi. S týmto úzko súvisí návrh verifikačných kritérií, na základe ktorých je možné výsledky z výpočtov objektívne posúdiť s výsledkami z experimentov. V príspevku sú hodnotené nánosové zmesi nové v porovnaní s degradovanými. Vyhodnotené sú formou porovnania závislosti ťahovej sily na predĺžení, získaných zo statických skúšok v ťahu. Na základe týchto závislostí sú stanovené Mooney-Rivlinové parametre. V príspevku bola navrhnutá metodika pre cyklické zaťaženie pre elastoméry vyskytujúce sa v plášťoch pneumatík. Meranie závislostí prebieha pre všetky jednotlivé zmesi, ako pre nové vzorky, tak aj pre vzorky po starnutí. Simuláciami môžeme nájsť potenciály v technológii procesov a produkcii plášťov pneumatiky, aby tieto typické degradačné starnutie bolo minimalizované. Na základe výsledkov možno zlepšiť výrobu nánosových zmesí plášťov pneumatík resp. navrhnúť opatrenia vedúce k zníženiu vplyvu starnutia na materiálové charakteristiky aj chemickým zložením gumárenských zmesí.

Kľúčové slová: *pneumatika, gumárenská zmes, degradácia, experiment, cyklické zaťažení*

Research is focused on tire rubber compounds in the interaction with reinforcing materials. Due to effect of various factors, the degradation of compounds may occur. One of the ways how to reduce or minimize the degradation effect is connected with the simulation of the degradation processes of rubber compounds using the software systems based on finite elements (FEM). By these simulations, we try to find the potential solution in relation to the degradation processes occurring during the process of tire manufacture.

Composite materials in tire casings

In the terms of material, the tire can be defined as very complex polycomponent material with specific properties. It is necessary to take into account these characteristics in relation to the computational models in the form of adequate material models and it can lead to the best description of the each part of composite casing. In relation to the tire composite casings, they are the composites with reinforcing fibers and polymer matrix called steel cord buffer, overlay buffer and carcass plies. The contact between the vehicle and the road is provided through the tire and its role is to

transfer forces. Basic material – the matrix is a binder and another component material has a firming effect (reinforcement) [1].

It is important to define composite materials in order to specify and utilize the individual material parameters and then we can create the computational model of the tire based on the given individual parametres. Composites with reinforcing fibers and composites with polymeric matrix are suitable to solve a given problem, because they are strong and tough fibers implemented into softer plastic matrix and by this way, the enhancement of the material mechanical properties can be gained. The given mechanical properties involve strength, toughness, fatigue resistance and tenacity of the composite. Elastomer degradation is caused by the influence of atmospheric oxygen and it is called oxidative aging. At normal temperatures and operating conditions for automobile tires, this aging can be observed after the long time. On average, it can be recognized after 4–8 years of tire service. Degradation of the rubber mixture is influenced by many factors and for good evaluation, it is necessary to know the chemical composition of the rubber compounds as well as their mechanical properties. After receiving the necessary information about rubber compounds, it is possible to carry out the simulations of the selected forms of degradation processes with the help of software systems based on FEM [1].

Overview of the tests performed

The rubber compounds had been provided from the production line of the tire casings and they were subsequently homogenized by help of the laboratory double cylinder at the temperature of 65–70 °C. Samples were left for at least 24 h at room temperature. We continued with determination of vulcanization characteristics using the rheometer Monsanto 100 at 150 °C and vulcanization curve was recorded for 60 min. Prepared rubber compounds were left to vulcanize by help of hydraulic press at 150 °C while the pressure was 20 MPa and it lasted 30 min. After leaving them for at least 16 h, the samples in form of double-sided blades with size A1 in accordance with ISO 37 [5] were subsequently cut [2].

Static tensile tests

Tested samples in the form of double-sided blade were pulled in uniaxial tension using the universal test machine Hounsfield H20K-W. During the test, the movement speed of jaws was 50 mm/min and temperature was 23 ± 2 °C. The values of strength and elongation to the break are necessary for the following evaluation of the required characteristics. The tensile strength and elongation to the break were evaluated parameters.

Hardness tests

The hardness was determined by indentation of the indentor which is a part of durometer IRHD. The indented depth of testing indentor pressed into the material was measured according to ISO 48 [6]. Hardness value is inversely proportional to the depth of indentation of the tip, representing indentor, into the material and depends on the elastic modulus and viscoelastic properties of the material. Hardness was measured at 23±2 °C and five tested samples were used and the thickness of each one was 6 mm [2].

Experimental results and discussion

The tested samples were made of rubber compounds which were blended 4 or more years ago. A significant factor affecting the degradation is the impact of air ozone which acts on the compound. Fig. 1 shows the evaluated dependency of force on the elongation of alluvial compounds with the specific designation as well as with its year of the manufacture (for example designation of sample B10 (2007) corresponds to rubber compound labeled B10 and this compound was blended in 2007). Material parameters of rubber compounds before and after degradation aging are evaluated in Table 1. For sample B10 (2007), it can be concluded that the elongation to break of sample after degradation was approx. 90 mm and the force 46 N stands for a curve approaching the value of the new sample B10 (2010). For higher values of elongation to break, the course of dependency is different in comparison to the other samples [3]. Significant difference of Mooney-Rivlin parameters can be seen in the Tab. 1.

Tab. 1 Elastomeric compounds before and after degradation aging
Tab. 1 Elastomérne zmesi pred a po degradačnom starnutí

sample number	measured F [N]	measured Δl [mm]	calculated E [MPa]	calculated A0 [mm^2]	calculated σ [MPa]	calculated ε [%]	C10* [MPa]	C01* [MPa]
B09 (2007)	168.7	112.7	8.63	13.87	12.16	140.9	0.040	0.187
B10 (2007)	152.0	203.6	4.65	12.84	11.84	254.5	0.025	0.597
B13 (2007)	259.3	180.1	8.93	12.91	20.09	225.1	0.046	1.040
44 (2009)	238.7	220.1	6.81	12.76	18.71	275.1	0.523	0.304
B07 (2010)	167.3	125.9	8.25	12.89	12.98	157.3	0.037	0.813
B08 (2010)	169.3	114.1	8.48	13.99	12.11	142.7	0.037	0.863
B09 (2010)	218.0	177.7	7.08	13.88	15.72	222.1	0.035	0.136
B10 (2010)	134.0	219.3	3.81	12.84	10.44	274.1	0.019	0.231
B13 (2010)	246.0	191.2	7.98	12.91	19.06	238.9	0.038	0.379
44 (2013)	305.6	217.8	7.75	14.50	21.09	272.2	0.033	0.019

*Calculated Mooney-Rivlin parameters

Hutnické listy č. 3/2014, roč. LXVII
ISSN 0018-8069

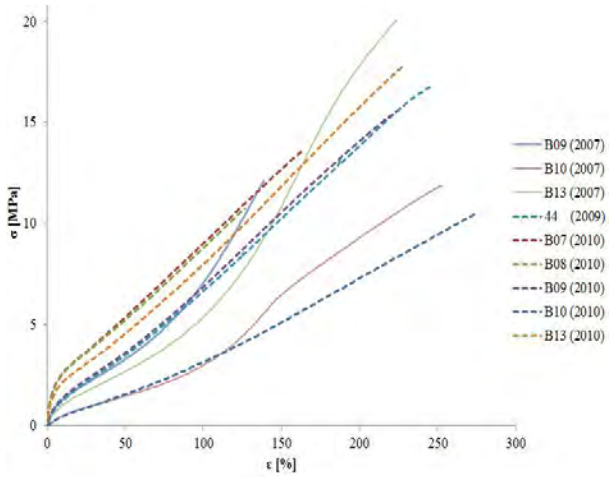

Fig. 1 Dependence of stress on the elongation to the break from the static tensile test in uniaxial tension
Obr. 1 Závislosť napätia od pomerného predĺženia zo statickej skúšky v ťahu v jednoosej napätosti

The dependences of stress on the elongation to the break of new samples as well as samples after aging were also measured and evaluated. In Fig. 2, there are the samples B13 (2007) and B13 (2010) which were evaluated and the evaluation is based on mutual comparison of parametres for these samples after and before aging. Based on the comparison of these two samples, there is significant difference in relation to the parameters for new samples compared to the samples after degradation. We can conclude that the change may be caused by the impact of air ozone acting on the given samples during the period of three years [3, 4].

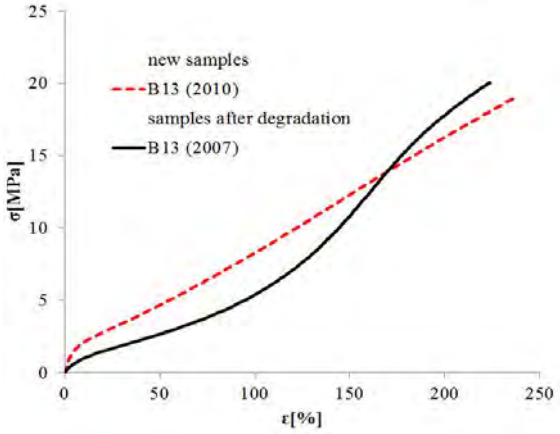

Fig. 2 Dependence of stress on the strain for samples B13 (2010) and B13 (2007)
Obr. 2 Závislosť napätia od pomerného predĺženia vzoriek B13 (2010) a B13 (2007)

Cyclic loading test of specimens in tension

Experiment was focused on cyclic loading of the selected compounds designated as B08 (2010), 44(2009) and 44 (2013). Samples in the form of double-sided blades were tested in uniaxial tension by test machine Hounsfield H20K-W. The sample was placed into the clamps of device (Fig. 3), where for the first tension, the initial value was 80 mm between the jaws and the speed of movement of jaws was 50 mm/min. Subsequently, the initial length of measurement at each cycle was varied in the range ± 0.25 mm due to the impossibility to stop the machine precisely at the desired length.

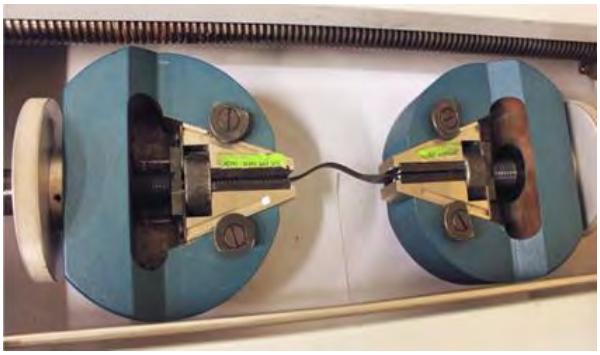

Fig. 3 Tested sample in clamps of testing machine
Obr. 3 Vzorka upevnená v čeľustiach skúšobného zariadenia

Evaluation of cyclic loading for samples designated as B08 (2010), 44 (2009) and 44(2013)

In relation to the strain, the sample was tested for 10 % (8 mm), 15 % (12 mm) and 20% (16 mm) with the reference to the initial values and five measurements were performed for the each one cycle. These values (strain) were selected because they are the closest values in relation to the conditions in practice. The each one cycle involved loading and releasing. After clamping into jaws and after requested strain in a given measured cycle, the sample was manually stopped for about 30 seconds to print the outputs of measured values from the testing machine in the form of graphs. The distance between the clamps was measured by sliding caliper gauge and this length became the input starting point for the next cycle. The sample was clamped in jaws during the whole measurement throughout the all cycles.

From dependence of the force on elongation for samples B08 (2010), 44 (2009) and 44 (2013), the dependence of stress on strain during cyclic loading was evaluated. Individual dependencies are shown in Figures 4 and 5.

Comparison of the measurement of rubber compound B08 (2010) represented by sample 1 and 2 showed that the compounds are identical and course of the curves, shown in the previous figures, is the same. This course was expected because there was the assumption that it was the same compound of the same composition as well as year of production. In the Fig. 5, the compounds 44 (2009) and 44 (2013) of the same composition can be seen but these compounds were not produced in the same year. In relation to the comparison of these compounds, there is the visible decrease of the stress values under the influence of the degradation to which the sample was exposed for 4 years.

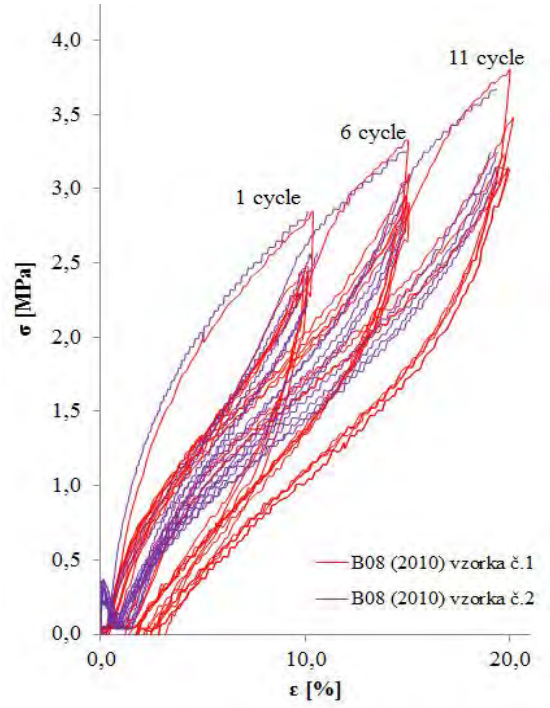

Fig. 4 Dependence of stress on the strain for samples B08 (2010) under cyclic loading
Obr. 4 Závislosti napätia od pomerného predĺženia vzorky B08 (2010)pri cyklickom zaťažení

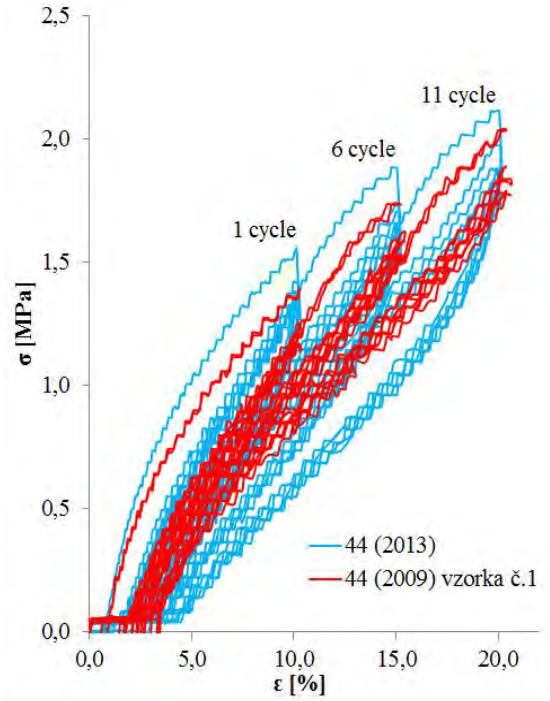

Fig. 5 Dependence of stress on the strain for samples 44(2013) and 44 (2009) under cyclic loading
Obr. 5 Závislosti napätia od pomerného predĺženia vzorky 44(2013) a 44 (2009) pri cyklickom zaťažení

Conclusions

Based on performed experiments, it can be concluded that aging process has a significant impact on the course of stress-strain characteristics from the aspect of static tensile tests. The methodology for cyclic loading of elastomers for the tire casings was determined. Measurement of the dependencies will continue for the each one individual compound relating to the new samples as well as the samples after aging. The results will be also used for calculations of Mooney-Rivlin parameters which will be the input data for calculations. Wrong evaluation of the investigated material and other characteristics can significantly affect their resulting values used for the calculations in FEM. These results are part of the research performed during the dissertation work of the author of the paper and the dissertation work is focused on „Verification of experimental results of the selected material characteristics of rubber compounds." On the basis of the results, the production of alluvial compounds for tire casings can be improved and it is also possible to propose measures leading to the reduction of the impact of aging on the material characteristics by changes of chemical composition of rubber compounds.

Literature

[1] DRDÁKOVÁ, J., STRUHARŇANSKÁ, M., KRMELA, J. *Selected physical – mechanical properties of specific composite materials with elastomer*. In ARSA 2012, Slovak Republik, 2012, ISBN 978–80–554–0606–0, p. 1785–1788

[2] DRDÁKOVÁ, J., STRUHARŇANSKÁ, M., KRMELA, J. *Vybrané fyzikálno – mechanické vlastnosti špecifických kompozitných materiálov s elastomérmi*. In Semdok 2013, Slovak Republik, 2013, ISBN 978–80–554–0629–9, p. 104-107

[3] KRMELA J., DRDÁKOVÁ, J., KOVÁČ I., VIDO P., PASTOREK M., STRUHARŇANSKÁ M. *Determination of Mooney–Rivlin Parameters of Rubber Used for Rubberizing of Steel cords as an Input for FEA Models of Tire*, Hutnícke listy, Czech Republic: 2012, 65, (7), ISSN 0018-8069, p. 104-106

[4] VIDO P., PASTOREK M., DRDÁKOVÁ, J., STRUHARŇANSKÁ, M, KRMELA, J. *Stanovenie materiálových charakteristík pre verifikáciu výpočtových modelov plášťou pneumatík.* QUAERE 2013, International Scientific Conference, Czech Republic, 2013, ISBN 978-80-905243-7-8, p. 2611-2616

[5] Standard ISO 37(orig. STN 62 1436), *Guma. Stanovenie ťahových vlastností*, edition 1982-03- 29

[6] Standard ISO 48(orig. STN 62 1433), *Guma. Stanovenie tvrdosti v medzinárodných jednotkách (tvrdosť od 30 do 85 IRHD)*, edition 1981-04- 14

Hutnické listy č. 3/2014, roč. LXVII
ISSN 0018-8069

Study of the Properties for Rubber Compounds with Fillers Based on PLA and PP Fibers

Štúdium vlastností kaučukových zmesí s obsahom plniva na báze PLA a PP vlákien

Ing. Katarína Holcová[1], prof. RNDr. Mariana Pajtášová, PhD.[1], Ing. Lenka Španiková [1], Ing. Jana Palieskova[1], Ing. Zuzana Jankurová PhD.[1], Ing. Marianna Janeková[1]

[1]Alexander Dubček University of Trenčín, Faculty of Industrial Technologies in Púchov, I. Krasku 491/30, 020 01 Púchov, Slovak Republic

This paper deals with the study of various non-conventional fillers, which were selected in order to replace a certain amount of conventional active fillers in rubber compounds. Investigation was connected with two types of fillers which were based on fibers. The polypropylene fibers (PP) and polylactide fibers (PLA) were subjected to the investigation process and the investigation of these two fibers was performed for the different amount which was 1 and 5 phr. Nowadays, the fibrous materials are quite popular subject of research because they offer such properties which can be the contribution for the future development of the industry. In addition, these materials are acceptable in the sphere of the environmental engineering because renewable raw materials are preferred including agricultural products. The current state of the preparation of textile fiber materials is influenced by several factors, such as technical, economic, environmental, qualitative and many others. Although the given factors have to be taken into account, the properties of the given fibrous materials highly influence the selection of the material. The paper is closely connected with measurement of vulcanization characteristics (minimum torque M_L, maximum torque M_H, time of start of vulcanization t_s, optimum vulcanization of t_{90}, rate coefficient of vulcanization R_V). Furthermore, the evaluation of the measured data in relation to non-vulcanized rubber compounds is also carried out. Moreover, the physical and mechanical properties (tensile strength, tensibility, hardness) of resultant vulcanizate were investigated. These characteristic features were compared to those which are typical for standard rubber compounds used in the rubber industry while standard filler was carbon black of N339 type.

Keywords: *polymeric materials, vulcanization characteristics, physical and mechanical properties, polypropylene fibers, polylactide fibers*

Práca sa zaoberá štúdiom vlákien vo funkcii plniva kaučukových zmesí. Pridaním plniva sa všeobecne menia všetky vlastnosti nevulkanizovaných zmesí, ale i vulkanizátov. Upravuje sa spracovateľnosť zmesí, mení sa merná hmotnosť vulkanizátov, pevnosť, ťažnosť, technický modul, dynamické vlastnosti a podobne. Zlepšenie vlastností vulkanizátu prídavkom plniva sa nazýva stuženie, čím sa rozumie súhrn všetkých zmien vlastností vulkanizátov s pozitívnym účinkom na vlastnosti výrobkov. Rozsah stuženia závisí nielen od veľkosti častíc plniva, ale aj od štruktúry a aktivity jeho povrchu. Všetky tieto charakteristiky ovplyvňujú interakciu medzi kaučukom a povrchom plniva. V práci boli použité dva druhy plnív na báze vlákien, a to polypropylénové vlákna (PP) a polylaktidové vlákna (PLA), ktoré boli pripravené v množstve 1dsk a 5dsk. Z celosvetového hľadiska sú vláknité materiály vysoko perspektívne pre budúci rozvoj priemyslu, pričom v súčasnosti sa presadzujú obnoviteľné zdroje surovín napr. poľnohospodárske produkty. Súčasný stav výroby na prípravu textilných vláknitých materiálov je podmienený viacerými faktormi a to technickými, ekonomickými, ekologickými, kvalitou a inými vlastnosťami. PLA je vhodnou náhradou polymérov na báze ropy pretože sa vyrába z biomasy a má vysokú biokompatibilitu a biodegradáciu. Vo všetkých gumárenských zmesiach bol použitý typ plniva kombinovaný s používaným aktívnym plnivom (sadze typu N339).U pripravených gumárenských zmesí boli hodnotené reologické vlastnosti a vulkanizačné charakteristiky (minimálny krútiaci moment M_L, maximálny krútiaci moment M_H, začiatok vulkanizácie t_S, optimálny čas vulkanizácie t_{90}, koeficient rýchlosti vulkanizácie R_V). U výsledných vulkanizátov, pripravených v tvare obojstranných lopatiek boli hodnotené fyzikálne a mechanické vlastnosti (pevnosť v ťahu, ťažnosť, tvrdosť) v zmysle platných noriem. Tieto vlastnosti boli porovnané so štandardnou gumárenskou zmesou, ktorá obsahovala plnivo sadze N339 a bola pripravená za rovnakých podmienok ako všetky gumárenské zmesi.

Kľúčové slová: *polymérne materiály, vulkanizačné charakteristiky, fyzikálne a mechanické vlastnosti, polypropylénové vlákna, polylaktidové vlákna*

Fillers in rubber compounds are very important because they have significant affect on properties of compounds and final product. In most cases, they are solid substances used in form of staple fiber or short fibers which represent the cut length of filament. Fillers help to improve the mechanical properties (such as strength, abrasion or wear resistance, toughness, and stiffness) and they also improve the resistance to heat, fire,

corrosion and aging and moreover, they affect the appearance of products [1]. Efficiency of fillers depends on the various parameters including the size of the filler particles, their shape, dispersion and surface, surface reactivity, structure of filler, ability of filler to form bonds with the rubber matrix [2, 3].

Experiment

Experimental evaluation is focused on the physical and mechanical properties of rubber compounds with an addition of polylactide fibers (PLA) and polypropylene fibres (PP).

The optical microscope LEICA was used for preparations of images of PLA and PP fibers (Fig. 1, 2; zoomed 200×).

Preparation and mixing of rubber compounds is one of the most important processes of rubber technology. The rubber compounds were prepared by two-step mixing in laboratory mixer of type Brabender, and the procedure was performed according to STN (Slovak Technical Standard) [4]. The given process of the investigation was performed under the special and determined conditions where the temperature was 120 °C and a rate of pinions rotation was 50 rpm/min. The rubber compounds consisted of synthetic rubber (SBR), carbon black of N339 type, polylactide fibers and polypropylene fibers. Mixing relating to the first step took 12 minutes. The second step of the preparation process took 6 minutes and the temperature was 90 °C while the sulphur was used as a vulcanization agent which was added to the compounds. The mixed rubber compounds were homogenized during the first and the second steps in laboratory double-cylinder device.

Prepared rubber compounds were left for 24 hours at laboratory temperature and then rheological properties and vulcanization characteristics (M_L, M_H, T_{S2}, t_{90}, R_v) were found out by vulcameter Monsanto 100 at the temperature of 150 °C during 60 min and the given mentioned procedure was performed according to specifications in STN [5]. Obtained values of vulcanization characteristics of rubber compounds containing prepared fillers were compared with the values of reference rubber compound.

Tensile properties were determined by help of tearing machine INSTRON according to STN [6]. The tensile strength, tensibility were evaluated properties. Hardness of vulcanizate was measured by hardness tester IRHD according to STN [7]. The measured values of model rubber compounds were compared to standard rubber compound.

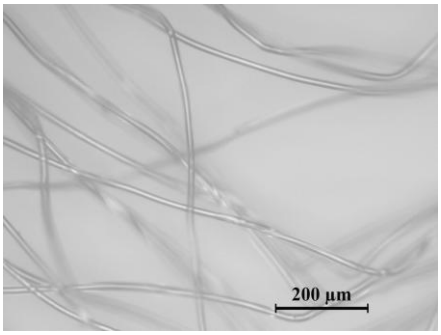

Fig. 1 Polylactide fibers
Obr. 1 Polylaktidové vlákna

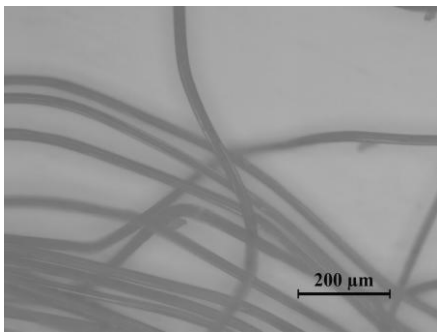

Fig. 2 Polypropylene fibers
Obr. 2 Polypropylénové vlákna

Results and discussion

Effect of fillers (*PLA, PP*) on the course of the sulfur vulcanization of rubber compounds was evaluated on the basis of vulcanization characteristics (minimum torque M_L, maximum torque M_H, time of start of vulcanization t_s, optimum time of vulcanization t_{90}, rate coefficient of vulcanization R_v). Using vulcanization curves, rheometric results based on evaluation of vulcanization characteristics were obtained and important parameters representing the vulcanization process are summarized in Tab. 1. Graphical presentations of the results relating to determination of vulcanization characteristics are shown in Figs. 3, 4.

Tab. 1 Vulcanization characteristics of rubber compounds
Tab. 1 Vulkanizačné charakteristiky gumárenských zmesí

		M_L [Nm]	M_H [Nm]	t_s [min]	t_{90} [min]	R_v [min^{-1}]
S		6.9	29.8	7.6	16.8	10.9
PLA	1 [phr]	6.6	30.1	7.5	17.9	9.6
	5 [phr]	6.5	33.1	7.6	43.0	2.8
PP	1 [phr]	6.5	30.3	7.3	16.5	10.9
	5 [phr]	6.1	29.9	8.0	17.4	10.7

The values of maximum torque (Fig. 3) for rubber compounds are lower in comparison to standard rubber compound.

Hutnické listy č. 3/2014, roč. LXVII
ISSN 0018-8069

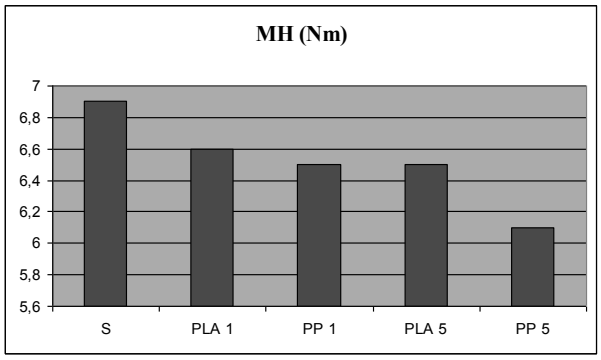

Fig. 3 Maximum torque of rubber compounds
Obr. 3 Maximálny krútiaci moment gumárenských zmesí

In comparison to standard compound, rubber compound with addition of 5 phr of PLA exhibited the highest value during the measurement of optimum time (Fig. 4) of vulcanization and it could have a positive impact on the quality of the resulting vulcanizate.

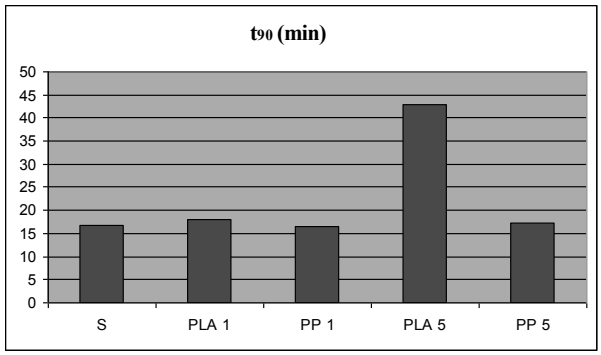

Fig. 4 Optimum time of rubber compounds
Obr. 4 Optimálny čas gumárenských zmesí

The selected physical and mechanical properties (strength, tensibility, hardness) were tested and evaluated in the case of the standard vulcanizate as well as vulcanizates with content of fillers containing PLA and PP. Effect of type and amount of the given filler with PLA and PP on selected physical and mechanical properties is presented in Tab. 2. Graphic images of the results for important physical and mechanical properties of vulcanizates are shown in Figs. 5 – 7.

Tab. 2 Physical and mechanical properties of resultant vulcanizates
Tab. 2 Fyzikálne a mechanické vlastnosti výsledných vulkanizátov

		Tensile strength [MPa]	Tensibility [%]	Hardness [IRHD]
S		17.7	321.4	66
PLA	1 [phr]	16.6	289.0	70
	5 [phr]	15.9	301.4	67
PP	1 [phr]	15.9	281.6	69
	5 [phr]	14.3	252.4	75

Evaluation of measured tensile properties showed that tensile strength (Fig. 5) of the added filler with 5 phr of PP was lower significantly in comparison to standard rubber compound.

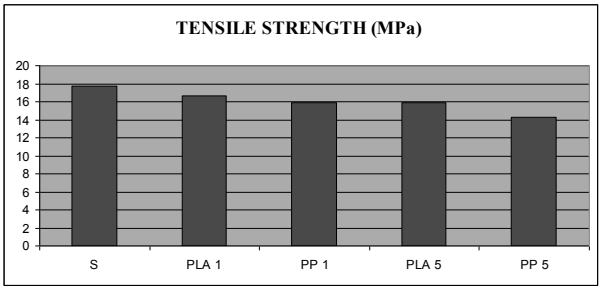

Fig. 5 Tensile strength of resultant vulcanizates
Obr. 5 Pevnosť v ťahu výsledných vulkanizátov

Evaluation of measured values showed that tensibility (Fig. 6) of the added fillers with PP or PLA in rubber compounds was lower significantly in comparison to standard rubber compound.

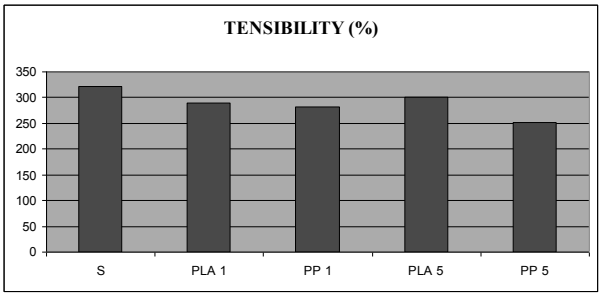

Fig. 6 Tensibility of resultant vulcanizates
Obr. 6 Ťažnosť výsledných vulkanizátov

In comparison with standard compound, the lower values of hardness (Fig. 7) were measured for tested rubber compounds and it means good integration of fillers into the compound and good compatibility with the rubber matrix.

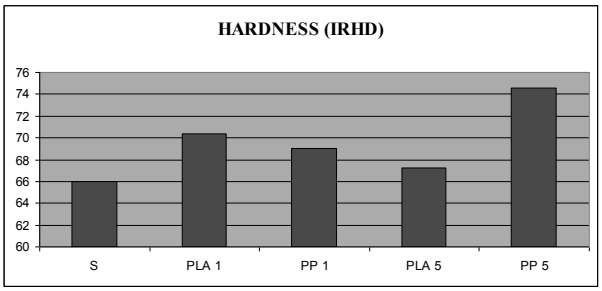

Fig. 7 Hardness of resultant vulcanizates
Obr. 7 Tvrdosť výsledných vulkanizátov

Conclusions

Vulcanization characteristics (minimum torque M_L, maximum torque M_H, time of start of vulcanization t_s, optimum time of vulcanization t_{90}, rate coefficient of vulcanization R_V) and physical as well as mechanical properties (tensile strength, tensibility, hardness) were evaluated for resulting vulcanizates according to STN. The obtained values of rubber compounds with the addition of fibers based on PLA, PP were compared with the characteristic features of standard rubber compound.

Acknowledgment

The authors are grateful to the Slovak Grant Agency KEGA No. 007 TnUAD – 4/2013 and KEGA No. 006 TnUAD – 4/2014 for financial support.

Literature

[1] LIPTÁKOVÁ, T., ALEXY, P., GONDÁR, E., KHUNOVÁ, V. *Polymérne konštrukčné materiály.* Žilina: ŽUŽ, 2012. 189s. ISBN 978-80-554-0505-6

[2] DUCHÁČEK, V. *Polymery - výroba, vlastnosti, zpracování, použití*, 2. vyd. Praha: VŠCHT, 2006

[3] PREKOP, Š. a kol.: *Gumárenská technológia I.* Žilina: Žilinská univerzita, 1998, p. 282, ISBN 80-7100-483-9.

[4] STN 62 1425: Príprava a vulkanizácia gumárenských zmesí, 1983.

[5] STN 62 1416: Stanovenie vulkanizačných charakteristík,1986.

[6] STN 62 1436: Stanovenie ťahových vlastností, 1982.

[7] STN 62 143: Stanovenie tvrdosti, 1981.

Hutnické listy č. 3/2014, roč. LXVII
ISSN 0018-8069

Effect of Structure of Knitted Fabric on the Transfer Properties

Vplyv väzby na transportné vlastnosti pletenín

Ing. Jela Legerská, PhD.[1]

[1]Alexander Dubček University of Trenčín, Faculty of Industrial Technologies in Púchov, I. Krasku 491/30, 020 01 Púchov, Slovak Republic

The properties of knitted fabrics should be able to ensure adequate state of comfort while wearing knitted garments. In inhomogeneous knitted fabrics, this goal is influenced by the percentage ratio of the structure as well as the air phase. The required shape and aesthetic properties are based on the structure of the knitted fabric. Air phase ensures good insulation properties of knitted fabrics. In relation to the knitted fabrics, the impact of used structure of the non-fibrous (air) ratio was evaluated in this paper. The evaluation was performed on the basis of the measurement of the air permeability and porosity. The selected tests were performed for the assortment of knitted fabrics with the different structure and different material composition. In this work, the properties of the knitted fabrics were mutually compared. In addition to the investigation of the different knitted fabrics, the most suitable structure of knitted fabric as well as the most suitable material composition was specified.

Keywords: *structure of knitted fabrics, porosity of knitted fabrics, covering of knitted fabrics, filling of knitted fabrics, air permeability*

V práci sa zaoberáme problematikou experimentálneho merania pórovitosti a prestupu vzduchu pleteninami. Analyzovali sme ako vplýva väzba a materiálové zloženie pletenín na sledované vlastnosti. Materiálom skúmaným v našej práci boli záťažné pleteniny patriace medzi mäkké tvarovo prispôsobivé materiály zachovávajúce voľnosť a pohodlnosť pohybu. Členitosť ich povrchovej štruktúry spôsobuje, že sa pletenina ani pri vysokej vlhkosti nelepí na pokožku a dobre odvádza vlhkosť. Pri zachovaní potrebnej hrúbky tiež dobre izoluje teplo. Spoločným cieľom vlastností týchto nehomogénnych pletenín je dosiahnutie stavu pohodlia pri nosení odevov. Tento cieľ je ovplyvnený percentuálnym pomerom väzbovej a vzduchovej fázy obsiahnutej v pletenine. Pričom väzba dodáva pletenine potrebné úžitkové a estetické vlastnosti. Vzduchová fáza zabezpečuje pletenine dobré prestupové a izolačné vlastnosti. Hľadanie vyváženého pomeru medzi obidvoma zložkami bolo tiež predmetom tohto príspevku. Bol tu hodnotený vplyv použitej väzby na obsah nevláknového podielu – vzduchu v pletenine. Hodnotenie sa robilo na základe merania prestup vzduchu na prístroji FF 12, plošnej pórovitosti prostredníctvom Obrazovej analýzy Nis Element a výpočte objemovej pórovitosti. Výsledky meraní objemovej pórovitosti a plošnej pórovitosti sú rôzne a dosť ťažko porovnateľné. Každý spôsob však vnáša iný pohľad na sledované vlastnosti. Hľadala sa tiež závislosť medzi pórovitosťou a prestupom vzduchu pleteninou. Rôzna väzba a materiálové zloženie záťažných pletenín do značnej miery vplývalo na sledované vlastnosti. Na záver bol uskutočnený výber optimálnej pletiarskej väzbovej techniky a materiálového zloženia skúšaných pletenín. Ako najvhodnejšie boli vybrané pletiarske väzby s vytiahnutými očkami (vz. 1, 3, 6).Väzba bude dobre transportovať vlhkosť od pokožky cez odev do prostredia a dobre izolovať teplo medzi pokožkou a prvou odevnou vrstvou. Na základe materiálového zloženia sa vybrali ako najvhodnejšie vz. 4 a 5 s podstatne väčšou hrúbkou a objemovou pórovitosťou a nižšou plošnou pórovitosťou.

Kľúčové slová: *väzba pleteniny, pórovitosť pleteniny, zakrytie pleteniny, zaplnenie pleteniny, prestup vzduchu*

Knitted fabrics are soft shape-adaptive materials which have to provide convenient and free movement. Irregular surface structure causes that the knitted fabric has a low adhesion even at high humidity and it is able to transfer humidity from the skin. Knitted fabric insulates heat when the required thickness is preserved. The determining factor relating to the inhomogeneous knitted fabrics is based on the achievement of comfort. This comfort is influenced by the percentage ratio of the volume as well as air phase in the knitted fabric. It is necessary to point out that the structure stands for the required shape and aesthetic properties of the knitted fabric. The air phase provides good transfer of the various media and it also provides the insulation properties. The main aim of the given paper is to find the adequate ratio in relation to the structure and air phase. The influence of the used structure of the knitted fabric on the volume of the non-fibrous ratio was evaluated (evaluation of the air in the knitted fabric). The mentioned evaluation was performed on the basis of the air transfer and porosity. In this paper, Nis Element image analysis was used for measurement of the porosity and FF12 device was used for measurement of permeability. The results of measurements are different but each method represents a different view in relation to the monitored property. The aim of this paper is connected with a comparison of inhomogeneous properties of knitted fabrics. The selected tests were performed for the assortment of knitted fabrics with the different structure and with the different material

composition. We investigated the correlation between porosity and air flow speed of knitted fabric. In addition, on the basis of the investigation, the most suitable structure of knitted fabric as well as material composition was specified.

Experimental part

Methods

Evaluation of the bulk porosity was based on the 3D model for knitted fabric. The values of weight per square meter, thickness values and density values from the table were determined as the initial values for calculation of the bulk porosity. The filling value represents the opposite value of the bulk porosity value in relation to the knitted fabric. The calculation of the bulk porosity can be done according to the equation [1]:

$$\mu = \frac{\rho_{pl}}{\rho_{vl}}.100 \qquad [\%] \qquad (1)$$

$$p = 100 - \mu \qquad [\%] \qquad (2)$$

where μ is filling of knitted fabrics, ρ_{pl} is specific bulk weight of knitted fabrics, ρ_{vl} is packing density of fibers, p is porosity of knitted fabrics.

Measurement of the surface porosity is based on the 2D model for knitted fabric and it is expressed as the ratio number between structure and air phase and it is in the range from 0 to 1 or from 0 % to 100 %. The porosity value represents the opposite value of the covering structure for knitted fabric. The measurements were based on the light transmittance through the air phase of knitted fabric (Nis Element image analysis) [2]. It was measured on the basis of the ratio between the surface of pore (A_p) and surface of image (A_o). The third dimension of knitted fabric – thickness was not taken into account during the measurements. Besides the value of the porosity, the distribution, the number and size of the pores in the knitted fabric were also measured. Expression of surface porosity in relation to the covering is determined from the following relationship:

$$p = \frac{A_p}{A_o}.100 \qquad [\%] \qquad (3)$$

$$z = 100 - p \qquad [\%] \qquad (4)$$

where z is surface covering for knitted fabrics.

Measurement of the amount of air permeability through the knitted fabrics – Q [l.hour^{-1}] has been performed with help of the FF 12 device [6]. The measured values of Q were calculated in order to obtain air flow speed – R. The calculation was done according to the equation:

$$R = \frac{Q}{A}.\frac{1}{3.6} \qquad [cm.s^{-1}] \qquad (5)$$

where R is the air flow speed [cm.s^{-1}], A is tested area [20 cm^{-2}], 1/3.6 is calculation factor of [l.hour.cm^{-2}] to [cm.s^{-1}].

Materials

Measurement of the porosity and air permeability has been performed using assortment of jersey knitted fabrics (see Fig. 1). These jersey knitted fabrics are designed in such a way that they can be used for production of T-shirts and other assortment of upper garments. Knitted fabrics are mostly in direct contact with the skin of the wearer. The higher porosity values of knitted fabric can improve the thermal-insulation properties (needed for winter clothing) and they can increase the speed of moisture transfer from the skin (needed for winter and summer clothing).

Tab. 1 Parameters of jersey knitting fabrics
Tab. 1 Parametre záťažných pletenín

n.	Material	ρ_s [kg.m^{-2}]	ρ_v [kg.m^{-3}]
1	100% PP	119	186
2	98% PP, 2% elastic	107	202
3	50% PP micro, 50% PP	98	136
4	50% PP, 50% cotton	179	140
5	50% wool, 50% PP	156	137
6	100% PP	116	181
7	100% PP	96	181
8	100% PP	133	190

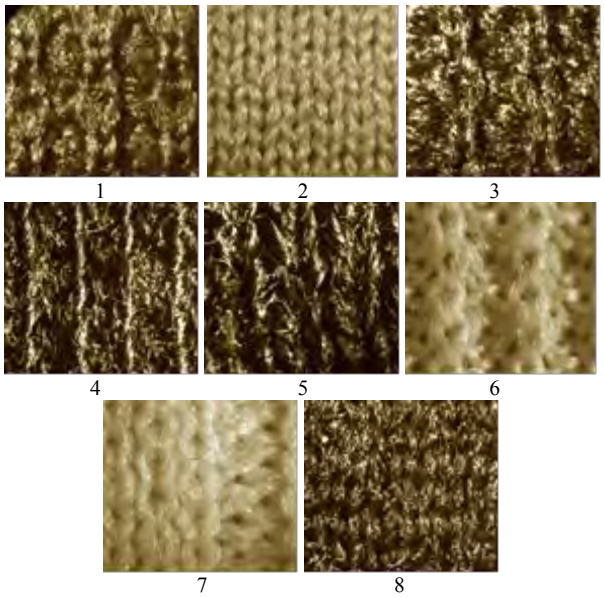

Fig. 1 Structure of jersey knitted fabrics
Obr. 1 Väzby záťažných pletenín

Knitted fabrics were made with help of the rib knitting machine. All measured knitted fabrics were made in such a way to represent jersey knitted fabrics [3] and they can be seen in Fig. 1. Samples designated as 1, 3, 6 have pulled loops to the outside in each fourth line. Every second needle of the machine operates in the front rib and all needles operate in the back rib. There was some deformation in relation to the structure of knitted fabric because loops are pulled out at the expense of the supplementary loops of kitted fabric. Change in shape of the knitted fabric is reflected in all

Hutnické listy č. 3/2014, roč. LXVII
ISSN 0018-8069

directions. The knitted fabric structure is airy, open and leisure. Knitted fabric designated as 2 is known as the transverse waves. The structure of knitted fabric is produced by interruption of all needles in the rear rib (in our case, after knitting of four lines). In terms of the front rib, the number of lines is increased by 3 knitted lines while the operation of the rear rib is interrupted. In relation to the structure of knitted fabrics, jersey double and jersey single lines are combined in this way. Structure of knitted fabrics is characterized by strength, elongation reduced in the line and good thermal-insulation [3]. Samples with designation of 4 and 5 had structure as velour with dense loops on the reverse side. Besides the base yarn, additional yarns were also used to create loops. Structure of the given knitted fabric is relatively thick, soft and good from the aspect of the thermal-insulation. Velour knitted fabric is significantly different from the other samples. Sample designated as 7 represents ribbed jersey knitted fabric. In relation to the manufacturing procedure, there are 4 operating needles and 2 non-operating needles in the front rip of the rib knitting machine while all the needles in the rear rib are operating. The structure of the knitted fabrics has a higher packing density, softness and thermal-insulation compared to single-ribbed knitted fabric. The sample of 8 is double jersey knitted fabric. Two separate structures of knitted fabrics are connected alternately in sinker part of loop in each third line. The mutual connection of yarns (from right side to the reverse side) allows each yarn to return to the initial rib. Double jersey knitted fabric can be understood as combination of all advantages of in single and double jersey knitted structure. The structure has a lower expansion, higher thickness and stable shape [3].

Results and discussion

Measurement permeability of air

During an experimental evaluation of air permeability for knitted fabric, the value of pressure-difference (Δp =50 Pa) was set for the measuring device [6]. The air flow speed (R) [cm.s^{-1}] through the areas between the structure points in the knitting fabric is the result of the measurement. On the basis of measurements, it can be concluded that the resultant flow of air is closely connected with the relationship between pressure gradient and air flow speed. In relation to the air permeability, there were the following changes during measurements [4]:

- the bulging and undesired shaping of knitted fabric and it is dependent on the material composition and structure,
- the movement of the free interconnected yarns in structure and it causes the change of shape of pores and moreover, there is also the increase of air flow,
- the change of the position of the protruded fibers which are close imposed to the yarn because of air flow.

These mentioned deformation changes can significantly distort the results of measurements of air permeability and they have to be taken into account mainly in the case of the knitted fabrics. According to the mentioned facts, it can be pointed out that the simple quantitative expression of porosity based on the air transfer is insufficient.

Measurement of porosity

The size of the pores, their distribution throughout the pattern repeat of the knitted structures is also important in relation to the evaluation and therefore, Nis Element image analysis is used. A lot of scientific disciplines use image analyses for verification or acquisition of information about structure and properties of investigated objects. The Image processing is defined as: “computerized routines for information extraction from remotely sensed images to obtain categories of information about specific features” [5]. The quality of visual information is based on the quality of the image. Therefore, sensing of image plays very important role in the image processing. In relation to the image processing, the images can be incorrect or wrong in some cases and it can be because of low resolution, noise or inhomogeneous or blurred background. However, these defects or incorrectness can be eliminated by the appropriate and known procedures in relation to the program system. The segmentation is the one of the methods used for information extraction in order to split an image up into segments or regions exhibiting distinguishable properties when these properties are compared to the surrounding neighbours. Segmentation of an image is based on the several techniques, such as thresholding, edge finding, binary mathematical morphology or grey-value mathematical morphology. From the aspect of the covering factor, tresholing plays important role for evaluation of the other structural characteristics of knitted fabrics, such as the areas of treads or pores, number, size and shape of pores.

The disadvantage of the mentioned method is that the image threshold is based on the subjective point of view. In relation to our investigation, the threshold value of 120 was chosen according to the histogram of grey. In relation to the image analysis, the microscope, the CCD camera and Nis Element software were used for performance of the investigation while the conditions for settings were as follows: image area (A_o) was 29212.04 μm^2, the mean intensity of exposure was 233, offset was 0, gamma was 0.75, saturation was 1, format for active image was1280×1024 px, RGB value was 1 / 1 / 1.8 (red, green, blue). The areas of single inter-yarns pores were measured and the distribution of pore size was monitored. The resulting values of the measurements are presented in the Tab. 2 and 3.

Tab. 2 Experimental data of the air permeability (Q) and calculated values of the air flow speed (R) according to the formula (5)
Tab. 2 Experimentálne hodnoty prestupu vzduchu Q a vypočítané hodnoty rýchlosti prechodu vzduchu R podľa vzťahu (5)

n.	Q_{mean} [l.h^{-1}]	V_q [%]	IS_Q [l.h^{-1}] lower/upper	R [cm.s^{-1}]
1	4435	7.79	4280/4590	61.60
2	3983	5.41	3886/4079	55.31
3	6855	2.43	6780/6930	95.21
4	3067	10.02	2929/3204	42.60
5	4930	3.61	4850/5010	68.47
6	6235	4.75	6234/9736	86.60
7	5430	6.24	5278/5582	75.42
8	5275	4.26	5175/5375	73.26

Tab. 3 Experimental data of the areas and size of pores
Tab. 3 Experimentálne hodnoty plochy a veľkosti pórov

n.	A_p [µm^2]			Number of pores		
	min	max	middle	min	max	middle
1	224	607	459	41	119	75
2	172	991	550	24	89	54
3	893	1207	1018	32	16	91
4	0.04	227	24	0	9	3
5	5	354	83	1	41	18
6	962	2908	1790	25	118	68
7	5	809	263	1	69	24
8	30	471	207	5	38	17

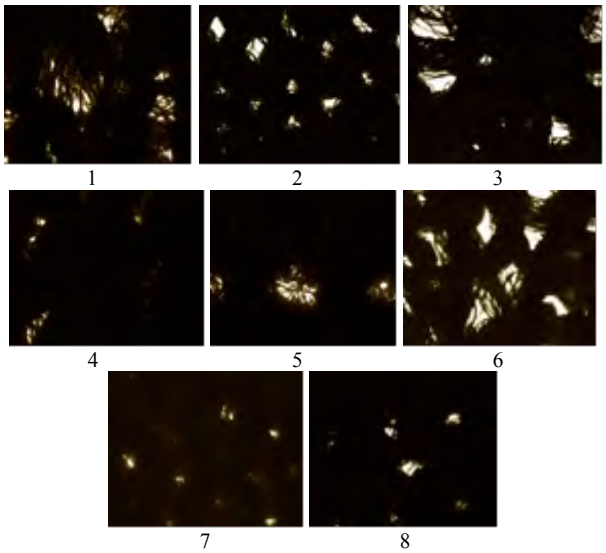

Fig. 2 Binary images of knitted fabrics
Obr. 2 Binárne obrazy pletenín

The binary images (Fig. 2) have a high informative value about porosity and are in the accordance with the measured values. The average value of porosity was obtained on the basis of 50 measurements.

Calculation of the bulk porosity and filling

The values of porosity and covering (Tab. 4) were calculated on the basis of the relationships (3), (4) and values of filling and bulk porosity (Tab. 5) were calculated according to the relationships (1), (2). Besides the calculated values of the filling and bulk porosity, the values of the thickness of the knitted fabrics are also presented in Tab. 5. The measured values of specific bulk weight of knitted fabrics (see. Tab. 1) and tabulated values of packing density were used for calculating.

Tab. 4 Values of the porosity and covering calculated according to the equations (3), (4)
Tab. 4 Hodnoty pórovitosti a zakrytia vypočítané podľa vzťahov (3), (4)

n.	p [%]	V_p [%]	IS_p [%] lower/upper	z [%]
1	1.57	31.92	1.43/1.71	98.43
2	1.88	3.96	1.67/2.09	98.12
3	3.49	26.71	4.47/2.5	96.51
4	0.08	83.3	0.06/0.1	99.92
5	0.28	91.91	0.21/0.35	99.72
6	6.13	25.2	5.69/6.57	93.87
7	0.90	9.0	0.69/1.13	99.1
8	0.71	66.97	0.57/0.84	99.29

Tab. 5 The calculated values of bulk porosity and filling according to the equation (1), (2) and measured values of thickness of knitted fabrics
Tab. 5 Výpočítané hodnoty objemovej pórovitosti a zaplnenia podla vzťahu (1), (2) a merané hodnoty hrúbky pletenín

n.	p [%]	μ [%]	h [mm]
1	79	21	0.64
2	78	22	0.53
3	85	15	0.72
4	89	11	1.28
5	88	12	1.14
6	80	20	0.64
7	80	20	0.53
8	79	21	0.70

This paper shows measurements of properties of knitted fabrics. Results of measurements relating to air permeability and surface and bulk porosity were compared. Correlation dependences show the significant tightness between the monitored properties (Fig. 3, 4). Porosity growth increased amount of air passing through the knitted fabric. The investigation shows that open structure of knitted fabric has influence on the measurement of air permeability and this influence can be mainly observed for knitted fabrics which were designated as samples of 1, 3, 6, 7 – these samples show less thickness and free structure. It is necessary to point out that the inaccuracy in the measurements of air permeability has to be taken into account. The structure of knitted fabrics also influenced the measurements of surface porosity. In relation to the all investigated knitted fabrics, the loop was used as the basic or initial constituent element in the structure. The increase of the length of yarn of the loop (samples of 1, 2, 3, 6) leads to the increase of the surface porosity. Samples of 4, 5 representing velour structure have higher thickness and inner pores. Therefore, the measurement of surface porosity by image analysis method is not suitable as well as inaccurate in this case. The use of cotton and wool fibers in these velour structures had also influence

Hutnické listy č. 3/2014, roč. LXVII
ISSN 0018-8069

on the increase of their thickness. The rib double jersey structure was represented by the sample of 7. This mentioned structure was tightly closed and therefore, it has a low surface porosity. Sample of 8 composed of two knitted fabrics connected together with the sinker loop also exhibited the low a surface porosity because these two connected knitted fabrics covered up the pores. Content of 50 % PP microfibers in the sample of 3 increased its areal porosity and thus the thermal insulation properties were increased too. Sample of 3 consisted of 50 % polypropylene microfibre which increased the surface porosity and thus thermal-insulation properties were increased too. The results of measurements of the bulk porosity are not comparable to the values of surface porosity. The numerical values of the bulk porosity can be considered as objective and accurate on the basis of a comparison to the literary resources [7]. They are mostly influenced by the thickness of knitted fabric. The bulk porosity increases with the increasing thickness of knitted fabric. From measurements of surface porosity, we can observe images for porous jersey knitted fabric (Fig. 2). Furthermore, we can also recognize the value of the number of pores as well as their size (Tab. 3) and these mentioned graphical and numerical values and results are more valuable than results referring to measurement of surface porosity.

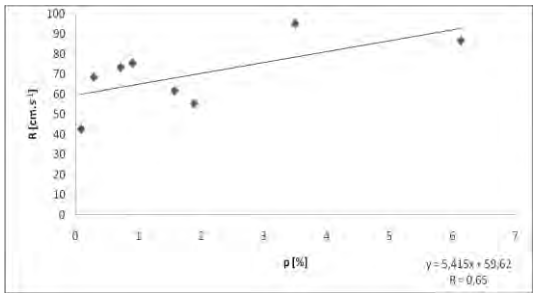

Fig. 3 Correlation dependency between the measurements of air permeability and surface porosity (Nis Element) of knitted fabrics
Obr. 3 Korelačná závislosť medzi prestupom vzduchu a plošnou pórovitosťou (Nis Element) pletenín.

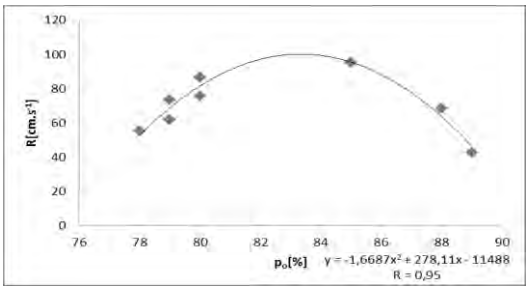

Fig. 4 Correlation dependency between the air permeability and bulk porosity of knitted fabrics
Obr. 4 Korelačná závislosť medzi prestupom vzduchu a objemovou pórovitosťou pletenín

Conclusions

The results of measurements of porosity and air permeability for the jersey knitted fabrics can be expressed in the following conclusions:

- Based on the measurements and results of image analysis, the increase of the surface porosity as well as the increase of the bulk porosity leads to the increase of the air permeability of knitted fabric (Fig. 3, 4).
- Measurements of surface porosity are not comparable to those of the bulk porosity (tab. 4, 5).
- The numerical values of the bulk porosity are in the range from 78 to 88 % and they are comparable to the tabular literary values [7].
- The significant influence of structure of knitted fabrics and material composition on the bulk porosity and filling was observed in the case of velour jersey knitted fabrics (samples designated as 4, 5). In relation to these knitted fabrics, the higher thickness led to the increase of the bulk porosity but there was the decrease of air permeability. In relation to these knitted fabrics, the results of measurements of surface porosity are not real.
- The content of polypropylene microfibbers in a mixture leads to the increase of the covering surface and bulk porosity as well as air permeability of knitted fabric and it means that there is an increase of the thermo-insulation properties.
- Measurement of surface porosity can be understood as valuable because of the image outputs giving accurate information about the pore surface, their number as well as their arrangement in the knitted fabric.
- The structure of knitted fabric where the loops are pulled out (samples of 3, 6) exhibits the most suitable results and it means that structure shows good transfer of moisture and it also has the perfect heat insulation.

Literature

[1] LEGERSKÁ, J. *Study of thermal transmittance depending on the structure of textiles*. (Dissertation). Púchov: FPT, 2009, p.49

[2] MILITKÝ, J. *Selected Topics-Technical textiles.* Liberec: TU, 2002, p. 172-175

[3] KOVAŘÍKOVÁ, M. *Structures and analyzes of knitted fabrics*. Bratislava: Alfa, 1985. p. 99, 101, 184

[4] HAVRDOVÁ, M. *Behavior of fabrics measurement of air permeability.* Strutex, 9 *International conference 200*2, TU Liberec, p. 225-262, ISBN 80-7083-668-7

[5] *Definition of image prosessing*. Available fromhttp:// www.extension.unm.edu//distribution/Naturalresources/components/DD607hr.htm

[6] STN EN ISO 9237. *The determination of air permeability textile fabric.* Bratislava: SÚTN, 1988

[7] NECKÁŘ B., *Fibers and fiber formations, Selected Chapter.* Liberec: TU, 1990

The Coefficient Influence of Knitted Fabric Packing Density on the Thermal Resistance and Resistance to Water Vapour

Vplyv koeficientu zaplnenia pleteniny na tepelnú odolnosť a odolnosť proti vodným parám

doc. Ing. Pavol Lizák, PhD.[1], Ing. Anton Schlosser[1], Ing. Ľubomír Žila[1]

[1]Alexander Dubček University of Trenčín, Faculty of Industrial Technologies in Púchov, I. Krasku 491/30, 020 01 Púchov, Slovak Republic

In our work, we deal with the influence of knitted fabric packing density on the thermal resistance and resistance to water vapour. The coefficient of knitted fabric packing density is influenced by the structure of the yarn used during its production and by the yarn structure itself. All these factors influence not only coefficient of filling but also other final knitted fabric properties. In our work we pay attention to the influence of these parameters on the thermal-physiological comfort. Thermo-regulation and humidity escape, belonging to thermal - physiological comfort, can be expressed by thermal resistance and resistance to water vapour. The textile materials differ one from another not only on the basis of the different kinds of fibres used for their production but the difference is also based on the way of mutual fibres arrangement and it is based on the influence by the structure and knitted fabric fineness.

Keywords: *knitted fabric, packing density, comfort, thermal resistance, resistance to water vapour*

V práci sa zaoberáme problematikou vplyvu koeficientu zaplnenia pleteniny na tepelnú odolnosť a odolnosť proti vodným parám. Koeficient zaplnenia pleteniny je ovplyvňovaný štruktúrou priadze použitej na jej výrobu a štruktúrou samotnej pleteniny. Všetky tieto faktory ovplyvňujú nie len koeficient zaplnenia ale aj ďalšie výsledné vlastnosti pleteniny. V našej práci sa sústreďujeme na vplyv týchto parametrov na termo-fyziologický komfort. Do oblasti termo-fyziologického komfortu patrí aj termoregulácia a odvod vlhkosti, čo môžeme vyjadriť tepelnou odolnosťou a odolnosťou proti vodným parám. Termoregulačný systém udržiava rovnováhu medzi teplotou pokožky a prostredím. Tam, kde už termoregulačný systém nie je schopný sám plniť svoju funkciu, nastupuje na pomoc odev napr. z pleteniny ako prostriedok ochrany organizmu pred prostredím. Základnou funkciou pleteného odevu od začiatku jeho existencie je funkcia ochranná. Táto funkcia bola určovaná prírodnými podmienkami a tieto určovali rozvoj a spracovanie používaných materiálov. Textilné materiály sa od seba odlišujú nielen odlišným druhom vlákien použitých na ich výrobu ale najmä spôsobom vzájomného usporiadania vlákien, čo ovplyvňuje hlavne väzba a jemnosť pleteniny. Cieľom tejto práce bolo posúdiť ovplyvňovanie tepelnej odolnosti a odolnosti proti vodným parám v závislosti na koeficiente zaplnenia pleteniny vyrobenej s POP vlákien. Takéto materiály sa používajú na výrobu športových odevov, pri ktorých je práve termo-fyziologický komfort jedným z najdôležitejších faktorov. Popis štruktúry pleteniny je veľmi zložitá problematika. Z tohto dôvodu sa niekedy vytvára určitý model očka a z neho je snaha matematicky vyjadriť krivku nite, ktorou je očko tvorené. Niť v očku je však veľmi zložitá priestorová krivka a jej zákonitosti je veľmi zložité vystihnúť. V práci sme použili postup, pri ktorom sme porovnávali koeficient zaplnenia objemu pleteniny polypropylénom a vplyv tohto zaplnenia na termo-fyziologický komfort vyjadrený tepelnou odolnosťou a odolnosťou proti vodným parám.

Kľúčové slová: *pletenina, zaplnenie, komfort, tepelná odolnosť, odolnosť voči vodným parám*

Knitted fabrics are often used for the production of clothes - mainly underwear and free time activities clothes. It is the comfort which is very important for underwear, sports clothes and similar clothes production [1]. Clothing comfort means good feelings and comfort during wearing and physiological functions of organism are in optimum. Ideal state of human body is connected with the basal metabolism. Human (healthy, hungry and undressed) in a horizontal position, at climatic conditions (T = 20 °C, φ = 65 %), has no feeling of cold or hot. There is only minimal substance transformation under these mentioned conditions, which are necessary for keeping the function of organs [2].

Clothing comfort is divided into:

1) functional – the influences which are given mainly by properties of fabric and by the construction;
   a) sensoric
   b) pathophysiological
   c) thermo-physiological;
2) psychological – individuality of human, cultural and social influences
   a) climatic conditions

Hutnické listy č. 3/2014, roč. LXVII
ISSN 0018-8069

b) traditions, customs, religions
c) age, education, social class
d) fashion, colours, trends

The clothing comfort is influenced by many processes, such as physical processes (the transport of heat and humidity into the clothes as well as mechanical action between the clothing and skin), physiological processes (the metabolic processes and heat balance conservation by the help of thermoregulatory actions), neurophysiological processes (the sensory perceptions obtained by skin, sight, etc.) and psychological processes (the processes in brain, which analyse a total sense on basis of previous information) [3].

In tab. 1, we can see physiological, psychological and physical harmony between human and environment.

Tab. 1 Comfort harmony between human and environment
Tab. 1 Harmonický komfort medzi človekom a prostredím

Thickness	0.8 – 2 [mm]
Area weight	0.11 – 0.4 [kg/m^2]
Thermal permeability	14 – 22 [J/m^2.s.K]
Moisture permeability	0.44 – 0.7 [g/m^2.s.bar]
Air permeability	10 – 100 [m^3/m^2.s]

Optimal comfort conditions are when the skin temperature is 33 – 35 °C, relative humidity near skin is 25 ± 10 %, air rate near skin is 25 ± 10 cm.s^{-1} and there is not liquid water on skin. Discomfort is when 25 % of skin surface is covered by sweat. Complex action is action of humidity at which there is swelling of hydrophilic fibres, porosity decrease, decrease of permeability of air and humidity through textiles and it cause the increase of the thermal conductivity.
The knitted fabric density is one of the most important properties because it can be easily influenced by the technology and it is the result of the basic technological parameters and the way of production. Density is also the property which influences other properties in a large scale. However, in spite of this, the expression of knitted fabric density is not unambiguous and uniform. From the physical point of view, the density means the amount of mass of given substance in unit volume. In the technology of knitting, the density has to correspond to percept conception. There are several systems of density expression [3]:

a) linear density expression represents the system which arises from loop length, however it does not correspond to the percept conception where we have to take in consideration also the thread thickness. This type of expression is usable only with certain types of knitted fabrics. In relation to the more complicated knitted fabrics, expression does not correspond to percept conception.

b) square density expression can be defined as the packing density of the knitted fabric area by the structure elements. The total density is expressed by the product of columns density and courses density on water. This expression has mainly technological importance. It corresponds to percept conception only when the knitted fabric is created by the threads of the same diameter.

c) volume density expression stands for packing density of knitted fabric volume by processing thread. It is more advantageous and it is more favorable for majority of knitted fabrics. It corresponds to percept conception provided with the respect to the knitted fabric thickness.

d) mass expression of density corresponds to a certain scale with the motion of density. Knitted fabric density can be defined as the ratio of density and volume. This expression is suitable mainly for the plastic knitted fabrics where previous procedures are difficult to be use.

Fibres density in the fibrous textile structure is characterized by the ratio of the total space of knitted fabric which is filled by fibres volume packing density [4, 5].

Packing density is a dimensionless quantity residing in the interval (0,1). In our work we were identifying the influence of the packing density characterized by the share of polypropylene polymer in the knitted fabric volume on the thermal physiological comfort. The measurements were performed for polypropylene knitted fabrics used for the production of sports and free-time activities clothes. The knitted fabrics were made of profiled polypropylene fibres which are made by company Chemosvit Fibrochem Inc. Svit. The square mass and the knitted fabric thickness were defined for the measured samples and with the help of these obtained data, the specific mass of the knitted fabric was defined too. The ratio between specific mass of the knitted fabric and specific mass of polypropylene is given by the coefficient of packing density. After measuring of thermal resistance and resistance to water vapour, it is possible to define the dependence of given quantity on the coefficient of packing density.

Experiment

Material

Polypropylene knitted fabrics which differ by used structure and also square mass were used for experiments. The surface structure was also different to be possible to compare appropriateness of given procedure in relation to different type of structure. The variety of surface structures are introduced hereinafter using the image from the image analyses Lucia (Fig. 1-4).

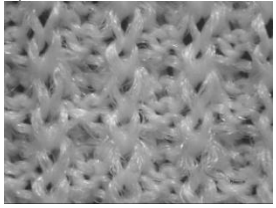

Fig. 1 Sample 1
Obr. 1 Vzorka 1

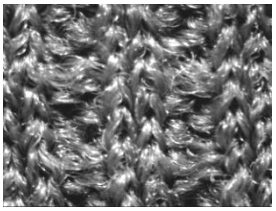

Fig. 2 Sample 2
Obr. 2 Vzorka 2

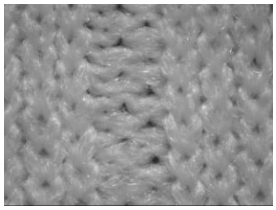

Fig. 3 Sample 3
Obr. 3 Vzorka 3

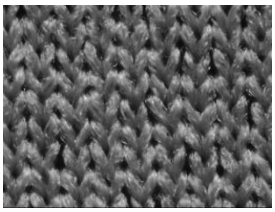

Fig. 4 Sample 4
Obr. 4 Vzorka 4

Sample 1 – Weft both-sided knitwear, rib stitch 1:1 with the decreased out – ripping secured by grasping loops.

Sample 2 – Weft both-sided knitwear with plastic rib pattern 2:2.

Sample 3 – Weft both-sided knitwear with rib pattern 4:2.

Sample 4 – Double knitwear created by joining of two jerseys with the help of grasping loop.

Methods and apparatuses

We defined square mass m_s [g.m^{-2}] for the material samples by weighing and we also measured the knitted fabric thickness h [mm]. From the given values it is possible to calculate specific knitted structure thickness ρ_{pl} [kg.m^{-3}]. The coefficient of knitted fabric packing density by polypropylene fibres can by calculated by relation:

$$\mu = \frac{\rho_{pl}}{\rho_v} \qquad (1)$$

Specific mass of fibre forming polypropylene ρ_v is 980 [kg.m^{-3}].

Thermal resistance

Thermal resistance R_{ct} is the difference of the temperatures between two surfaces of material divided by resulting thermal flow on the surface unit in the gradients direction. This flow of dry heat can have conductive, conventional and radiant component or only some of these mentioned components. Thermal resistance R_{ct} expressed in [m^{-2}.K.W^{-1}] is the property specific for textile materials or stratified compositions which is connected with the regulation of the dry heat flow on the given area corresponding to stable heat gradient.

Heat resistance R_{ct} is defined in the following way - heat resistance of marginal air layer above the surface of testing devices is deducted from heat resistance of testing sample and marginal air layer above it, both are measured in the equal conditions according to formula:

$$R_{ct} = \frac{(T_m - T_a).\ A}{H - \Delta Hc} - R_{ct0} \qquad (2)$$

where T_m is the temperature of measuring unit [°C], T_a is the air temperature in the experimental space [°C], A is the area of measuring unit [m^{-2}], H is a heating input transported to measuring unit [W], ΔH_c is a correcting element for heating input by the measurement of heat resistance, R_{cto} is the constant of apparatus on heat resistance measurement [m^{-2}.K.W^{-1}].

Resistance to water vapour R_{et} is the difference of water vapour pressure between surfaces of material divided by resulting evaporating thermal flow on the unit of area in the gradient direction.

Evaporating flow can consist of diffuse and conventional component. Resistance to water vapour R_{et} expressed in [m^{-2}.Pa.W^{-1}] is a specific property for textile materials or composites which defines latent evaporating thermal flow running across given area and corresponding to stable water vapour gradient. To define resistance to water vapour, the electric heated plate is covered by membrane which leaks vapour, but not water. For testing sample located on a membrane, the thermal flow is necessary for keeping constant temperature on the plate by the measure of the vapour water speed and based on these data, the sample resistance to vapours is defined:

$$R_{et} = \frac{(p_m - p_a).\ A}{H - \Delta He} - R_{et0} \qquad (3)$$

where p_m is a balanced partial pressure of water vapours on the surface of measuring unit [Pa], p_a is a partial pressure in the air in the testing area [Pa], A is the area of measuring unit [m^{-2}], H is a heating input given to measuring unit [W], ΔH_e is a correcting element for heating input by measurement of resistance to water vapour, R_{eto} is an apparatus constant for measurement of resistance to water vapours [m^{-2}.Pa.W^{-1}].

Results and discussion

Resulting values of individual knitted fabric samples and their coefficient of packing density are introduced in the Tab. 2.

Tab. 2 Parameters for individual knitted fabric samples
Tab. 2 Parametre jednotlivých vzoriek pleteniny

sample	h [mm]	m_S [g.m^{-2}]	ρ_{pl} [kg.m^{-3}]	ρ_v [kg.m^{-3}]	μ [0,1]
1	0.668	113.027	169.202	980	0.172
2	0.898	131.333	146.250	980	0.149
3	0.533	100.889	189.285	980	0.193
4	0.67	136.224	203.319	980	0.207

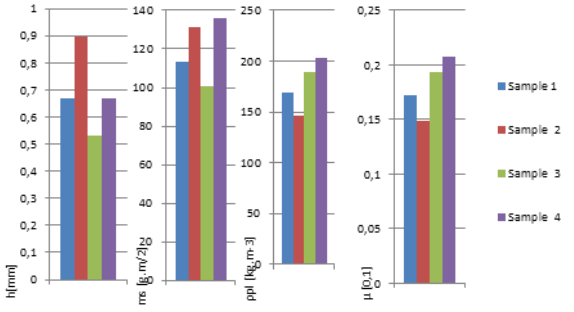

Fig. 5 Packing density coefficient of parameters for individual knitted fabric samples
Obr. 5 Koeficient zaplnenia jednotlivých vzoriek pleteniny

Hutnické listy č. 3/2014, roč. LXVII
ISSN 0018-8069

In the Tab. 3, the thermal resistance values for individual kinds of knitted fabrics are introduced. Graph displays the dependence of thermal resistance on packing density coefficient (Fig. 6).

Tab. 3 Thermal resistance and coefficient of packing density
Tab. 3 Tepelná odolnosť a koeficient zaplnenia

sample	R_{ct} [$m^{-2}.K.W^{-1}$]	μ [0,1]
1	0.003	0.172
2	0.025	0.149
3	0.011	0.193
4	0.014	0.207

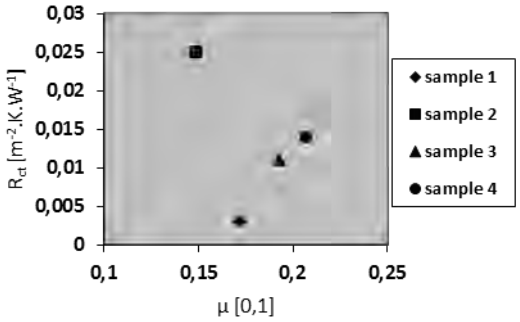

Fig. 6 Coefficient of packing density influence on thermal resistance
Obr. 6 Vplyv koeficientu zaplnenia na tepelnú odolnosť

In the Tab. 4, there are the values of resistance to water vapour for the individual kinds of knitted fabrics. The graph displays the dependence of water vapour resistance to water vapour on packing density coefficient (Fig.7)

Tab. 4 Resistance to water vapours and packing density coefficient
Tab. 4 Odolnosť proti vodným parám a koeficient zaplnenia

sample	R_{et} [$m^{-2}.Pa.W^{-1}$]	μ [0,1]
1	7.07	0.172
2	16.88	0.149
3	8.87	0.193
4	10.44	0.207

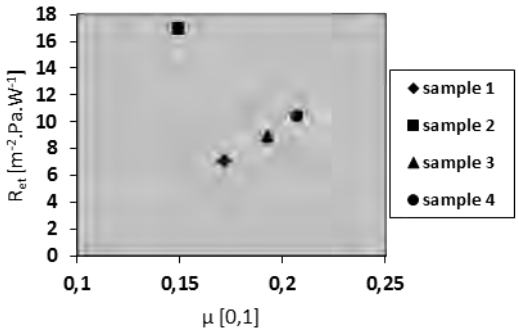

Fig. 7 Coefficient packing density influence on the resistance to water vapour
Obr. 7 Vplyv koeficientu zaplnenia na odolnosť proti vodným parám

Conclusions

As we can see from the results of thermal resistance dependence on packing density coefficient and resistance to water vapour (Fig. 7), knitted fabric structure has the impact on the thermo-physiological properties. Knitted fabric structure can be also expressed by packing density coefficient because the values standing for the thermal resistance and resistance to water vapour are increased along with the increasing packing density coefficient.

Based on the evaluation of the measured values, we can conclude that one of knitted fabrics does not show the supposed dependence (sample 2) because the fibres distribution in the knitted fabric volume is strongly influenced by the rib structure. This dependence can be supposed only for the knitted fabrics which have even special fibres distribution and surface structure. In relation to the rib structure (sample 2), the ribs strongly influence the knitted fabric thickness as well as the knitted fabric packing density coefficient. In the case of very broken knitted fabrics, it is not possible to use standard measured thickness for the calculation of specific thickness. However it would be possible to set a mean thickness from the cross-section.

Literature

[1] KOČÍ, V. *Vazby pletenin,* SNTL - Nakladatelství technické literatury, Praha 1980, 04-825-80

[2] LEGERSKA, J., KOPAL, I. *Measurement of thermal properties of car seat covers using pulse transient method*, In: Hutnické listy. ISSN 0018-8069. Roč. LXVI, č.7(2013), s. 110-113

[3] LEGERSKA, J. *Evaluation of heat transfer and moisture transfer in the selected assortment of home fabrics*, In: Hutnické listy. ISSN 0018-8069. Roč. LXVI, č.7(2013), s. 102-105

[4] LIZÁK, P. *Evaluation methods of materials structure,* 1st ed., Krakow, Towarzystwo Slowaków w Polsce, 2011, ISBN 978-83-7490-384-4

[5] LEGERSKA, J., DROBNÝ, M. Evaluation of total hand value of fabrics, In: Hutnické listy. ISSN 0018-8069. Roč. LXVI, č.7(2013), s. 106-109

Physiological Function in the Clothing Design

Fyziologická funkcia v odevnom dizajne

doc. Ing. Pavol Lizák, PhD.[1]

[1] Alexander Dubček University of Trenčín, Faculty of Industrial Technologies in Púchov, I. Krasku 491/30, 020 01 Púchov, Slovak Republic

More and more scientific, technical and artistic disciplines are combined in the design. At the beginning, there is an inspiration and notion of each designer and the result of this idea is connected with creation of the product representing innovative ideas, well-designed shape, effective content and all these mentioned approaches correspond to practical application. In the clothing design, it is important to combine the beauty, elegance and functionality. The cloth should correspond to the requirements of the comfort. Optimal choice of material and good quality of technical treatment should be also in a harmony with the color, shape and line of thought-shear structure. Design represents a specific and internally differentiated professional activity which is combined with the elements of technical and artistic creation in order to shape or form the different aspects of the world and human communication positively.

Keywords: *design, inspiration, aesthetic comfort, clothing comfort, functional comfort*

Dizajn zlučuje v sebe stále viac vedeckých, technických a umeleckých disciplín. Na začiatku každého dizajnéra je nápad s inšpiráciou a výsledok by mal byť výrobok s inovatívnymi myšlienkami, dobre navrhnutý tvar, s účinným obsahom, čo zodpovedá praktickému využitiu. V odevnom dizajne je dôležité kombinovať krásu, eleganciu a funkčnosť. Látka by mala zodpovedať požiadavkám na pohodlie. Optimálna voľba materiálu a kvalitné technické spracovanie by mala byť v súlade s farbou, tvarom a líniami vnútornej štruktúry. Návrh predstavuje špecifickú a vnútorne diferencovanú profesionálnu činnosť, kombinovanú prvkami technickej a umeleckej tvorby, ktoré sa používajú, aby bolo možné pozitívne tvarovať rôzne svetové aspekty a ľudskej komunikácie. Dizajn dnes predstavuje špecifickú a vnútorne diferencovanú odbornú činnosť, spájajúcu v sebe prvky technickej a umeleckej tvorby, ktorá je vykonávaná s cieľom pozitívne formovať rôzne stránky predmetného sveta a ľudskej komunikácie. Vzišiel z lona výtvarnej a architektonickej činnosti, syntetizuje v sebe stále viac vedeckých, technických a umeleckých disciplín. Cieľom každého správneho dizajnérskeho nápadu by mal byť produkt s inovatívnym nápadom, dôkladne vypracovaným tvarom a povrchom, s efektívnym obsahom, ktorý zodpovedá funkčnému použitiu. Skĺbiť „rozum“ a „cit“, krásu s inteligenciou. Ergonomická funkcia odevu sa dá zistiť už pri prvom skúšaní. Dobrý funkčný odev pri nosení sa takmer nevníma. Naopak, nevhodný strih odevu obmedzuje pohyb, vyvoláva nepríjemné pocity a znižuje fyzický výkon. Strih odevu a jeho módnosť vyjadrujú zovňajšok človeka. Fyziologická funkcia odevu sa nedá zistiť pri jeho kúpe. Vyžaduje sa k tomu dlhší čas nosenia odevu v kľude a pri fyzickej záťaži. Odev sa používa celý deň, a preto požiadavky na fyziologické funkcie odevov sa rozlišujú podľa účelu použitia. Odevný komfort charakterizuje stav organizmu, kedy sú fyziologické funkcie organizmu v optime, a kedy prostredie vrátane odevu nevytvára žiadne nepríjemné pocity vnímané našimi zmyslami.

Kľúčové slová: *dizajn, inšpirácie, estetický komfort, odevný komfort, funkčný komfort*

Design as finished product of specific and internally differentiated professional activity combines elements of technical and artistic creation which are used in order to shape the different aspects of the world and human communication positively.

The aim of the design as a creative professional activity is to achieve a comprehensive quality of objects, processes, services and systems for the specified duration of their performance and thus contribute to the quality of life. Despite of the fact that the design as a type of creative activity arose from the base of art and architectural activities, there is the tendency to involve more and more scientific, technical and artistic disciplines into this mentioned base of design and it means that design output can affect very diverse spheres of human activity, economy, starting and ending art.

As a three dimensional object of designer's activity, the apparel has to be understandable from the several aspects that mutually overlap each other. Deeper philosophical dimension of fashion design is based on seeking new and creative ideas, links and grows in the process of creating the shape and transferring it to a material form. The continuity of the process from initial inspiration to handcrafting is subjected to the physiological knowledge and social aspects affecting the apparel. Understanding the patterns and functions of

Hutnické listy č. 3/2014, roč. LXVII
ISSN 0018-8069

clothing, fashion variability in the lifetime of specific historical periods and artistic directions and movements lead to respect of the requirements of clothing comfort by designer.

Consumer wearing the clothes registers the perceptions that can very significantly affect the mood, well-being and confidence. Claims that society puts on individuals in the current rapid, dynamic process of life, are resulting in specific tasks and solutions in the process of clothes designing for specific occasions. The requirement of the comfort clothing is at the forefront of the current generation in relation to clothing. Clothing comfort oscillates between two poles because of functional and aesthetic components. Aesthetic vision and its fulfillment should be in accordance with the functionality of the apparel. Functional comfort implies the physiological, sensorial and physiological comfort and is influenced by the characteristics of clothing materials used in apparel making [1]. The protection of an organism as a primary function of clothing, maintenance of thermal equilibrium and creation of a microclimate factors are not always in the forefront of clothing design. Specificity of individual cloths, depending on function, for which they are designed, allows a deviation from this requirement.

Clothes of people working in extreme climatic conditions are the opposite solution in comparison to the extravagant clothing originals, the role of which is to draw attention to the holder. In relation to the fashion and extravagant clothes, the aesthetic comfort is very important from the aspect of wearer. It has to be also pointed out that aesthetic comfort is very subjective and subtle fashion aspect. In the history of a fashion we can find periods, when the prevailing aesthetics and apparel site literally distort the body and cause health problems and despite these problems, this fact has been literally ignored by many people. Currently, demand for clothing comfort is based on the research and development of high quality materials while the necessary physical and physiological properties are also taken into account [2].

Design of the models

To find a suitable material for the implementation of ideas is a task on which a great idea of a designer can wreck. In the creation of clothing, it is mainly the experience which allows us to “discover” a good sense for the material. Besides the study of aesthetic patterns, art history, principles and compositional studies, the study of physiological properties of materials, design fabrics, knits and ties is an important part of training of young designers.

In Fig. 1 and Fig 2, we can see the part of the analysis of the materials from the fashion design aspect and the photos show how the combination of technical and artistic components is important.

Fig. 1 Men's jacket
Obr. 1 Pánske sako

Fig. 2 Lady's party dress
Obr. 2 Dámske večerné šaty

Men's jacket

As the most appropriate material, the woolen fabric was selected and its trade name is tweed. It is flexible soft-contrast material, which provides good wearing comfort to user (Fig. 3). For lining, the viscose fabric was used.

The construction is derived from the basic pattern of men's jacket using the principle of asymmetry. Decor was created by technique of printing with utilization of the template.

Lady's party dress

The short dress was created by combination of two different colored and structured fabrics creating an interesting contrast: black taffeta and white lace (Fig. 4). Taffeta is a fine silk fabric with fine cross waled effects and slight sheen. Lace is translucent embossing knitted fabric with floral pattern.

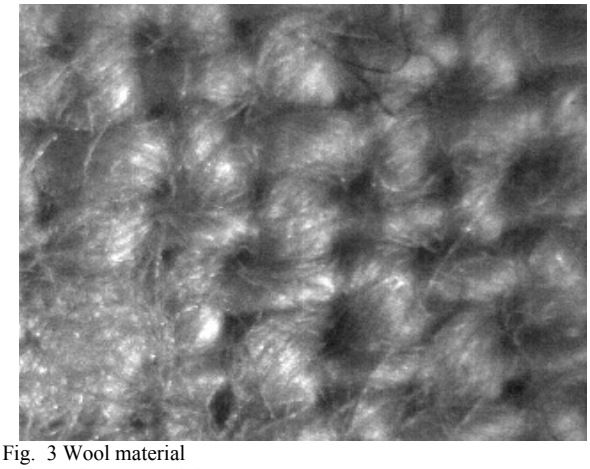

Fig. 3 Wool material
Obr. 3 Vlnený materiál

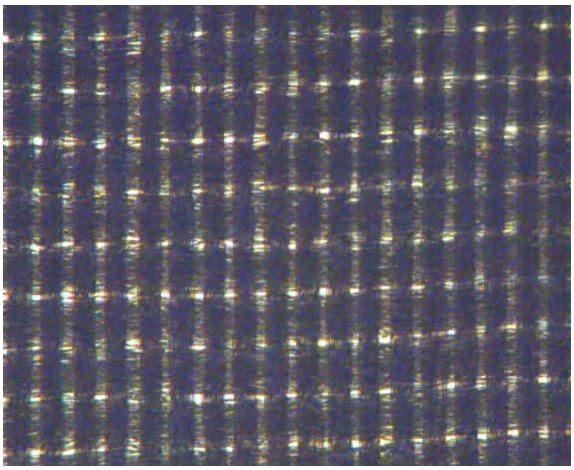

Fig. 4 Silk material
Obr. 4 Hodvábny materiál

Parameters of fabrics

The suitability of these materials was verified by measurements of properties which are necessary for the processing of the clothing as well as the use of the models. In the Tab. 1, the basic variables are presented.

Tab. 1 Parameters of material
Tab. 1 Parametre materiálu

Type of material	Material composition	Surface weight (kg/m^2)	Dimensional variety warp/weft (%)	Keeping color in wash (1..5)
Wool fabrics	40 % wool 60 % PES	350	1/1	5
Silk fabrics	100 % PES	90	04/0.6	5
Lace	100 % PAD	140	-	-

Conclusions

We attached two designed models as example while these models were made at the Department of Industrial Design in Ružomberok in 2009. The common denominator of the work is connected with the inspiration standing for modern art. Each of the authors elaborated the model in different ways. Author of man´s jacket benefited from a minimalist approach and simple shape and author of the lady´s dress emphasized interesting details and contrast. The utilization of selected material and its combination with the authors´ ideas leads to excellent harmony in relation to the clothing design - "idea is consistent with the form". Before the design and preparation of the models, analysis of the materials was carried out and this analysis confirmed that selected materials were a good choice for emphasis of the required and specified features.

Literature

[1] LIZÁK, P. *Textilný dizajn*. Dizajn n.o. Ružomberok, 2006, ISBN 80 -969610 – 0 – 4, EAN 978809691009, p. 126

[2] BHASKARAN, B. *Podoby moderního designu*, ISBN 80-7209-864-0, Slovart, s.r.o., Praha, 2007

hutní výroba v ČR a SR

Meziroční porovnání měsíčních a postupných hutních výrob roku 2014 a 2013

	Výroba *)			Výroba	Index	Výroba	Index	Výroba	Index
	březen	duben	leden-duben	březen		duben		leden-duben	
	2014	2014	2014	2013	2014/13	2013	2014/13	2013	2014/13
		tis.t		tis.t	%	tis.t	%	tis.t	%
KOKS									
CELKEM	291,63	280,91	1 132,56	284,72	102,43	276,00	101,78	1 105,66	102,43
z toho (HŽ) ČR	157,28	149,88	610,37	153,47	102,48	151,23	99,11	600,07	101,72
(HŽ) SR	134,35	131,03	522,19	131,24	102,37	124,77	105,02	505,59	103,28
AGLOMERÁT									
CELKEM	871,28	787,22	3 161,64	690,47	126,19	690,82	113,96	2 732,99	115,68
z toho ČR	520,38	480,82	1 891,04	459,97	113,13	447,12	107,54	1 759,29	107,49
SR	350,90	306,40	1 270,60	230,50	152,23	243,70	125,73	973,70	130,49
SUROVÉ ŽELEZO									
CELKEM	672,31	686,66	2 652,67	687,48	97,79	631,75	108,69	2 593,89	102,27
z toho ČR	366,54	358,41	1 415,11	353,37	103,73	324,99	110,28	1 338,88	105,69
SR	305,77	328,25	1 237,56	334,11	91,52	306,76	107,01	1 255,01	98,61
SUROVÁ OCEL									
CELKEM	858,53	864,67	3 359,28	886,00	96,90	792,01	109,17	3 303,17	101,70
z toho ČR	477,79	467,69	1 835,95	460,35	103,79	404,43	115,64	1 726,30	106,35
SR	380,74	396,99	1 523,33	425,65	89,45	387,58	102,43	1 576,88	96,60
KONTISLITKY									
CELKEM	817,69	826,28	3 203,92	842,55	97,05	749,86	110,19	3 140,58	102,02
z toho ČR	437,88	430,23	1 684,32	417,88	104,79	363,25	118,44	1 567,58	107,45
SR	379,81	396,06	1 519,61	424,68	89,43	386,61	102,44	1 573,00	96,61
BLOKOVNY									
CELKEM	49,00	49,49	192,51	52,85	92,71	41,91	118,07	188,00	102,40
z toho ČR	49,00	49,49	192,51	52,85	92,71	41,91	118,07	188,00	102,40
SR	0,00	0,00	0,00	0,00	0,00	0,00	0,00	0,00	0,00
VÁLCOVANÝ MATERIÁL									
CELKEM	770,19	773,93	3 043,69	755,02	102,01	756,27	102,34	3 016,76	100,89
z toho ČR	425,33	404,04	1 661,36	408,47	104,13	408,07	99,01	1 640,62	101,26
SR	344,87	369,89	1 382,32	346,55	99,52	348,21	106,23	1 376,14	100,45
TRUBKY									
CELKEM	65,25	66,71	256,42	71,66	91,06	67,64	98,62	254,42	100,79
z toho ČR	45,77	46,03	177,59	49,98	91,57	47,06	97,81	172,44	102,98
SR	19,48	20,68	78,83	21,68	89,87	20,58	100,46	81,98	96,16
TAŽENÁ, LOUPANÁ, BROUŠENÁ OCEL									
CELKEM= (HŽ)Č	17,44	16,54	67,33	17,58	99,23	16,00	103,43	63,85	105,45
STUDENÁ PÁSKA KLASICKÁ									
CELKEM= (HŽ)Č	2,78	2,76	10,96	2,51	110,81	2,68	102,95	9,96	110,06

POZNÁMKA: *) Za poslední měsíc jsou údaje předběžné

Zpracoval: Hutnictví železa, a.s. - ing. Vala

ze spolkové činnosti a odborných akcí

Tradiční konference Oceláři

Ve dnech 3. – 4. 4. 2014 se konala v Lázeňském domě Libuše v Karlově Studánce tradiční, již 30. celostátní konference s mezinárodní účastí s názvem „Teorie a praxe výroby a zpracování oceli“.

Konference se zúčastnilo celkem 71 odborníků, z toho jeden účastník z Německa, dva účastníci z Polska a 6 účastníků ze Slovenské republiky. Přítomni odborníci zastupovali celkem 30 podniků a organizací, 3 vysoké školy a 2 výzkumné ústavy. Celkem bylo předneseno 21 odborných referátů.

Vlastní přednášky se zabývaly hlavně:

- technologiemi primárních výrob oceli,
- plynulým odléváním oceli,
- sekundární metalurgií,
- odléváním ingotů.

Dalšími přednesenými tématy úzce navazujícími na primární výrobu a zpracování oceli byly:

- vnitřní čistota, kvalita oceli,
- fyzikální a numerické modelování procesů,
- struskové režimy při výrobě a aplikaci nových struskotvorných směsí,
- využití žárovzdorných materiálů,
- nákladovost výroby, řízení výroby a optimalizace procesů.

Mnohé z přednesených příspěvků prezentovaly výsledky projektů podporovaných finančními zdroji z operačních programů vědy a výzkumu Ministerstva průmyslu a obchodu ČR, Technologické agentury ČR a Ministerstva školství, mládeže a tělovýchovy ČR. Prezentaci doprovázela bohatá diskuse, která probíhala i v rámci závěrečného společenského setkání.

Organizační výbor konference

nová literatura

Jiří Stýblo, Otto Hain

Manažerské trumfy

(Recenze Ing. RNDr. Bohumil Tesařík)

Manažerské trumfy: hodí se naprosto všude a ke všemu. "Lidé tápou. Není to tím, že nevidí řešení. Je to tím, že nevidí problém." (cit. G. K. Chesterton). "Doba je zlá a bude možná ještě horší, věř mi." (cit. Pohádky bratří Grimmů, z rozhovoru dvou skřítků). "Leader a manažer využívá sílu učení nápodobou. Jde o příklad vzorem, založený na osobní autoritě a důvěře." (cit. S. R. M. Covey). "Dnešní problémy nemohou být řešeny, jestliže stále myslíme způsobem, kterým jsme mysleli, když jsme je vytvářeli." (cit. Albert Einstein).

Svět se mění natolik, že včerejší recepty neplatí. Společnost ovládají nové síly, řídí se novými hodnotami. Fakta, která ještě před několika lety představovala ekonomickou realitu, jsou nejen nepopulární, ale pro mnohé podniky přímo sebevražedná. Staré zdroje podnikání a řízení (spotřeba tažená populační explozí, příkazový systém práce s lidmi, úkolující a normující vedení, politické zázemí vycházející a nacházející oporu v podvodech a korupci, management spoléhající na jistotu, opatrnost, předem dané procedury a minimalizace rizika) již přestávají být životné. Všeobecně je uznáváno pět hlavních příčin, nazývaných oprávněně "zabijáci" katarze (očisty) byznysu. Jedná se o strategickou impotenci, strategické mezery, manažerský akademismus, firemní turistiku a ulpívání na konformních zónách bytí a existence. Moderní management dospívá k poznání, že budoucnost do roku 2020 budou vytvářet především tři síly:

1. Globalizace, boj o inovace, schopné zaměstnance a zejména o talenty. Právě souhrnný přístup k trhům, inovacím a talentům zcela určuje a přetváří byznys jako specifický okruh podnikatelských aktivit.
2. Sociální sítě a sociální média intenzivně propojující zaměstnance, zákazníky a dodavatele k okamžité komunikaci.
3. Demografický vývoj: v organizacích bude vedle sebe pracovat několik generací lidí společně (aktuální se stává týmová práce, pravidlo rovnosti apod.).

Hybateli dění jsou leadři (lidé, které ostatní následují a následovat chtějí, aniž by je k tomu musel někdo donucovat; pokud nemají nikoho, kdo by je následoval, jsou jen "lidmi na procházce"), talentovaní pracovníci, jednotlivci i týmy, které přijmou pravidla hry a chtějí hrát s trumfovými kartami. Vítězí ten, kdo má v ruce lepší karty – manažerská esa. Právě o nich, byť z poněkud nezvyklého pohledu, pojednává nová knížka "Manažerské trumfy" (Professional Publishing, Praha 2013, 1. vyd., 170 s.), která chce být příspěvkem k současné aktuální problematice zvyšování výkonnosti a konkurenční schopnosti podniků prostřednictvím lidského kapitálu a jeho podstatného fenoménu leadershipu. Vychází z ověřené hypotézy, že zásadní roli v procesu změn hrají lidé, jejich znalosti, motivace a inspirace, pracovní i osobní uspokojení a připravenost vyrovnat se se změnami v předstihu. Autorem díla je Ing. PhDr. Jiří Stýblo, CSc., patřící ke špičkovým lektorům vědecké a vzdělávací instituce Ústav práva a právní vědy, o.p.s.. Jako pedagog působil nebo působí v několika státních a soukromých vysokých školách, angažuje se v představenstvech v řadě velkých a nadnárodních společností, vydal několik stovek časopiseckých i knižních prací (jmenujme např. knihu "Leadership - realita nebo vize") z oboru řízení, zvláště personálního. Dnes působí jako výkonný ředitel České manažerské asociace. Ke spoluautorství (kapitola "Žaludské eso") přizval dalšího experta v této oblasti PaedDr. Ing. Otto Haina.

Publikace začíná krátkou retrospekcí nedávné minulosti, ale soustřeďuje se na leadery a manažery jako vizionáře, stratégy a vůdce trvale udržitelného rozvoje konkurenční schopnosti firem. Proto je první kapitola nazvána "Neuvěřitelná dobrodružství managementu". Lidé mohou dosáhnout vysoké výkonnosti a produktivity svého konání a jednání pouze tehdy, jsou-li zralými, kompetentními odborníky. Pak se mohou rozvíjet, růst a vydávat plody svého potenciálu. To je žaludský trumf, protože žaludy zrají, nesou své plody, rostou a vydávají svoji sílu a energii v rozpuku.

Člověk, který je vysoce kvalifikován, ale nedělá svoji práci srdcem, nedociluje pracovní ani osobní spokojenosti, na které je jeho výkonnost závislá. Tedy další trumf, srdcové eso, představuje tep firmy. Správná

motivace, inspirace a synergie jsou silou koloběhu života, ať již osobního nebo pracovního.

Firma, která má produktivní výsledky, konkurenceschopné postavení na trhu a chce být na špici peletonu, potřebuje silné a rozumné vedení, kvalitní lídry a otevřenou komunikaci. To jsou trefy mířící do černého – takovým trumfem je kulové eso.

Současná doba je neúprosná. Vyžaduje nové myšlenky, nápady, invenci a inovativnost. To vše přinášejí především talentovaní lidé. Cesta vpřed na první příčky světové konkurenční schopnosti vyžaduje mít v ruce také zelené trumfové eso, otevírající netušené šance a příležitosti. Spolehlivý směr, kterým se musí firmy vydat, je cesta k zákazníkovi a k lidem.

Manažerské trumfy jsou aplikacemi, přidávajícími hodnotu. Významnými součástmi celého textu jsou četné inspirativní příklady z reálného života našich i zahraničních firem a korporací, vybrané úryvky z knih a časopiseckých článků z oblasti moderního i klasického managementu a citace vůdčích osobností ve světě znalostí, inovací, informatiky, technologií, talentů a lidského kapitálu. Kniha je určena nejen pro manažery, kteří mají zájem na zvyšování výkonnosti a konkurenční schopnosti podniků a korporací, ale i pro širší ekonomickou, technickou a další odbornou praxi, pro experty ve firemní strategii (zejména se zaměřením na rozvoj personálních znalostí a lidského kapitálu, podnikovou etiku) a informačních technologiích, pro odborné publicisty, pedagogy a studující vysokoškolských programů i pro všechny ty, kteří se o problematiku vůdcovství laicky zajímají.

Petr Martinovský, Tomáš Šmíd a kol.

Přírodní zdroje a ozbrojené konflikty – aktuální trendy

(Recenze Ing. RNDr. Bohumil Tesařík)

Soubor studií pro orientaci ve světovém soupeření o dostupné suroviny a s ním spojených bezpečnostních hrozbách. "Všechny války vznikají pro hmotné statky." (cit. Platón). "Války nemohou přestat, dokud národy žijí v tak různorodých životních podmínkách." (cit. Sigmund Freud). "Nevím, čím se bude bojovat ve třetí světové válce, ale ve čtvrté to budou klacky a kameny." (cit. Albert Einstein).

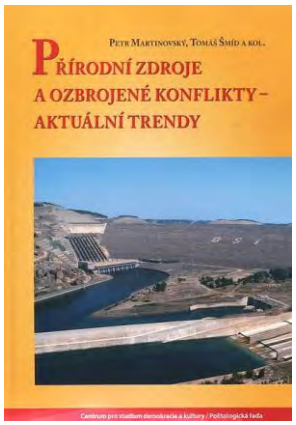

Dlouhodobé udržení dnešní výše spotřeby nejen energetických, ale všech ostatních nerostných surovin, nezbytných pro zachování civilizační úrovně, se začíná jevit jako velmi obtížné až nemožné. V celých dějinách lidstva nám v současné době poskytují výjimečnou příležitost vytvořit zcela reálný souhrnný pohled na význam nerostných surovin a prognózy dalšího celosvětového vývoje tři skutečnosti: 1. rozvoj výpočetní techniky, zejména možnost tvorby a zpracování rozsáhlých databází a možnost přenosu a sdílení informací internetem; 2. vysoká prozkoumatelnost zemské kůry z hlediska výskytu nerostných surovin; 3. stále širší používání angličtiny jako prostředku globální komunikace. Díky těmto třem faktorům lze dnes sestavit skutečně věrohodné dlouhodobé odhady vývoje globálního směřování v oblasti nerostných surovin, což se také děje. Bohužel, převažující většina oficiálních prognóz budoucího vývoje je konstruována a obhajována z pozice zájmů a názorů silnějších aktérů (tzn. pravicově); zájem slabší většiny, ať jedinců, či států, není akceptován a současně nikdo nemyslí na celek – planetu Zemi. Objektivita vládních analýz je přirozeně ovlivněná silou politického zadání. Některé pasáže takových elaborátů se proto mohou jevit až příliš propagandistické. Stále se všeobecně pracuje s doktrínou trvalého růstu, ačkoli nerostné zdroje jsou konečné. Z logiky věci bychom se měli soustředit spíše na "nerůst" či řízené zpomalení produkce a spotřeby. Veškeré souhrnné práce, ať pocházejí z vládního, či soukromého zadání, "cudně" také mlčí o neustálém zbrojení, které masivně odčerpává přírodní zdroje.

Podtrženo a sečteno – před lidstvem se vynořuje vážný problém mizejících zdrojů přírodních surovin, nedostatku energetických a potravinových zdrojů, úbytku půdy a lesů, znečištění vody a celého přírodního prostředí, ale také hrozba populačního růstu a přelidnění. Ačkoliv zvláště v mediálním světě stále víceméně převládají tyto chmurné předpovědi, existuje významná skupina vědců a prognostiků z různých oborů, kteří na základě obsáhlého souboru empirických dat, kvantitativní a historické analýzy, dospívají k přesvědčení, že veškeré naše přírodní zdroje jsou v každém směru neomezené, protože jsou produktem nejen samotné přírody, ale především lidské práce, vynalézavosti a myšlení. Největším našim skutečným bohatstvím, o které musíme nejvíce pečovat, jsou lidé a jejich svoboda.

Zdá se, že z hlediska přístupu k nerostným zdrojům, v nichž má klíčové postavení ropa, jde v tuto chvíli o globální závod v tom, kdo déle vydrží. Hlavní otázka, která by měla znít v pozadí všech rozhodování vlád, finančníků, představitelů armád a dalších mocenských činitelů a seskupení, zní, jak rychle a jakým způsobem bude probíhat nezbytná a očekávaná civilizační regrese. Avšak stále více jsou nerostné suroviny vnímány jako jedno z klíčových témat při tvorbě národních bezpečnostních politik včetně vyzbrojování a budování moderních akceschopných armád. Kromě toho se vlády stále častěji a důrazněji soustřeďují na sledování vnitropolitické situace v oblastech nerostných zdrojů, které jsou nerovnoměrně rozloženy po celé zeměkouli. Podle současných názorů mnohých odborníků budou ještě v tomto století dominantním typem ozbrojených konfliktů právě války o přírodní suroviny. Nárůst poptávky, stálé vyčerpávání snadno dostupných ložisek ropy a dalších komodit, stejně tak jako vnitropolitický a sociální neklid v mnoha producentských zemích, zintenzivňují mezinárodní soupeření o dostupné prameny zejména fosilních paliv. Jiné charakteristiky obsahují často opomíjené konflikty o obnovitelné přírodní zdroje – vodu, půdu či dřevo. Napětí v mnoha oblastech světa narůstá a soupeření se často odehrává nikoli na mezinárodní, ale spíše vnitrostátní rovině. U řady přírodních zdrojů je základní příčinou problémů nejen zvyšování poptávky či spotřeby, ale také zvyšující se znečištění životního prostředí. Jen jeden takový charakteristický příklad: enormní zátěž přírody v Číně se stane podle některých analytiků hlavním spouštěčem radikální transformace tamního politického systému.

Podrobný vhled do šesti takových konfliktních oblastí světa přináší nová fundovaná monografie Petra Martinovského, Tomáše Šmída a kolektivu "Přírodní zdroje a ozbrojené konflikty – aktuální trendy", vydaná obecně prospěšnou společností zaměřenou na vzdělávací, analytickou a kulturní činnost (ve společensko-politické oblasti se hlásící ke konzervativně-liberálním ideovým pozicím), Centrem pro studium demokracie a kultury (Praha 2013, 1. vyd., 186 s., Politologická řada, č. 449, IBSN 978-80-7325-329-5). Publikace rozebírá například vysoce aktuální příští exploataci ohromných zásob nerostných surovin v Afganistanu, který nemá téměř žádný těžební průmysl ani odpovídající infrastrukturu. Jde především o nedávno objevená ložiska kovů (podle odhadu amerických geologů v hodnotě bilion USD), především lithia (používaného pro výrobu baterií do většiny moderních elektronických přístrojů), ale také železa, mědi, zlata, kobaltu, uranu a dalších prvků; zajímavé jsou i naleziště kamenů moderní doby - turmalinů, či tmavě modré silikátové horniny lapis lazuli. Podle vyjádření zahraničních odborníků by se dokonce mohl stát Afganistan "Saudskou Arábií lithia", přirovnávající zásoby tohoto strategického lehkého kovu k zásobám ropy na Arabském poloostrově. Nesmírné přírodní bohatství sice představuje budoucí naději pro tuto zaostalou zemi, na druhé straně však může způsobit další zintenzivnění bojů, protože evidentně představuje pro Taliban ještě větší motivaci k dalším pokusům o trvalé převzetí moci v zemi. "Prokletí Konga se jmenuje coltan", tak označují politologové a novináři situaci v Demokratické republice Kongo, ve které se nachází 80 % světových zásob coltanu, což je obchodní název směsi dvou rud, kolumbitu a tantalitu, ze kterých se získává niob a tantal, tj. kovů nezbytných pro výrobu kondenzátorů a dalších součástek mobilů, notebooků a ostatních elektronických přístrojů. Málo známé a diskutované jsou také konflikty o vodní zdroje na horním Nilu a další konflikty.

Publikace je určena pro odbornou i širší veřejnost jako zajímavá pomůcka pro orientaci v ekonomicko-politických problémech současného světa. Využití nalezne v rukou politiků, ekonomických a vojenských analytiků a prognostiků, vlastníků a manažerů těžebních, zpracovatelských nebo obchodních společností, novinářů, odborných publicistů i učitelů a studentů politologie, mezinárodních vztahů, bezpečnostních studií aj.

konference, výstavy, veletrhy

Veletrh zpracování plechu EuroBLECH 2014

Průmysl zpracování plechu se 21. – 25. 10. 2014 opět sejde na výstavišti v Hannoveru na svém největším světovém odborném veletrhu EuroBLECH. Výstavní stánky si už objednalo přes 14 tisíc vystavovatelů ze 41 zemí, kteří obsadí v halách č. 11, 12, 13, 14, 15, 16, 17 a 27 výstavní plochu o velikosti 86.500 m^2. EuroBLECH 2014 tak už dnes dosahuje ve srovnání s minulými ročníky mírný nárůst 3 %.

Největšími vystavovateli po Německu jsou Itálie, Čína, Turecko, Nizozemsko, Španělsko, Švýcarsko, Rakousko a USA. Podíl zahraničních podniků, které budou na veletrhu vystavovat, činí 50 %. Tento značně vysoký podíl zahraničních vystavovatelů opět dokládá významné postavení veletrhu EuroBLECH jako vedoucího mezinárodního veletrhu oboru. Ukazuje ale také, že průmysl zpracování plechu při zajišťování dlouhodobé úspěšnosti svých produktů sází na mezinárodní obchodní kontakty.

Průmysl zpracování plechu se v globalizovaném světě uplatňuje na velmi rozdílných trzích, kde je poptávka po stále větší rozmanitosti produktů. Pro jejich výrobu jsou nutné nové, flexibilní výrobní procesy. Ukazuje se, že pro průmysl zpracování plechu jsou důležité investice do efektivních zařízení a systémů na míru. Ve výrobě jsou bezpodmínečně nutné inteligentní procesové řetězce a vytváření sítí. Výstavní nabídka 23. Mezinárodního technologického veletrhu pro zpracování plechu zahrnuje celý procesový řetězec zpracování plechu: předvalky, dodavatelské díly, handling, řezání, tvarování, pružné zpracování plechu, spojování, svařování, zpracování trubek a profilů, zpracování hybridních struktur, úpravu povrchů, nástroje, řídicí a regulační techniku, systémy CAD/CAM, kontrolu kvality, zařízení továren, výzkum a vývoj.

K dispozici je pro návštěvníky veletrhu už nyní brožura ve dvanácti jazycích s podrobnými informacemi. Lze ji získat na adrese www.euroblech.de. EuroBLECH Bulletin, pravidelně vycházející elektronický newsletter, je možné rovněž získat na webové stránce veletrhu. Newsletter obsahuje aktuální informace o veletrhu EuroBLECH 2014, zajímavé zprávy z oboru a informace o produktech, které budou na veletrhu v říjnu vystavené.

red.

(podle zdroje: Susanne Neuner, PR Direktor, Tiskové oddělení EuroBLECH, Mack Brooks Exhibitions Ltd., Romeland House, Romeland Hill, St Albans, Herts AL3 4ET, Velká Británie, 0044 (0)1727 814400, press@mackbrooks.co.uk)

Úsporná opatření Tata Steel Scunthorpe

Steel Guru/Steel Trade Today 27. 3. 2014

Zaměstnanci na válcovně kolejnic a profilů v ocelárnách Tata Steel v Scunthorpe nasadili všechny páky, aby společnosti pomohli do 31.3.2014 dosáhnout úspory 34,5 mil. GBP. Většina střešního a nástěnného osvětlení byla konvertována na vytváření úspor okolo 800 GBP denně. Od r. 2008 je v ocelárně velký tlak na redukci spotřeby energie. Ze zlepšení, které dosáhli, šetří okolo 800 tis. GBP ročně. Některé z velkých úspor přicházejí ze změn, které provedli také v osvětlení. I v nadcházejících měsících se budou zaměřovat na redukci nákladů na energii.

hutnictví ve světě

Hlavní vývojové tendence české ekonomiky v roce 2013 a výhled na rok 2014

Vývoj průmyslu v roce 2013

Průmyslová výroba v roce 2013 zaznamenala meziroční růst o 0,5 %. Výsledek průmyslové výroby však nebyl od počátku roku jednoznačný, neboť průmysl navázal na pokles z roku 2012. Již v 1. čtvrtletí roku 2013 dosáhla produkce svého dna, když se meziročně snížila o 5,4 %. Ve 2. čtvrtletí se propad zmírnil na 2,4 % a ve 3. a 4. čtvrtletí se průmyslová produkce vrátila k růstu a vzrostla o 3,9 %, resp. 6,1 %. Na celkovém ročním výsledku se projevilo oživení průmyslu v eurozóně, zejména v Německu, a lepšící se situace na evropském automobilovém trhu, která přinesla růst domácí výroby automobilů a na ni navazujících oborů. Oživení průmyslu bylo predikováno nejen zahraničními předstihovými ukazateli, ale i domácím konjunkturálním průzkumem ČSÚ, který od poloviny roku signalizoval zvýšení výrobní činnosti a posilování důvěry podnikatelů.

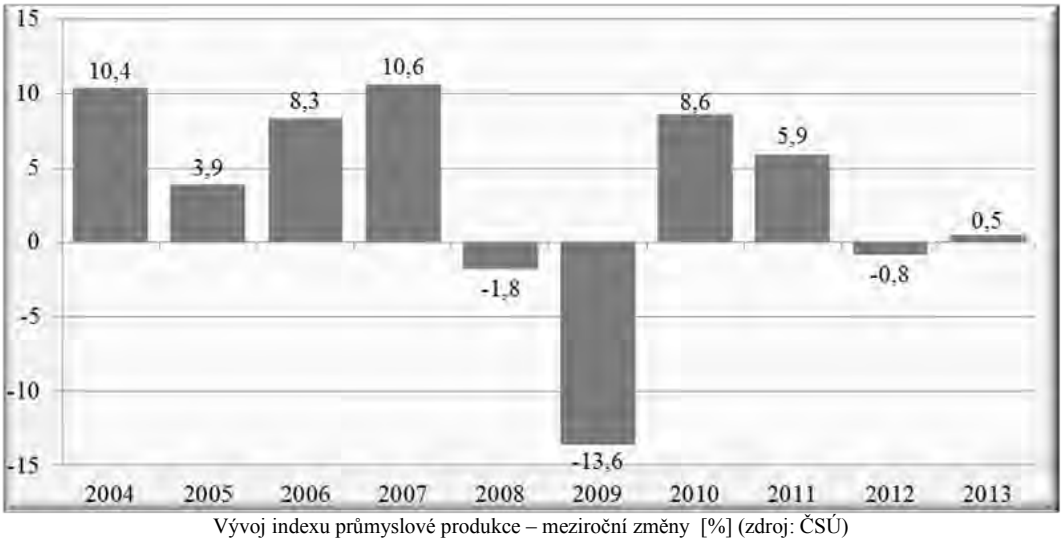

Vývoj indexu průmyslové produkce – meziroční změny [%] (zdroj: ČSÚ)

V roce 2013 se ve zpracovatelském průmyslu produkce zvýšila ve 14 odvětvích (o 1,4 %, měřeno indexem průmyslové produkce – IPP). Na celkových tržbách průmyslu se růstová odvětví podílela 63,3 %. Růst ovlivnila především zahraniční poptávka a projevila se zejména v odvětvích s uplatněním produkce na trhu EU. Z odvětví zpracovatelského průmyslu se produkce nejvíce zvýšila ve výrobě ostatních dopravních prostředků (o 9,1 %), ve výrobě farmaceutických výrobků a přípravků (o 7,6 %), ve zpracování dřeva a výrobě dřevěných výrobků (o 6,7 %), v ostatním zpracovatelském průmyslu (o 6,1 %), ve výrobě kovových konstrukcí a kovových výrobků (o 5,3 %), ve výrobě oděvů (o 3,3 %), ve výrobě nápojů (o 2,8 %), ve výrobě strojů a zařízení (o 2,7 %) a ve výrobě dopravních prostředků (o 2,5 %). Ostatní růstová odvětví evidovala nárůst produkce do 2 %.

Ve zpracovatelském průmyslu ke snížení produkce došlo u devíti odvětví (na celkové průmyslové produkci se podílela 27,6 %). Nejvíce poklesla výroba počítačů, elektronických a optických přístrojů (o 8,7 %), opravy a instalace strojů a zařízení (o 8,4 %), tisk a rozmnožování nahraných nosičů (o 7,5 %) a koksování a rafinérské zpracování ropy (o 6,6 %). Ostatní odvětví evidovala nižší meziroční pokles produkce pod 5 %.

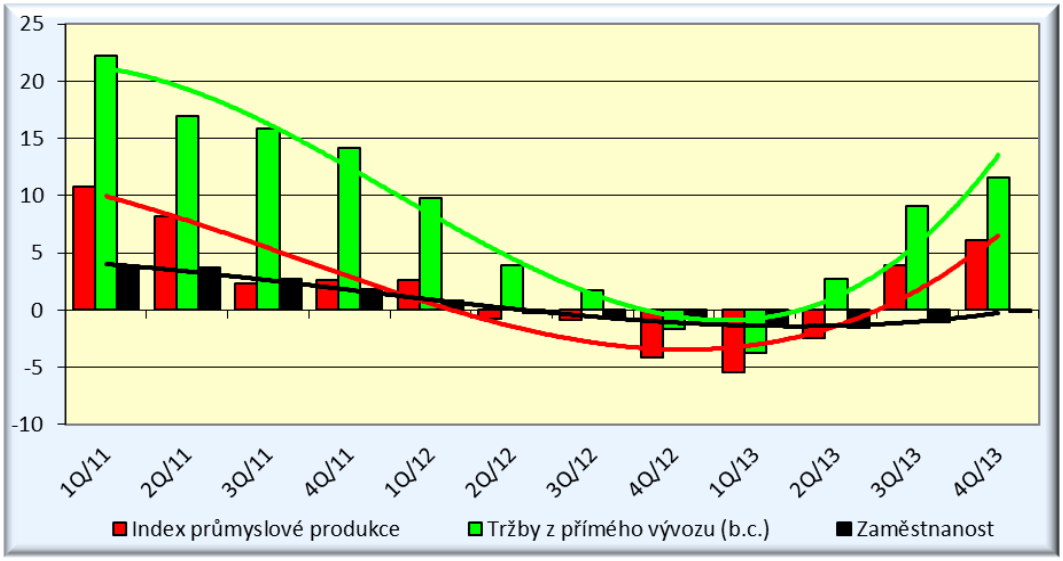

Vývoj průmyslové produkce, tržeb z přímého vývozu a zaměstnanosti u organizací s 50 a více zaměstnanci – meziroční změna [%] (zdroj: ČSÚ)

Průmyslová produkce se v roce 2013 podle propočtů MPO zpracovaných podle dostupných údajů Eurostatu meziročně snížila v zemích EU o 0,5 %, v eurozóně o 0,8 %. Oživení ekonomik se odrazilo růstem produkce ve 4. čtvrtletí 2013. V EU ekonomika vzrostla o 1,6 %, v eurozóně o 1,3 %. Mezi vývojem v ČR, Německu a eurozóně je velmi úzká vazba, která je patrná z následujícího grafu.

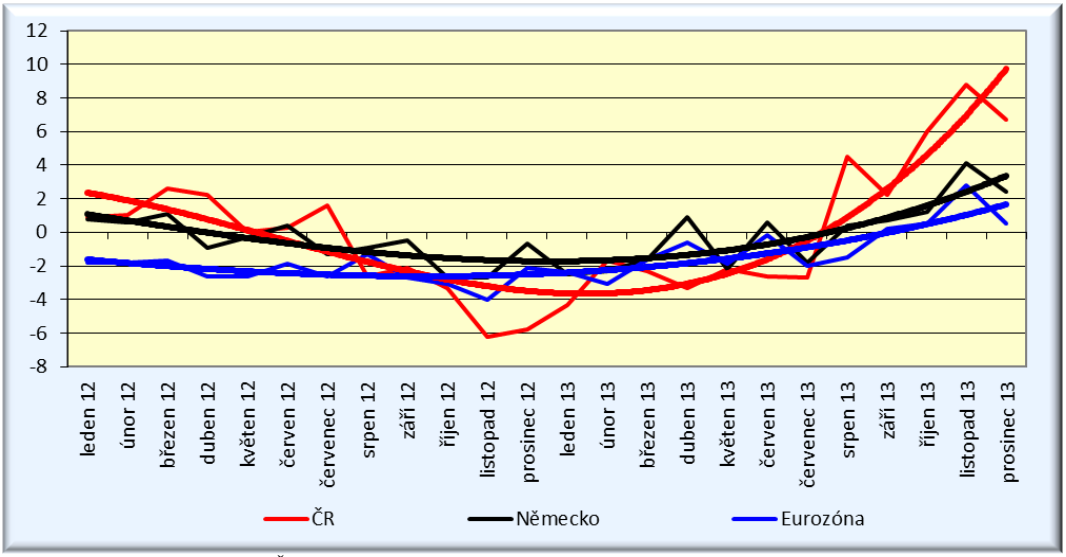

Vývoj průmyslové produkce v ČR, v Německu a eurozóně – meziroční změna [%] (zdroj: Eurostat, graf a propočty MPO)

Nastartování růstu průmyslové produkce v eurozóně v polovině roku 2013 se projevilo růstovou tendencí i v ČR. Vývoj v ČR byl v závěru roku 2012 ovlivněn nižším počtem pracovních dní o tři dny, což se projevilo vyšším růstem v závěru roku 2013.

Podle hlavních průmyslových seskupení se růst produkce v druhé polovině roku projevil v celoročních výsledcích zvýšením výroby pro mezispotřebu (o 1,9 %), dlouhodobou spotřebu (o 1,3 %), investice (o 1,2 %) a krátkodobou spotřebu (o 0,4 %). Snížení produkce evidovala pouze výroba energií (o 3,9 %). Zvýšená investiční aktivita průmyslových podniků byla zahájena ve 3. a 4. čtvrtletí 2013.

V dělení výroby zpracovatelského průmyslu podle technologické náročnosti měl nejvýznamnější pozici sektor „medium high-tech“ zabezpečující více než polovinu tržeb (50,6 %, při zvýšení podílu o 1 bod). Jeho produkce se meziročně zvýšila o 3,6 %. V tomto sektoru je zahrnut automobilový, elektrotechnický, chemický a strojírenský průmysl. Růst tržeb evidoval i sektor „low-tech“ o 2,6 %. Jeho podíl se mírně zvýšil (o 0,2 bodu na 15,2 %). V tomto sektoru jsou zahrnuta méně významná odvětví průmyslu: potravinářský, oděvní, kožedělný a dřevozpracující průmysl. Produkce u ostatních sektorů se snížila. Tržby u „medium low-tech“ byly mírně nižší o 0,1 % a více než čtvrtinový podíl se snížil (o 0,4 bodu na 25,8 %). Sem patří odvětví

napojená na automobilový průmysl (výroba pryžových a plastových výrobků), dále hutnictví, výroba kovových konstrukcí, koksování a rafinérské zpracování ropy a výroba ostatních nekovových minerálních výrobků.

Hlubší pokles tržeb zaznamenal sektor „high-tech“ o 6,7 %, při snížení podílu (o 0,7 bodu na 8,5 %). Vývoj v tomto sektoru byl nepříznivě ovlivněn poklesem rozhodující výroby počítačů.

Vývoj produkce zpracovatelského průmyslu podle technologické náročnosti výroby [%, rozdíl v p.b.] (zdroj: ČSÚ, propočty MPO)

CZ-NACE	Tržby z průmyslové činnosti - meziroční změna	Podíl na tržbách zpracov. prům. 2012	Podíl na tržbách zpracov. prům. 2013	Rozdíl 2013-2012
Zpracovatelský průmysl celkem	1,5	100,0	100,0	0,0
High-tech	-3,7	9,2	8,5	-0,7
Medium high-tech	3,6	49,6	50,6	1,0
Medium low-tecg	-0,1	26,2	25,8	-0,4
Low-tech	2,6	15,0	15,2	0,2

Ukazatelem vypovídajícím o směřování dalšího vývoje průmyslu byl objem celkových nových zakázek ve vybraných oborech, který se v roce 2013 zvýšil o 4,8 %. Rozhodující pozici mělo zvýšení zahraničních zakázek o 5,8 %, které se na celkových zakázkách podílely 70,8 %. Zahraniční zakázky se vlivem oživení produkce a zakázek v eurozóně (zejména v Německu ve druhé polovině roku) a vlivem silné provázanosti ekonomik staly hlavním tahounem domácího růstu. Ve 3. čtvrtletí se zvýšily o 16 % a ve 4. čtvrtletí o 18,2 %. Největší zvýšení těchto zakázek z vybraných oborů v roce 2013 evidovala výroba ostatních dopravních prostředků (o 22,4 %), výroba kovových konstrukcí a kovodělných výrobků (o 14,3 %), výroba motorových vozidel (o 12,5 %) a výroba farmaceutických výroků a přípravků (o 9,7 %). Domácí zakázky posílily o 2,5 %, z vybraných odvětví nejvýrazněji ve výrobě oděvů (o 18,3 %), ve výrobě strojů a zařízení (o 11,3 %), ve výrobě kovových konstrukcí a kovodělných výrobků (o 11,2 %) a ve výrobě elektrických zařízení (o 8,2 %).

Mírný růst tržeb (o 1,7 %) a snížení zaměstnanosti (o 1 %) se projevily zvýšením produktivity práce o 2,7 %. Vývoj produktivity práce předstihl růst reálných mezd o 3,7 bodu a dále se projevil poklesem jednotkových mzdových nákladů nominálních a reálných. Produktivita práce zvýšila ve většině odvětví zpracovatelského průmyslu (v 18 odvětvích), naopak pokles evidovalo pět odvětví.

Očekávaný vývoj průmyslu v roce 2014

Růst průmyslové produkce, nastartovaný v druhé polovině roku 2013, bude pokračovat i v roce 2014. Jeho udržení bude záležet na dalším vývoji v eurozóně a především v Německu. Z vývoje průmyslu v závěru roku 2013 je patrné oživení ekonomik eurozóny. Z tohoto důvodu můžeme očekávat pokračování růstu zahraniční poptávky, což se vlivem silné vzájemné provázanosti bude projevovat i na růstu průmyslu ČR. V první polovině roku 2014 bude průmysl dosahovat díky nízké srovnávací základně vyššího růstu, v druhé polovině roku se však tento růst mírně zpomalí.

Zahraniční předstihové ukazatele na začátku roku 2014 (např. index nákupních manažerů - PMI) dosahují dlouhodobě nadprůměrných hodnot, za kterými stojí zrychlený růst nových objednávek. Na počátku roku se zlepšila i podnikatelská nálada v Německu a potvrdila odhady, podle nichž největší evropská ekonomika v roce 2014 urychlí růst. Březnové výsledky však optimismus, vlivem situace na Ukrajině, mírně snížily. Naopak, podle konjunkturálního průzkumu ČSÚ u vybraných průmyslových podniků, se zvýšila důvěra i k hodnocení celkové poptávky.

Důležitý bude i vývoj domácího automobilového průmyslu, který má na tržbách průmyslu ČR rozhodující podíl (zhruba čtvrtina tržeb průmyslu). Vývoj automobilek bude záviset na růstu prodejů, které v závěru roku 2013 dynamicky rostly. Příznivý vývoj automobilového průmyslu bude mít pozitivní vliv i na dodavatelská odvětví a obory.

Pro rok 2014 můžeme předpokládat pokračování růstu průmyslové produkce nastartované v druhé polovině roku 2013. Vzhledem k dosavadnímu vývoji, postupnému oživení evropských ekonomik a pokračování příznivého vývoje automobilového průmyslu, můžeme pro rok 2014 očekávat růst průmyslové produkce v rozmezí o 3 až 5 %**.** Tuto prognózu podporují i dosažené výsledky na začátku roku, kdy se průmyslová produkce v lednu meziročně zvýšila o 5,5 % a v únoru o 6,7 %.

red. (podle zdroje: Analýza MPO, duben 2014)

(Pokračování)

Proexportní program Vlády ČR podporuje zaměstnanost

„Export je jedním z hlavních pilířů naší ekonomiky a podpora exportu musí být prioritním zájmem státu na všech úrovních, přičemž nejsledovanějším cílem je zajištění stávajících a tvorba nových pracovních míst v České republice," uvedl na své dubnové tiskové konferenci věnované nové hospodářsko-obchodní strategii ministr průmyslu a obchodu Jan Mládek. Připomněl, že efektivní export úzce souvisí s ekonomickou rovnováhou země, se stabilitou měny, kvalitním mezinárodním ratingem a důvěryhodností.

ČR jako malá a otevřená ekonomika je na úspěšném vývozu kvalitních produktů a služeb s co nejvyšší mírou přidané hodnoty životně závislá. Jestliže 81 % exportu směřuje do partnerských zemí EU, další potenciál růstu lze spatřovat zejména mimo EU. V souladu s exportní strategií proto vláda zahajuje exportní ofenzívu v oblasti 12 prioritních zemí a 26 zájmových zemí, které byly vybrány na základě požadavků podnikatelských reprezentací. Pro etapu do roku 2020 sem patří například Brazílie, Čína, Indie, Irák, Kazachstán, Mexiko, Srbsko, Turecko, USA či Vietnam. Již v květnu byla realizace tohoto scénáře zahájena návštěvou více než dvou desítek podnikatelů vedených ministrem Mládkem ve Vietnamu. Důležitou roli v podpoře českých exportérů bude hrát zejména síť zahraničních kanceláří MPO a CzechTrade.

Ministr Mládek vyjádřil svou myšlenku, že se nespokojí pouze s dosažením kvantity v podobě cílového počtu 70 zahraničních kanceláří MPO, jejichž otevření bylo plánováno v minulých obdobích. Podstatně důležitější než celkový počet zahraničních zastoupení jsou jejich kompetence, personální obsazení nejlepšími lidmi s obchodním duchem a zejména pak zvýšená pozornost vůči trhům s velkým obchodním a investičním potenciálem.

Naše exportní strategie je založena na třech pilířích: zpravodajství pro export, rozvoj exportu a podpora obchodních příležitostí. Již byl zahájen proces optimalizace marketingových služeb státu, aby české firmy dobře věděly, jakou podporu mohou od státu ve svém exportním úsilí očekávat. Proto se klade velký důraz na spolupráci s podnikatelským sektorem. Zásadní je restart samostatných, agilních a vzájemně se doplňujících aktivit CzechTrade a CzechInvest. Jejich činnost se musí přizpůsobit vládním prioritám a především potřebám jednak tuzemských exportérů a jednak zahraničních investorů. Obě agentury musí pružně a rychle reagovat na neustále se měnící podmínky na globálním trhu a stát jim prostřednictvím MPO poskytne maximální podporu.

V ekonomické diplomacii musí co nejdříve nastoupit synergický efekt spolupráce a sdílení infrastruktury vytvářením klientských center podpory exportu založených na spolupráci ministerstva průmyslu a obchodu, ministerstva zahraničních věcí a agentury CzechTrade. Agentura poskytuje široké poradenské, vzdělávací a asistenční služby především pro malé a střední firmy a ministerstvo zahraničních věcí bude koordinátorem vnějších ekonomických vztahů a efektivně podpoří ekonomickou diplomacii prostřednictvím zastupitelských úřadů po celém světě.

Generální ředitel agentury CzechInvest Ondřej Votruba na tiskové konferenci uvedl, že po dlouhé době zaznamenává podporu ministerstva průmyslu a obchodu a celé vlády, a proto se agentura můžeme opět soustředit na lákání investic, díky kterým v ČR ročně vznikají tisíce nových pracovních míst. Cílem je, aby se CzechInvest znovu dostal mezi špičky světových investičních agentur. Rovněž pověřený generální ředitel CzechTrade Milan Ráž sdělil, že přáním agentury je, aby ji firmy vnímaly jako proklientskou a komunikaci otevřenou agenturu, jako stabilního partnera, který jim může nabídnout své zkušenosti a teritoriální a oborovou znalost. Do struktury institucí podporujících export patří i Česká exportní banka (ČEB) a Exportní garanční a pojišťovací společnost (EGAP), které poskytují státem podporované financování a pojištění exportu. Letos půjde na podporu činnosti ČEB asi 1 mld. Kč a počítá se také se státní zárukou na závazky banky ve výši 130 mld. Kč. Rozpočet zahrnuje i navýšení pojistných fondů EGAP ve výši 1,25 mld. Kč.

Příkladem může být například perspektivní Čína, kde dosud působily kanceláře MPO pouze v Shanghai a Chengu. Začala fungovat kancelář v Pekingu a do konce roku by měla být otevřena rovněž kancelář v Kantonu. V současné době se projevuje velmi dobře započatá propagace zejména českého leteckého průmyslu. Jistě však je potenciál podstatně větší a zahrnuje i další obory.

red. (podle zdroje: Tisková zpráva MPO, 25.4.2014)

Poptávka po nerezové oceli v EU roste

Steel Business Briefing 24. 3. 2014

Reálná poptávka po nerezové oceli v Evropě sílí, a logickým důsledkem by měl být podle výrobce, jehož vedení sídlí v Lucemburku, případný nárůst základních cen. Zvětšuje se důvěra zákazníků, zlepšují se objednávkové knihy a prodlužují se dodací lhůty. Základní ceny (bez přirážek za slitiny) pro studený svitek typu 304, pásu o tloušťce 2 mm, se ze 1005 Euro/t na začátku roku zvýšily v březnu na 1015 Euro/t. Další nárůst základních cen je logicky dán poptávkou, objednávkovými knihami a dodacími lhůtami. Firma uvádí, že lepší makroekonomické podmínky generují mnohem pozitivnější a důvěryhodnější klima mezi spotřebiteli nerezové oceli. Zjevná spotřeba v Evropě je nejlepší za 2 – 3 roky, v r. 2013 posílila o 3 %. Nedochází k žádnému podstatnému doplňování zásob a to naznačuje, že reálná spotřeba je na zlepšené úrovni. Přispívají k tomu všechny sektory konečné spotřeby, od investičního zboží až po segmenty ve vztahu ke spotřebě, jako je bílé zboží. Dopředu směřující objednávkové knihy jsou proto zdravější. Objednávkové knihy firmy Aperam jsou o 8 – 10 % vyšší, než v téže době minulého roku, dodací lhůty se prodloužily. Výhledově se nepředpokládá žádné oslabení ve 3. čtvrtletí. Léto je vždy o něco napjatější a vytvoří tlak na příští dodávky. Asijští výrobci zvyšují ceny, což bude mít pozitivní vliv. Nárůst ceny niklu má také vliv na efektivní transakční cenu nerezové oceli. Je naděje, že se cena niklu udrží v rozpětí 16 až 16,5 tis. USD/t a vyhne se velkým výkyvům, zaznamenaným v předchozích letech.

US Steel plánuje výstavbu další elektrické obloukové pece

Reuters 25. 3. 2014

US Steel Co. by měla nahradit jednu další ze svých starších vysokých pecí elektrickou obloukovou pecí. Požádala již o povolení instalovat elektrickou obloukovou pec (EOP) náhradou za vysokou pec ve svém zařízení ve Fairfieldu, Alabama, jako součást svého úsilí o redukci nákladů. Rentabilní rival US Steel, Nucor Corp., se dlouhodobě specializuje na výrobu oceli v elektrických obloukových pecích v rámci minioceláren. US Steel a Nucor jsou největší výrobci oceli sídlící v USA. Trvalý ppřechod k miniocelárnám by byl velkou změnou ve strategii US Steel, která se všeobecně zaměřuje na udržení své flotily vysokých pecí. EOP využívají ocelový šrot namísto železné rudy. Provoz EOP snižuje náklady spojené s dopravou surovin a chrání výrobce oceli před nárůstem cen železné rudy a uhlí. Jedním z faktorů pro zastavení jedné z vyskokých pecí je jejich věk a doba opravy vyzdívky. Oprava vyzdívky vysoké pece může stát 100 mil. USD nebo více.

Na téma užití hliníku oproti oceli US Steel říká, že v automobilovém průmyslu hliník velmi expanduje. Ocel, pokud jde o jjeí užití při výrobě kol, poněkud zaspala. Ocelářský průmysl zaostává ve výzkumu a vývoji, ale US Steel zintenzivňuje své práce v této oblasti. Poptávka výrobců automobilů po hliníku, který je dražší a také lehčí než konvenční ocel, rychle roste, protože výrobci automobilů tlačí na snížení spotřeby paliva.

Skupina Simec z ICH investuje do dvou oceláren v Mexiku

Steel Guru/Steel Trade Today 27. 3. 2014

Business News Americas informovaly, že skupina Simec bude investovat více než 700 mil. USD do dvou nových oceláren v Mexiku. Mateřská firma Industrias CH řekla, že společnost sídlící v Guadalajara plánuje vybudovat provoz na výrobu tyčí ze speciální oceli s kapacitou 600 tis. t/r. na severu země za 700 mil. USD z vlastních zdrojů. Vedení ICH také schválilo nový provoz na výrobu tlustých plechů, což společnosti umožní výrobu svařovaných trubek ve šroubovici až do průměru 100 inch (2.54 m) a s tloušťkou stěn 1 inch (25.4 mm). Nové provozy pomohou uspokojit rostoucí poptávku od automobilového průmyslu a těžebního průmyslu ropy a plynu, které jsou považovány za klíčové oblasti růstu pro mexický ocelářský sektor. Simec dosud vyrábí tvarové produkty, jako jsou konstrukční profily, tyče a speciální ocelové výrobky, a to především pro stavební sektor, automobilový průmysl a pro další výrobní sektory. ICH má 12 oceláenských provozů, 4 zařízení na zpracování šrotu v Mexiku a také 8 provozů v USA a Kanadě.

Bochumská Outokumpu se uzavře v září 2015

www.derwesten.de 30. 3. 2014

Závod v Bochumi na výrobu nerezavějící oceli se uzavře nejdříve v září 2015, jak se dohodly IG Metall a finská ocelářská skupina Outokumpu. Asi nejdůležitějším bodem je budoucnost 450 zaměstnanců, kteří si tak prozatím nemusí hledat práci. Mezi vedením závodu a odbory při jednání k dohodě. Outokumpu bude zkoumat technické možnosti přemístění tavicí kapacity do Finska a Švédska. Všichni zaměstnanci dostanou kompenzaci do výše jejich zaměstnání do konce 2016 a dodatečně 10 tis. Eur na jednoho zaměstnance. Bude jim také nabídnuto alternativní zaměstnání u ThyssenKrupp, HKM nebo v jiném výrobním závodě Outokumpu.

Hodnocení výsledků řešení ve výzkumných projektech

Rada vlády ČR pro výzkum, vývoj, inovace (VVI) zavádí nový bodový systém pro hodnocení výsledků řešení ve výzkumných projektech, platný pro léta 2013 – 2015. Toto hodnocení se dotýká autorských publikací v odborných časopisech, tedy i recenzovaných článků v Hutnických listech a dalších časopisech vydávaných v ČR. Autoři sami jistě novou situaci znají. Zde redakce jen připomíná, že podle nové metodiky jsou nyní recenzované články v technických, informatických a ještě dalších oborech hodnoceny nulovým počtem bodů. Původní počet bodů 4 zůstal jen v hodnocení společenských, humanitních a uměleckých věd. Nová metodika může mít dalekosáhlé negativní následky nejen pro odborné časopisy z takto postižených oborů, ale i pro proces VVI v řadě pracovišť a v důsledku toho může ohrozit konkurenční schopnost českého průmyslu.

Redakce Hutnických listů na nastalou situaci reagovala dopisem Radě vlády ČR pro VVI s vyjádřením stanoviska a podnětů k nové metodice. Zde je uveden plný text dopisu ze dne 5.5.2014, adresovaný na Úřad vlády ČR, Odbor rady pro VVI, jejího předsedu MVDr. Pavla Bělobrádka, Ph.D., MPA a zároveň místopředsedu vlády pro VVI:

„Vážený pane předsedo,

obracíme se na Vás ve věci změn v Metodice hodnocení výsledků výzkumných organizací a hodnocení výsledků ukončených programů platné pro období let 2013 – 2015 a dopadů těchto změn na neimpaktovaná recenzovaná odborná periodika vydávaná v ČR.

Podle této metodiky dochází k úpravě Hodnocení publikačních výsledků (příloha 1, tabulka 1.1 a 1.2) v tom smyslu, že jen recenzované články zahrnuté do oborové skupiny společenských, humanitních a uměleckých věd (SHVa, SHVb) mají hodnocení ve výši 4 bodů. Ostatní obory, tj. technické a informatické obory, ale i řada dalších oborů, které podle předešlé metodiky platné do r. 2012 byly hodnoceny 4 body, zůstávají bez bodového hodnocení, resp. s nulovým hodnocením výstupů výzkumných projektů, tj. recenzovaných článků kategorie J_{rec} publikovaných v neimpaktovaných recenzovaných periodikách vydávaných v ČR.

Vyloučení kategorie technických a informatických věd, spolu s dalšími obory, může mít dalekosáhlé negativní dopady na recenzované odborné časopisy. Recenzovaný časopis Hutnické listy se řadí k této ohrožené skupině. Hutnické listy jsou odborným časopisem pro metalurgii a materiálové inženýrství s hlubokou tradicí od r. 1946. Vždy představovaly kvalitní platformu pro odborné publikace výsledků vědeckých, výzkumných a rozvojových programů řešených na akademických pracovištích, ve výzkumné i výrobní sféře. Z tohoto pohledu mají dnes Hutnické listy nezastupitelnou úlohu pro řešitelská pracoviště v oboru hutnictví a materiálového inženýrství i v souvisejících a navazujících oborech, protože poskytují uvedeným řešitelským pracovištím kvalitní publikační platformu s možností veřejné oponentury formou objektivního recenzního řízení u všech hlavních článků. Absence bodového hodnocení publikačních výsledků podle platné Metodiky vyvolá nejen problémy ve vydávání technických odborných časopisů, ale i v prezentaci aplikovaného výzkumu, vývoje a inovací, které jsou hlavním prostředkem k uvádění novinek do výrobní praxe a udržení konkurenční schopnosti českých výrobců.

Na důkaz podpory tohoto stanoviska jsou zde připojeny podpisy zástupců některých organizací, které v Hutnických listech prezentují výsledky řešení projektů výzkumu, vývoje a inovací, mají své zastoupení v redakční radě časopisu nebo se pravidelně zúčastňují recenzních řízení. Jmenovitě i výrobní podniky jsou zainteresovány na výsledcích výzkumných a vývojových programů, a to nejen po stránce aplikační, ale přímo i řešitelské.

Hutnické listy jsou dlužny dát odpověď řešitelům pracovišť, která v časopise publikují své výsledky, svému orgánu – redakční radě i výrobním podnikům na otázku, jaká bude pozice časopisu dle nové Metodiky hodnocení výsledků výzkumných organizací a hodnocení výsledků ukončených programů. Řadu nápravných podnětů obsahuje stanovisko Svazu průmyslu a dopravy ČR ze dne 12.3.2013, ale ani v materiálu pro jednání Rady vlády ČR pro výzkum, vývoj a inovace k metodice ze září 2013 nelze najít odpověď v tom smyslu, že by kategorie technické a informatické obory a další obory byly zařazeny do skupiny oborů s bodovým hodnocením výsledků výzkumu, vývoje a inovací stejně jako oborová skupina SHVa nebo SHVb.

Vážený pane předsedo, považujte toto naše stanovisko za podnět k optimalizaci Metodiky hodnocení výsledků výzkumu, vývoje a inovací a k objektivizaci postavení zmíněných technických a informatických oborů a dalších oborů v systému bodování.

Přejeme Vám a Vašemu pracovnímu týmu mnoho úspěchů ve snaze o nápravu metodiky a jsme s pozdravem .....“

ISSN 0018-8069

Kromě vedoucího redaktora dopis podepsal předseda redakční rady Hutnických listů prof. Ing. Ľudovít Dobrovský, CSc., dr.h.c., děkanka Fakulty metalurgie a materiálového inženýrství, VŠB-TU Ostrava prof. Ing. Jana Dobrovská, CSc., předseda dozorčí rady vydavatelské firmy OCELOT s.r.o. a jednatel Materiálového a metalurgického výzkumu s.r.o. Ing. Jaroslav Pindor, Ph.D., předseda představenstva a výkonný ředitel Hutnictví železa, a.s. RNDr. Jaroslav Raab, 2. místopředseda představenstva a technický ředitel Třineckých železáren, a.s. Ing. Henryk Huczala, vedoucí elektroocelárny ŽĎAS a.s. Ing.. Ludvík Martínek, Ph.D., ředitel pro strategii VÍTKOVICE, a.s. Ing. Jiří Michálek, Ph.D. a technický ředitel EVRAZ Vítkovice Steel, a.s. Ing. Ludvík Strakoš.

Stanovisko s podněty ve stejném duchu obdržela Rada vlády ČR pro VVI ve společném dopise redakce časopisu Slévárenství a Svazu sléváren. Tento dopis je podpořen také podpisy sedmi význačných pedagogů a odborníků v oboru slévárenství, strojírenských technologií a materiálového inženýrství z VUT v Brně. V době zpracování tohoto příspěvku je v přípravě opět stejné stanovisko ve formě dopisu na stejnou adresu, který vypracovává Česká slévárenská společnost a který bude podpořen podpisy představitelů řady významných závodů v ČR.

Všechny subjekty, které podaly své podněty k nové metodice budou nyní bedlivě sledovat reakci a vývoj v metodice, aby v případě, že technické obory nebudou zrovnoprávněny s těmi obory, jimž zůstalo hodnocení 4 body, použili v dalším kroku pro svou argumentaci silnější kalibr a zaujali jednotný a společný postup.

red.

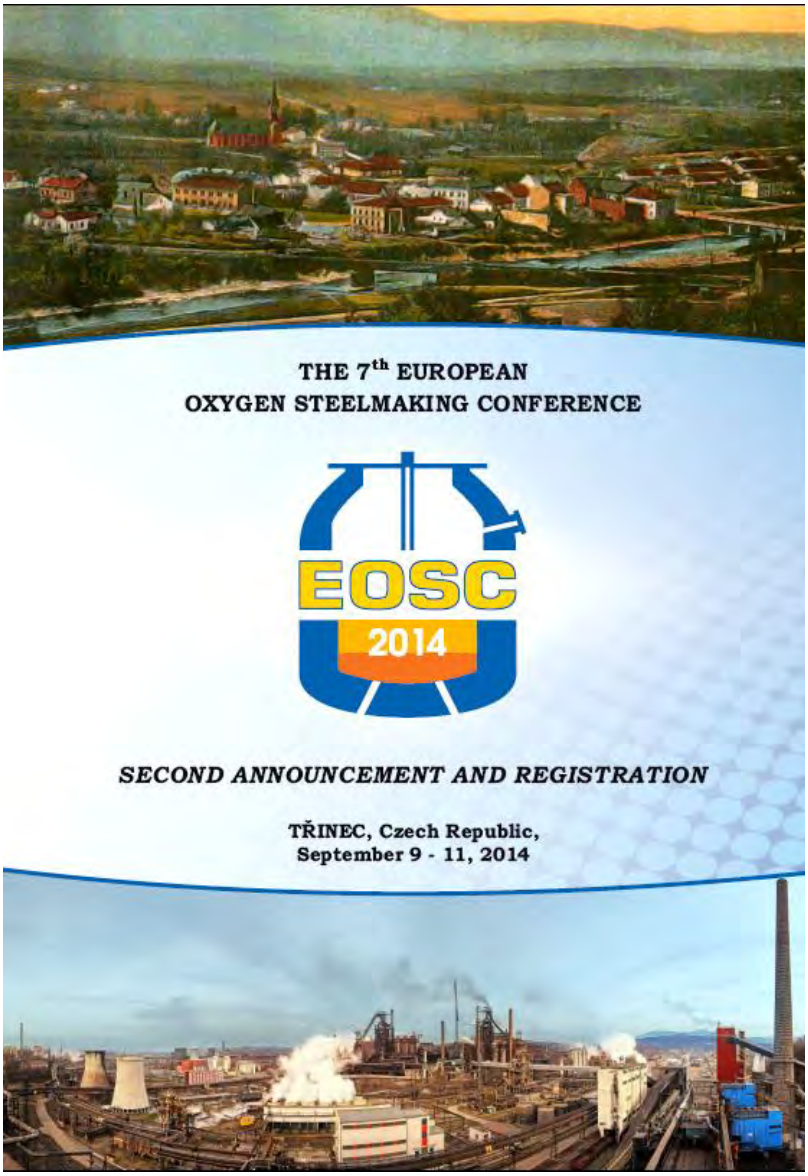

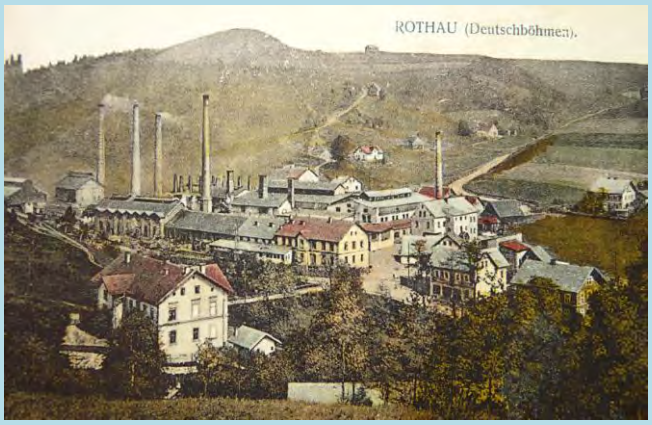

Na Rotavském potoce v horské osadě Rhodaw, která se v toku času přeměnila na město **Rotava**, vznikaly již od r. 1543 doly na železnou rudu a hamry. Nejstarší zprávy o zpracování železa však pocházejí již ze 14. stol. Do r. 1628 (některé zdroje uvádějí 1627) Rotavské panství vlastnili Šlikové. Poté v době, kdy po porážce české reformace došlo k masivním majetkovým převodům na šlechtické rody věrné císaři, získal panství hrabě Otto Nostitz. Jeho rodu pak panství patřilo až do r. 1908.

Na území panství vyrostly železárny, které přestavovaly vždy význačnou železářskou základnu habsburského mocnářství. V r. 1615 zde pracovalo 6 hamrů, v r. 1670 již dřevouhelná vysoká pec, v 18. stol. přibyly další hamry, v. r. 1800 zde pracovaly již 2 dřevouhelné vysoké pece a 10 hamrů. Specialitou zpracování železa v hamrech byla výroba plechu, přičemž již v 17. století se zde poprvé v Evropě plechy válcovaly. Od poč. 19. stol. se závod rychle rozrůstal a intenzifikoval. V r. 1826 zaměstnával již 400 pracovníků a v 60. letech 19. stol. prošel významnou modernizací. Byla postavena profilová válcovna, která byla později (v letech 1906 – 1907) vybavena parním pohonem 1000 HP, dále žíhárna se 2 pecemi na generátorový plyn, v r. 1880 byla rozšířena válcovna plechu s parním pohonem 250 HP, od r. 1901 dimenzovaným až na 700 HP. Byla to nejvýznamnější válcovna plechu v Rakousku-Uhersku. Závod jako první v Evropě již ve své historické podobě uvedl do provozu technologii žárového pocínování plechu, která se připomíná již v r. 1597. Z důvodu úspory cínu bylo v r. 1886 zavedeno i pozinkování plechu. Pocínovna doznala svého největšího rozmachu v době, kdy ve formě potravinových konzerv dodávala válečný erár na bojiště 1. světové války. Zajímavostí je, že z rotavského plechu byly raženy válečné železné pětníky a šestáky.

Ještě v r. 1880 pracovaly v Rotavě pudlovny. Do r. 1905 byly spolu s ostatními pudlovnami v Českých zemích zrušeny. V r. 1888 byla spuštěna do provozu první martinská pec 6 t, následujícího roku slévárna a v r. 1893 další martinská pec 8 t, v letech 1902 a 1906 další dvě martinské pece 20 t. Závod byl propojen železničními vlečkami s okolními železárnami a hlavními železničními tratěmi. V r. 1900 vyráběl 15 tis. t oceli, většinou pro plechy, v r. 1915 již 57 tis. t oceli a po spojení s železárnami v nedalekém Nejdku a Šindelové měl celý závod Železárny Rotava-Nejdek roční kapacitu 100 tis. t oceli.

Rotava vyráběla ploštiny pro novou válcovnu tenkých plechů v Nejdku, vybudovanou v r. 1908. V provoze v Rotavě pracovala plechotrať a dále hrubá, střední a jemná profilová trať. Šindelová pak provozovala plechotrať, pozinkovnu a slévárnu. Prvenství ve výrobě bílých plechů zůstalo spojeným železárnám i po vzniku ČSR, a to až do zastavení provozů v letech 1930 – 1932 v důsledku světové hospodářské krize. Po odeznění krize a po spojení s Báňskou a hutní společností se obnovilo válcování plechu. Vznikla také samostatná a.s. Válcovny plechu. Nová vlastnická společnost totiž ve snaze přiblížit finální výrobu plechu místu původu polotovarů, tj. Třineckým železárnám (dosud totiž ploštiny dodávalo Německo), postavila v letech 1920 – 1930 novou válcovnu plechu při Karlově huti v Lískovci. Ale to je již novodobá historie a zde vstupujeme na samotný práh současnosti. Za 2. světové války byl podnik německým majitelem Vereinigte Stahlwerke AG orientován plně na zbrojní výrobu. V poválečných letech se provozy v Rotavě zastavily. Až v r. 1957, kdy závod patřil pod Škoda Plzeň, se výroba znovu rozjela. Posléze byla postavena nová slévárna a závod přešel na strojírenskou výrobu, jejímž předmětem byly především úpravenské stroje, válcovací zařízení a vulkanizační lisy. V r. 2003 byla zrušena stará slévárna, jejíž žalostné torzo v areálu závodu dosud stojí. Dnes pracují provozy orientované na strojírenskou výrobu pod souhrnným názvem ROTAS Strojírny spol. s r.o.

První fotografie ze sbírky Petra Berana ukazuje celkový pohled na závod Rotava v r. 1900. Druhá fotografie z r. 2011 ukazuje pohled na správní budovu závodu postavenou v r. 1939. Fasáda budovy, jejímž autorem je patrně stejný architekt, který se podílel na výstavbě závodu pro braniborskou firmu Vereinigte Stahlwerke AG, Eberswalde, do jejíhož vlastnictví tehdy závod v Rotavě patřil, je tvořena režným zdivem, typickým pro průmyslovou architekturu i v dalších průmyslových lokalitách u nás.

Literatura

[1] Kol.: Industriální topografie Karlovarského kraje. Praha: ČVUT v Praze, Výzkumné centrum průmyslového dědictví Fakulty architektury, autorská položka – Jan Zikmund, foto Miroslav Kindl, 2011, 217 s. ISBN 978-80-01-04919-8

[2] Kol.: Dějiny hutnictví železa v Československu I, II. Praha: SNTL, 1984, 1988,www.rotas-strojirny.cz [cit. 20.01.2014] Beran, P. Sbírka hist. fotografií, nedat.

[3] Kol.: Dějiny hutnictví železa v Československu. Praha: Academia, 1986

FAKULTA PRIEMYSELNÝCH TECHNOLÓGIÍ V PÚCHOVE

Trenčianska Univerzita Alexandra Dubčeka v Trenčíne

Fakulta priemyselných technológií (FPT) svojím zameraním predstavuje unikát v rámci **SR** vo výchove odborníkov v oblasti kovových a nekovových materiálov, najmä gumy, silikátových materiálov a textilu. Je výnimočná predovšetkým priamou väzbou na výrobnú prax, a to ako prípravou odborníkov pre jej potreby, tak i štruktúrou štúdia špecializovanou v rámci akreditovaných študijných programov, čím je plne kompatibilnou s modelmi vzdelávania na popredných univerzitách v krajinách **EU**.

Kvalitu **Fakulty priemyselných technológií** potvrdzuje aj hodnotenie nezávislých agentúr **ARRA** a **profesia.sk**. V hodnotení **ARRA** (od roku 2005) sa **FPT** každoročne umiestňuje v prvej desiatke všetkých technických fakúlt na Slovensku. Agentúra **profesia.sk** hodnotí poradie fakúlt slovenských vysokých škôl podľa záujmu zamestnávateľov o absolventov fakúlt. **FPT** bola vyhodnotená na 7. mieste medzi fakultami s najvyšším záujmom zamestnávateľov.

Fakulta priemyselných technológií ponúka kvalitné štúdium v akreditovaných študijných programoch v študijnom odbore 5.2.26 materiály. Študenti majú možnosť absolvovať časť štúdia na zahraničných vysokoškolských inštitúciách prostredníctvom programu **ERAZMUS**.

Akreditované študijné programy na FPT v Púchove:

- **Bakalárske študijné programy:**
  - ✓ Počítačová podpora materiálového inžinierstva
  - ✓ Materiálová inžinierstvo
  - ✓ Materiálová Technológia
  - ✓ Textilná technológia a návrhárstvo
- **Inžiniersky študijný program:**
  - ✓ Materiálové inžinierstvo
- **Doktorandský študijný program:**
  - ✓ Materiály

Ivana Krasku 491/30
020 01 Púchov

tel.:032/7400 814
www.fpt.tnuni.sk